THE ORIGIN OF JUVENILE MYELOMONOCYTIC LEUKEMIA:

INSIGHTS FROM DEVELOPMENTAL HEMATOPOIESIS

Stefan Pasichnyk Tarnawsky

Submitted to the faculty of the University Graduate School
in partial fulfillment of the requirements
for the degree of
Doctor of Philosophy
in the Department of Biochemistry and Molecular Biology
Indiana University

June 2017

Accepted by the Graduate Faculty of Indiana University, in partial fulfilment of the requirements for the degree of Doctor of Philosophy.

Doctoral Committee

_____
Mervin C. Yoder, M.D., Chair

_____
Rebecca J. Chan, M.D., Ph.D.

_____
Reuben Kapur, Ph.D.

April 25, 2017

_____
Raghu G. Mirmira, M.D., Ph.D.

DEDICATION

To my parents and to my brother.

For unwavering love and support.

Дякую.

ACKNOWLEDGEMENTS

Mervin C. Yoder, M.D. and Rebecca J. Chan, M.D., Ph.D.
For invaluable mentorship.

Reuben Kapur, Ph.D. and Raghu G. Mirmira, M.D., Ph.D.
For serving on my Doctoral Committee.

Momoko Yoshimoto, M.D., Ph.D.
For expert advice, experimental help, and excellent technical training.

Yang Lin, Christopher Shelley, Ph.D., Michael J. Ferkowicz, Ph.D.
For expert advice and experimental help.

Kimihiko Banno, M.D., Ph.D., Lisa Deng, Victoria N. Jideonwo-Auman, Ph.D., Elizabeth Virts, Ph.D., Xingjun Li, Ph.D., Charles B. Goodwin, M.D., Ph.D., Michi Kobayashi, M.D., Ph.D., Donna M. Edwards, Benjamin J. Ulrich, Michelle L. Block, Ph.D., and Edward F. Srour Ph.D.
For expert advice.

Cheng-Kui Qu, M.D., Ph.D., Slava Epelman M.D., Ph.D., Anthony B. Firulli, Ph.D., Murray Korc, M.D., and Mitchell Weiss, M.D., Ph.D.
For providing reagents.

Susan E. Rice, Kimberly D. Stoner, Anthony L. Sinn, Keith W. Condon, Ph.D., and Julie A. Mund,
For assistance with core facilities and equipment.

Nancy Long, Dennis V. Renner, Dana L. Gonzales, Jayne M. Silver, and Keely L. Szilagyi, D.V.M.
For animal care.

Maureen A. Harrington, Ph.D., and Mark G. Goebl, Ph.D.
For programmatic advice.

Jan Receveur, Tiffany L Lewallen, Tracy A. Winkle, Twila P. Johnson, Sheila Reynolds, and Darlene A. Lambert.
For administrative assistance.

NHLBI, NIDDK, IUSM MSTP, IU Simon Cancer Center, Riley Children's Foundation, and The JMML Foundation
For research funding.

Stefan Pasichnyk Tarnawsky

THE ORIGIN OF JUVENILE MYELOMONOCYTIC LEUKEMIA: INSIGHTS FROM DEVELOPMENTAL HEMATOPOIESIS

Hematopoiesis proceeds through three developmental phases, each with a unique and indispensable function. The individual roles of these phases in the pathogenesis of blood disorders is unknown. We have adapted murine lineage trace models to identify the relative contributions of embryonic, fetal, and adult hematopoietic phases to the origin of Juvenile Myelomonocytic Leukemia. We hypothesized that the fetal phase would have the most pronounced contribution to the development of JMML, a pediatric myeloproliferative disorder whose disease-initiating somatic mutations occur *in utero.* Progenitors expressing PTPN11^{E76K} from all three waves were growth hypersensitive to GM-CSF due to hyperactive *RAS-ERK* signaling. However, fulminant myeloproliferation was only seen in fetal and adult cohorts. We observed equal disease severity in FLT3Cre; PTPN11^{E76K}; ROSA26^{mTmG} and CSF1R-MCM; PTPN11^{E76K}; ROSA26^{YFP} cohorts, which had high and low mutant allele frequencies, respectively. This led to the revelation that all progenitors in the BM niche of mutant animals have equal growth hypersensitivity and *RAS-ERK* hyperactivation due to non-cell autonomous effects of PTPN11^{E76K}. We further identified that FLT3Cre has hematopoietic-restricted expression, and thereby circumvented morbidity from PTPN11^{E76K} expression in endothelial and stromal cells. This led us to hypothesize that FLT3Cre; Kras^{G12D}; ROSA26^{mTmG} would be the first faithful model of JMML to express this disease-initiating mutation. Indeed, FLT3Cre; Kras^{G12D} mice were born at expected Mendelian ratio and showed normal weight gain to 2 weeks of age. Thereafter, they acquired defining features of JMML including monocytosis, anaemia, thrombocytopenia, and hepatosplenomegaly. All FLT3Cre; Kras^{G12D} mice succumb to a

JMML-like disease, which was propagated following transplantation. This is in contrast with CSF1R-MCM; $Kras^{G12D}$; $ROSA26^{YFP}$ mice, in which low mutant allele frequencies in either fetal or adult HSCs uniformly resulted in T-ALL. Our models reveal previously underappreciated features of JMML including an expansion of dendritic cells and a pronounced defect in T-lymphocyte development. We are the first to demonstrate non-cell autonomous effects of hematopoietic-restricted $PTPN11^{E76K}$ expression. Most importantly, we have shown that both the spatial and the temporal origin of JMML-initiating mutations will affect disease manifestations. Each of our findings suggest novel strategies to treat this intractable disease.

Mervin C. Yoder, M.D., Chair

TABLE OF CONTENTS

Curriculum Vitae

LIST OF TABLES

LIST OF FIGURES

LIST OF ABBREVIATIONS

AKT ..... Protein Kinase B

AML ..... Acute Myelogenous Leukemia

BM ..... Bone Marrow

CBC ..... Complete Blood Count

CD ..... Cluster of Differentiation

CLP ..... Common Lymphoid Progenitor

CMoP ..... Common Monocyte progenitor

CSF1R ..... Colony Stimulating Factor 1 Receptor

CT ..... Threshold Cycle

(E) ..... Embryonic Day

EDTA ..... Ethylenediaminetetraacetic acid

Erk1/2 ..... Extracellular Signal–Regulated Kinase 1/2

FBS ..... Fetal Bovine Serum

FL ..... Fetal Liver

Flk2 ..... Fetal Liver Kinase 2

FLT3 ..... FMS-Like Tyrosine Kinase 3

GAPDH ..... Glyceraldehyde 3-phosphate dehydrogenase

GFP ..... Green Florescent Protein

GM-CSF ..... Granulocyte-Macrophage Colony Stimulating Factor

HSC ..... Hematopoietic Stem Cell

HSCT ..... Hematopoietic Stem Cell Transplantation

HSPC ..... Hematoietic Stem and Progenitor Cells

i.p. ..... Intraperitoneal

i.v. ..... Intravenous

IHC ..... Immunohistochemistry

IMDM ..... Iscove's Modified Dulbecco's Medium

JMML ..... Juvenile Myelomonocytic Leukemia

KRAS .....Kirsten rat sarcoma viral oncogene homolog

LK .....Lin- cKit+

LSK .....Lin- cKit+ Sca1+

M-CSF .....Macrophage Colony Stimulating Factor

MDP ..... Monocyte-Dendritic Cell Progenitor

MDS ..... Myelodysplastic Syndrome

MER ..... Mutated Estrogen Receptor

MHCII .....Major Histocompatibility Complex II

MPN ..... Myeloproliferative neoplasm

MPP .....Multipotent Progenitor

mTmG .....membrane tdTomato LSL membrane GFP

P/S .....Penicillin-Streptomycin

PBS ..... Phosphate Buffered Saline

PCR..... Polymerase Chain Reaction

PFA .....Paraformaldehyde

PI3K ..... Phosphoinositide 3-kinase

PSp ..... Para-aortic Splanchnopleura

PTPN11.....Protein Tyrosine Phosphatase 11

RBC..... Red Blood Cell

STAT5 ..... Signal Transducer and Activator of Transcription 5

T-ALL .....T-cell Acute Lymphoblastic Leukemia/Lymphoma

tdTomato .....tandem dimer Tomato

YFP ..... Yellow Fluorescent Protein

YS .....Yolk Sac

CHAPTER I

INTRODUCTION

Outline

Hematopoiesis is a hierarchical process. Stem cells divide and progressively commit themselves to the production of a single mature blood cell lineage. This commitment occurs through a series intermediary progenitors that lose differentiation potential in a stepwise fashion. The textbook dogma suggests that all blood progeny trace their origin to a single progenitor type: the hematopoietic stem cell (HSC, see Figure I-1). Whereas this schematic is a useful heuristic tool it overlooks the nuanced origin of hematopoiesis. In reality, blood cells emerge in distinct hematopoietic phases, each with its own spatial and temporal origin. These phases require different signals for their emergence and they contain distinct progenitors whose differentiation potentials are unique. Progenitors in each phase may share cell surface markers, but nonetheless have different function and longevity. As such, it is imperative to appreciate the distinctions of hematopoietic phases in order to understand the scope of blood cell development.

This work will consider three sequential phases of hematopoiesis: embryonic, fetal, and adult (Figure I-2). The embryonic phase emerges independently and prior to the first HSC, whereas the fetal and adult phases are HSC-dependent. We will describe the spatial and temporal origin of each phase as well as their unique functions. Finally, we will consider the significance of these phases in the context of a pediatric blood disorder with a known *in utero* origin: Juvenile Myelomonocytic Leukemia. We will do so by describing the contribution of these phases to murine models of JMML.

Three Phases of Hematopoiesis

The first hematopoietic cells produced in a developing mammal arise directly from mesoderm in the extraembryonic yolk sac (YS) (Maximow 1909; Lux et al. 2008;

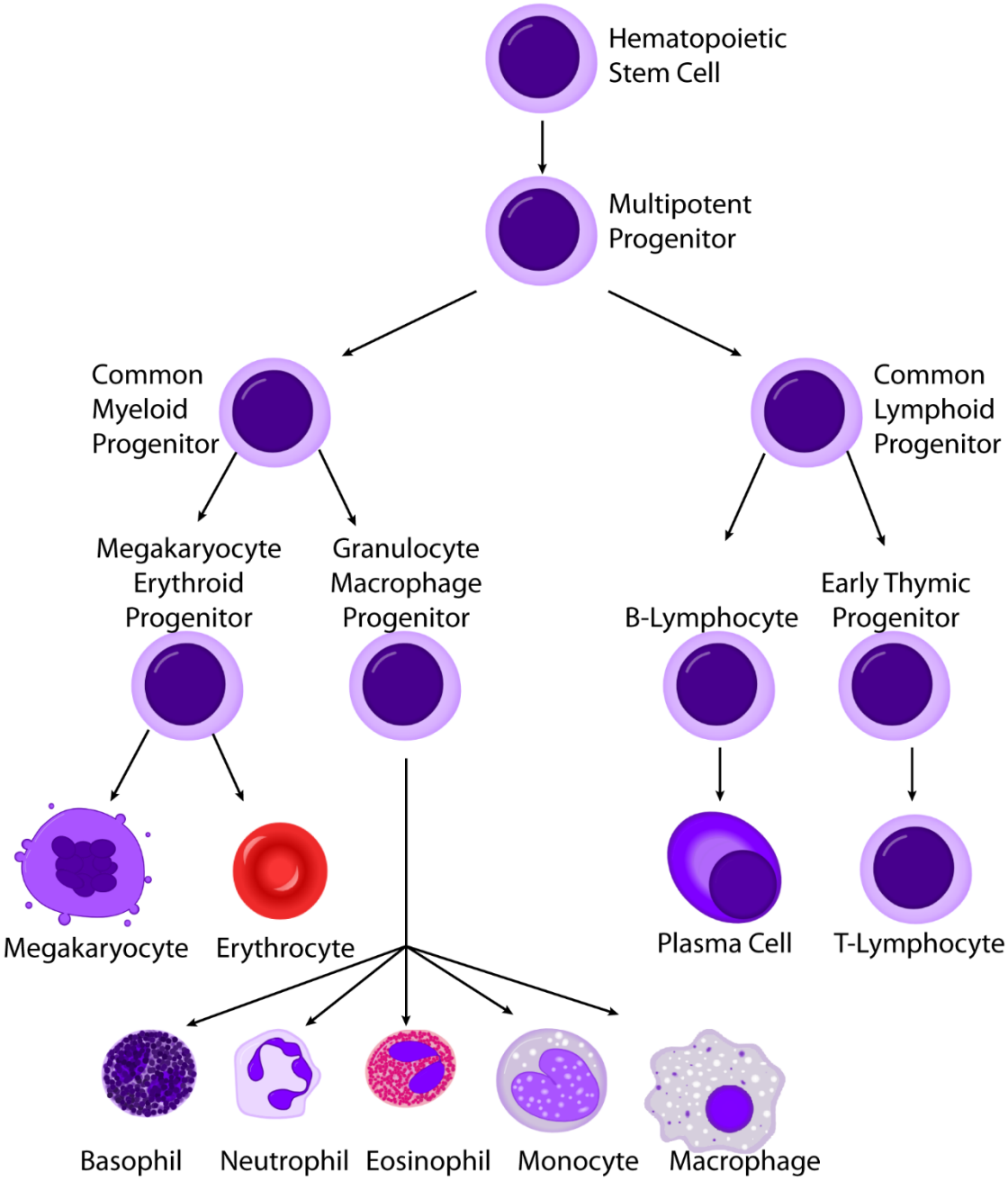

Figure I-1. The Traditional Hierarchy of Hematopoiesis. The classic hierarchy suggests that all hematopoietic cells are progeny of the hematopoietic stem cell, which gives rise to mature cells through a series of progenitors with progressively more committed lineage differentiation potential.

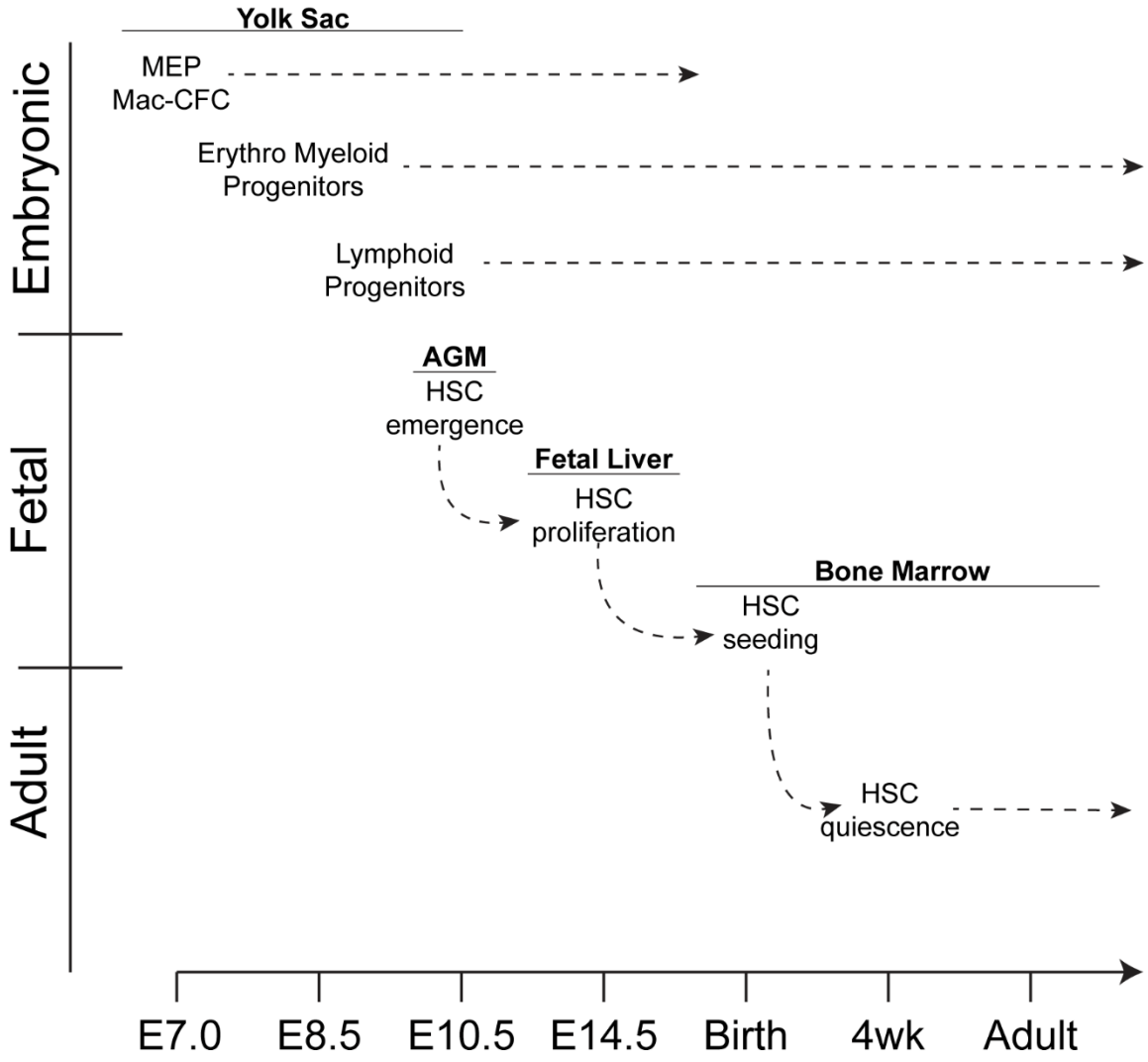

Figure I-2. The Three Phases of Hematopoiesis. The first hematopoietic cells emerge in the extraembryonic yolk sac around embryonic day (E)7.0. Erythromyeloid progenitors emerge around E8.25 followed by lymphoid progenitors around E9.0. The first definite hematopoietic stem cells (HSCs) emerge in the aorta-gonad mesonephros (AGM) region around E10.5. They migrate to the fetal liver and proliferate before seeding the bone marrow around birth. They continue to proliferate and differentiate until 4 weeks of age when they enter quiescence. This marks the fetal to adult phase transition. This graphic highlights the relevant developmental events for studies performed in this work. See (Lin Y, MC Yoder, Yoshimoto M, 2014) for in-depth review of embryonic hematopoiesis.

Ferkowicz 2003; Palis et al. 2001; Migliaccio et al. 1986). These are bipotent megakaryocytic-erythroid progenitors (MEP) that produce large, nucleated erythrocytes (Tober et al. 2007). Because these features resemble similar previously-characterized avian and reptilian cells, this lineage was termed primitive (Frame, McGrath, and Palis 2013). This designation distinguished these cells from definitive erythrocytes that shrink in size following enucleation. It was later shown that a myeloid-restricted progenitor (Mac-CFC) emerged concurrently with the primitive MEP (Bertrand et al., 2005; Moore and Metcalf, 1969). The progeny of Mac-CFC had morphological and functional properties of phagocytes and these were named primitive macrophages (Bertrand et al. 2005; Moore and Metcalf 1969).

Shortly following the emergence of this first hematopoietic wave were bipotent erythromyeloid progenitors (EMPs). These arise from an endothelial-to-hematopoietic transition in the YS around E8.25 (Frame et al. 2016). They seed the fetal liver around E10.5, where they contribute to monocytes, granulocyte, and erythroid progeny that sustain the conceptus as the HSC-dependent phase emerges and proliferates (Palis et al. 1999; Chen et al. 2011; McGrath et al. 2015). Whereas initial studies suggested EMPs had a transient role in development, recent evidence conclude that the progeny of EMPs persist into adulthood as tissue resident macrophages (Schulz et al. 2012; Gomez Perdiguero et al. 2015; Epelman et al. 2014; Kierdorf et al. 2013; Ginhoux et al. 2010; Samokhvalov, Samokhvalova, and Nishikawa 2007). This contribution is most significant in the brain; all microglia are thought to arise from HSC-independent yolk sac progenitors in unperturbed hematopoiesis. Microglia are only replenished by BM progenitors or CNS stromal precursors in the context of inflammation (Ajami et al. 2007; Mildner et al. 2007; Ginhoux et al. 2010; Elmore et al. 2014).

The embryonic phase of hematopoiesis also contributes to lymphoid progeny. Whereas neither MEPs, Mac-CFCs nor EMPs have lymphoid potential, B and T-

lymphocytes emerge in the yolk sac prior to and independently from HSCs (Yoshimoto et al. 2010; Yoshimoto et al. 2012). Beginning around E9.0, B-lymphoid progenitors emerge in the YS via an endothelial to hematopoietic transition. These progenitors preferentially contribute to peritoneal B1 cells and marginal zone cells in the spleen. This suggests that YS B-cell progenitors preferentially give rise to innate-type cells rather that adaptive B2 cells that preferentially arise from HSCs. Additional work has identified that multipotent progenitors with of tri-lineage lymphocyte potential arise in the YS independently of HSCs (Yoder and Hiatt 1997; Inlay et al. 2014). As such, the yolk sac produces blood cells from all lineages and does so prior to the emergence of the first HSC. Together, these progenitors constitute the HSC-independent hematopoietic phase.

The HSC is functionally defined as a cell that can i) give rise to all blood cell lineages and ii) that can self-renew indefinitely upon serial transplantations into adult recipients. This definition distinguishes it from neonatal HSCs, which first arise in the yolk sac, give rise to all lineages, but can only engraft neonatal recipients (Yoder et al. 1997; Yoder and Hiatt 1997; Johnson and Yoder 2005). Other progenitors from the embryonic phase are equally incapable of durable contributions in adult recipients (McGrath et al. 2015). The HSC definition further draws the distinction with non-self-renewing progenitors in adults that are capable of clonal contributions to all lineages but cannot self-renew upon serial transplantation (Yamamoto et al. 2013).

The current standard to evaluate of an HSC is the single-cell transplant (Wilson et al. 2015). Therein a single cell is injected into a conditioned adult recipient and the engraftment is monitored for at least 16 weeks. To be considered an HSC, the cell must contribute to a minimum of 1% of peripheral blood cells from all lineages and must be able to sustain this contribution for a minimum of two additional sequential transplantations. This definition, however, is problematic. Historically HSCs have been variously defined as cells able to give rise to multilineage colonies in methylcellulose, cells able to give rise to

grossly-visible colonies in recipients' spleens, cells able to rescue a lethally-ablated recipient, among others (Eaves 2015). Additionally, the current definition requires a functional test that irrevocably alters the assayed cell. As such, you cannot have your HSC and test it too. Furthermore, since the HSC assay requires transplantation, there is no accepted definition for an HSC in its native host (Busch and Rodewald 2016). Indeed, recent studies demonstrate major differences between post-transplant and unperturbed hematopoiesis (Henninger et al. 2017; Sun et al. 2014; Busch et al. 2015); these will be discussed in detail below. In short, these difficulties make it challenging to compare HSCs from different studies. Herein HSCs will be defined as single cells capable of multilineage serial reconstitution in adult recipients.

The first HSCs arise in the mouse around E10.5-E11.0 on the ventral wall of the dorsal aorta (Muller et al. 1994; Medvinsky and Dzierzak 1996; Boisset et al. 2010). This occurs through an endothelial to hematopoietic transition that is dependent on Runx1 and Sox17 signaling (Chen et al. 2009; Zovein et al. 2008; Kim, Saunders, and Morrison 2007). Shortly thereafter, HSCs also emerge in other tissues including the placenta and the yolk sac (Samokhvalov, Samokhvalova, and Nishikawa 2007; Gekas et al. 2005). They migrate to the fetal liver where they rapidly proliferate (Taoudi and Medvinsky 2007; Ema and Nakauchi 2000). Chemotactic signals later induce migration to the spleen and/or the thymus before HSCs seed the bone marrow (BM) around birth (Kiel et al. 2005; Christensen et al. 2004). There, HSCs undergo gradual functional changes that define the fetal to adult phase transition.

The distinction between fetal and adult HSC-dependent phases is not arbitrary. Fetal progenitors are highly proliferative and have greater repopulating ability than adult progenitors, which are predominantly quiescent (Bowie et al. 2006; Bowie et al. 2007; Dykstra et al. 2007). Genetic or microenvironmental alterations that force adult HSCs to enter the cell cycle result in bone marrow failure (Ye et al. 2013; Kunisaki et al. 2013). The

differentiation potential of the two phases is also different. Fetal HSCs are biased to produce lymphoid progeny whereas adult HSCs are biased to produce myeloid progeny (Benz et al. 2012). Nonetheless, due to their enhanced proliferative potential, fetal progenitors produce greater numbers of myeloid colonies in methylcellulose assays that can be serially replated (Ema and Nakauchi 2000; Lansdorp, Dragowska, and Mayani 1993). With respect to lymphoid progeny, fetal progenitors are capable of robust contributions to innate immune cells, whereas adult progenitors predominantly contribute to adaptive immune cells (Benz et al. 2012; Yuan et al. 2012; Beaudin et al. 2016). Fetal HSCs have a unique immunophenotype that includes expression of CD11b and CD144 (Kim, Yilmaz, and Morrison 2005) and have differential response to exogenous cytokines and signaling mediators than their adult counterparts (Chanda et al. 2013; Kim, Saunders, and Morrison 2007; Park et al. 2003; Ye et al. 2013; Copley and Eaves 2013). Importantly, parallel studies in humans have also identified developmental changes in hematopoietic progenitors: fetal progenitors are more proliferative and transition into the adult phase at approximately two years of age (Lansdorp, Dragowska, and Mayani 1993; Sidorov et al. 2009). Fetal and adult HSC-dependent phases are also differentially susceptible to transformation. For instance, fetal progenitors are relatively resistant to transformation by FLT3ITD mutations and are more likely to produce myeloid rather than lymphoid malignancies (Porter et al. 2016; Man et al. 2016).

We have described the origin and function of three hematopoietic phases: HSC-independent, fetal, and adult. These phases, however, do not exist in isolation. Their interdependence is highlighted by seminal experiments that showed the emergence of HSCs from hemogenic endothelium is dependent on sterile inflammatory signals (Espin-Palazon et al. 2014). These signals come from myeloid cells that are descended from YS EMPs (Li et al. 2014). Loss of EMPs is not compatible with life, as they are required to sustain the embryo during the late fetal period when HSC-dependent progenitors are

proliferating (Mucenski et al. 1991). Furthermore, the high proliferation rate of fetal progenitors may be a requirement for the prompt population of rapidly growing tissues during development. Additionally, the propensity of fetal HSCs to preferentially contribute to lymphoid tissues may be an adaptation to protect neonates from the abrupt exposure to exogenous pathogens at birth. Finally, the high proliferative rate of fetal HSCs is not suitable for life-long maintenance of hematopoiesis. As such, the transition from fetal to adult phases is likely an adaptation to prevent exhaustion of progenitors and lessen the acquisition of deleterious mutations that occurs at each cell division.

Given that each phase has a defined role in mammalian development, it is surprising that their respective contributions to hematologic disease have not been evaluated. Pediatric hematologic disorders are markedly different from adult ones (Greaves 2015). Nonetheless, the majority of animal models do not consider distinctions between embryonic, fetal, and adult hematopoiesis. In this study, we sought to evaluate the contribution of these three phases to the pediatric myeloproliferative neoplasm Juvenile Myelomonocytic Leukemia.

Case Report

The patient is a 16 month-old Caucasian male that presented to his pediatrician with lethargy, abdominal distention, and skin lesions. Parents relate that the patient was healthy until 2 months ago when they noticed weakness and a progressive weight loss. Physical exam revealed a palpable liver and spleen 7cm and 4cm below the costal margin, respectively, with skin pallor, widespread bruising, and dyspnea. Peripheral blood exam showed thrombocytopenia (16500/uL), and anaemia (7 g/dL), and marked leukocytosis (104 600/uL; 9% band forms; 71% neutrophils; 7% monocytes; 12% leukocytes, 0.8% eosinophils) with elevated fetal hemoglobin (15.3%). BM aspirate showed hypercellularity with dysplastic neutrophils and 11% blast cells. Patient karyotype shows monosomy 7

without translocations. A diagnosis of JMML was suspected and sequencing analysis of peripheral blood cells confirmed a somatic PTPN11 226G>A mutation. Two months after presentation two 5/6HLA-matched cord blood units were transplanted following a Bu-Cy-Mel conditioning regimen. The patient developed mild GVHD 46 days after transplant and was treated with steroids. 167 days after transplant monosomy 7 was identified in 37% of peripheral leukocytes indicating disease relapse. 13 months after initial presentation, the patient underwent a second transplant with matched sibling donor. 90 days after HSCT complete donor chimerism was confirmed and the patient remains disease-free 3 years later. [Based on published studies (Osumi et al. 2017; Locatelli and Niemeyer 2015; Inagaki et al. 2013)].

Juvenile Myelomonocytic Leukemia

JMML is a pediatric myeloproliferative neoplasm (MPN). The World Health Organization also classifies JMML as a myelodysplastic syndrome (MDS) due to an abundance of abnormal myeloid cells in patients' BM and blood (Arber et al. 2016). The diagnosis of JMML is clinically challenging (Locatelli and Niemeyer 2015). Patients present very young with a mean age of <2 years. They show hepatosplenomegaly, failure to thrive, non-specific dermatologic features, and they are prone to infections. Blood analysis will reveal an absolute monocytosis along with anaemia and thrombocytopenia. BM biopsy will reveal a moderate elevation of blasts (<20%) that lack AML and CMML-associated translocations. These features are non-specific and the differential diagnosis is broad. Definitive diagnosis of JMML requires its distinction from viral infections, non-malignant hematologic disorders, and pediatric AML.

A breakthrough for JMML diagnosis came when researchers discovered that hematopoietic progenitors from JMML patients had unique growth hypersensitivity to the cytokine GM-CSF (Emanuel et al. 1991). The search for the causative mechanism

subsequently revealed that >90% of patients have somatic mutations in signaling mediators downstream of the GM-CSF receptor (Figure I-3). These gain of function mutations in *PTPN11*, *Kras*, *Nras*, or loss of function mutations in *NF1* or *c-CBL* caused hyperactivation of RAS-ERK and led to disease. More recent exome-wide sequencing studies have identified that a minority of JMML patients have secondary mutations in overlapping or parallel signaling pathways, such as *SETBP1*, *JAK3*, *RAC2*, and *ASXL1* (Sakaguchi et al. 2013; Caye et al. 2015; Stieglitz, Taylor-Weiner, et al. 2015). In so doing, however, these studies confirmed that single nucleotide polymorphisms and single gene deletions are sufficient for JMML emergence and are the sole drivers of disease in the majority of patients.

JMML has a low incidence of only 1 in $1.2x10^6$ births. This is fortunate given its poor prognosis. Chemotherapy is ineffective; the only curative treatment is allogeneic HSC transplantation (HSCT). Nonetheless, the 5 year overall survival of JMML patients following HSCT is only 52%, considerably lower than that of pediatric AML patients treated with HSCT (Locatelli et al. 2013). The reason for this poor efficacy is unclear. Atypical histiocytes infiltrate the tissues of JMML patients (Ng et al. 1988; Ozono et al. 2011). Such populations are relatively resistant to myeloablation and thus may contribute to disease recurrence (Haniffa et al. 2009; Hashimoto et al. 2013). Additionally, these histiocytes and other granulocytes may irrevocably damage patients' hematopoietic niche, possibly through oxidative damage or alterations in stromal cell populations (Zheng et al. 2013; Dong et al. 2016). This could lead to engraftment failure and subsequent relapse (Chan and Yoder 2013). Finally, whereas JMML unquestionably has a clonal origin, it has been proposed that the disease-initiating cell may not be the *bona fide* HSC. This hypothesis stems from findings that lymphocytes in patients frequently do not express the disease-initiating mutation (Sakaguchi et al. 2013; Stieglitz, Taylor-Weiner, et al. 2015; Flotho et al. 1999). If true, this could explain why HSCT may not cure an HSC-independent disease.

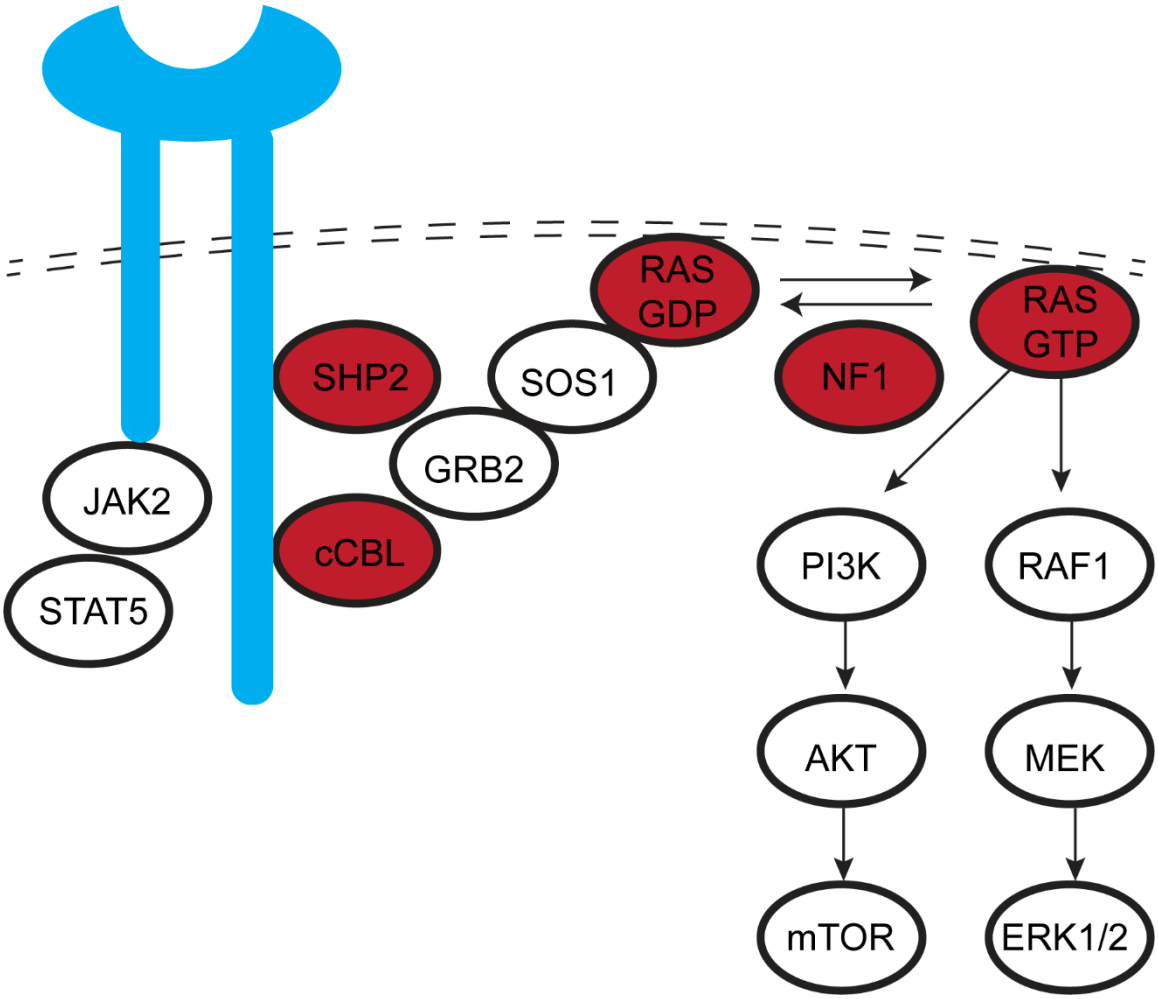

Figure I-3. Aberrant Signaling in Juvenile Myelomonocytic Leukemia. Mutations frequently found in JMML patients are highlighted in red. The growth factor receptor is shown in blue. The GM-CSF receptor is frequently implicated in human disease; in murine models other cytokine receptors, including the SCF receptor and the IL-3 receptor, are involved.

Groups have hypothesized that progenitors from JMML patients may have differentiation blocks and/or biased differentiation that impedes the production of mature progeny in certain lineages. Murine studies suggest hyperactive Ras induces a block in erythroid maturation in the BM (Braun et al. 2006), which may thereby prompt common myeloid progenitors to commit to the granulocyte-monocyte lineage rather than to the megakaryocyte-erythroid lineage. Additionally, groups have identified that JMML patients have relatively fewer T-lymphocytes in the blood, BM, and spleen compared to age-matched controls (Oliveira et al. 2016; Krombholz et al. 2016). This hints at a mechanism for the lack of mutation expression in lymphocytes; progenitors from JMML patients may undergo a lineage-specific differentiation block that prevents the production of mature progeny. This notion of aberrant differentiation is further supported by studies that showed progenitors from JMML patients spontaneously differentiate into dendritic-like cells (Longoni et al. 2002; Estrov et al. 1986). These *in vitro* findings parallel the histiocytic infiltrates that have been documented in the skin and spleen of JMML patients.

Evidence from recent studies has converged to implicate a fetal origin for JMML. This disease is unique in causing a persistently elevated fetal hemoglobin (Weinberg et al. 1990). Additionally, retrospective analysis determined that disease-initiating mutations were present in the majority of JMML patient samples collected at birth (Kratz et al. 2005; Matsuda et al. 2010). This confirms an *in utero* origin for this disease. Finally, gene expression analysis of unfractionated BM cells from JMML patients revealed a signature that was pathognomonic of fetal progenitors (Helsmoortel, Bresolin, et al. 2016). It was characterized by elevated expression of Lin28B, a master-regulator of stem cell-like features (Shyh-Chang and Daley 2013). This signature was present in the majority of JMML patients and was associated with an inferior overall survival. In contrast, only 10% of pediatric AML patients, 2% of pediatric ALL patients and no pediatric MDS patients had a similar gene expression signature (Helsmoortel, De Moerloose, et al. 2016).

In summary, JMML is a clonal pediatric MPN caused by somatic mutations in *PTPN11*, *K/N-Ras*, *NF1*, and *c-CBL*. These mutations evoke two defining disease features: growth hypersensitivity in response to GM-CSF and hyperactive RAS-ERK signaling. HSCT is the only curative therapy, which nonetheless has a very high failure rate. Hypotheses for this failure include an HSC-independent origin, myeloablation-resistant tumour cells, and irrevocable alterations to hematopoietic niches. Whereas the cellular origin of JMML is debated, there is strong evidence for a fetal origin: mutations occur *in utero*, patients have elevated fetal hemoglobin, and gene expression from tumour cells bears hallmarks of fetal progenitors.

Current Mouse Models of JMML

JMML is an ideal disease model because it can be evoked by a single nucleotide polymorphism. As such, minimal genetic manipulations are required to create a model. Since *Ras* mutations are sufficient to cause JMML, and since *Ras* mutations are the most common genetic abnormality seen in human cancers, findings from JMML models have broad applicability to other malignancies (McCormick 2015). Initial studies utilized retroviral vectors to introduce gain of function *PTPN11* or *Ras* mutations in cultured cells (Chan et al. 2005; Serrano et al. 1997; Mohi et al. 2005). Such *in vitro* studies of JMML-disease initiating mutations helped resolve the aberrant signaling mechanisms that underlie this disease. It became clear that a linear pathway could not account for all observed disease manifestations. Rather, crosstalk between multiple signaling mediators converged to enhance proliferation and mediate cell-intrinsic and cell-extrinsic defects (Goodwin et al. 2012). As such, it was crucial to develop animal models to study the mutations' effects *in vivo*.

The Cre-loxP system is the most widespread tool for genetic manipulation in mice (Kuhn and Torres 2002). This technique replaces a portion of an existing allele with an *in*

vitro designed vector using homologous recombination. The modified allele has two components: i) the mutation of interest and ii) a loxP-flanked stop cassette 5' of the mutation. The stop cassette encodes tandem polyadenylation signals that cause premature transcriptional termination. As such, the knocked-in locus is silenced and the animal is haploinsufficient for the gene of interest. However, the loxP sites that flank the stop cassette are recognized by the Cre recombinase. This enzyme will cut out the intervening DNA sequence. Thus, in the presence of an active Cre enzyme, the stop cassette will be removed and the conditional mutant allele will be transcribed.

Therefore, in the Cre-loxP system two mouse strains must be bred together: i) a strain that encodes the Cre recombinase and ii) a strain that encodes a conditional mutation flanked by loxP sites. Since a single genetic alteration is sufficient to give rise to JMML, only one mutation must be introduced into a mouse to recapitulate the underlying cause of the patient disease. The $Kras^{G12D}$ mouse was the first conditional animal model of JMML (Braun et al. 2004) and was shortly followed by numerous others including multiple *PTPN11* mutations, *NF1*, and *c-CBL* (Chan, Kalaitzidis, et al. 2009; Xu et al. 2011; Le et al. 2004; Naramura et al. 2010 and see Table I-1).

Expressing the mutation, however, is not sufficient to produce a faithful disease model. The expression must be restricted to the cellular compartment that matches the pathophysiology of the studied disease. As such, the specificity of Cre expression is the major determinant of Cre-loxP model success. A variety of murine Cre strains have been created in which tissue-specific and/or developmentally-regulated *cis* regulatory elements drive Cre expression. In designing a conditional mouse model, one must identify a Cre stain whose spatial and temporal activity recapitulates that observed in patients.

JMML is caused by somatic *in utero* mutations within hematopoietic progenitors. Successful modelling of this disease, therefore, requires the Cre enzyme to have developmentally controlled and hematopoietic restricted expression. Unfortunately, it has

proven very challenging to find Cre strains with these criteria (Table I-1). The most commonly used hematopoietic Cre stain is Mx1Cre (Kuhn et al. 1995). Therein, interferon-responsive cells begin to express Cre following stress. Typically, this is experientially introduced through the administration of polyI:polyC (pI:pC) to mice. However, Mx1Cre is active in up to 10% of hematopoietic progenitors in the absence of exogenous pI:pC (Sabnis et al. 2009). Furthermore, Mx1Cre activity is not restricted to hematopoietic cells; it is also expressed in stromal, endothelial, and intestinal cells (Staffas et al. 2015; Dong et al. 2016). Finally, pI:pC administration is toxic to the growing fetus (Liu and Hansen 1993). As such, this system's use is typically restricted to adult mice.

The VavCre and LysMCre strains are also widely disseminated and largely regarded as hematopoietic-restricted. Their expression is developmentally controlled and does begin *in utero* (Clausen et al. 1999; Ghiaur et al. 2008). However, these models have their drawbacks. Like Mx1Cre, VavCre and LysMCre will introduce mutations in all cells in which their promoter is active. As such, they cannot recapitulate the clonal origin of JMML. Additionally, their constitutive activity cannot be turned off. Each time a progenitor acquires *Vav* or *LysM* promoter activity it will activate *de novo* mutations. This never-ending cascade of mutations makes drug studies a challenge; even if a treatment eradicates all mutation-expressing cells, new clones with freshly-acquired mutations will inevitably emerge to take their place. Finally, VavCre and LysMCre activity is also not restricted to hematopoietic cells (Siegemund et al. 2015; Stadtfeld, Ye, and Graf 2007). As such it is unclear which symptoms in these models are the result of hematopoietic expression and which stem from stromal or alveolar cell expression (Xu et al. 2011).

To circumvent the non-specific expression patterns of Cre strains, researchers have turned to transplantation studies (Till and McCulloch 1961). In these experiments, a recipient animal's hematopoietic system is ablated and replaced with donor HSCs. If donor cells express a mutation the reconstituted mouse may be a model for the corresponding

Cre	Expression Pattern	Oncogene	Disease Phenotype	Median Survival (weeks)
Mx1Cre	>90% HSCs Endothelial cells Osteoblasts MSPCs	$PTPN11^{E76K}$	MPN (?)	11
		$Kras^{G12D}$	T-ALL	28
VavCre	>90% HSCs Endothelial cells	$PTPN11^{E76K}$	MPN (?)	Not reported.
		$Kras^{G12D}$	*In utero* lethal	N/A
LysMCre	~80% monocytes ~5% HSCs Alveolar cells Heart septum	$PTPN11^{E76K}$	MPN (?)	36
		$Kras^{G12D}$	Lung adenocarcinoma	3

Table I-1. Existing Murine Models of Conditional $PTPN11^{E76K}$ and $Kras^{G12D}$. MSPCs mesenchymal stem and progenitor cells; MPN myeloproliferative neoplasm; T-ALL T-lymphocyte acute lymphoblastic leukemia/lymphoma. (?) Indicates that a MPN phenotype was reported but that effects of non-hematopoietic expression were not explicitly characterized. In this work we will restrict our analysis to PTPN11 and Ras models of JMML. Other models that evaluate loss of function mutations in NF1 and c-CBL have equally been studied using Cre strains with non-hematopoietic expression (Le et al. 2004; Naramura et al. 2010; An et al. 2015).

disease. Control transplants with healthy donor cells must be performed to account for irradiation-induced injuries. Since donor cells are hematopoietic any disease manifestations can be attributed to hematopoietic causes. Such studies have identified disease features that were mistakenly attributed to hematopoietic effects in Cre-loxP systems. For instance, Mx1Cre;$Kras^{G12D}$ mice develop progressive anaemia but transplant recipients of $Kras^{G12D}$ expressing cells do not (Braun et al. 2004). It was determined that Mx1Cre;$Kras^{G12D}$ animals become anaemic from intestinal bleeding caused from endothelial and intestinal expression of the oncogene (Staffas et al. 2015).

Transplantation studies are also the cornerstone of cancer stem cell studies (Bonnet and Dick 1997). This hypothesis proposes that malignancies emulate the progenitor hierarchy observed in normal hematopoiesis. At the top of the malignant hierarchy is the leukemia stem cell, which is defined by its ability to propagate the malignancy upon transplantation (Kreso and Dick 2014). As such, transplantations permit researchers to seek the cellular origins of a disease. Specific populations are separately transplanted into recipient cohorts and disease burden in these cohorts are compared. This technique can identify the progenitor capable of initiating a disease. It determined that myeloid-restricted progenitors in Mx1Cre;$Kras^{G12D}$ mice cannot initiate disease in recipients, in contrast to HSCs which do initiate T-ALL following transplantation (Zhang et al. 2009; Sabnis et al. 2009).

Transplantation experiments, however, have notable shortcomings. Donor cells are removed from their native environment, required to engraft a foreign host, and are forced to proliferate. As such, developmental context is lost in transplantation studies. This can be mitigated by selecting recipients that permit engraftment of the desired hematopoietic phase (Arora et al. 2014). For instance, sublethally-irradiated immunodeficient neonates readily permit engraftment of yolk sac progenitors, whereas lethally-irradiated adult congenic mice are the best recipients of BM donors (Yoder and

Hiatt 1997; Johnson and Yoder 2005). However, these developmentally-synchronous transplants are technically challenging and the overwhelming majority of studies restrict themselves to BM donor cells and adult recipient mice.

More troubling still are the striking differences between post-transplant and unperturbed hematopoiesis (Busch and Rodewald 2016). Only a small fraction of donor cells contribute to hematopoiesis 16 weeks after transplantation (Yamamoto et al. 2013). In contrast, progenitors in their native hosts have much longer lifespans and are capable of significant clonal contributions to mature cell populations (Sun et al. 2014). Additionally, studies of unperturbed hematopoiesis suggest a periodicity of HSC activity, in which only 1% of HSCs contribute to peripheral populations at any given time. Furthermore, these authors estimated that only ~30% of transplantable HSCs will have any significant contribution to mature progeny in the course of a lifetime (Busch et al. 2015). Finally, the differentiation patterns following transplantation do not mirror those of unperturbed hematopoiesis. For instance, ~90% of myeloid cells will be labelled by FLT3Cre under native conditions, but only ~50% of cells will be labelled following transplantation with 100 HSCs (Boyer et al. 2011). Additionally, the diversity of hematopoiesis in recipient animals is greatly reduced from that of the donor HSC pool due to the engraftment and cycling stresses imposed by transplantation (Henninger et al. 2017). As such, both existing Cre-loxP and animal transplantation models of JMML have notable shortcomings that have inadequately recapitulated the defining features of the human disease.

In an effort to circumvent these challenges, researchers have taken advantage of recent technologies to develop humanized models of JMML. Two groups have established induced pluripotent stem cell (iPSC) lines from JMML patients (Gandre-Babbe et al. 2013; Mulero-Navarro et al. 2015). These lines demonstrate disease-defining features: growth hypersensitivity to GM-CSF due to hyperactive *RAS-ERK* signaling. Additionally, these studies identified novel microRNAs that may contribute to myeloid dysregulation and may

thus be targets for future therapies. However, iPSCs can only recapitulate the HSC-independent hematopoietic phase (Vanhee et al. 2014; Buchrieser, James, and Moore 2017). Despite increasingly innovative and complex strategies, human iPSC-derived HSCs have remained elusive (Doulatov et al. 2013; Sturgeon et al. 2014). As such, JMML-specific iPSCs are a useful tool to study signaling mechanisms in human samples. However, they cannot be used to probe the developmental origins of the disease.

Several groups have also modeled JMML in xenograph experiments. They transplanted progenitors from patients into immunodeficient mice and monitored disease progression using species-specific reagents (Lapidot et al. 1996; Nakamura et al. 2005). Initial attempts showed varying engraftment efficiency, were dependent on supplementation with human cytokines, and were difficult to reproduce. A more recent study (Krombholz et al. 2016) was able to engraft 4/5 tested patient samples in the majority of recipient animals without the use of exogenous cytokines. Engrafted recipients showed clinical features of JMML such as enhanced myeloid populations, decreased lymphocyte populations, histiocytic tissue infiltrates and early death. However, this study was not able to identify the JMML-initiating cell and relied on large bulk donor cell populations. It remains to be seen whether this model will be suitable for drug studies and if it will help identify new disease mechanisms and therapeutic targets.

In summary, JMML is ideally suited for animal studies. The disease-initiating mutations can be readily introduced and their signaling mechanisms have been thoroughly validated. However, previous studies have failed to address the *in utero* and hematopoietic-restricted origin of this disease. The relative contributions of the three hematopoietic phases to JMML are not known. The clonal nature of the disease has not been recapitulated and it is not known which disease manifestations are the result of cell-autonomous vs. non-cell autonomous effects of the mutation. Finally, it has proven challenging to interpret existing studies due to non-hematopoietic expression of mutations

or due to uncertainties as to the physiologic-appropriateness of post-transplant hematopoiesis. In the studies presented herein we sought to circumvent these previous shortcomings to create the most representative animal model of JMML.

CHAPTER II

HEMATOPOIETIC PHASE-SPECIFIC MODELS OF MUTANT PTPN11

Abstract

Somatic mutations in PTPN11 are the most common cause of JMML and are a prognostic indicator of poor overall survival. Existing murine models of JMML using PTPN11 mutations have demonstrated molecular characteristics of the disease. However, these studies have not recapitulated two defining pathophysiologic features of JMML: hematopoietic restricted expression, and a clonal origin. Furthermore, they have not considered the independent consequences of PTPN11 mutations in the embryonic, fetal, and adult phases of hematopoiesis. In this study, we show that progenitors expressing mutant PTPN11 from all three phases will show growth hypersensitivity following GM-CSF stimulation due to hyperactive *RAS-ERK*. We use conditional models and transplant studies to show that embryonic progenitors that express either $PTPN11^{D61Y}$ or $PTPN11^{E76K}$ cannot cause myeloproliferation in adult mice. We validate the CSF1R-MCM as a hematopoietic-restricted Cre that targets HSCs with a physiologically-appropriate low efficiency. We generate CSF1R-MCM; $PTPN11^{E76K}$; $ROSA^{YFP}$ cohorts that express the mutation in either the fetal or adult phases. We show that both fetal and adult cohorts develop a JMML-like disease despite a very low mutant allele frequency. They develop monocytosis, anaemia, thrombocytopenia and have a paucity of peripheral T-lymphocytes. Tissue examination reveals pronounced extramedullary hematopoiesis. Both YFP+ and YFP- progenitors from mutant mice have equal growth hypersensitivity and RAS-ERK activation following stimulation with GM-CSF, indicating non-cell autonomous effects of hematopoietic-restricted $PTPN11^{E76K}$. In summary, we demonstrate that both fetal and adult phases have a pronounced contribution to $PTPN11^{E76K}$-evoked MPN. Additionally, we demonstrate that low mutant allele frequencies are sufficient to cause disease due to non-cell autonomous effects of this mutation.

Materials and Methods

Mice

C57BL/6J, B6.SJL-*Ptprc*^{a} *Pepc*^{b}/ (BoyJ), and NOD.Cg-*Prkdc*^{scid} *Il2rg*^{tm1Wjl}/SzJ (NSG) mice were bred in-house and/or obtained from the IUSM *In Vivo* Therapeutics Core. LSL-PTPN11^{D61Y}/+ mice were obtained from Dr. Gordon Chan and Dr. Benjamin Neel. LSL-PTPN11$^{E76K/+}$ mice were obtained from Dr. Cheng-Kui Qu. FLT3Cre+; ROSA$^{mTmG/mTmG}$ mice were obtained from Dr. Slava Epelman. ROSA$^{YFP/YFP}$ mice were obtained from Dr. Anthony Firulli. CSF1R-Mer-Cre-Mer mice (#019098) and LSL-Kras^{G12D}/+ mice (#008179) were purchased from Jackson Labs. Mice were identified by ear notches or toe clips. Genomic DNA was obtained from tails snips by boiling for 1hr in 50mM NaOH, 2mM EDTA and genotyping was performed with conventional PCR using primers listed in the Appendix. Experimental and control animals were housed together in the same cages. All animal studies were performed with prior approval from the IUSM Institutional Animal Care and Use Committee.

Mouse hematologic analysis

Blood collections were done via tail vein into EDTA-coated tubes (Fisher #NC9628695). Counts were obtained using a HemaVet 950 (Drew Scientific) or Element HT5 (Heska). Blood smears and cytospins were stained using Modified Wright-Giemsa dyes on a Hematek 3000 system (Siemens). For subsequent flow cytometric analysis, up to 60ul of blood was aliquoted into 1ml of Blood Collection Medium (IMDM +10%FBS +1% Pen/Strep + 20U/ml Heparin (Sigma #H3149)).

Timed Matings

Male studs (10-26 weeks of age) were housed in separately and mated after at least 2-3 days of acclimatization to their cage. In the evening one or two female mice (8-26 weeks of age) were moved to the stud cage. The following morning, successful matings were confirmed by visual inspection of a vaginal plug and assigned a gestational age of E0.5.

Embryo Harvests

Pregnant females were euthanized by cervical dislocation followed by bilateral pneumothorax. The abdominal cavity was opened using sterile scissors and forceps. The uterine horns were removed and placed in a petri dish with sterile PBS. The uterine fascia, musculature, and placental tissues were sequentially removed using forceps to expose the YS-enclosed embryo. Embryo age was confirmed by counting somite pairs. Desired tissues were dissected out and placed into collection tubes containing PBS. Tissue digests were performed for 5-30min at 37ºC in 0.2% collagenase D (Sigma #11088866001).

Ex Vivo Culture

All cells were cultured in a humidified incubator at 37ºC, 5% CO_2 in IMDM (Fisher #12440079), 10% FBS (Fisher #SH30070.03), and 100 U/ml P/S (Fisher #15140122). As needed, the culture was further supplemented with 440nM β-Mercaptoethanol (Sigma #M6250), 2mM L-Glutamine (Fisher # 25030-081) and specified concentrations of the following murine cytokines: GM-CSF (Peprotech #315-03), M-CSF (Peprotech #315-02, SCF (Peprotech #), IL-3 (Peprotech #213-13), IL-6 (Peprotech #216-16), TPO (Peprotech #315-14), and Epoetin Alfa (Epogen). BMDM were generated by plating BM cells for 7d in IMDM medium containing 10ng/ml M-CSF. Cells were serum-starved for 16h in plain IMDM prior to stimulation with specified concentrations of cytokine in serum-free medium.

Hematopoietic Cell Isolations

All tissues were kept on ice in PBS +2mM EDTA. Bone marrow cells were flushed from forelimb and hindlimb bones using a 23G of 27G needle. Spleens and thymuses were triturated with glass cover slides. Livers, hearts, and brains were minced with razors and digested at 37ºC in 0.2% collagenase D (Sigma #11088866001), 0.5% Dispase (Fisher # 17105-041) and 50U/ml DNase I (Sigma # 10104159001) for 60min. BM stromal cells were isolated from flushed long bones by crushing with mortar and pestle, and digested as above for 3hrs. All cells were strained through a 70um mesh. Enucleated RBCs were

depleted as necessary using density gradient centrifugation (Sigma #10771) or RBC lysis buffer (Quiagen #158904). As needed, liver and brain suspensions were depleted of parenchymal cells and lipids via centrifugation through a gradient of 37% and 50% Percoll (Sigma #P1644) gradient, respectively.

Flow Cytometry

Cells were stained at a concentration of 1-5 x 10^7/ml in PBS +2% FBS + 2mM EDTA. Antibodies were purchased from Biolegend, eBioscience, or BD Biosciences and required concentrations were determined experimentally. If required, cells were fixed in 1% PFA (Fisher #50-980-487). For cell cycle analysis, stained cells were permeabilized with eBioscience Intracellular Fixation & Permeabilization Buffer Set (#88-8824-00). For Intracellular phosphor-flow, cells were fixed with 1% PFA and permeabilized using BD Perm Buffer III (#558050). Stained cells were analyzed using the BD LSR Fortessa, BD FACS CANTO II, or BD Accuri C6. Post run analysis was performed using FlowJo (Treestar).

Tissue Histopathology

Tissue samples were fixed in 4% PFA, dehydrated with ethanol, cleared with xylenes and embedded in paraffin. 5um sections were cut on a rotary microtome and stained with hematoxylin and eosin.

DNA isolation

Murine tails were digested for 1hr at 95^{o}C in 50mM NaOH + 0.2mM EDTA, vortexed, pelleted, and then diluted to 100mM Tris buffer. Alternatively, DNA was isolated from tissues using the DNeasy Blood & Tissue Kit (Quiagen # 69504).

PCR

The GoTaq Green Master Mix (Promega #M712) was used with primers listed in the Appendix. Reaction products were run out on a 2% agarose gel and strained with ethidium bromide (Sigma # E1510).

Hematopoietic Progenitor Colony Forming Assay

$5x10^4$ BM mononuclear cells were plated in 1ml of 30% methylcellulose in IMDM (Stemcell Technologies #M3120) supplemented with 30% FBS, 2.2% Pen/Strep, 2.45mM L-Glutamine, and 440nM β-Mercaptoethanol (Sigma #M6250) and defined concentration of murine GM-CSF. For inhibitor studies, 100 nM PD0325901 (Selleck Chemicals) solubilized in DMSO was added to methylcellulose media.

Quantitative PCR

mRNA was isolated from 0.5-$10x10^6$ freshly-harvested or previously flash-frozen cells using RNeasy kits (Qiagen #74034 or 74134). cDNA was obtained using the QuantiTect Reverse Transcription Kit (Qiagen #205310). qPCR was run on a 7500 Real-Time PCR System (Applied Biosystems) using a SYBR Green kit (Roche # 4913850001) using 250nM of each primer pair listed in the Appendix.

Transplantations

Adult recipients (8-24wks) were lethally irradiated with 950cGy or 700cGy+400cGy. Within 16hrs, donor cells were adoptively transferred via tail vein in 250ul PBS using a 28G insulin syringe (Fisher #BD 329461). A heat lamp and alcohol swab was used to engorge the vein. Neonatal recipients (2-3d) were sublethally irradiated with 350cGy. Immediately after irradiation, donor cells were adoptively transferred via facial vein or intraperitoneally in 30ul PBS using 30G needle and 0.1ml syringe (Hamilton #1710). Donor cell numbers are listed in Table II-1.

Tamoxifen Treatment

To induce recombinase activity in adult mice 75ug/g tamoxifen (Sigma #T5648), dissolved in sunflower oil, was injected i.p. To induce recombinase activity *in utero,* pregnant dams were injected i.p. with 75ug/g 4-hydroxy tamoxifen (Sigma #H6278) along with 37.5ug/g progesterone (Sigma # P0130). Litters of tamoxifen-treated dams were routinely delivered by C-section and raised by foster females.

Western blots

Protein extracts were obtained by lysing cultured or primary cells for 30min on ice in 50mM HEPES, 150mM NaCl, 10% Glycerol, 1% Triton X100, 1.5mM $MgCl_2$, 1mM EGTA, 100mM NaF, 10mM NaPP, along with a protease inhibitor cocktail containing sodium vanadate, ZnCl2, PMSF, and enzymatic inhibitors (Sigma # 10837091001). Protein lysates were run using SDS-PAGE, transferred to nitrocellulose membranes. Blots were exposed using SuperSignal West Pico Chemiluminescent Substrate (Fisher #34080).

Statistical analyses

P-values were calculated using Graph Pad Prism 7.0. Two-tailed t-tests were used to compare two-variable experiments. Chi-squared analyses were used to compare birth ratios. Survival analyses were performed by Mantel-Cox log-rank tests. Two-way ANOVA analyses were used to compare changes in variables over time. All error bars represent S.E.M. Notation of statistical significance: * p-value<0.05; ** p-value<0.01; *** p-value<0.001; n.s. not significant.

Results

A. HSC-Independent Disease Manifestations of PTPN11^{D61Y}

We hypothesized that *in utero* expression in early development of the PTPN11^{D61Y} JMML-initiating mutation would result in the rapid onset of MPN in mice. To test this hypothesis we evaluated the mutation's effect on isolated *in utero* hematopoietic progenitors. The expression of VavCre in fetal liver HSCs is well documented (Chen et al. 2009). VavCre; PTPN11^{D61Y} mice were viable and born at expected Mendelian ratio (Figure II-1A). They developed leukocytosis and monocytosis before 8 weeks of age, indicative of early-onset MPN (Figure II-1B). This early onset suggested that hyperactive *RAS-ERK* signaling may be contributing to disease emergence in these animals. To test this notion, we plated FL cells in methylcellulose colony forming assays at increasing doses of GM-CSF. VavCre;PTPN11^{D61Y} mutant cells showed marked increase in colony formation at low cytokine doses compared with cells from littermates (Figure II-1C). Additionally, FL cells differentiated into myeloid cells demonstrated elevated phosphorylation of ERK both at baseline and following 30min stimulation with 5ng/ml GM-CSF (Figure II-1D). These findings confirm that FL progenitors in VavCre;PTPN11^{D61Y} animals demonstrate GM-CSF hypersensitivity and *RAS-ERK* hyperactivation; two defining features of JMML.

E14.5 fetal livers contain progenitors from both embryonic and fetal phases. As such, our results could not determine whether HSC-independent progenitors from the embryonic phase demonstrated JMML-like features. Therefore, we isolated cells from E9.5 yolk sacs, a full day prior to the emergence of the first HSC. We confirmed that VavCre labels the majority of hematopoietic cells, including Ter119- CD45+ CD41+ cKit+ EMPs, in the E9.5 YS (Figure II-2A). Progenitors from mutant YS at this time also demonstrated GM-CSF growth hypersensitivity in colony forming assays and had greater RAS-ERK signaling following cytokine stimulation compared to littermate controls (Figure

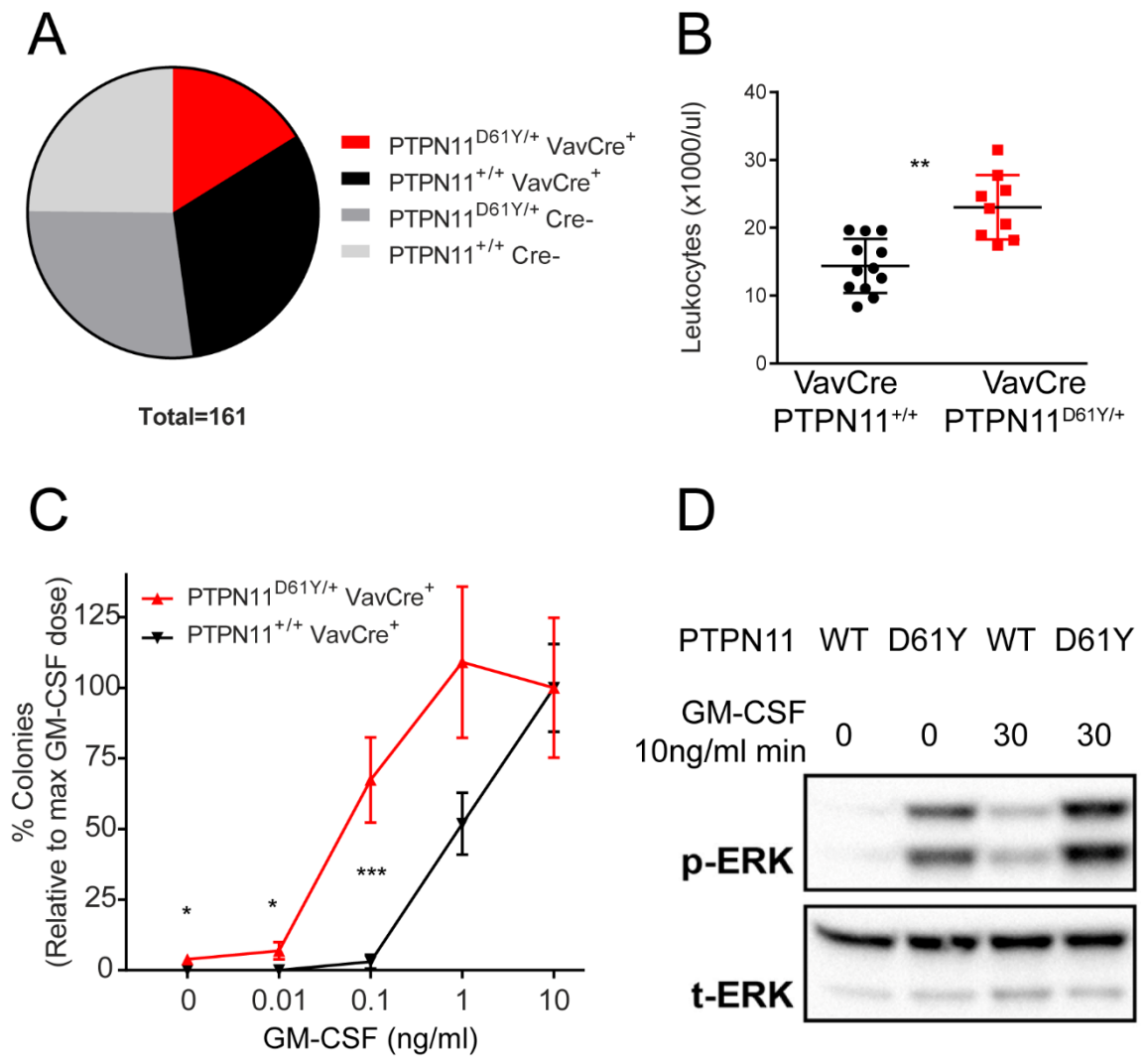

Figure II-1. VavCre+;PTPN11$^{D61Y/+}$ Mice Have Defined Features of JMML. A) Genotype ratios at weaning of VavCre+ x PTPN11$^{D61Y/+}$ matings; Chi-Squared p-value=0.04. B) Leukocyte counts at 8 weeks of age. C) Methylcellulose colony forming assays from E14.5 fetal liver cells. D) M-CSF cultured fetal liver cells were stimulated for 30min with 10ng/ml GM-CSF and lysates were probed with indicated antibodies.

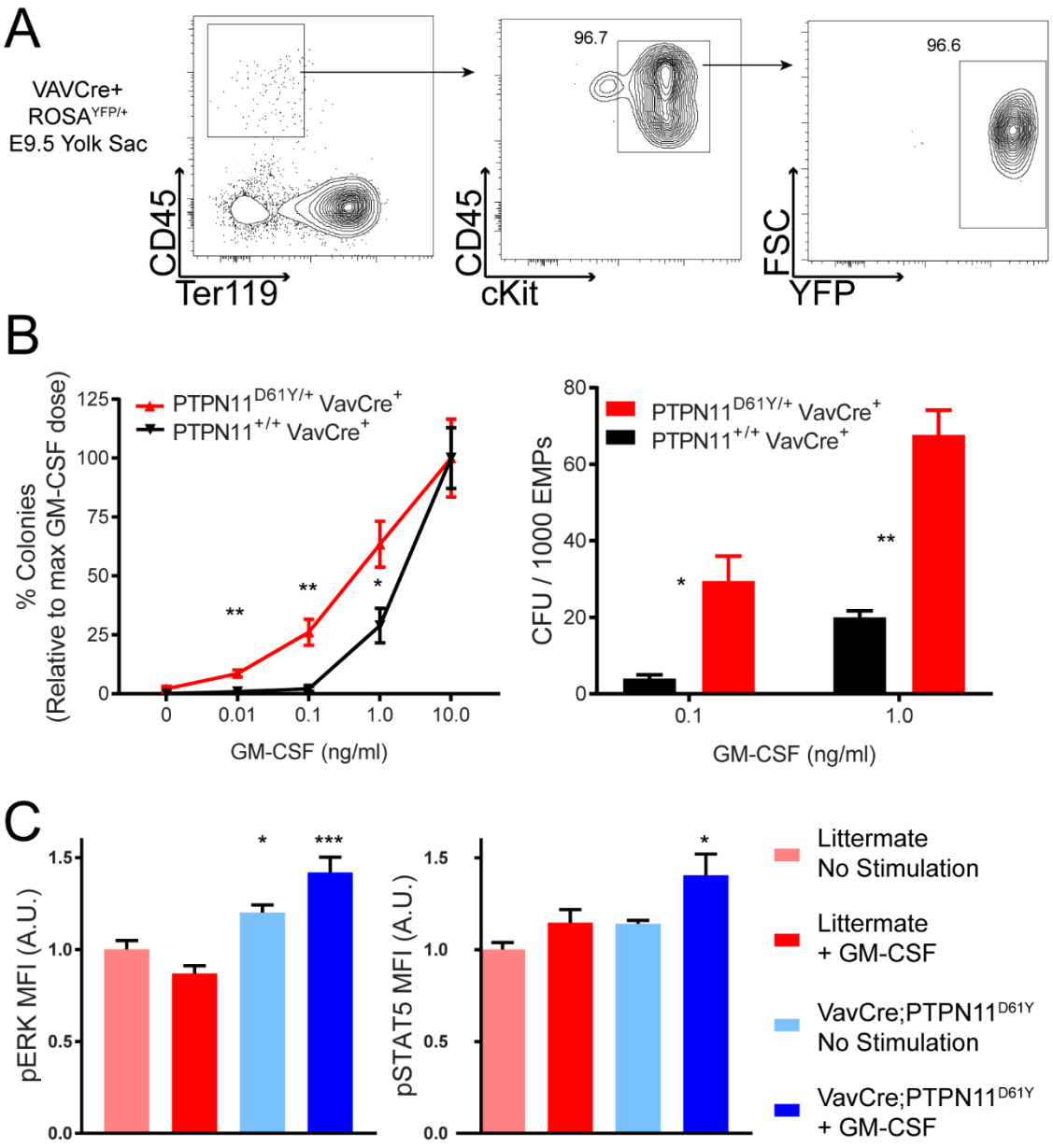

Figure II-2. Yolk Sac EMPs from VavCre+;PTPN11$^{D61Y/+}$ Mice Have Defined Features of JMML. A) VavCre is active in E9.5 YS EMPs (representative gating of 2 litters). B) Methylcellulose assay with E9.5 yolk sac unfractionated cells or sorted Ter119- cKit+ CD41^{dim} EMPs (N=8 unfractionated litters and 2 sorted litters). C) pERK and pSTAT5 signaling in M-CSF cultures of E9.5 YS progenitors following 30min of 5ng/ml GM-CSF stimulation (N=5 biological replicates/group from 2 independent experiments).

II-2B-C). These results confirmed that JMML disease-defining mutations cause features of MPN in HSC-independent progenitors. The presumptive YS progenitor targeted by the mutation was the erythromyeloid progenitor (EMP), which is the dominant myeloid progenitor in the YS at this developmental stage (McGrath et al. 2015). To confirm, we sorted Ter119- cKit+ $CD41^{dim}$ EMP progenitors from mutants and littermates and plated them in colony forming assays. Mutant EMPs produced greater numbers of colonies at the tested concentrations of GM-CSF (Figure II-2B). This proved that the EMP is the YS progenitor responsible for the observed JMML features in the YS of VavCre;$PTPN11^{D61Y}$ animals.

Nearly all JMML patients undergo HSC transplantation as first-line therapy. Half of these treated patients will relapse and will require a second transplant (Locatelli and Niemeyer 2015). Since the therapeutic efficacy of HSCT in JMML patients is significantly inferior to that of pediatric leukemias, we reasoned that long-lived HSC-independent hematopoietic cells may contribute to disease relapse. The progeny of YS EMPs persist in murine tissues as tissue resident macrophages in the brain, heart, liver, and spleen (Epelman et al. 2014; Gomez Perdiguero et al. 2015; Schulz et al. 2012; Hoeffel et al. 2015). Under non-inflammatory conditions, these macrophages self-renew independently of HSC contributions. Furthermore, they are relatively resistant to myeloablation in the setting of transplantation (Hashimoto et al. 2013). Complementary studies in humans have demonstrated that macrophages and dendritic cells also resist replacement by donor cells following transplantation (Haniffa et al. 2009). These findings suggest the tantalizing possibility that JMML mutations in YS progenitors may persist in tissue resident myeloid cells and contribute to disease relapse in children following HSCT.

We therefore hypothesized that VavCre;$PTPN11^{D61Y}$ mice would relapse following transplantation with healthy donor BM cells. We reasoned this relapse would occur due to poor donor engraftment resulting from a hyperinflammatory niche caused by ablation-

resistant and mutation-expressing YS-derived macrophages. We transplanted 12-24week old lethally irradiated mutant and littermate animals (CD45.2+) with $5x10^5$ heathy congenic CD45.1+ BM cells (Figure II-3A). We were surprised to observe that healthy donor cells engrafted more readily in mutant recipients that in control recipients (Figure II-3B). Furthermore, the engrafted cells preferentially gave rise to CD11b+ myeloid cells and to fewer CD3+ T-lymphocytes (Figure II-3C). Despite this robust engraftment, mutant recipient mice rapidly succumbed after transplantation, with a mean survival of 16 weeks (Figure II-3D).

We hypothesized that the increased engraftment in our mutant animals stemmed from enhanced proliferation of healthy lineage-committed progenitors. This enhanced cycling may have been due to abnormal signaling cues in the mutants' microenvironment. We reasoned that, as reported in pediatric transplant studies, a saturating dose of donor cells would improve the survival of our mutant recipients by diminishing the proliferative requirements of the donor cells (Kalwak et al. 2010). We therefore repeated the transplantation with $1x10^7$ donor cells (Figure II-4A). In this setting no difference in donor chimerism was observed between mutant and littermate recipients (Figure II-4B). Furthermore, donor cells gave rise to myeloid, B, and T cells with equivalent frequencies in both groups (Figure II-4C). Nonetheless, mutant recipients had a mean survival of only 18 weeks following transplantation (Figure II-4E).

At analysis, moribund mutant recipients had a hypercellular BM with an effacement of the normal splenic follicular architecture (Figure II-5A). Blast-like cells were observed in the peripheral blood and mutant recipients had larger spleens than littermates. We were surprised, however, to find markedly enlarged thymuses in moribund mice. Subsequent immunophenotye analysis confirmed that both the BM and spleen were filled with recipient CD45.2+ CD4+ CD8+ abnormal T-lymphocytes (Figure II-5B). Transplantations of BM or spleen cells from HSCT-treated mutants into BoyJ recipients confirmed that the CD45.2+

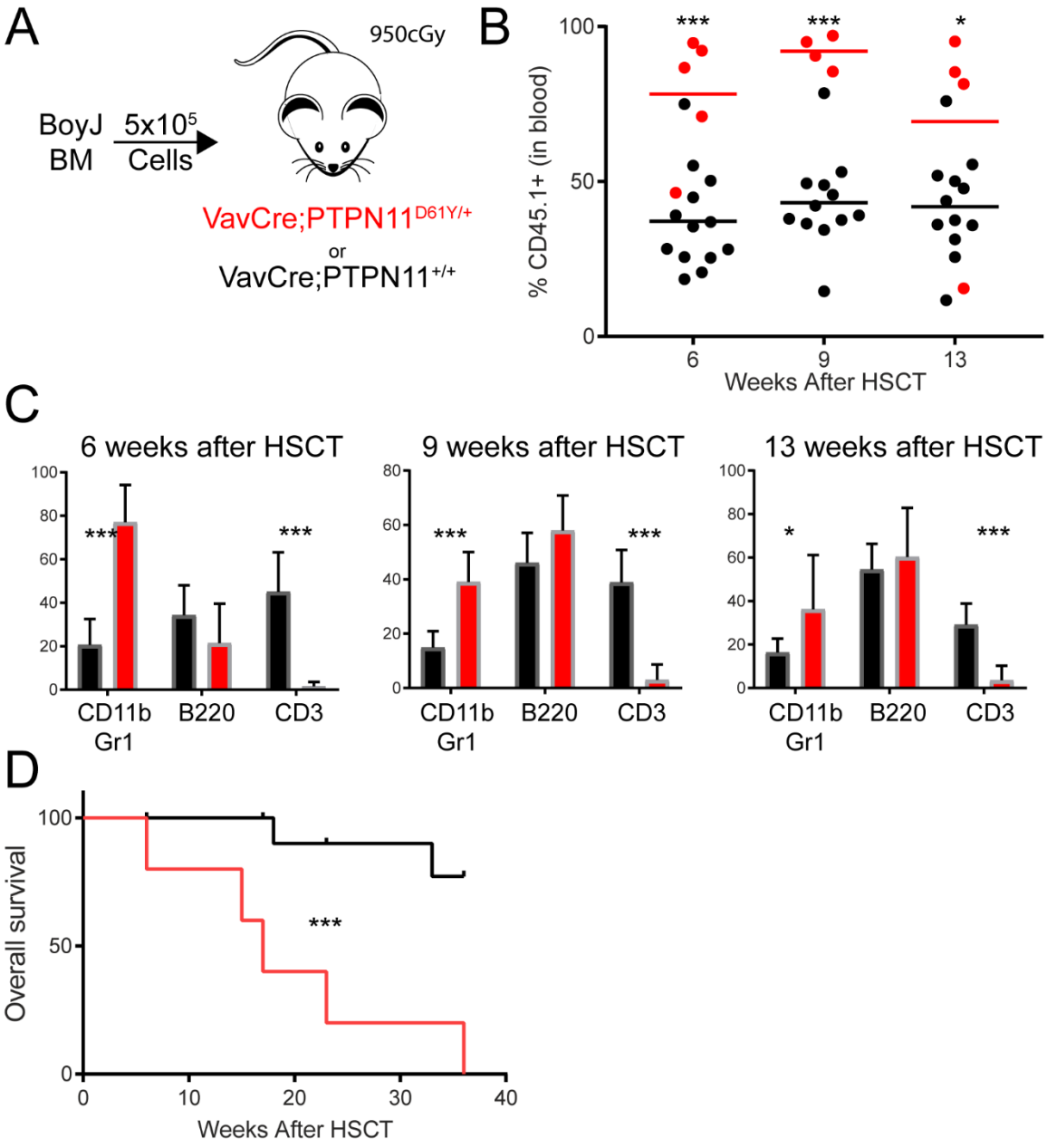

Figure II-3. HSCT of VavCre+;PTPN11$^{D61Y/+}$ Mice with 5x10^5 Healthy Donor Cells. A) Schematic of transplant. B) Donor engraftment in blood at indicates times after transplant. C) Analysis of lineages produced by engrafted cells at indicated times after transplant. D) Overall survival of mutant and control recipients following healthy donor HSCT (N=5 mutant and 13 control recipients).

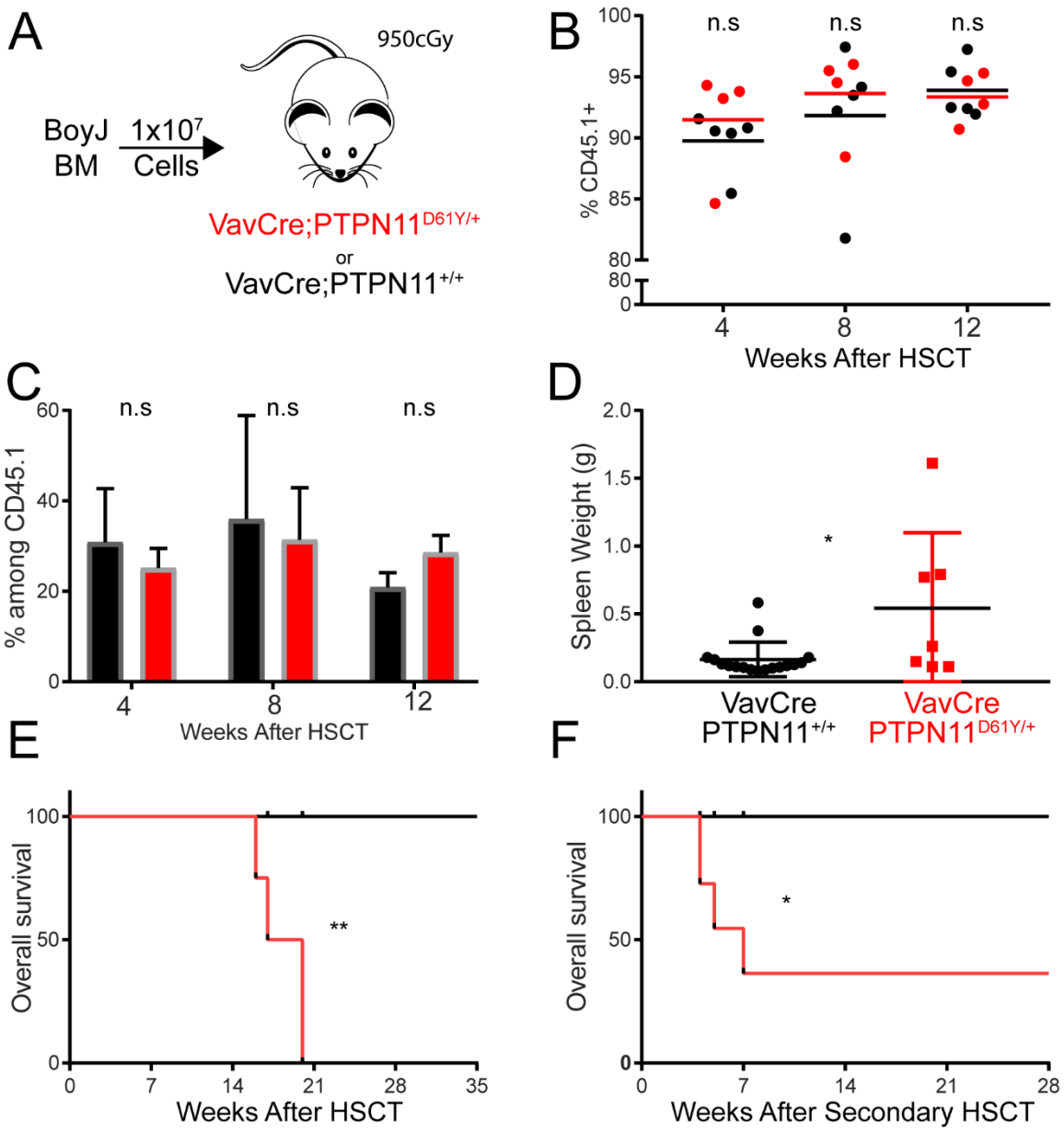

Figure II-4. HSCT of VavCre+;PTPN11$^{D61Y/+}$ Mice with 1x10^7 Healthy Donor Cells. A) Schematic of transplant. B) Donor engraftment in blood. C) Donor contribution to CD11b+ cells D) Spleen weights at analysis of mutant and control recipients (pooled from 5x10^5 and 1x10^7 donor cohorts). E) Overall survival of animals transplanted with 1x10^7 healthy donor cells (N=4 mutants, 5 controls). F) Survival of animals transplanted with 2x10^6 BM or 4x10^6 spleen cells from moribund mutant primary recipients or healthy control primary recipients (N=7 mutant donors and 5 control donors).

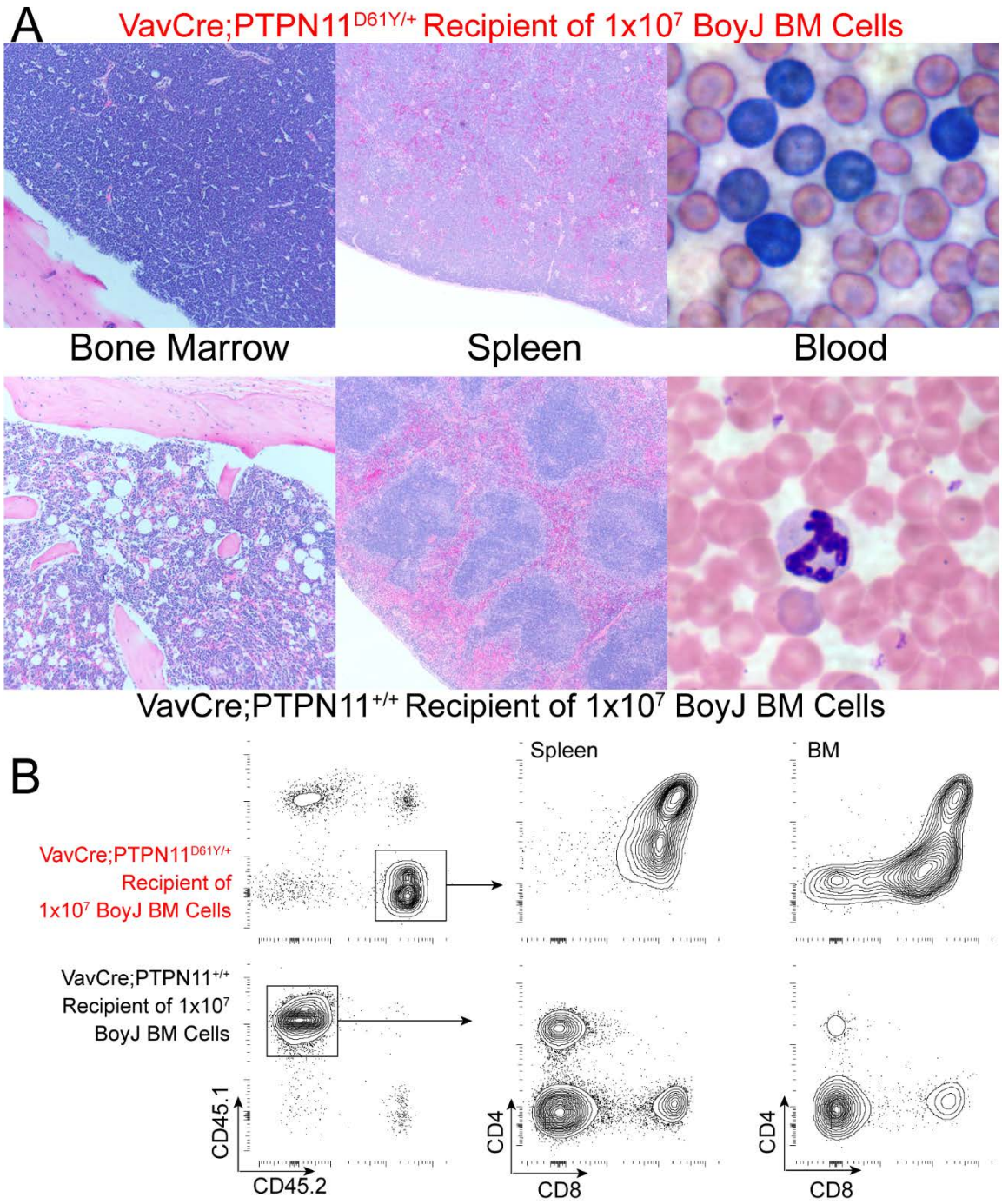

Figure II-5. VavCre+;PTPN11$^{D61Y/+}$ Recipients Die of Host-Derived T-ALL. A) Immunohistochemistry of BM, spleen, and blood of mutant and littermate transplant recipients. B) Representative flow cytometry of CD45.2+ host-derived abnormal T-lymphocytes in the BM and spleen of mutant recipients.

T-ALL disease could be propagated and was neoplastic (Figure II-4F). From these experiments we concluded that healthy donor cells could efficiently engraft mutant recipients and preferentially gave rise to myeloid progeny. Despite this robust engraftment, mutants died after transplantation due to the emergence of a recipient-derived T-ALL This relapsed disease could be propagated via transplantation and could not be prevented with a saturating dose of healthy donor cells.

B. Insights from the VavCre;PTPN11^{E76K} JMML model

The PTPN11^{D61Y} murine model has indolent disease progression. We reasoned that a different JMML-associated PTPN11 mutation that causes more rapid disease onset would aid our studies. The PTPN11^{E76K} model fit this criteria. The mutation is functionally similar to PTPN11^{D61Y}; both target the N-terminal SH2 domain and prevent its inhibition of the PTP catalytic domain (Loh et al. 2004). As such, both PTPN11^{E76K} and PTPN11^{D61Y} mutations enable constitutive phosphatase activity. However, PTPN11^{E76K} murine models succumb to disease more rapidly than PTPN11^{D61Y} models (Xu et al. 2011). Additionally, the PTPN11^{E76K} mutation has been documented to occur *in utero* (Matsuda et al. 2010). We therefore hypothesized that repeating our studies with the more potent PTPN11^{E76K} mouse model may permit emergence of disease manifestations that had been masked in our PTPN11^{D61Y} model.

Sorted EMPs from E10.0 VavCre;PTPN11^{E76K} YS demonstrated GM-CSF growth hypersensitivity, again showing embryonic progenitors can have features of JMML (Figure II-6B-C). Surprisingly, when we mated VavCre mice with PTPN11$^{E76K/+}$ mice we did not get viable VavCre;PTPN11^{E76K} progeny (Figure II-7A). Analyses of E10.5 embryos showed mutants were smaller, less developed, and had a pale YS and AGM region (Figure II-7B). Subsequent analysis of E17.5 embryos confirmed that VavCre;PTPN11^{E76K} embryos were dying *in utero.* These findings were surprising given that JMML patients

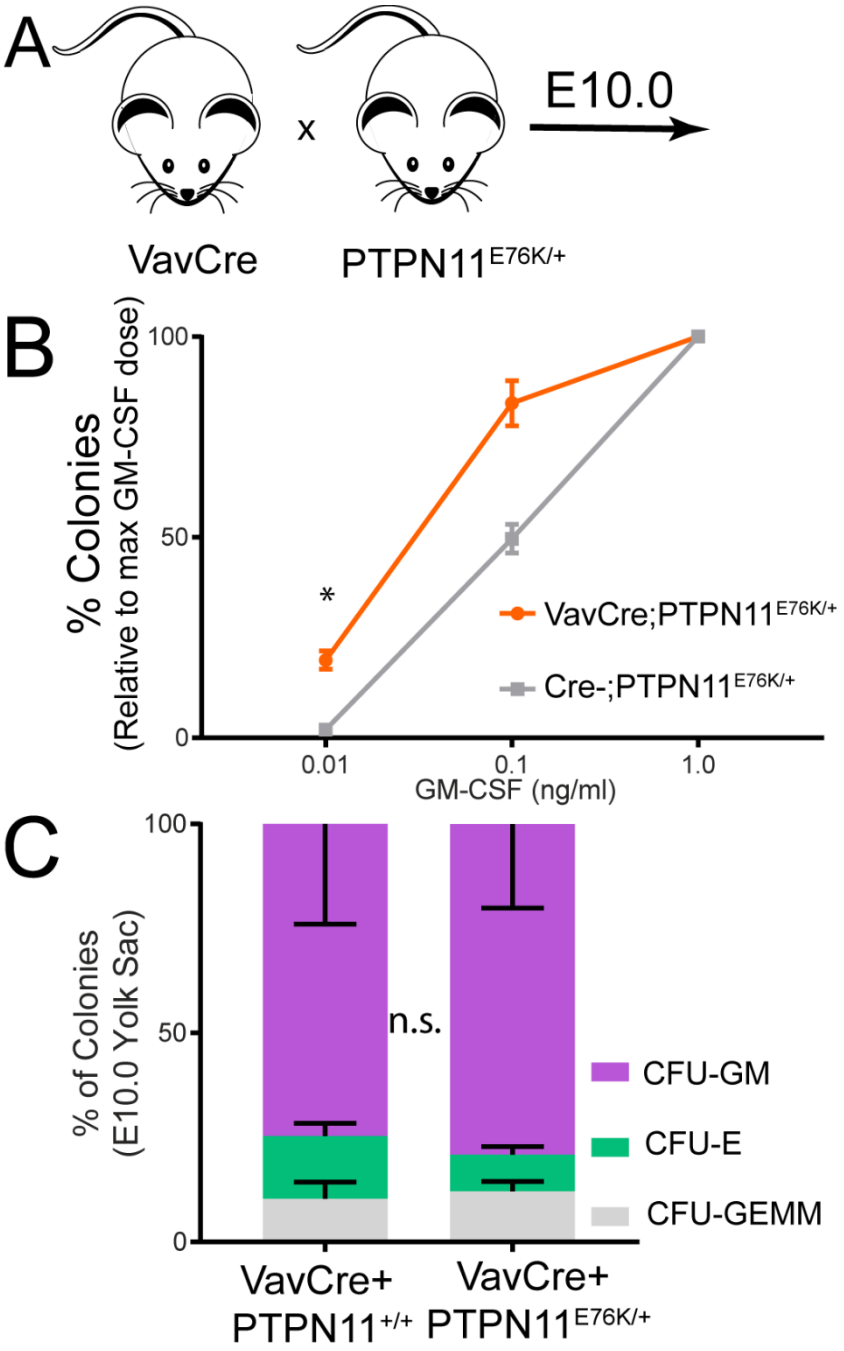

Figure II-6. EMPs from E10.0 VavCre+;PTPN11$^{E76K/+}$ Yolk Sacs Are Hypersensitive to GM-CSF. A) Mating strategy. B) Colony formation from sorted Ter119- cKit+ CD41^{dim} E10.0 YS EMPs (n=4 embryos/group from 2 litters). C) Methylcellulose colony differentiation of mutant and littermate YS progenitors (N=3 litters).

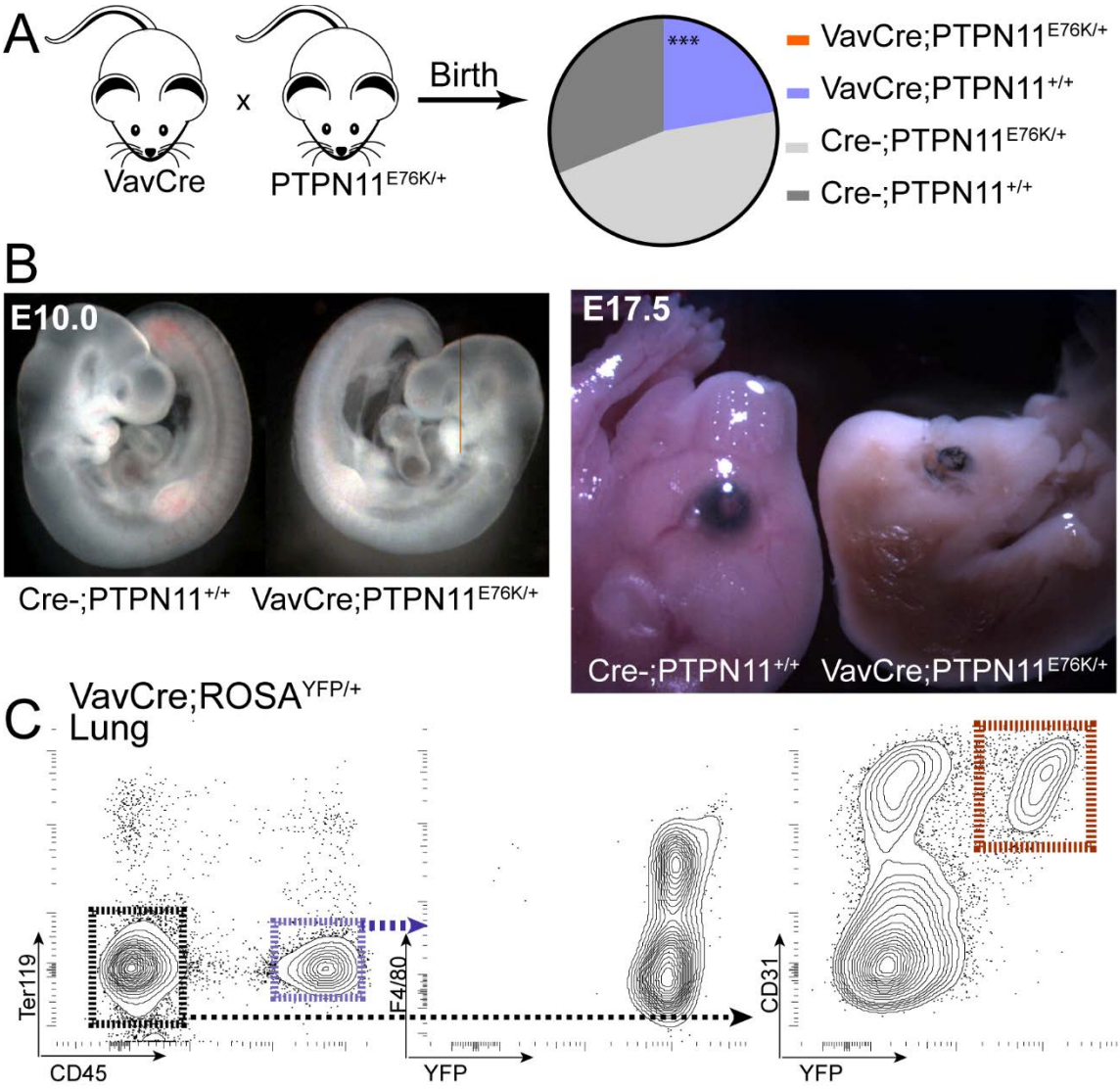

Figure II-7. VavCre+;PTPN11$^{E76K/+}$ Mice Die *In Utero* with Non-Hematopoietic Oncogene Expression. A) Genotype ratio of animals weaned from VavCre(Croker *et al*) x PTPN11$^{E76K/+}$ matings (N=45 births). B) Representative images of E10.0 and E17.5 embryos. F) Representative flow cytometric analysis of VavCre;ROSA$^{YFP/+}$ lung, demonstrated highly efficient VavCre activity in both CD45+ F4/80+ macrophages and CD45- Ter119- CD31+ endothelial cells (gated in red) (experiment performed with Yang Lin).

can acquire their somatic PTPN11 mutations before birth (Matsuda et al. 2010; Kratz et al. 2005). Furthermore, other groups had previously shown VavCre;PTPN11^{E76K} mice to be viable and live into adulthood (Liu et al. 2016; Dong et al. 2016). This prompted us to more closely characterize the identity of the model we were using.

We discovered that there are at least 4 distinct versions of the VavCre strain, each with different expression patterns (de Boer et al. 2003; Stadtfeld and Graf 2005; Croker et al. 2004; Georgiades et al. 2002). The de Boer *et al* VavCre animal was used for our PTPN11^{D61Y} studies because it had been bred into the mixed background of these animals. The original characterization of this strain showed that in addition to hematopoietic expression, the de Boer VavCre also labelled the testis and ovaries. As such, the expression could have been transmitted through the germline and subsequently expressed in other lineage, including endothelium. The Croker *et al* VavCre was used in our matings with PTPN11^{E76K} mice because both were available on a pure C57B6 background. Its initial characterization documented expression in the endothelium as did the Georgiades P *et al* strain. We independently confirmed that this strain labels lung CD45- Ter119- CD31+ endothelial cells (Figure II7-C).

The studies that produced viable VavCre;PTPN11^{E76K} animals used the animal developed by Stadtfeld M & Graf T. Of the four available strains this is the only one whose expression appears limited to hematopoietic cells. Indeed, studies that sought to induce mutations after the endothelial to hematopoietic transition have relied on this strain (Chen et al. 2009). Even so, personal communications to our lab suggests that careful curation of animals is required to achieve this specificity.

Despite the *in utero* lethality, EMPs from VavCre;PTPN11^{E76K} animals at E10.0 gave rise to a normal distribution of BFU-E, CFU-GM, and CFU-GEMM colonies (Figure II-6C). Since it was not possible to monitor their contribution to disease in host animals, we performed transplantation experiments to determine their potential to give rise to

disease in recipients (Figure II-8A). We transplanted 1 embryo equivalent (e.e.) FACS-sorted EMPs from E10.5 yolk sac cells from VavCre;PTPN11^{E76K} mice i.v. into 150cGy sublethally irradiated neonatal NOD.Cg-*Prkdc*^{scid} *Il2rg*^{tm1Wjl}/SzJ (NSG) CD45.1+ recipients. We also transplanted CD45- Ter119- cKit+ VECadherin+ hemogenic endothelial populations from the YS and AGM of the same embryos. Prior work has demonstrated that this model is uniquely capable of supporting YS progenitor engraftment (Yoder et al. 1997; Yoder and Hiatt 1997; Johnson and Yoder 2005; Yoshimoto et al. 2010; Yoshimoto et al. 2012; Arora et al. 2014). Nonetheless, we did not observe peripheral blood engraftment or elevated leukocytes in neonatal recipients of either YS or AGM cells (Figure II-8B). This was consistent with recent studies that showed purified YS EMPs did not contribute to the circulation of neonatal recipients (McGrath et al. 2015). NSG animals are immune compromised and prone to infections. Our recipient animals became moribund due to presumed C. Bovis infection and were euthanized for humane reasons per the directions of the IUPUI LARC veterinary staff.

At analysis, we were surprised to discover that donor EMPs had engrafted in recipient spleens as F4/80^{+} CD11b^{dim} macrophages (Figure II-8C. The engraftment of splenic macrophages was more robust in recipients of YS EMPs than of AGM VECad+ cells. Notably, whereas the most prominent progeny of YS EMPs in unperturbed animals are microglia, we did not detect any CD45.2+ cells in the brains of YS recipients (Figure II-8D). These results are consistent with previous studies that showed differences in progenitor differentiation under native and transplant settings (Boyer et al. 2011; Beaudin et al. 2016; Busch et al. 2015). This highlights the pitfalls of models that rely on transplantation, which identify progenitor potentials under non-native conditions (Busch and Rodewald 2016; Hofer et al. 2016; Schlenner and Rodewald 2010; Feil et al. 2014). These results made it clear that evaluating the contribution of distinct hematopoietic phases to JMML would not be feasible using the VavCre model.

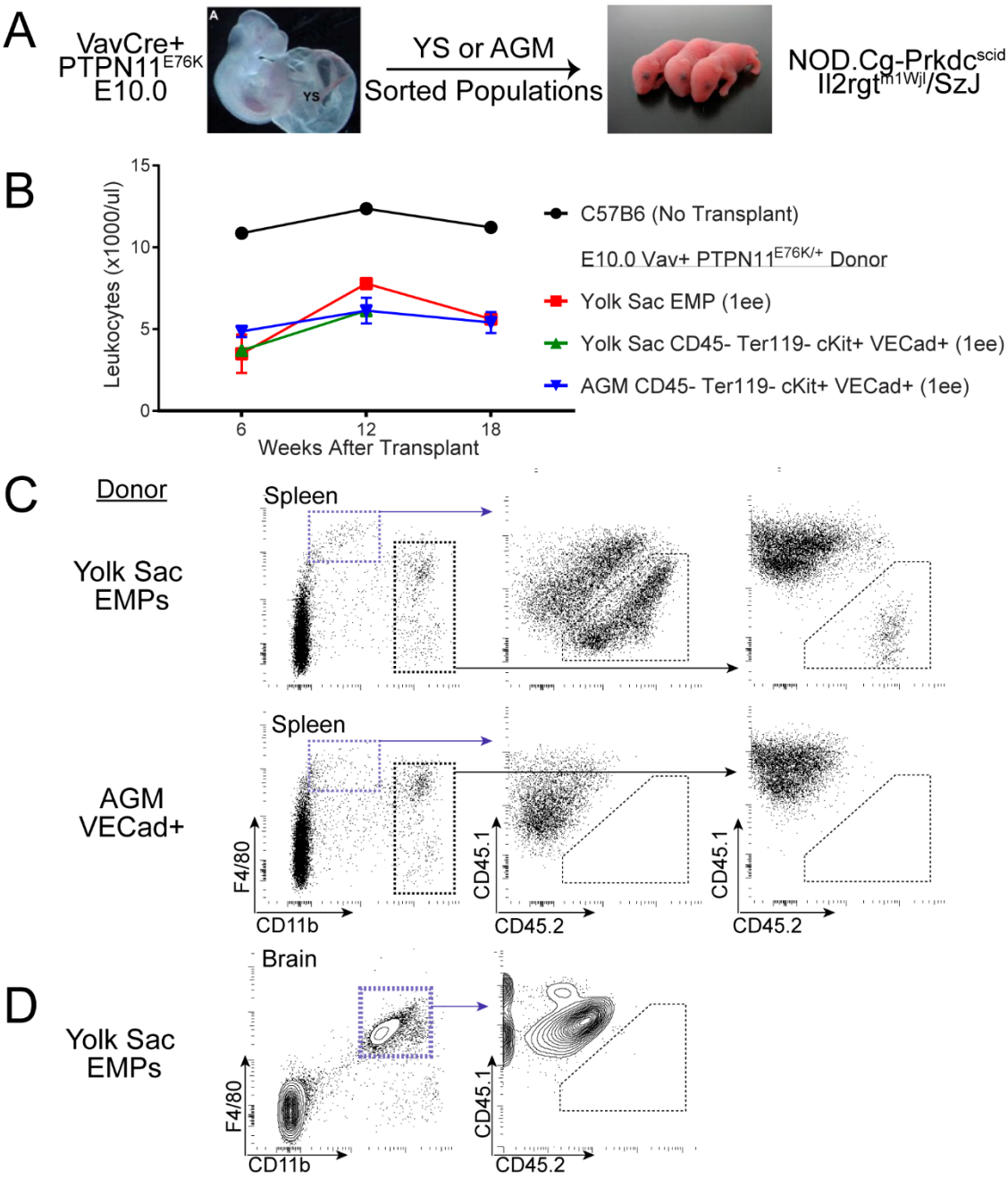

Figure II-8 Neonatal Transplantation with Embryonic VavCre;PTPN11^{E76K} Populations. A) Schematic of transplantations. Recipients were conditioned with 150cGy. B) Leukocyte counts of indicated recipients (N=2 recipients/group). C) Representative gating of YS EMP-derived splenic F4/80+ CD11b^{dim} macrophages in neonatal recipients. D) YS EMPs do not contribute to microglial populations in engrafted animals. (Experiment performed with assistance from Dr. Momoko Yoshimoto).

C. CSF1R-MER-Cre-MER: A Hematopoietic-Restricted and Phase-Specific Model

We set out in search of a new Cre strain that could model JMML with the $PTPN11^{E76K}$ mutation. Our criteria for this strain were as follows: i) Hematopoietic-restricted Cre expression; ii) Well-defined expression within the hematopoietic phases; iii) The ability to monitor which cells express the mutation using a fluorescent marker; and iv) low level expression that would emulate the clonal nature of JMML We ultimately chose to use the CSF1R MER-Cre-MER system (Figure II-9A) (Qian et al. 2011). Therein, the expression of the Cre recombinase occurs in cells that actively transcribe the CSF1R (M-CSF Receptor) gene. The N- and C-terminal ends of the Cre enzyme are linked to mutated estrogen receptor (MER) domains, which prevent the translocation of the enzyme to the nucleus. Only following the administration of tamoxifen and its hepatic conversion to the active 4-hydroxy tamoxifen (4-OHT) metabolite will the MER domains acquire nuclear-localizing signals (Zhang et al. 1996). Then the MER-Cre-MER enzyme can bind to loxP sites, remove intervening DNA sequences through recombination, and permit the expression of desired genes. The recombination reaction is irreversible: once an allele is recombined in a progenitor then all of its progeny will also have a recombined allele. Nonetheless, the half-life of tamoxifen is approximately 24h (Wilson et al. 2014). Thereafter, the metabolite dissociates from the MER domains, whose localization once again becomes restricted to the cytoplasm—preventing Cre activity. Therefore, there is only a narrow window of time following tamoxifen administration in which recombination is possible in the CSF1R MER-Cre-Mer stain. As such, by timing the administration of tamoxifen we reasoned we would be able to specifically target each individual phase of hematopoiesis (Figure II-9B).

Indeed, seminal lineage-trace studies demonstrated that E8.5 4-OHT administration would uniquely label YS EMPs in CSF1R-MCM;$ROSA^{YFP}$ embryos (Schulz et al. 2012; Gomez Perdiguero et al. 2015). No labelling of fetal liver HSCs, adult HSCs,

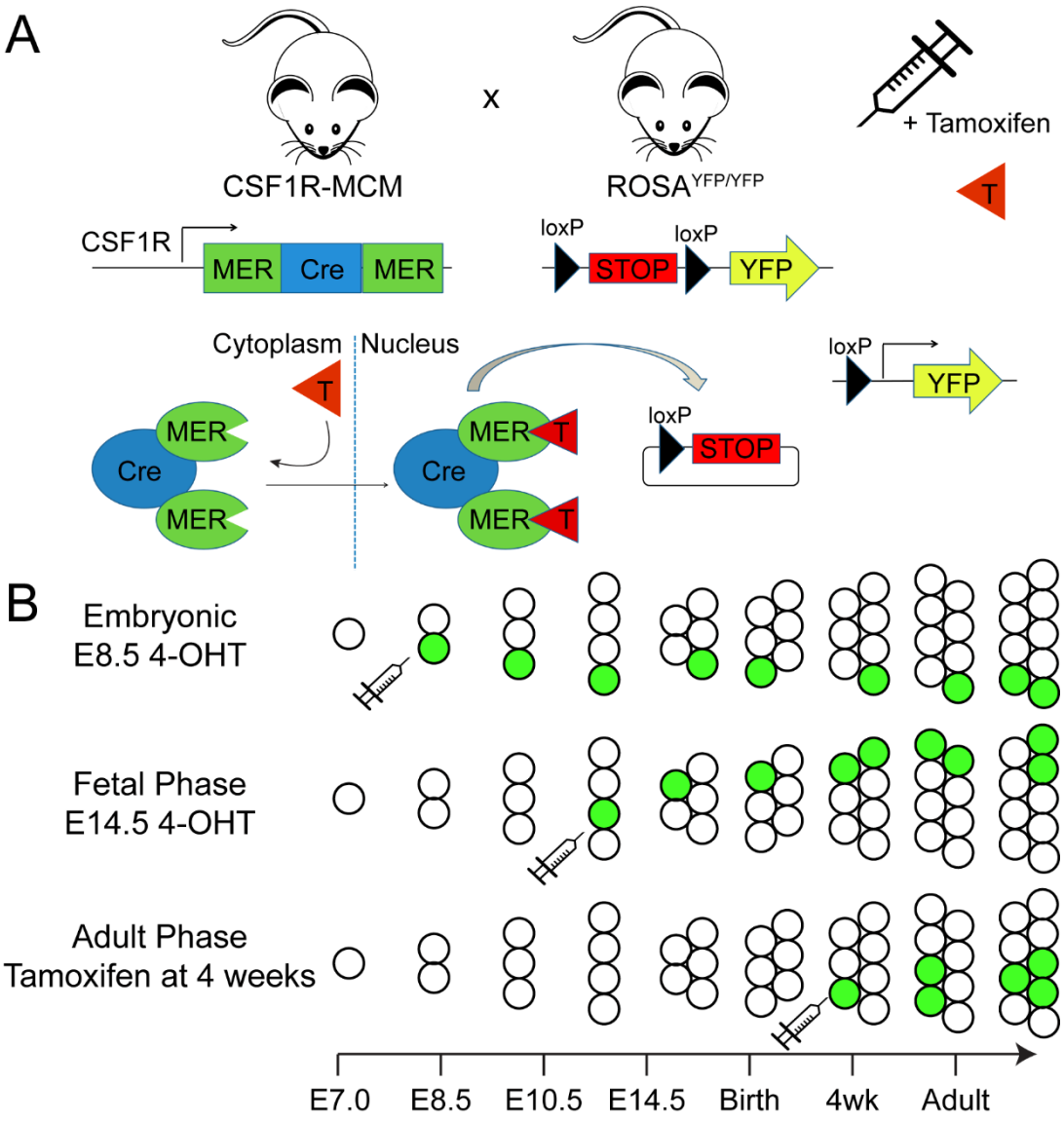

Figure II-9. The CSF1R MER-Cre-MER System. A) Tamoxifen administration permits Cre activity as measured by expression of the YFP fluorescent protein. Tamoxifen binds the MER domains and permits nuclear localization of the MER-Cre-MER enzyme. Cre recognizes the loxP sites, removes the intervening DNA sequence containing the STOP cassette, and thereby permits expression of YFP. B) Timing the administration of tamoxifen permits targeting Cre activity to the three phases of hematopoiesis. MER=mutated estrogen receptor; T, TAM=tamoxifen; 4-OHT=4-hydroxy tamoxifen; YFP=yellow fluorescent protein.

or adult peripheral blood cells was observed. Additional studies that administered tamoxifen in adulthood suggested that tumour-associated myeloid cells were uniquely labelled (Qian et al. 2011). However, these studies restricted their analysis to peripheral tissues and to one week after injection. Personal communication with the authors (J.W.P. and B-Z .Q.) confirmed that weeks after adult administration of tamoxifen they saw labelling in circulating myeloid, B, and T cells—strongly suggesting that a multipotent progenitor was labelled. As such, we had strong evidence that the CSF1R-MCM model could be used to selectively label HSC-independent as well as both fetal and adult HSC-dependent phases. Furthermore, by tittering the dose of tamoxifen, we would be able to modulate the efficiency of labelling to near-clonal levels. And by breeding the CSF1R-MCM animals to the ROSA26$^{YFP/YFP}$ reporter strain, we would be able to distinguish mutation-expressing YFP+ cells from non-mutated YFP- cells in the same animal (Srinivas et al. 2001).

A note on terminology. We outline below three cohorts of mice that were exposed to tamoxifen at E8.5, E14.5, or at 4 weeks of age. These cohorts had Cre activated in the embryonic, fetal, and adult hematopoietic phases, respectively (see Figure II-9). For simplicity we will name these cohort by phase. For instance, animals born following tamoxifen exposure at E14.5 will be the fetal cohort. As such, we will present embryonic, fetal, and adult cohorts of mutant and control mice. Since all CSF1R-MCM+ animals also possess a ROSA^{YFP} allele, we will shorten our notation. For example: CSF1R MER-Cre-Mer+; PTPN11$^{E76K/+;}$ ROSA$^{YFP/+}$ mice as CSF1R-MCM;PTPN11^{E76K}. Additionally, since these animals have YFP+ and YFP- cells we will refer to the sum of YFP+ and YFP- cells in a tissue as unfractionated cells or as net cells.

D. CSF1R-MCM; PTPN11^{E76K}: Expression within the Embryonic Phase

To generate animals that specifically express gain of function mutations in yolk sac erythromyeloid progenitors (YS EMPs) and their progeny, we performed timed matings between CSF1R-MCM+;ROSA$^{YFP/YFP}$ males and PTPN11$^{E76K/+}$ females (Figure II-10). On E8.5, pregnant dams were injected i.p. with 75ug/g 4-OHT with 37.5ug/g progesterone to mitigate late-term abortions cause by pro-estrogenic effects of tamoxifen. We confirmed that at E9.5 EMPs were labelled with high efficiency and that no labelling was observed in fetal liver HSCs at E14.5 (Figure II-10D). Mutant and littermate YS had comparable frequencies of EMPs and they were labelled with YFP at comparable efficiencies (Figure II-11B,C). However, we did not observe a proliferative advantage in either YFP+ or YFP- EMPs in mutant yolk sacs compared to controls as measured by Ki67 expression (Figure II-12A,C). Furthermore, we did not observe a hyperactive *RAS* signaling in progeny of mutant EMPs following GM-CSF stimulation as measured by pERK expression (Figure II-12B,D).

The lack of cell cycle and signaling differences was attributed to the high proliferative nature of all embryonic progenitors as compared with their adult counterparts. We reasoned that any oncogenic effects of PTPN11^{E76K} mutation would only be manifest in their long-lived tissue macrophage progeny.

We proceeded to generate a cohort of CSF1R-MCM; PTPN11^{E76K} animals whose EMPs had been activated with 4-OHT at E8.5. Despite the co-administration of progesterone, dams frequently experienced late-term abortions. Therefore, the majority of litters were delivered by C-section. Mutants were weaned at a Mendelian frequency of 24% and were physically indistinguishable from littermates (Figure II-13A). We monitored all animals in this embryonic cohort with monthly peripheral blood draws (Figure II-13B-F). As expected, we did not observe YFP+ cells in the peripheral blood. Over a 52week period, we did not observe leukocytosis, anaemia, or thrombocytopenia in mutant animals.

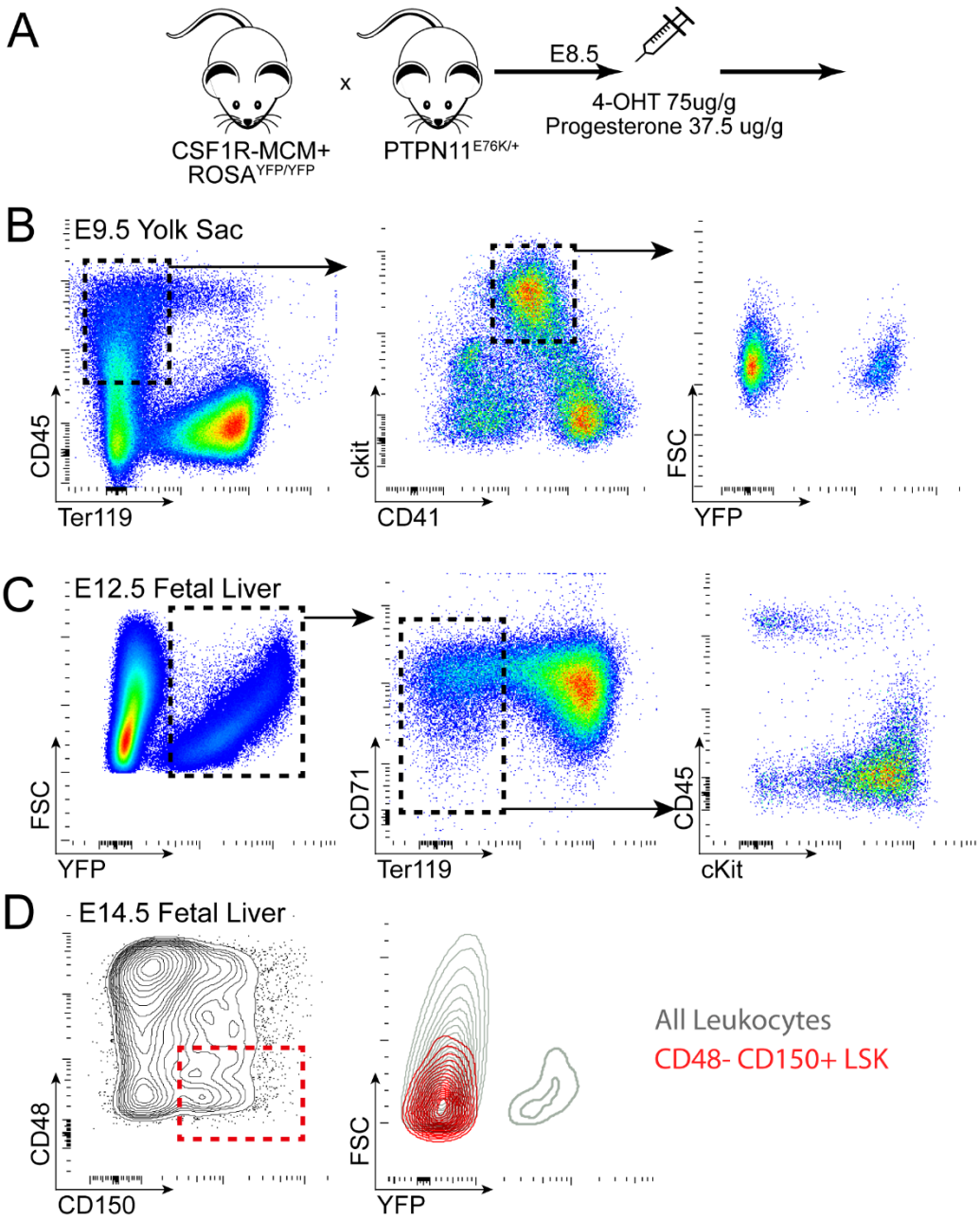

Figure II-10. CSF1R-MCM Labels YS Erythromyeloid Progenitors. A) Schematic of mating strategy and 4-hyroxy tamoxifen (4-OHT) administration to pregnant dams. B) Representative flow gating demonstrating CSF1R-MCM drives ROSA^{YFP} expression in E9.5 yolk sac EMPs (Ter119- CD45+ cKit+ CD41^{dim}). C) Representative gating of CSF1R-MCM (E8.5 4-OHT) contribution to E12.5 fetal liver cells. D) No CSF1R-MCM activity was observed in HSC-dependent fetal liver populations at E14.5.

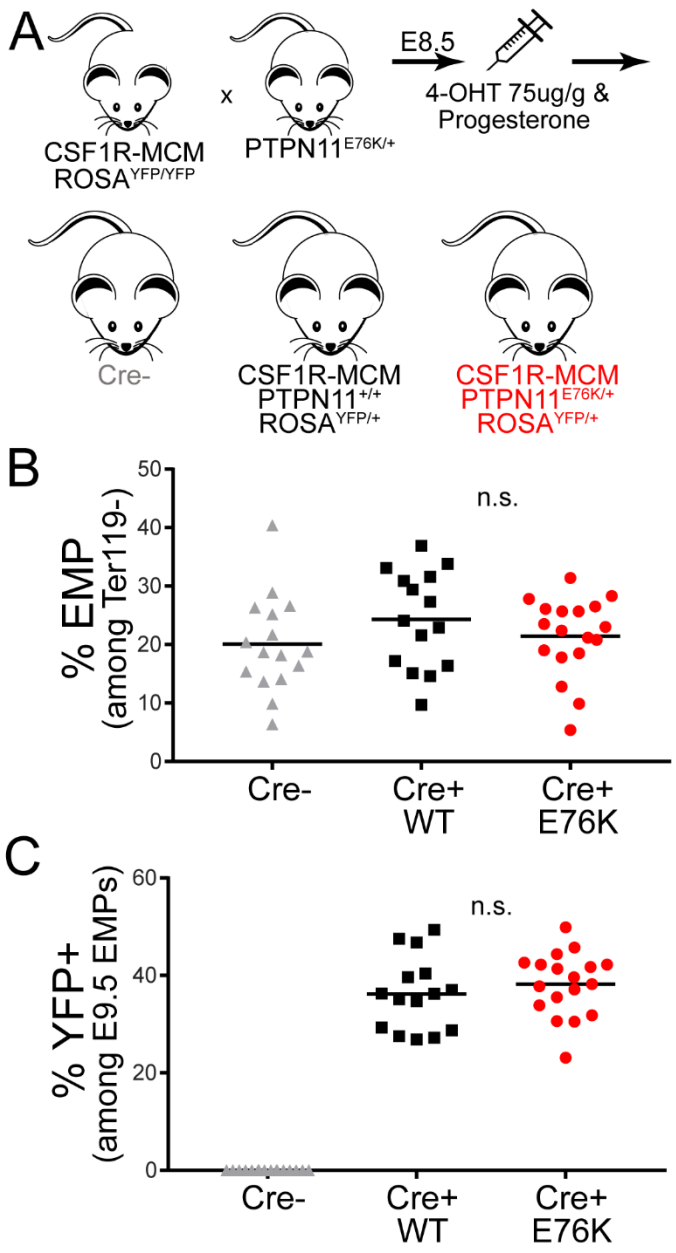

Figure II-11. Embryonic Phase CSF1R-MCM; PTPN11^{E76K}: Yolk Sac EMP Frequency and Labeling Efficiency. A) Legend of analyzed genotypes. B) Frequency of EMPs in E9.5 yolk sacs. C) Proportion of EMPs that are YFP+ following E8.5 4-OHT.

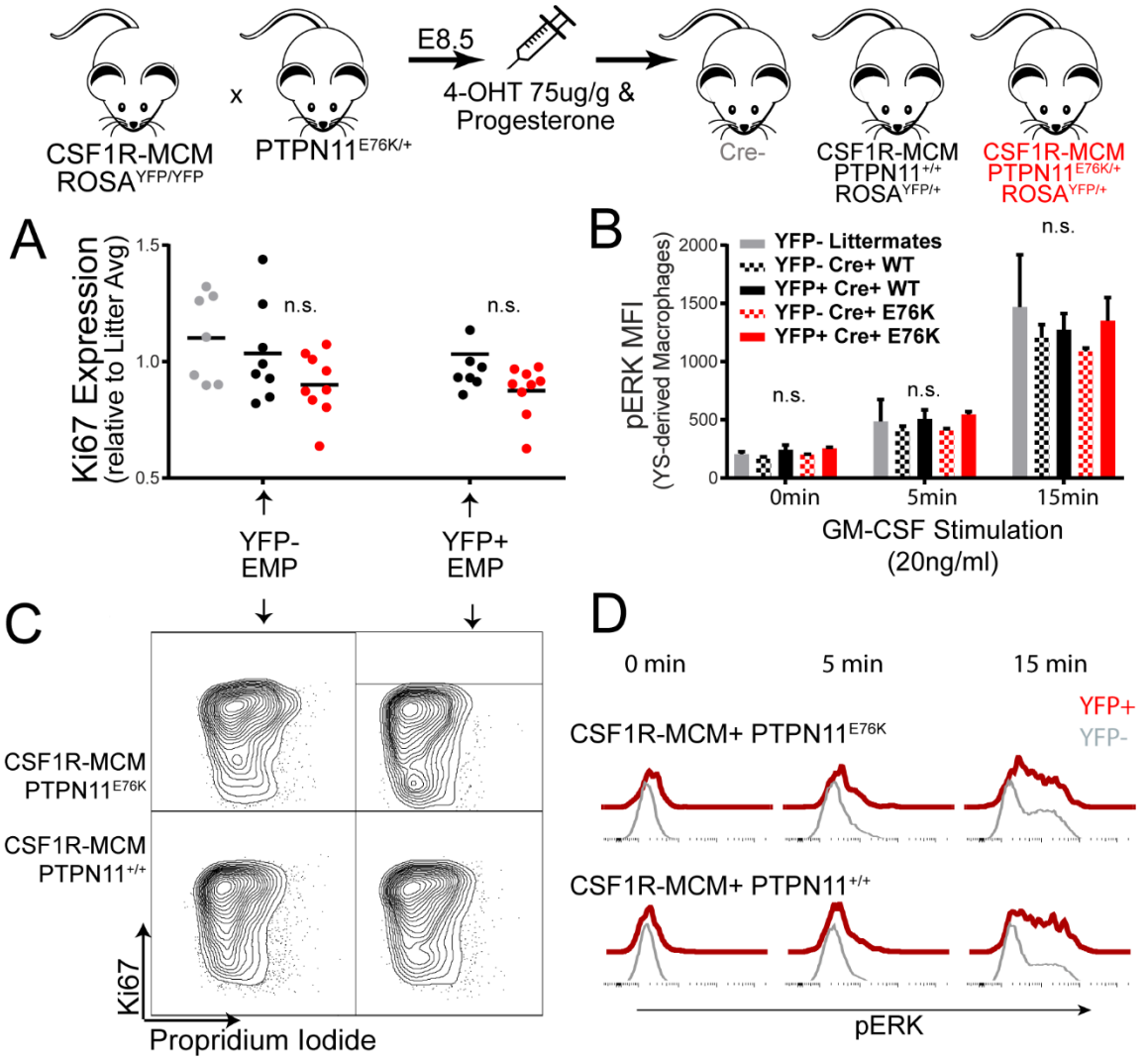

Figure II-12. Embryonic Phase CSF1R-MCM; PTPN11^{E76K}: E9.5 EMP Cell Cycle and Signaling Analysis. A) Ki67 expression in E9.5 yolk sac EMPs (expression normalized to average MFI among EMPs in each litter). B) pERK expression among YS EMP-derived macrophages after stimulation with 20ng/ml. C) Representative cell cycle gating of YFP+ and YFP- YS EMPs from mutant and control yolk sacs. D) Representative gating of pERK expression in YFP+ and YFP- YS-derived macrophages from mutant and control embryos stimulated with 20ng/ml GM-CSF for indicated durations. MFI=mean fluorescence intensity; 4-OHT=4 hydroxy tamoxifen.

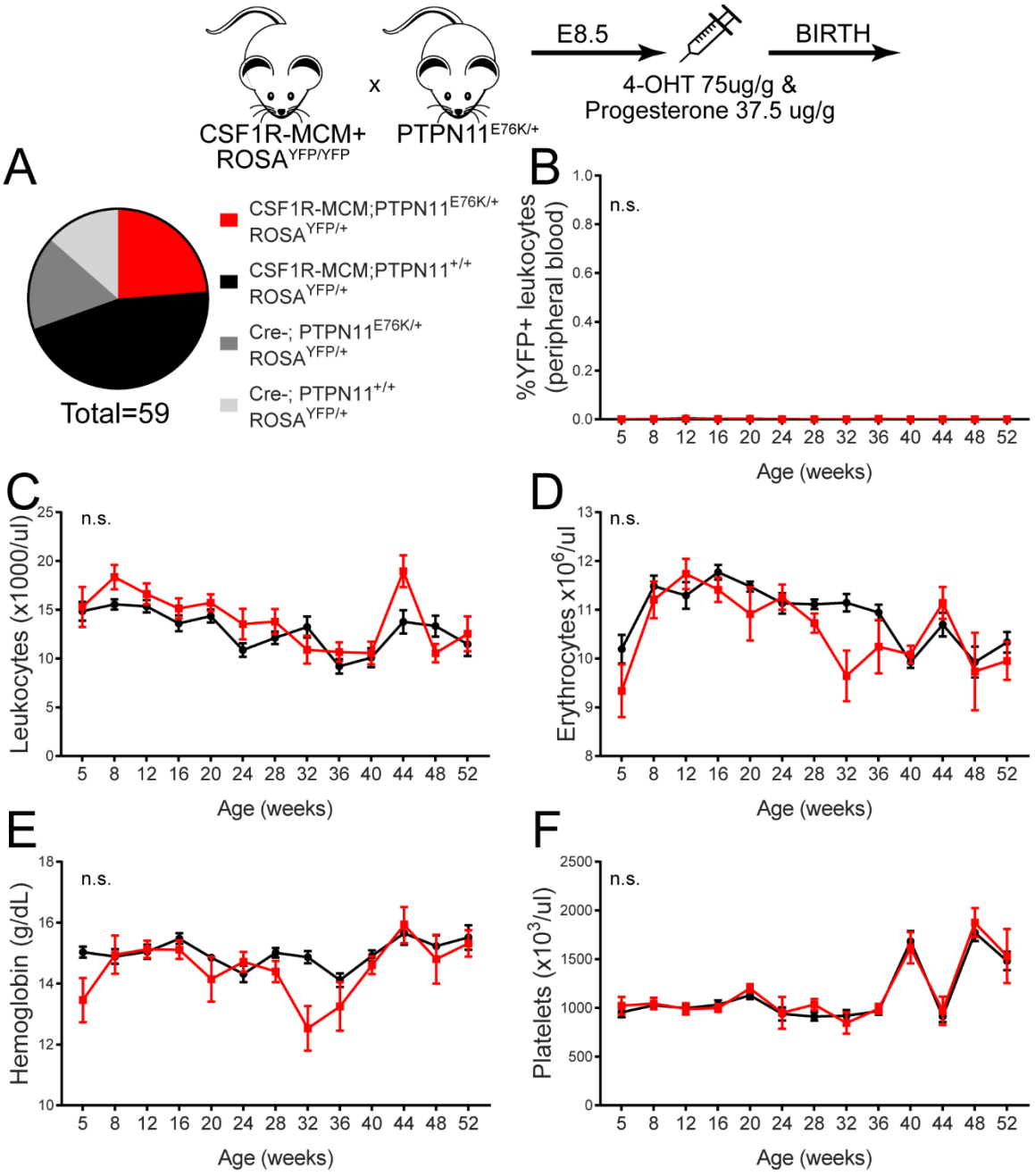

Figure II-13. Embryonic Phase CSF1R-MCM; PTPN11^{E76K}: Birth Ratio and CBC Analysis. A) Genotype ratios at weaning of indicated matings (Chi-squared p-value=0.002). B) Frequency of YFP+ leukocytes in peripheral blood. C-F) CBC analysis of leukocyte frequency, erythrocyte frequency, hemoglobin density and platelet abundance. Statistical analyses were performed by two-way ANOVA.

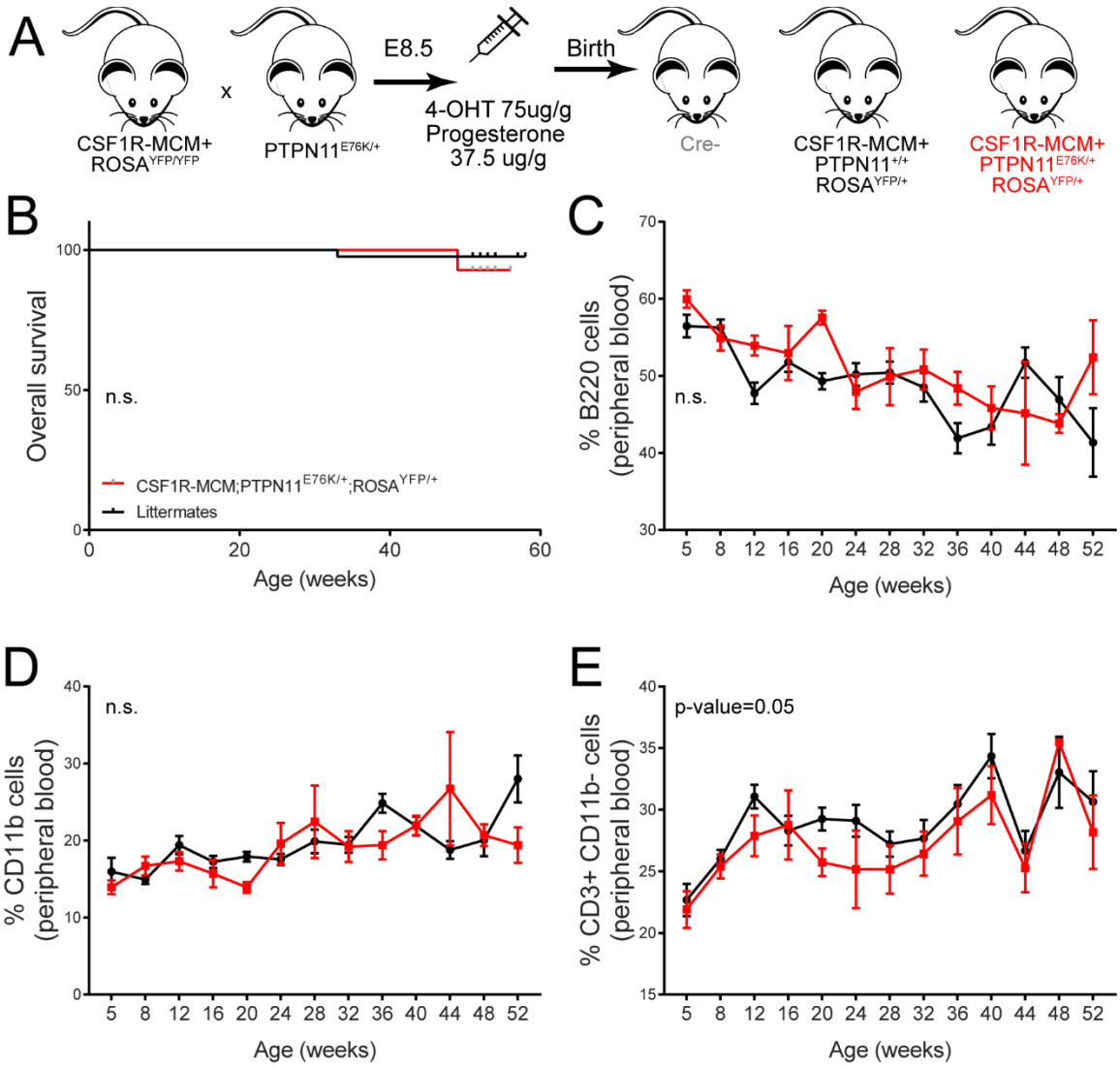

Figure II-14. Embryonic Phase CSF1R-MCM; PTPN11^{E76K}: Survival and Blood Leukocyte Analysis. A) Schematic of mating and analysis (N=14 mutants and 43 controls). B) Overall survival of CSF1R-MCM; PTPN11^{E76K}; ROSA$^{YFP/+}$ animals from the HSC-independent (E8.5 4-OHT) cohort (p-value=0.409 by log-rank test) C-E) Frequency of CD11b+ myeloid cells, B220+ B-lymphocytes, and CD3+ CD11b- T-lymphocytes in peripheral blood. Lineage frequency statistics performed with two-way ANOVA.

Furthermore, we did not see evidence of myeloproliferation or skewing of other blood lineages (Figure II-14). Over the course of the study, one mutant animal succumbed from an unclear cause. One littermate control developed sporadic T-ALL and was euthanized for humane reasons as per the request of IUPUI LARC veterinary staff.

We considered that indolent MPN progression in this embryonic cohort may not manifest in the peripheral blood and would only be evident upon tissue examination. Upon analysis, mutant animals did not have enlarged spleens or livers and their thymuses were the same size as those of littermates (Figure II-15 B-E). There was no evidence of leukocyte lineage skewing in the BM and spleen of mutants, which was consistent with the findings obtained from our year-long analysis of peripheral blood (Figure II-15F,G). We proceeded to characterize the macrophage populations in the brain, heart, liver, and spleen, which have the greatest contribution from YS EMPs (Figure II-16) (Epelman et al. 2014; Gomez Perdiguero et al. 2015; Bain et al. 2014). Consistent with previous reports we saw high proportions of YFP+ microglia and measureable proportions of YFP+ heart and liver macrophages. No labelled cells were detected in the BM or spleen. PCR analysis confirmed the loxP-STOP-loxP cassette of the PTPN11^{E76K} allele was recombined in the brain of mutant animals, demonstrating that the mutation should be expressed in microglia (Figure II-16F). Nonetheless, we did not observe differences in the frequency of YFP+ macrophages between CSF1R-MCM; PTPN11^{E76K} and controls in any tissue. This suggests that the PTPN11 mutation did not confer a proliferative advantage to macrophages. Furthermore, whereas all CSF1R-MCM+ animals had YFP+ microglia, their frequency was strikingly different among analyzed litters (Figure II-16E). This suggests that small differences in the timing or dosing of *in utero* tamoxifen may result in markedly different labelling efficiency, irrespective of whether a mutant allele is present. As such, any difference in the frequency of YFP+ microglia is more likely to be attributed to litter than to the expression of a mutation (two-way ANOVA: p-value<0.001). Nonetheless, we

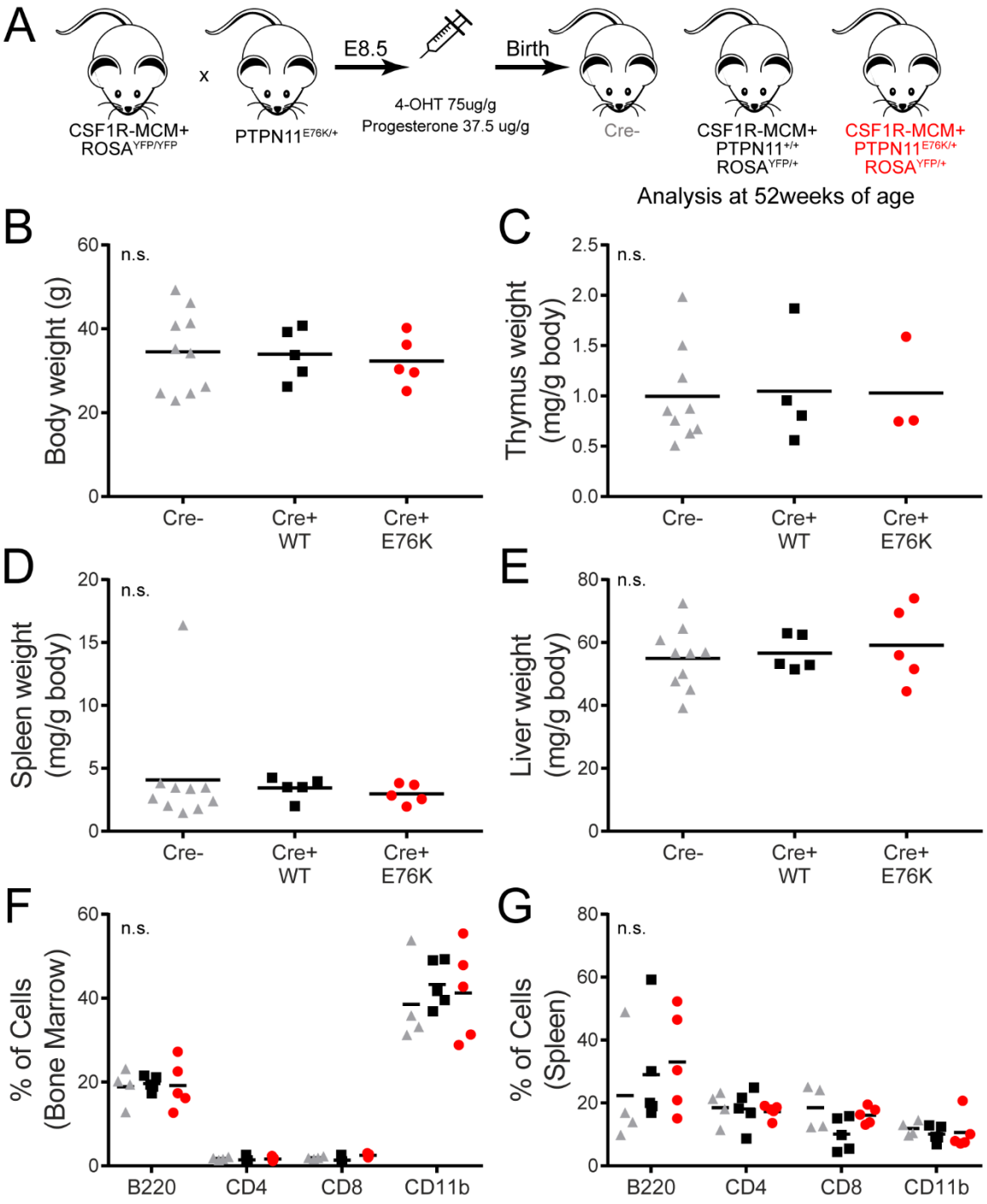

Figure II-15. Embryonic Phase CSF1R-MCM; PTPN11^{E76K}: Tissue Analysis. A) Animals were analyzed a 52 weeks of age. B-E) Weights of body, thymus, spleen, and liver. F,G) Frequency of B-cells, T-cells, and myeloid cells in the bone marrow and spleen of mutants and littermates as measured by flow cytometry.

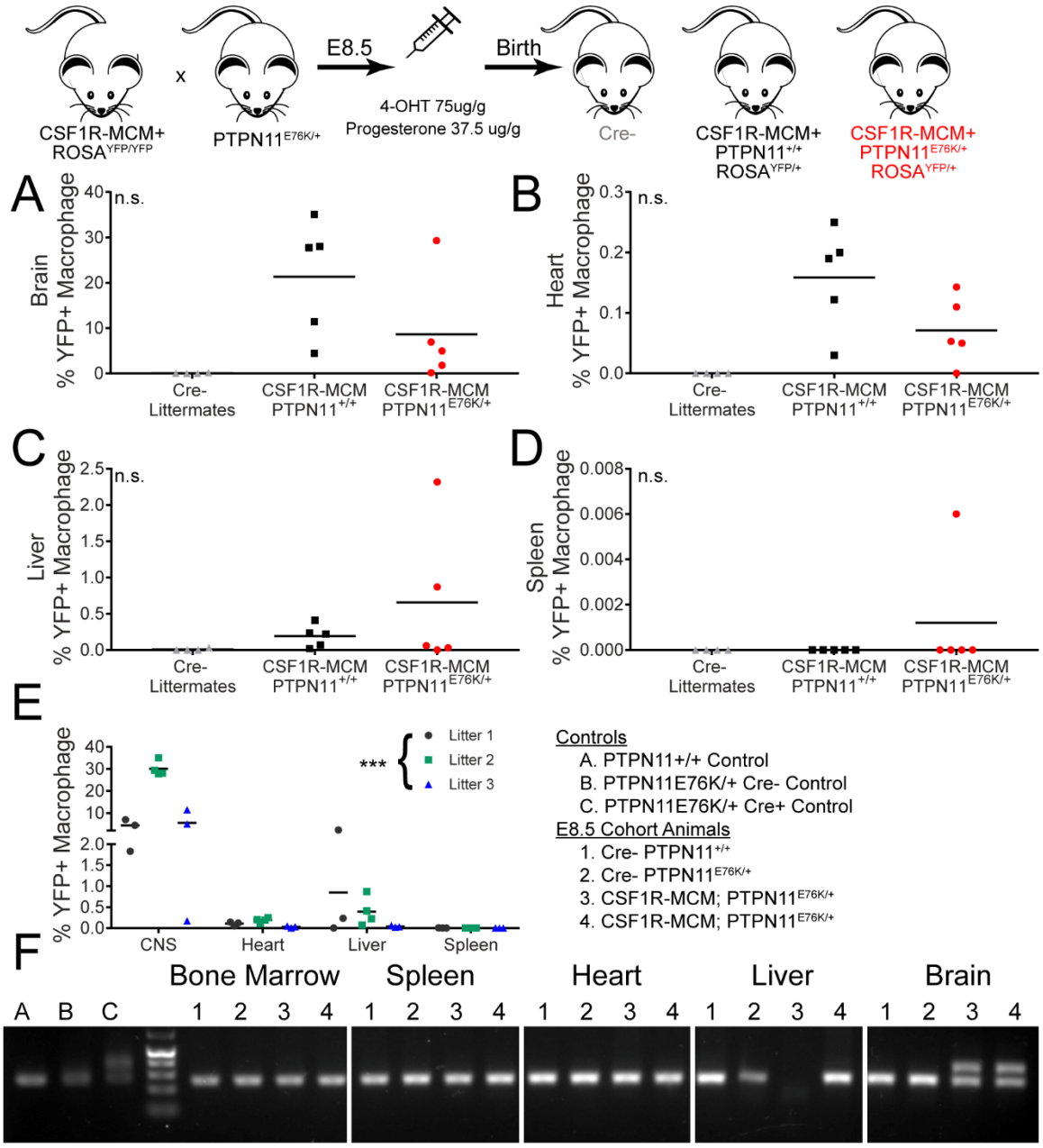

Figure II-16. Embryonic Phase CSF1R-MCM; PTPN11^{E76K}: Macrophages Analysis. A-D) Frequency of YFP+ macrophages in the brain, heart, liver, and spleen of mutant animals and controls at 52 weeks of age. E) Frequency of YFP+ macrophages in CSF1R-MCM+ animals in each litter (variation due to litter: two-way ANOVA p-value<0.001). F) PCR analysis of genomic DNA demonstrates populations in the brain have recombination of LSL-PTPN11^{E76K} locus.

are able to conclude that expression of PTPN11^{E76K} in a subset of YS EMPs is not sufficient for the emergence of a MPN.

E. CSF1R-MCM Activity within Fetal and Adult Phases

Having analyzed the contribution of the embryonic HSC-independent phase to MPN development, we proceeded to compare the effects of PTPN11^{E76K} expression in progenitors of the fetal and adult HSC-dependent phases. We modified the timing of tamoxifen administration (see Figure II-9).; the fetal cohort obtained one 75ug/g 4-OHT +37.5ug/g progesterone injection at E14.5, whereas the adult cohort received 3 daily 75ug/g tamoxifen injections beginning at 4 weeks of age We had strong reason to be confident that the timing of our doses would activate progenitors solely from the desired phase. Previous studies have shown that tamoxifen exposure after E10.5 no longer labels EMPs in the CSF1R-MCM model (Hoeffel et al. 2015). Furthermore, between 3-4 weeks of age mouse HSCs undergo a pronounced functional change that defines the fetal to adult transition: they enter quiescence, they alter their gene expression, they have differential responses to cytokine signals, and they acquire biased lineage differentiation (Bowie et al. 2006; Benz et al. 2012; Copley et al. 2013; He et al. 2011; Yuan et al. 2012; Kim, Saunders, and Morrison 2007). As such, we reasoned the timing of our tamoxifen doses would target distinct phases of hematopoiesis and would permit evaluation of the specific contribution of each to MPN development.

CSF1R is transcriptionally active in numerous hematopoietic progenitor populations (Wilson et al. 2015), each of which can be identified by immune phenotype using flow cytometry (see Figure II-17). These CSF1R-expressing progenitors include HSCs, multipotent progenitors (MPP), Myeloid-Dendritic cell progenitors (MDP), common monocyte progenitors (CMoP), early thymic progenitors (ETP), and myeloid restricted Lin- cKit+ Sca1- (LK) cell subsets: common myeloid progenitors (CMP), granulocyte-

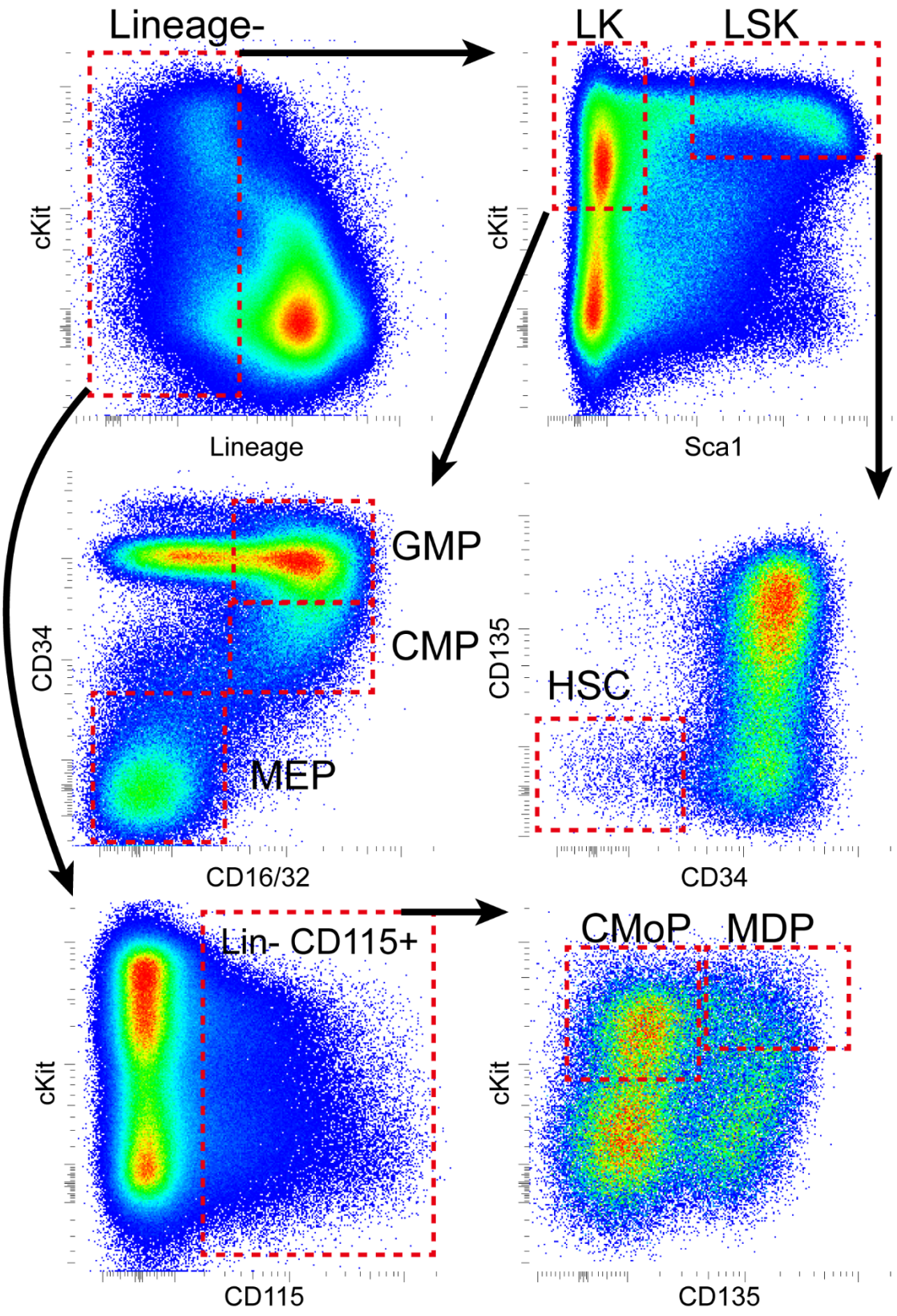

Figure II-17. Flow Cytometric Gating Strategy of Hematopoietic Progenitors.

macrophage progenitors (GMP) and megakaryocyte-erythroid progenitors (MEP) (Luc et al. 2012; Waskow et al. 2008; Hettinger et al. 2013). Therefore, we hypothesized that tamoxifen injection into CSF1R MCM;ROSA$^{YFP/+}$ mice would label a diverse progenitor population. To test this hypothesis, we analyzed 4 week-old mice 24hr after the third tamoxifen injection (Figure II-18). We observed 1.1 +/- 0.5(S.D.)% and 1.1 +/- 0.4% labelling of BM LK and LSK cells, respectively. We further observed 0.67 +/-0.28% and 1.5 +/-0.5% labelling of spleen LK and LSK cells, respectively. This demonstrates that our model has reproducible, low efficiency labelling of hematopoietic progenitors. Further analysis demonstrated that short-lived myeloid biased progenitors, such as MDPs, CMoPs, and GMPs, were labelled at higher efficiencies. LK cells, LSK cells, and HSCs were labeled at similar efficiencies in the fetal liver following 4-OHT injection at E14.5. (Figure II-19). Strikingly, thymic progenitors were labelled at 6.1 +/- 3.0%, confirming that both myeloid and lymphoid progenitors were targeted in our model (Figure II-20). Finally, we determined that CSF1R-MCM was not active in non-hematopoietic mesenchymal stem cells or osteoblasts and had negligible activity in endothelial cells (Figure II-21). Having confirmed that CSF1R-MCM has hematopoietic-restricted activity and labels progenitors of all lineages, we proceeded to use this model to express PTPN11^{E76K} in both adult and fetal progenitors.

F. Comparison of PTPN11$^{E76K/+}$ Expression in Fetal and Adult Phases of Hematopoiesis

We hypothesized that YFP+ cells in mutant animals would have a proliferative advantage over YFP- cells due to the expression of PTPN11^{E76K}. We reasoned this increase in mutant allele frequency could be quantified by the %YFP+ leukocytes in the blood. In our adult cohort, mutant and control animals had an equal %YFP+ cells 1 week after injection. Thereafter, the %YFP+ leukocytes were significantly expanded in mutant

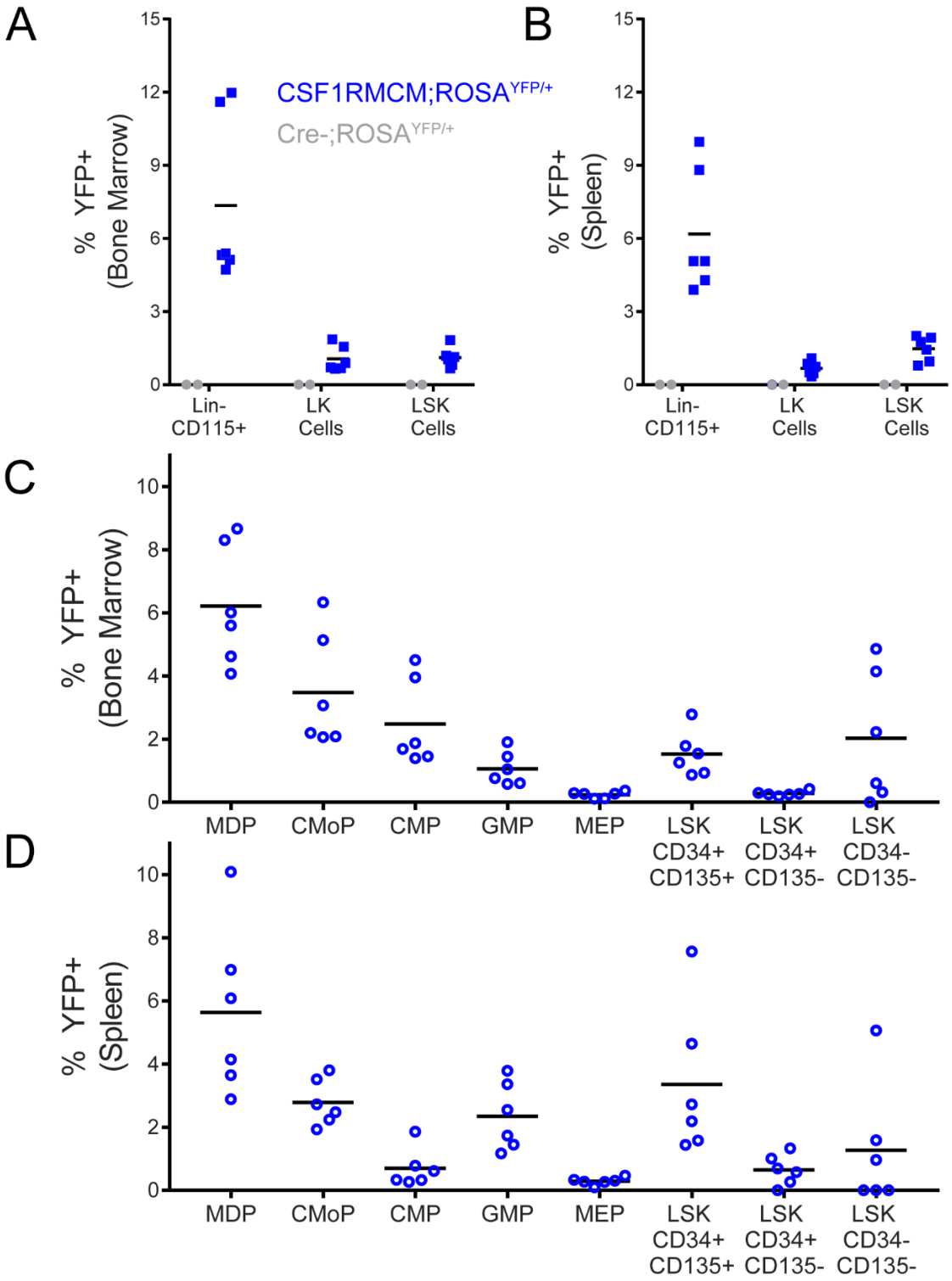

Figure II-18. CSF1R-MCM Labels Progenitors in the Adult Phase. Frequency of YFP+ cells in A,C) BM and B,D) spleen 48hrs after tamoxifen injection at 4weeks of age.

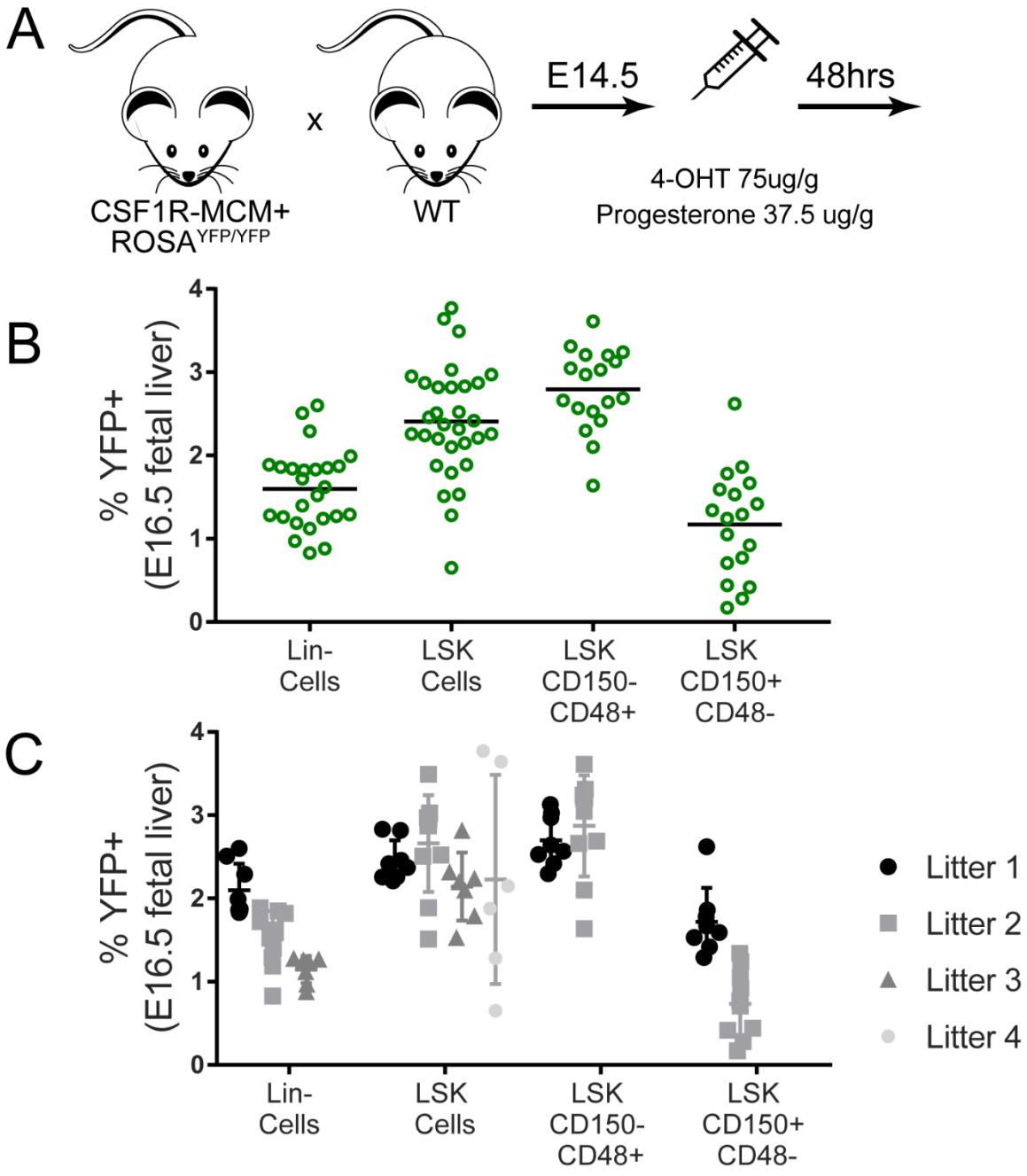

Figure II-19. CSF1R-MCM Labels Progenitors in the Fetal Phase. Frequency of YFP+ cells in the fetal liver 48hrs after 4-OHT injection at E14.5. B) Grouped analysis. C) Analysis by litter shows minimal differences in LSK labeling efficiency between litters (two-away ANOVA p-value =0.09).

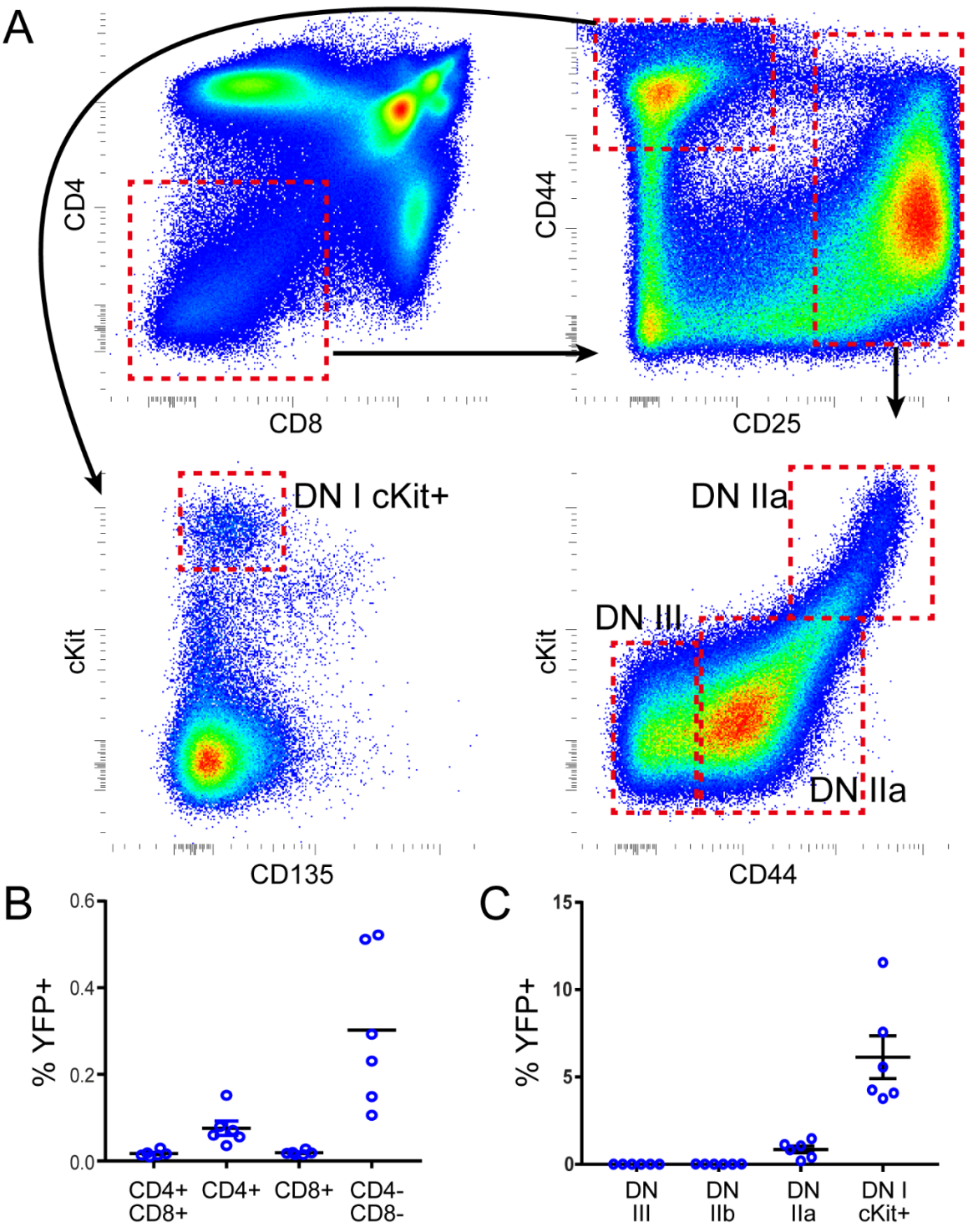

Figure II-20. CSF1R-MCM Labels Progenitors in the Thymus. A) Gating strategy to analyze thymic progenitors. B,C) Frequency of YFP+ cells in thymus 48hrs after tamoxifen injection at 4weeks of age.

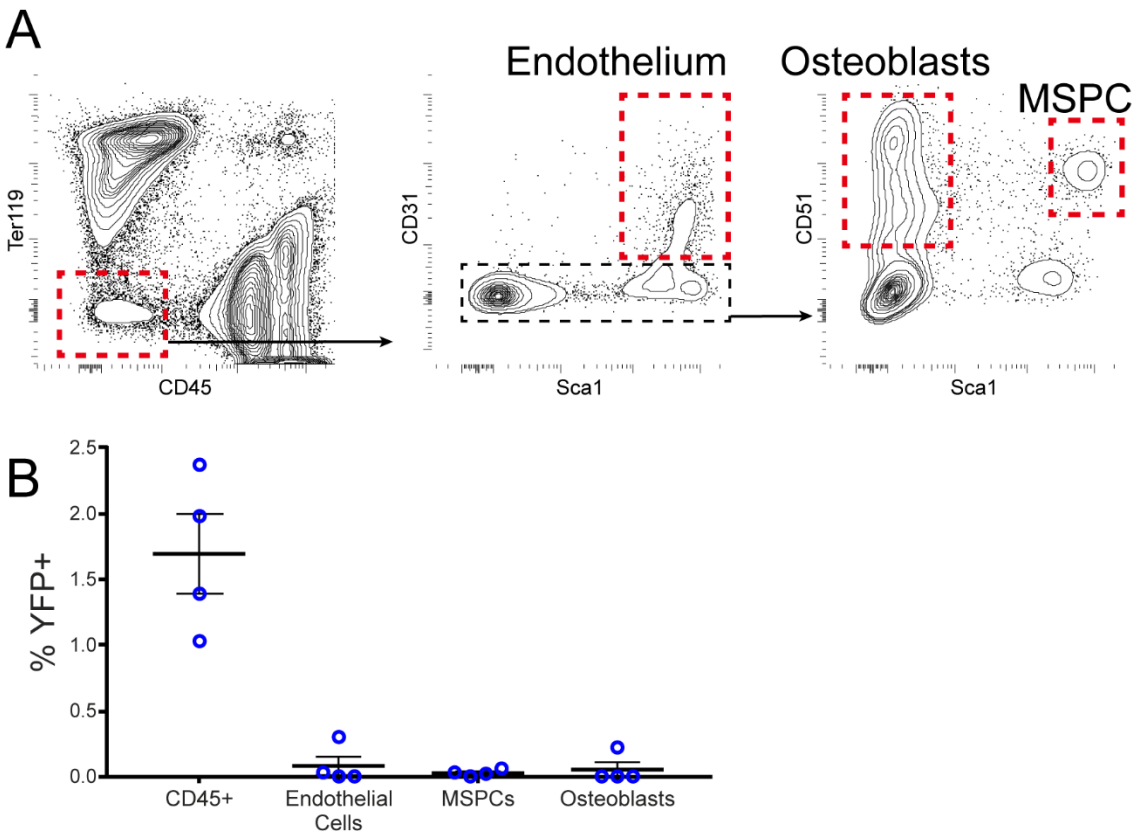

Figure II-21. CSF1R-MCM Does Not Label Endothelial Cells or BM Stromal Cells. A) Gating strategy to analyze BM endothelial cells and stromal cell populations. B) Frequency of YFP+ cells in BM 7 days after tamoxifen injection in 4 week old CSF1R-MCM;ROSA$^{YFP/+}$ animals. MSPC=mesenchymal stem and progenitor cells.

animals at all analyzed time points (Figure II-22B). This difference was greatest at 24-36 weeks after tamoxifen treatment and declined thereafter. Strikingly, mutant animals demonstrated overall leukocytosis compared to littermates at 5-8 weeks after treatment and again at 32 weeks, coinciding with the peak of %YFP+ cells. This suggested that oncogene expression in a minor subset of progenitors was sufficient to cause leukocytosis. The distribution of YFP+ cells in mutant animals was myeloid biased and there was a paucity of YFP+ T cells (Figure II-23A,B). Strikingly, albeit the frequency of YFP+ cells was never greater than 10% of leukocytes, mutant animals showed a decrease in net (YFP+ and YFP- combined) T-lymphocytes in older age with a concomitant increase in net CD11b+ neutrophils (Figure II-24A,B). Combined, these results suggest that low frequency expression of $PTPN11^{E76K}$ in adult progenitors result in a marked expansion of that subset with myeloid-biased differentiation and overt hematologic abnormalities in mutant animals.

We performed the same analysis in our fetal cohort, in which the $PTPN11^{E76K}$ mutation was expressed *in utero* at E14.5. We did not observe leukocytosis or an increased frequency of YFP+ cells in mutant animals in the fetal cohort (Figure II-22,A,B). Additionally, we did not observe biased lineage distribution among YFP+ cells (Figure II-23). Nonetheless, mutants from the fetal cohort did show increased net CD11b+ myeloid cells and decreases in net CD3+ T-lymphocytes (Figure II-24A,B). This suggests that mutant cells from the fetal phase disrupted the microenvironment and are contributing to MPN development in a non-cell autonomous fashion. This finding parallels the observations from the adult cohort. Indeed, mutant animals from both fetal and adult cohorts showed thrombocytopenia with increased platelet size at all analyzed time intervals, suggestive of a consumptive coagulopathy (Figure II-25B,C).

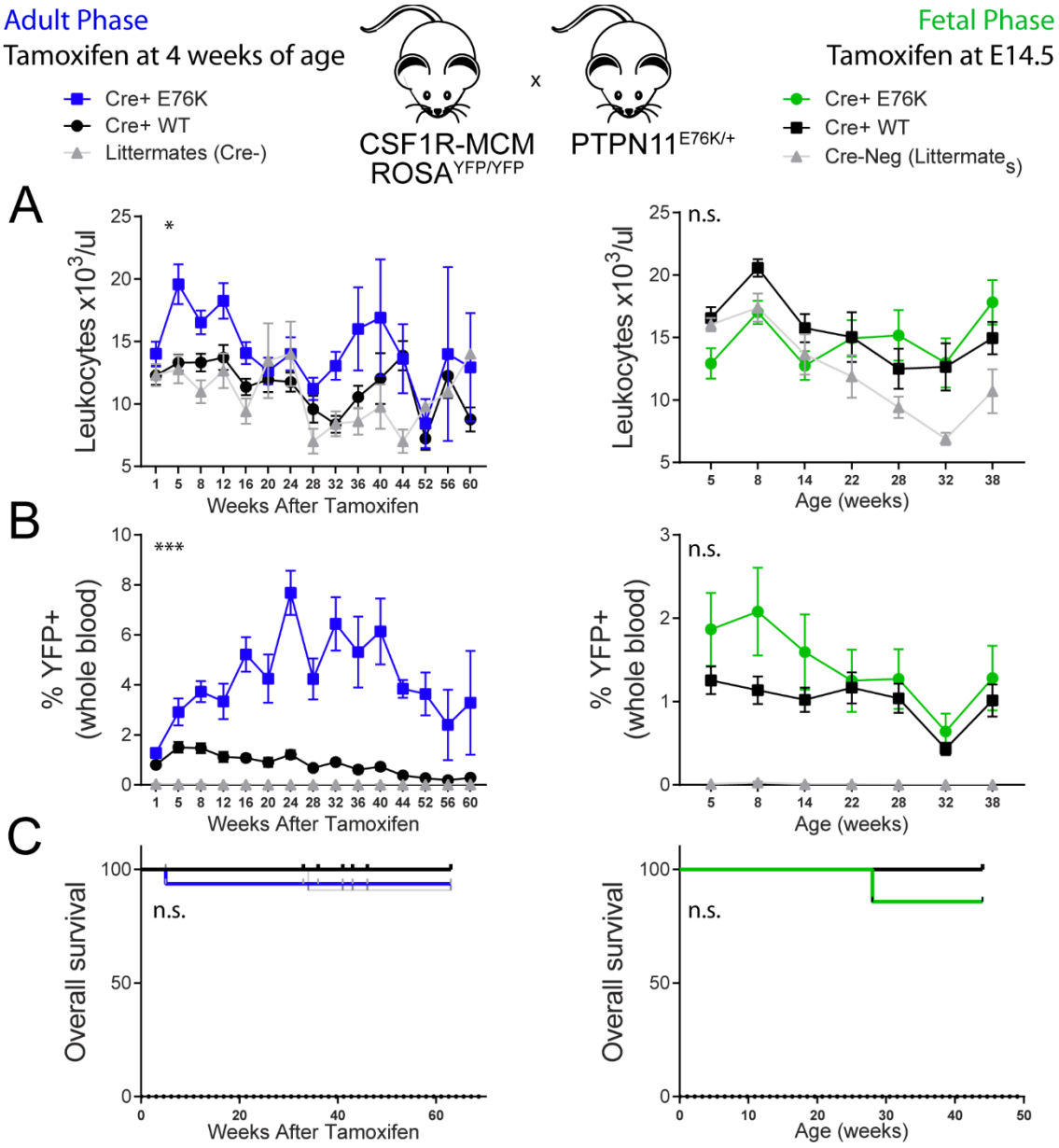

Figure II-22. Comparison of PTPN11^{E76K} Expression in Adult and Fetal Phases: Leukocytes, %YFP+, Survival. A) Leukocyte counts of cohorts over time (peripheral blood N=14 adult mutants, 25 adult littermates, 7 fetal mutants, 15 fetal littermates). B) %YFP+ leukocytes in blood as measured by flow cytometry. C) Overall survival (Survival analysis N= 32 adult mutants, 48 adult littermates, 7 fetal mutants, 15 fetal littermates).

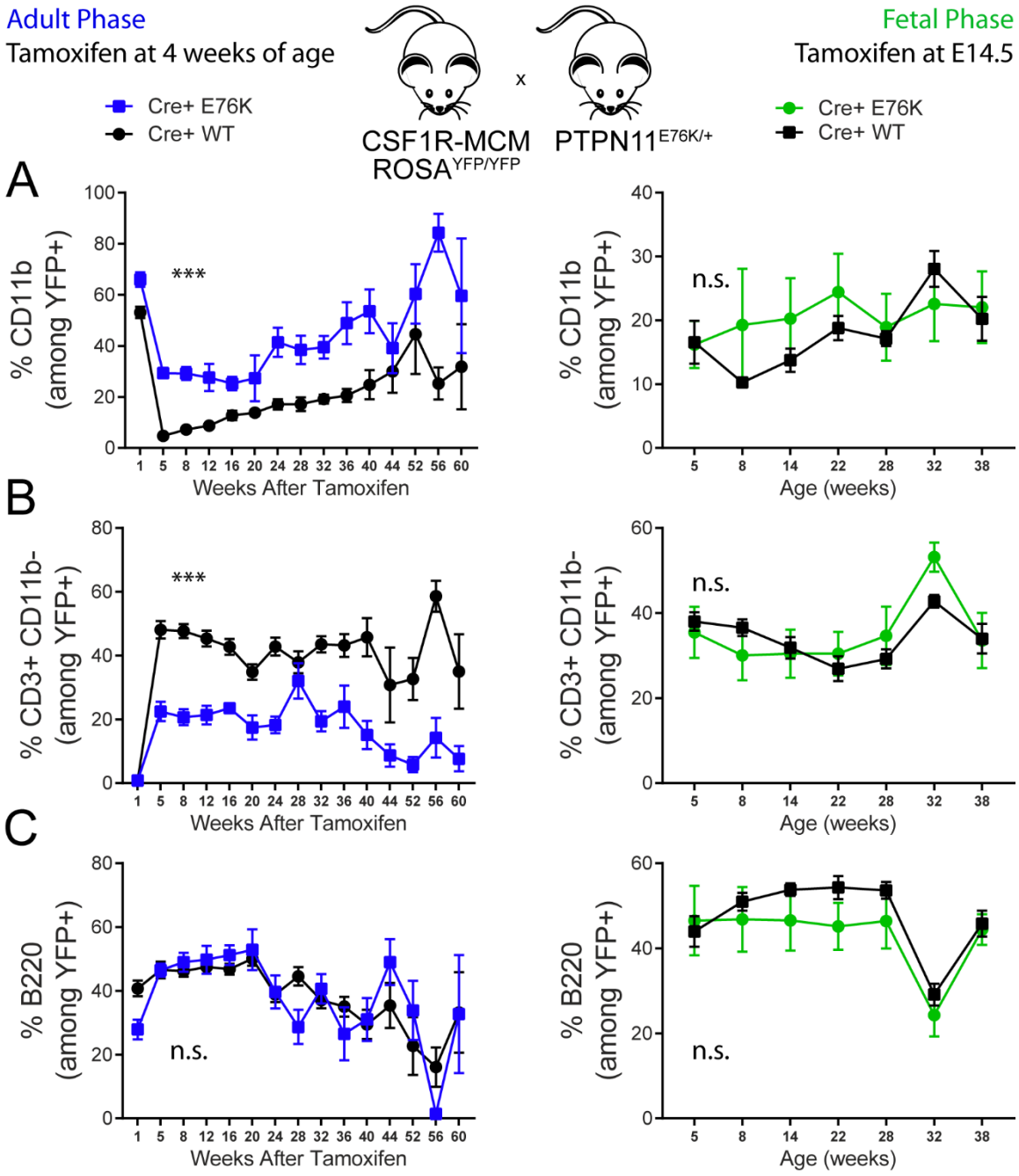

Figure II-23. Comparison of PTPN11^{E76K} Expression in Adult and Fetal Phases: Lineage Bias of YFP+ Cells. A-C) Analysis of frequencies of CD11b+ myeloid cells, CD3+ CD11b- T-cells, and B220+ B-cells among YFP+ cells the peripheral blood of adult & fetal cohort CSF1R-MCM;PTPN11$^{E76K/+;}$ROSA$^{YFP/+}$ animals and their controls.

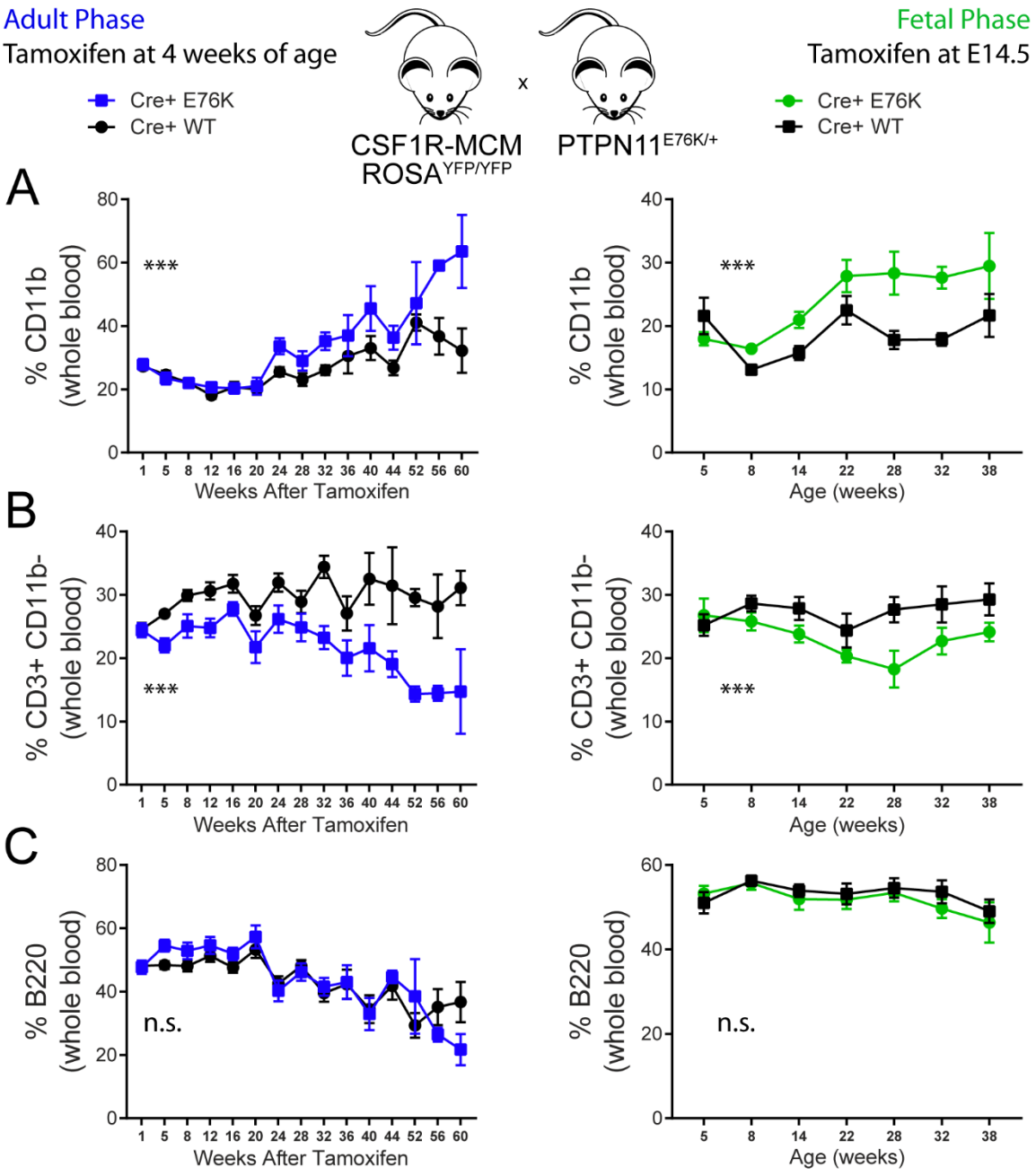

Figure II-24. Comparison of PTPN11^{E76K} Expression in Adult and Fetal Phases: Lineage Bias of Unfractionated Peripheral Leukocytes. A-C) Analysis of frequencies of CD11b+ myeloid cells, CD3+ CD11b- T-cells, and B220+ B-cells among all leukocytes cells the peripheral blood of adult & fetal cohort CSF1R-MCM;PTPN11$^{E76K/+}$;ROSA$^{YFP/+}$ animals and their controls.

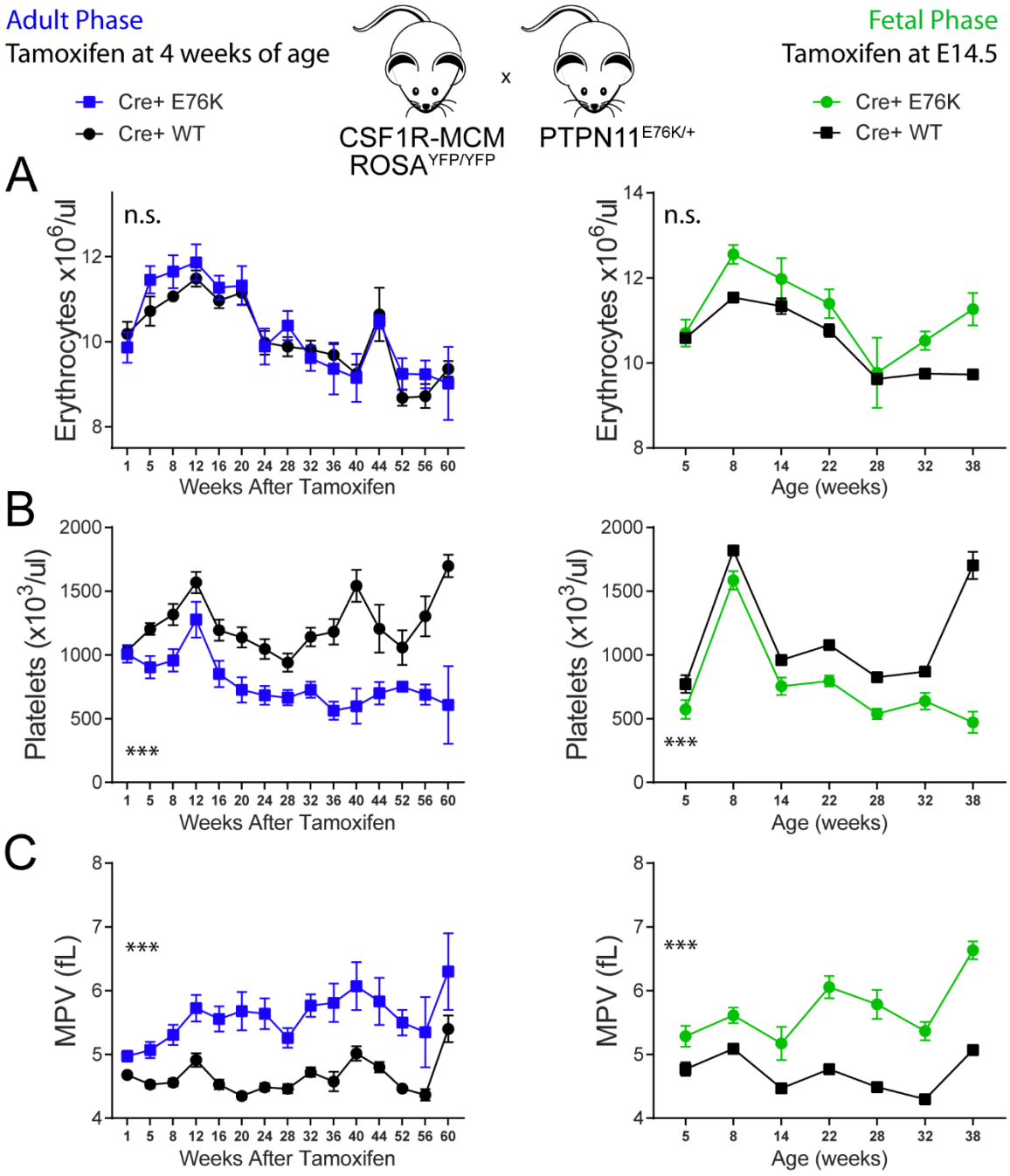

Figure II-25. Comparison of PTPN11^{E76K} Expression in Adult and Fetal Phases: Erythrocyte and Platelet Analysis. A-C) Analysis of erythrocyte abundance, platelet abundance, and the mean platelet volume (MPV) of adult & fetal cohort CSF1R-MCM;PTPN11$^{E76K/+;}$ROSA$^{YFP/+}$ animals and their controls.

F. Non-Cell Autonomous Effects of Hematopoietic-Restricted PTPN11^{E76K} Expression

To evaluate the effects of low mutant allele frequency on the microenvironment, we proceeded to analyze hematopoietic tissue compartments. We chose to look at our adult cohort 32 weeks after tamoxifen injection because this coincided with the most pronounced leukocytosis and %YFP+ cells. We observed marked hepatosplenomegaly in mutant animals (Figure II-26B,C). This further supports our assumption of a consumptive coagulopathy, as was suggested by our CBC analysis. The frequency of YFP+ cells was increased in mutant animals in all analyzed mature leukocyte populations in the BM, spleen, and thymus (Figure II-27). This confirms that the oncogene is active in progenitors that are multipotent and that the oncogene confers a proliferative and/or survival advantage to these progenitors. Nevertheless, the mean frequency of YFP+ cells never exceeded 12%, suggesting that the majority of cells in the tissues of mutant animals did not express the mutation. We reasoned, therefore, that any observed net differences in population frequency would likely be the result of non-cell autonomous effects of oncogene-expressing cells.

We observed a net reduction of CD8+ cells in the BM and spleen of mutant animals (Figure II-27D,E). In the thymus, however, we did not detect differences in the frequencies of CD4+, CD8+, or double positive (DP) cells (Figure II-28B). Furthermore, we did not observe differences in the frequency of committed T cell progenitors: the double negative (DN) IIa, IIb, and III populations. However, we did observe a marked expansion of early thymic progenitors (ETPs, Lin- CD44+ cKit+) as well as thymic dendritic cells (Lin- CD44+ CD11c+) (see Figure II-28C). The increase in ETPs without a concomitant increase in downstream progenitors is suggestive of a block in ETP commitment to the T cell lineage. This is supported by our finding that the expression of CD25 among committed T cell progenitors was decreased in mutant animals compared to controls (Figure II-28D). These

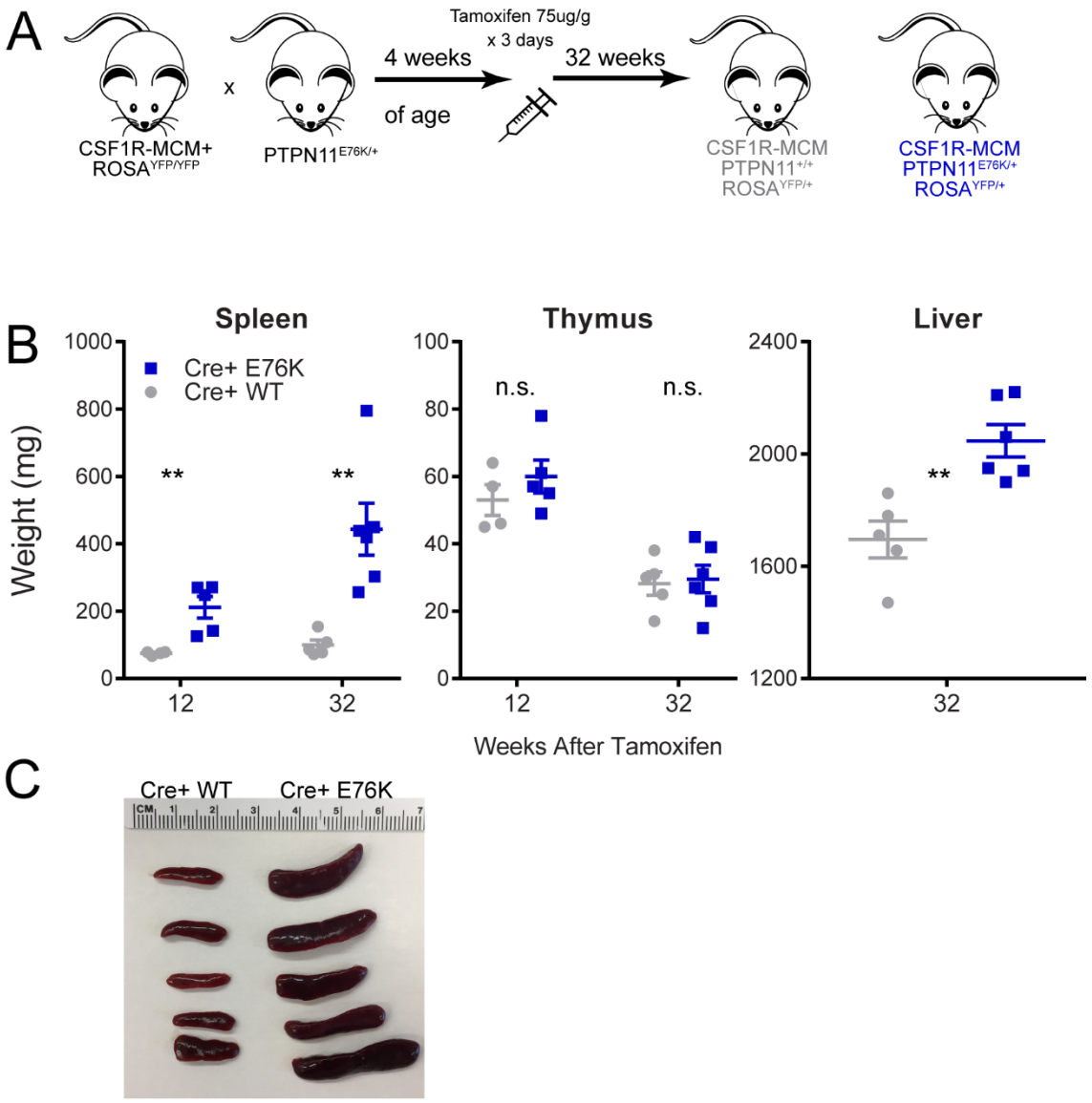

Figure II-26. Adult CSF1R-MCM; PTPN11^{E76K}: Hepatosplenomegaly. A) Mutant animals and controls were analyzed 12 and 32weeks after tamoxifen injection. B) Spleen, thymus, and liver weights among mutants and controls and indicated intervals after tamoxifen treatment. C) Images of mutant & control spleens 32 weeks after tamoxifen.

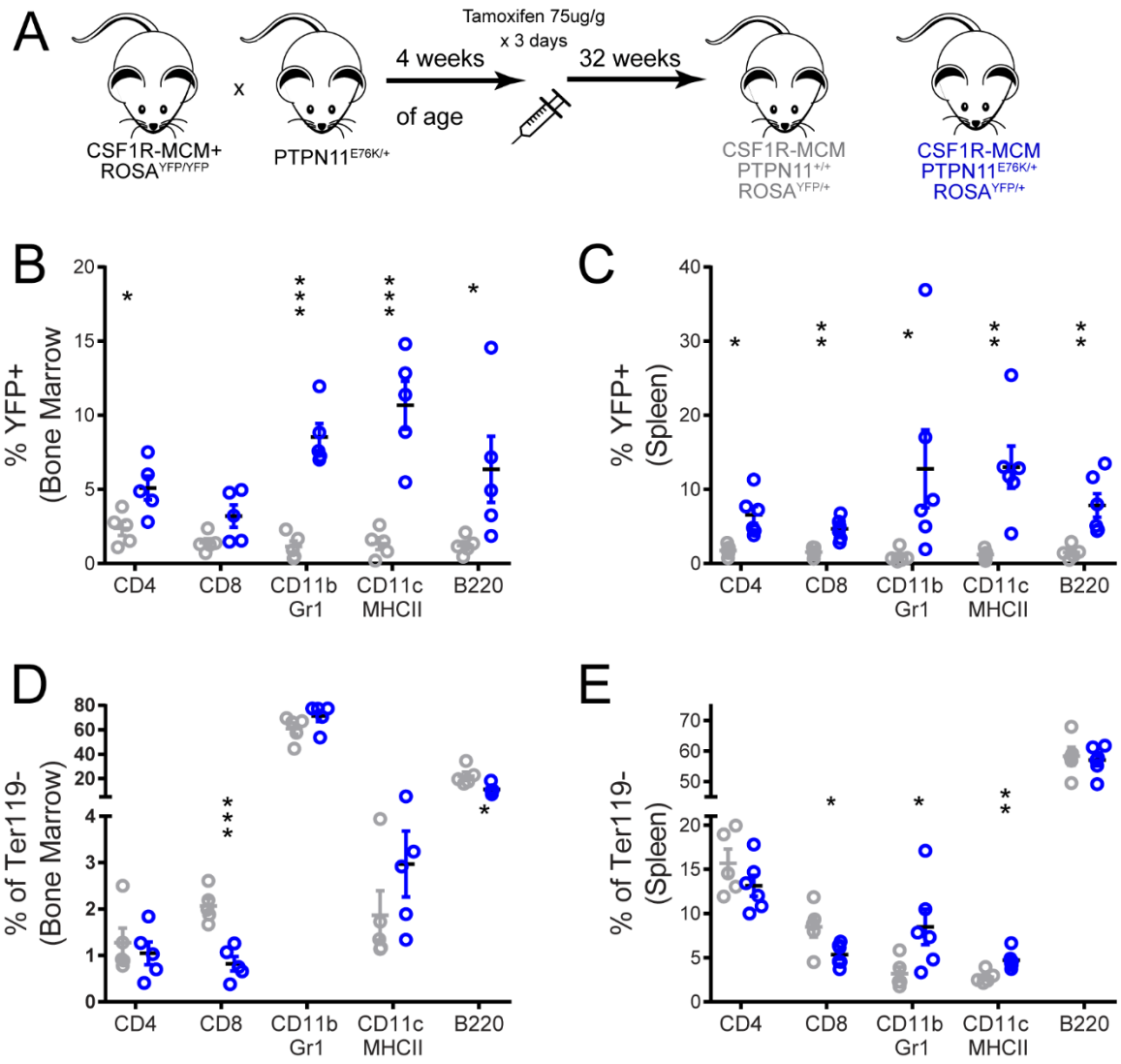

Figure II-27. Adult CSF1R-MCM; PTPN11^{E76K}: Leukocytes in BM and Spleen. A) Analysis was performed 32 weeks after tamoxifen treatment. B,C) Frequency of YFP+ cells among lymphoid and myeloid populations in the BM and spleen of mutants and controls. D,E) Overall (YFP+ and YFP-) frequency of myeloid and lymphoid cells in BM and spleen of mutants and controls.

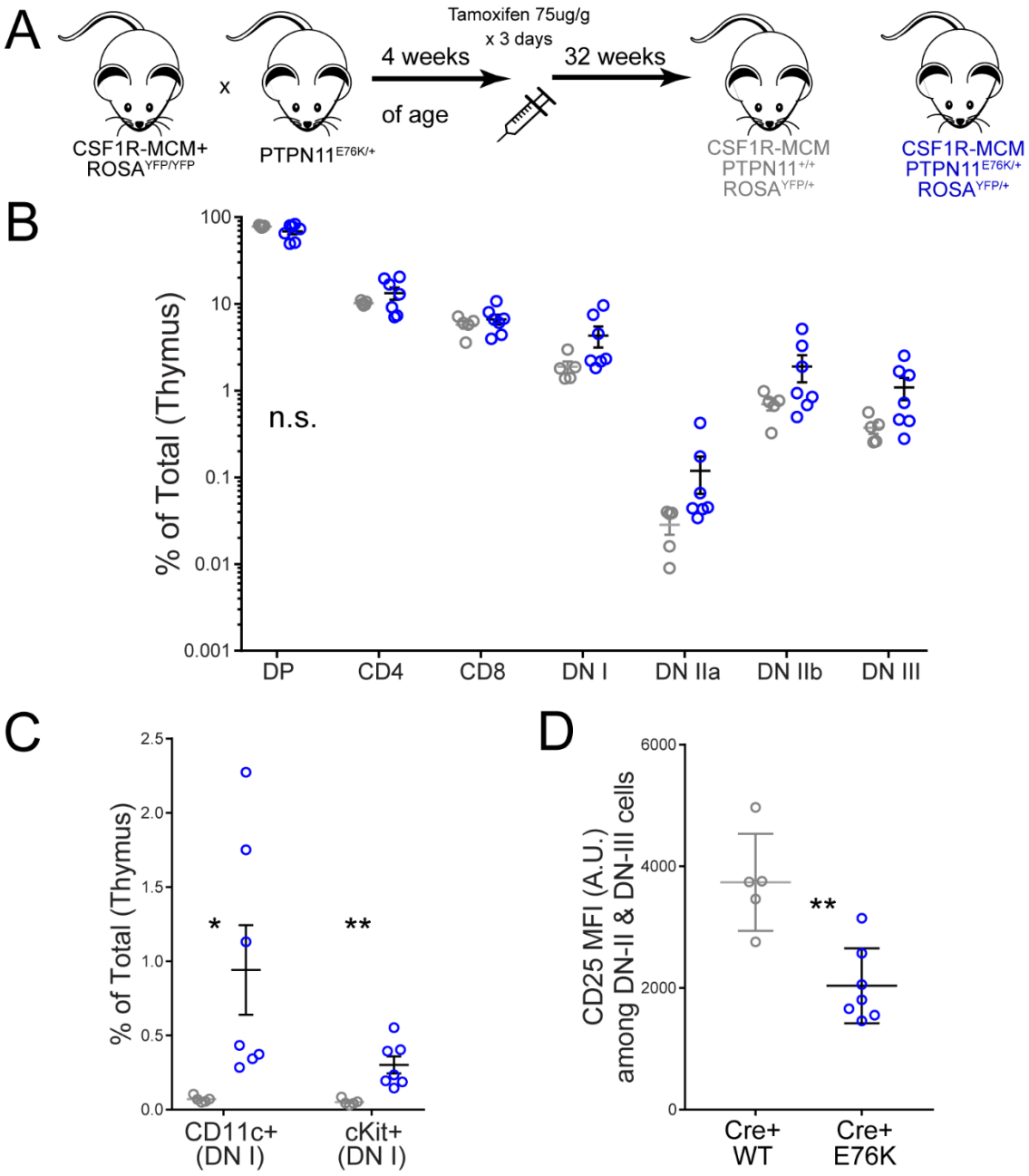

Figure II-28. Adult CSF1R-MCM; PTPN11^{E76K}: Thymocytes. A) Analysis was performed 32 weeks after tamoxifen treatment. B) Overall (YFP+ and YFP-) frequency of T and lymphoid cells in thymuses of mutants and controls. C) Frequency of CD11c+ dendritic cells and cKit+ early thymic progenitors in mutant and control thymuses. D) CD25 Mean florescence intensity (MFI) among DN-IIa, DN-IIb, and DN-III populations in mutant and control thymuses.

findings suggest that oncogene expression within the thymus causes defects in T cell production, which may be exacerbated over time.

We proceeded to analyze myeloid cells in our mutant animals. In the spleen we observed an increase in net neutrophils and dendritic cells (Figure II-27D,E). This finding paralleled our peripheral blood analyses. However, differences in these populations were not detected in the BM. We proceeded to analyze the frequency of YFP expression amongst BM and splenic progenitors (Figure II-29). All analyzed progenitor subsets had a greater frequency of YFP+ cells in mutants compared to controls. However, their proportion never exceeded 13%. Therefore, this expansion of YFP+ cells was unlikely to account cell autonomously for any observed net differences.

Indeed, we did not observe any differences in the absolute number of progenitors in the BM (Figure II-30B). However, we did observe an increase in the absolute number of splenic HSCs in mutant animals (Figure II-30C). We also observed an increase in mutant MEPs, which is suggestive of increased non-medullary erythropoiesis – a defining feature of JMML (Figure II-30E). Subsequent analysis of splenic erythroid committed progenitors confirmed an expansion of CD71+ Ter119- pro-erythroblasts, CD71+ Ter119+ early erythroblasts, and CD71- Ter119+ FSC^{Hi} late erythroblasts (Koulnis et al. 2011) (see Figure II-31). Similar trends were seen in the BM, albeit the differences were less pronounced. These findings, along with the observation of increased HSCs in the spleens of mutant animals, strongly suggest that non-cell autonomous effects in the context of low mutant allele frequency cause hematopoietic stress that promotes non-medullary hematopoiesis.

We sought to further probe the functional consequences of oncogene expression in the tissue microenvironment of our animals. We plated unsorted (YFP+ and YFP-) BM cells from mutant animals in methylcellulose medium with increasing doses of GM-CSF. Surprisingly, we observed a marked increase in colony formation among mutant

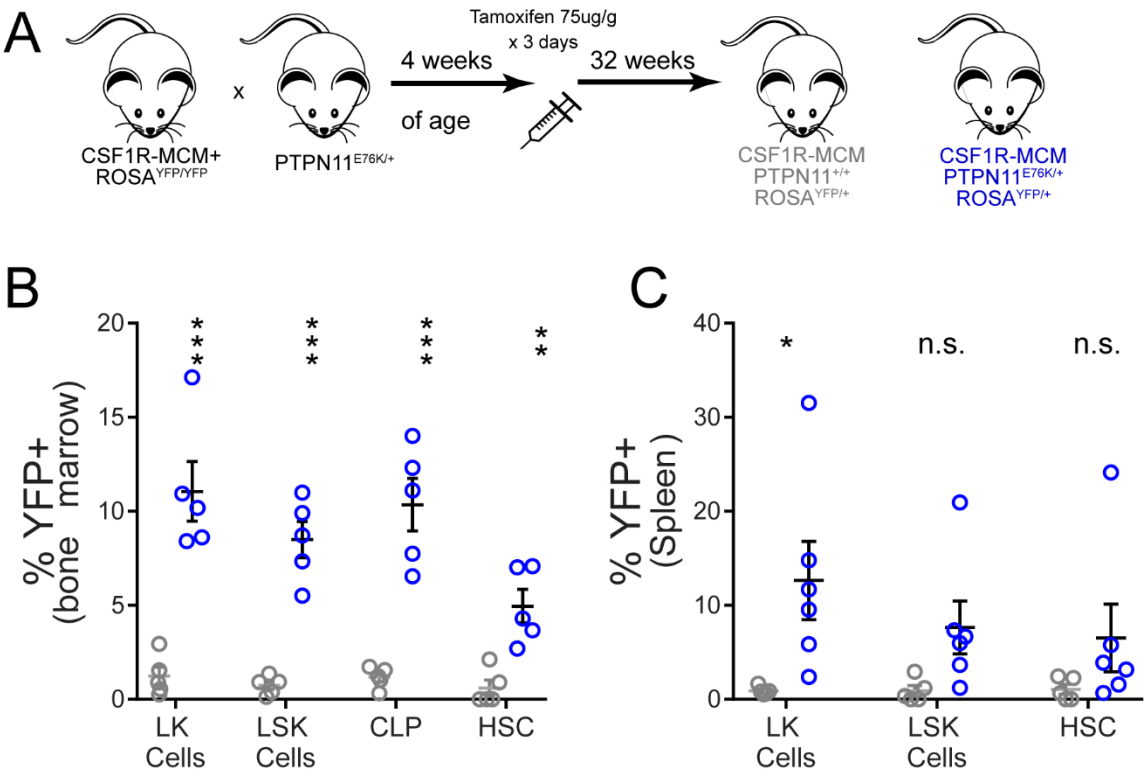

Figure II-29. Adult CSF1R-MCM; PTPN11^{E76K}: YFP+ Progenitor Frequencies. A) Analysis was performed 32 weeks after tamoxifen treatment. B,C) Proportion of BM and splenic progenitors that express YFP.

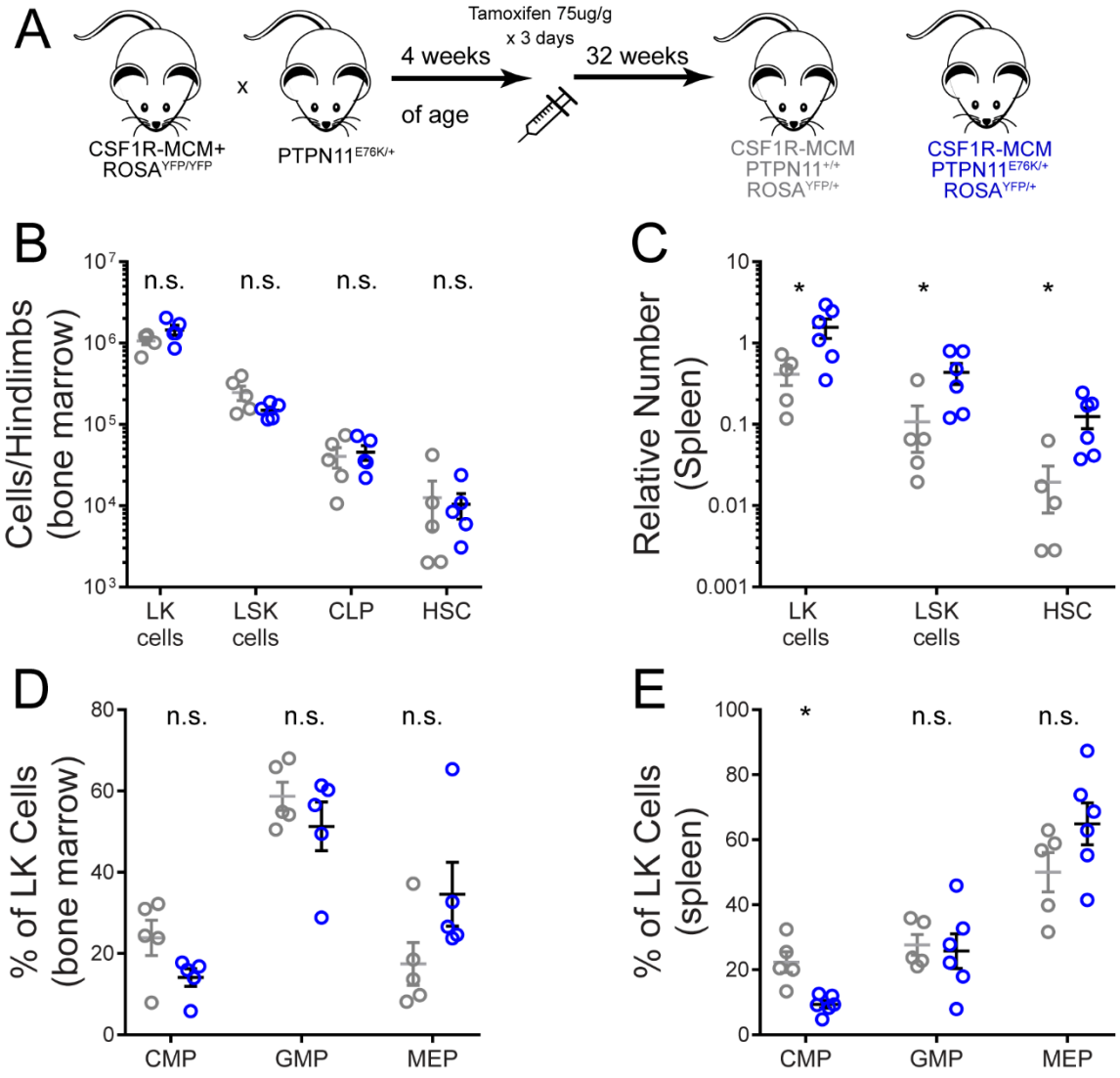

Figure II-30. Adult CSF1R-MCM; PTPN11^{E76K}: Absolute Progenitor Frequencies. A) Analysis was performed 32 weeks after tamoxifen treatment. B) Absolute cell number of YFP+ and YFP- BM progenitors in mutant and controls. C) Relative cell number of YFP+ and YFP- BM progenitors in mutant and controls calculated by multiplying the frequency of progenitors by each animal's spleen weight. D,E) Distribution of CMP, GMP, and MEP populations among LK cells in the BM and spleen of mutants and controls.

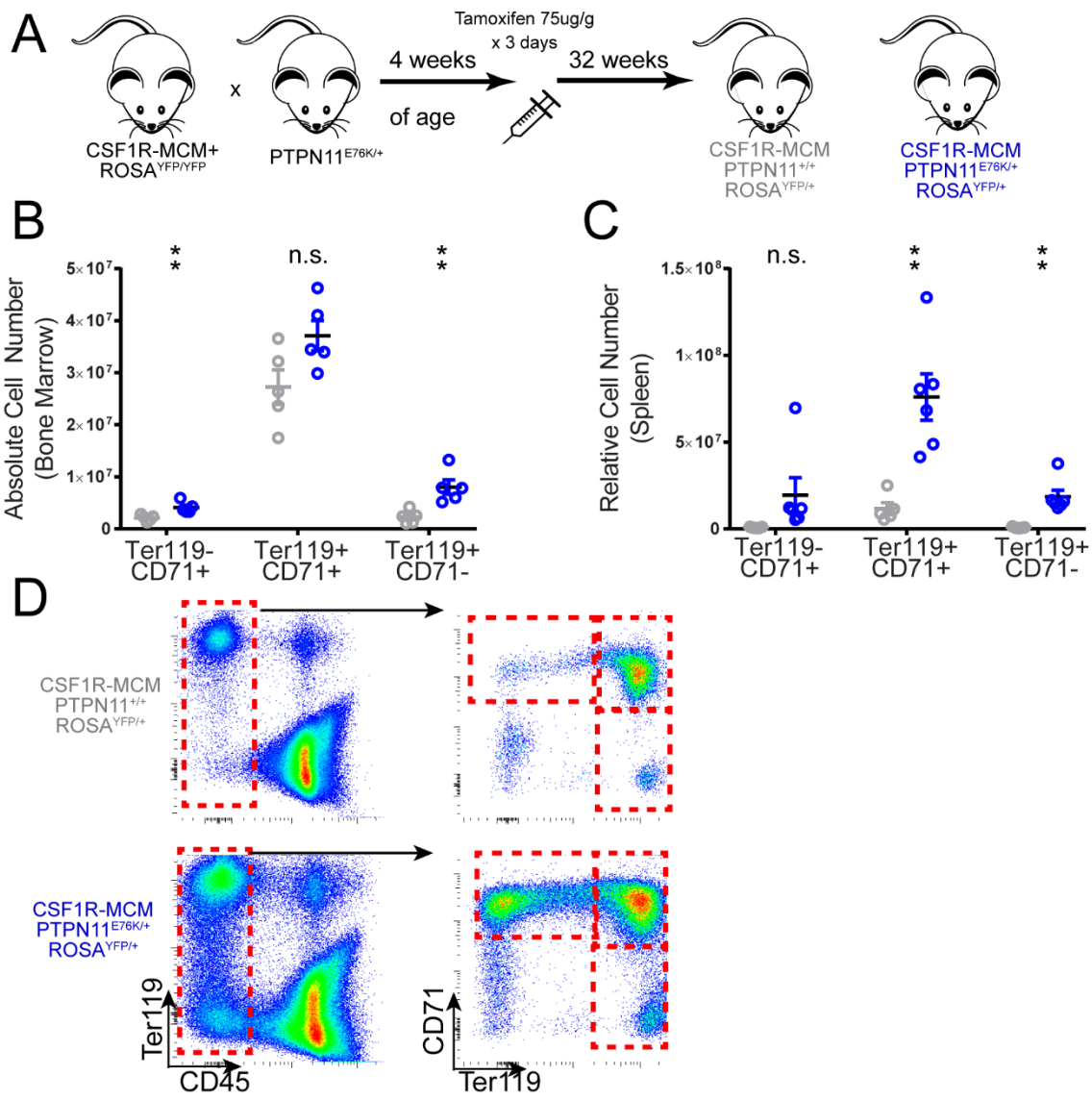

Figure II-31. Adult CSF1R-MCM; PTPN11^{E76K}: Erythroid Progenitors. A) Analysis was performed 32 weeks after tamoxifen treatment. B) Absolute cell number of BM erythroid progenitors in mutant and controls. E) Relative number of splenic erythroid progenitors in mutant and controls calculated by multiplying the frequency of progenitors by each animal's spleen weight. D) Representative flow cytometric plot of erythroid progenitors in mutant and control spleens.

progenitors at low cytokine doses (Figure II-32B). Since the frequency of YFP+ oncogene-expressing progenitors in these samples was only 10%, it is very unlikely for them to account cell-autonomously for the observed hypersensitivity. We proceeded to evaluate *RAS-ERK* signaling following GM-CSF stimulation in mutant animals (Figure II-33). Progenitors were cultured for 7days in medium containing 10ng/ml M-CSF in order to differentiate them into myeloid cells. Cells were then starved of serum for 4hrs and stimulated with 10ng/ml GM-CSF for 0, 10, or 30min. The level of pERK expression was measured using flow cytometry. YFP+ and YFP- cells had equal pERK expression at all doses of GM-CSF. In contrast, YFP+ and YFP- mutant cells both had higher pERK expression at 10min of stimulation compared to cells from littermates. However this preliminary study was not adequately powered and will be repeated. Importantly, when the same experiment was performed with sorted YFP+ and YFP- cells that were assayed independently, only YFP+ cells demonstrated features of JMML (Figure II-34). This finding strongly suggests that non-cell autonomous effects of oncogene-expressing YFP+ cells alter the GM-CSF sensitivity healthy YFP- progenitors that cohabit the same BM niche.

Discussion

We present the first study to directly compare the expression of a JMML mutation within three distinct hematopoietic phases. We demonstrate that both HSC-dependent and HSC-independent *in utero* progenitors that express the PTPN11^{D61Y} mutation bear defining molecular features of JMML patients: growth hypersensitivity in response to GM-CSF and hyperactive RAS-ERK signaling. We go on to show that YS EMPs are the HSC-independent progenitor responsible for this phenotype. Restricted expression of the PTPN11^{E76K} mutation in YS EMPs was unable to produce disease manifestations after transplantation into neonatal recipients or under unperturbed conditions following *in utero*

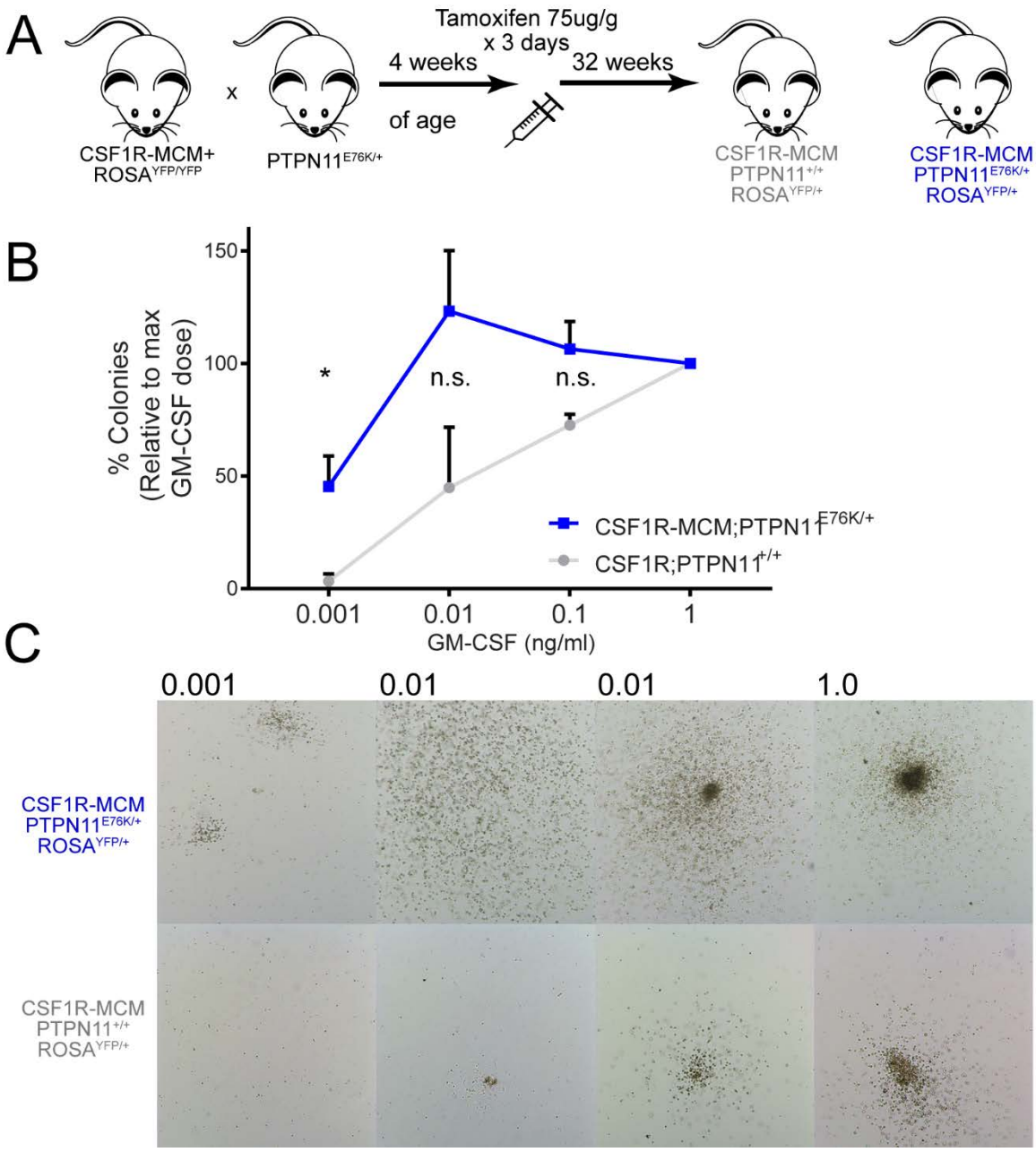

Figure II-32. Adult CSF1R-MCM; PTPN11^{E76K}: BM Progenitors are Growth Hypersensitive to GM-CSF. A) Methylcellulose assays were performed using unsorted BM from mutants and controls 32 weeks after tamoxifen. B) Relative colony number after 7days in culture. N=3 mutant and 3 control animals, each condition plated in triplicate. C) Representative images of colonies plated at indicated doses of GM-CSF (ng/ml).

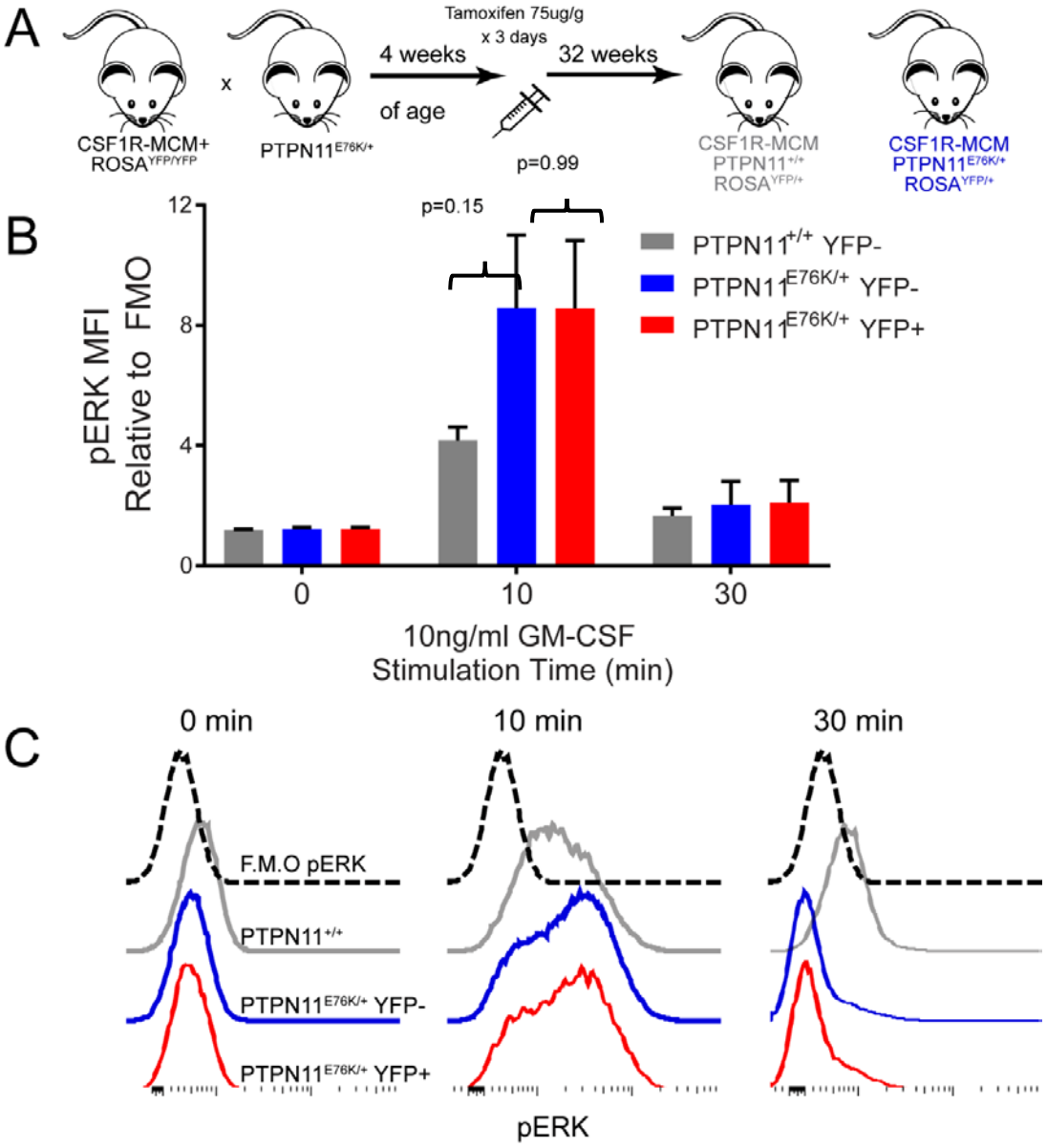

Figure II-33. Adult CSF1R-MCM; PTPN11^{E76K}: Co-Cultured YFP+ and YFP- Progenitors Have Equally Hyperactive *RAS* signaling. A) Signaling assays were performed using unsorted BM from mutants and control that was cultured in M-CSF for 7days (N=3/genotype). B) pERK mean fluorescence intensity (MFI) among control and mutant cells stimulated with 10ng/ml GM-CSF. Mutant YFP+ and YFP- cells were co-cultured and co-stimulated. C) Representative histograms of pERK in YFP+ mutant cells, YFP- mutant cells, and control cells. FMO=fluorescence minus one.

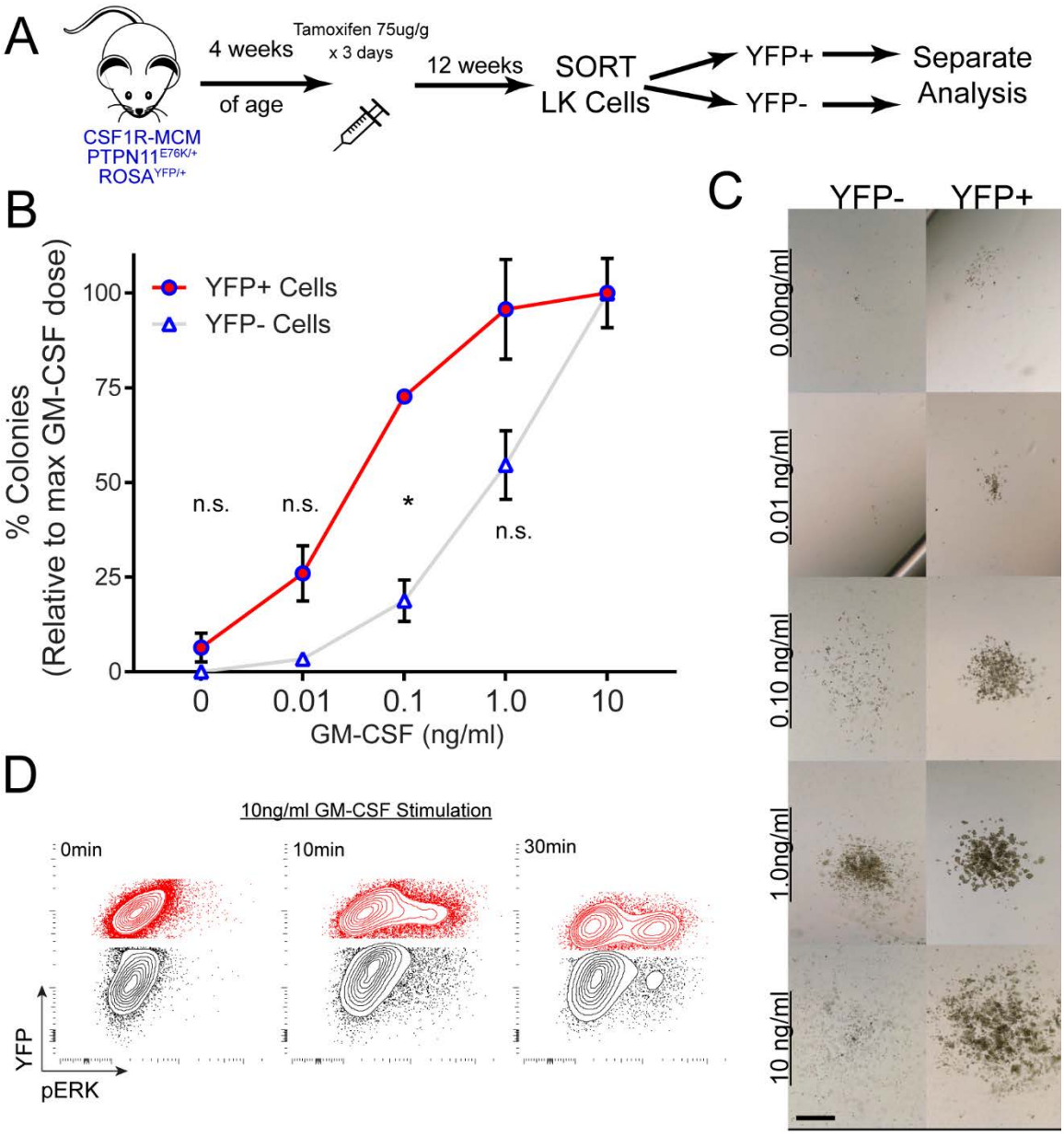

Figure II-34. Adult CSF1R-MCM; PTPN11^{E76K}: Sorted YFP+ and YFP- BM Progenitors Have Distinct Responses to GM-CSF. A) YFP+ and YFP- progenitors were sorted from mutant animals (N=2). B) Colony formation of YFP+ and YFP- progenitors from the same animal, plated separately. C) Representative images of colonies at indicated doses of GM-CSF, scale bar=0.5mm. D) Representative pERK expression in YFP+ and YFP- progenitors cultured separately in M-CSF for 7 days and stimulated separately with 10ng/ml GM-CSF.

expression with tamoxifen-inducible CSF1R-MCM. In contrast, PTPN11^{E76K} expression in fetal or adult HSC-dependent progenitors did produce evidence of MPN emergence.

In the adult cohort, we saw a striking expansion of mutant YFP+ cells in myeloid, B cell, and T cell lineages in the blood, BM, spleen, and thymus. This was accompanied by a concomitant increase of YFP+ multipotent, myeloid-restricted, and lymphoid-biased progenitors in the BM, spleen, and thymus. We also observed non-cell autonomous effects of the PTPN11^{E76K} mutation. There was a net increase in dendritic cells, neutrophils, and erythroid progenitors in the spleen along with a decrease of CD8+ T-lymphocytes. The thymus had an increase in net ETPs and dendritic cells and showed evidence of defective T-lymphocyte commitment 32 weeks after PTPN11^{E76K} expression. Finally, HSCs numbers were increased in the spleens of mutant animals and we observed GM-CSF hypersensitivity and *RAS-ERK* hyperactivation in both YFP+ and YFP- BM progenitors.

Previous studies have provided tantalizing evidence for the potential contribution of embryonic HSC-independent hematopoiesis to JMML. First, the strikingly high relapse rate following HSCT suggests that HSC-independent and myeloablation-resistant populations contribute to disease emergence (Locatelli et al. 2013). YS EMPs admirably match these criteria: they contribute to tissue macrophage populations in diverse tissues that are long-lived and relatively resistant to myeloablation (Gomez Perdiguero et al. 2015; Epelman et al. 2014; Hashimoto et al. 2013; Haniffa et al. 2009). Second, JMML patients acquire their disease-initiating mutations *in utero* (Matsuda et al. 2010). Finally, several studies have successfully modelled JMML using patient-derived iPSCs, whose differentiation pathways mimic that of embryonic—and not HSC-dependent—hematopoiesis (Gandre-Babbe et al. 2013; Mulero-Navarro et al. 2015; Vanhee et al. 2015; Buchrieser, James, and Moore 2017). This reasoning prompted us to hypothesize that expression of JMML-initiating mutations in embryonic HSC-independent progenitors would be sufficient for disease development (Chan and Yoder 2013).

We demonstrated the feasibility of this hypothesis with our initial VavCre; PTPN11^{D61Y} experiments. HSC-independent yolk sac EMPs from these embryos had two disease-defining features of JMML: growth hypersensitivity to GM-CSF and hyperactive *RAS-ERK* signaling. However, they were unable to give rise to disease manifestations either upon transplantation or following spatiotemporal-restricted expression using CSF1R-MCM. This lack of symptoms was not the result of experimental failures. Amazingly, and in contrast to previous reports (McGrath et al. 2015), we were able to show that mutation-bearing VavCre;PTPN11^{E76K} YS EMPs engrafted neonatal recipients and contributed to a self-replenishing macrophage population for at least 18 weeks after transplantation. Furthermore, in our CSF1R-MCM lineage trace studies, we demonstrated that all 1 year old mutant animals had YFP+ myeloid cells that had recombined their mutant PTPN11 locus. As such, we have strong evidence that in both of these studies HSC-independent progenitors persisted in adult tissues, expressed the JMML-initiating mutation, but were unable to give rise to a MPN.

There are several possible explanations for the lack of disease in our embryonic cohorts. First, YS EMPs may not possess the differentiation potential required for fulminant MPN emergence. Indeed, the long lived progeny of EMPs are tissue resident macrophages, which are functionally, transcriptionally, and epigenetically distinct from the monocytes/neutrophil lineage that is expanded in JMML patients (Lavin et al. 2014; Gosselin et al. 2014). Indeed, healthy EMPs are already so proliferative that oncogene expression had no effect on their expression of the cell-cycle marker Ki67. Furthermore, only 35% of E9.5 EMPs were targeted in our model. This is a much lower frequency than the >90% efficiency obtained from most published conditional mouse models, such as Mx1Cre or VavCre. Finally, whereas the CSF1R-MCM can only label EMPs between E8.5 and E9.5 (Gomez Perdiguero et al. 2015; Hoeffel et al. 2015), the transcriptional program that drives the emergence of EMPs begins between E6.5 and E7.5. The first EMPs

emerge at E8.25, continue to arise until as late as E11.5, and EMPs will proliferate until birth (Tanaka et al. 2012; Tober et al. 2013; Chen et al. 2011). As such, our system labels only a minority of one subset of EMPs and it is possible that other HSC-independent progenitors, including distinct EMP subpopulations and neonatal repopulating cells, may respond differently when expressing PTPN11 mutations (Frame et al. 2016; Sheng, Ruedl, and Karjalainen 2015; Yoder et al. 1997). Nonetheless, our results permit the conclusion that PTPN11^{E76K} expression in a subset of E9.5 YS EMPs does not result in an expansion of mutant macrophages and is not sufficient for MPN emergence in a mouse model of JMML.

HSC-dependent hematopoiesis is markedly different from that of yolk sac EMPs. HSC-dependent progenitors from the fetal and adult phases are more numerous, self-renew indefinitely, and produce cells from all lineages. Nonetheless, fetal progenitors differ from adult ones: the former are more proliferative, have greater repopulating potential, give rise to more myeloid colonies in semi-solid culture, have unique gene expression signatures, and have more lymphoid-biased long-term differentiation potential (Lansdorp, Dragowska, and Mayani 1993; Bowie et al. 2006; Bowie et al. 2007; Copley, Beer, and Eaves 2012; Copley et al. 2013). Additionally, strong evidence suggests that it is a fetal progenitor that is responsible for the emergence of JMML. Disease-initiating mutations are known to occur in utero and JMML is the only malignancy characterized by persistently elevated levels of fetal hemoglobin (Matsuda et al. 2010; Kratz et al. 2005; Weinberg et al. 1990).The fetal to adult transition has been inferred to occur at 2 years of age, which coincides with the mean JMML age of onset (Rufer et al. 1999; Sidorov et al. 2009). The majority of JMML patients have BM cells with a fetal-like gene expression signature, which further correlates with inferior prognosis. This same signature is present in only 10% of pediatric AML, 2% of pediatric ALL, and is absent from other pediatric MDS (Helsmoortel, De Moerloose, et al. 2016; Helsmoortel, Bresolin, et al. 2016) For this reason, we

hypothesized that PTPN11^{E76K} expression within a fetal progenitors would produce a more faithful JMML model than expression within adult progenitors.

Our study used fluorescent lineage trace methods to define the expression pattern of CSF1R-MCM following tamoxifen administration at E14.5 and at 4weeks of age. We show durable year-long contributions to peripheral lymphocytes from all lineages. This was the result of low efficiency labelling of HSCs either in the fetal liver or in the BM and spleen. In addition, we simultaneous labeled more committed progenitors including MPPs, and myeloid- and lymphoid-committed progenitors in the BM, spleen, and thymus. Importantly, we showed that there was negligible activity of CSF1R-MCM in mesenchymal, osteoblast, and endothelial lineages. As such, we confirmed that this model would meet our *a priori* criteria for evaluating the contribution of distinct hematopoietic phases to MPN. Namely: i) hematopoietic restricted expression; ii) spatiotemporally regulated; iii) low level efficiency to mimic the disease clonality; and iv), the ability to trace mutation-expressing cells using fluorescent molecules.

Both fetal and adult cohorts of CSF1R-MCM; PTPN11^{E76K} mice had evidence of MPN. The fetal cohort had an increase in net CD11b+ peripheral leukocytes compared to controls. It was surprising, however, that these animals did not show a net increase in %YFP+ cells and that there was no myeloid-biased differentiation among YFP+ cells. In contrast, the adult cohort showed a pronounced increase in %YFP+ cells. YFP+ cells in the adult cohort preferentially contributed to CD11b+ myeloid cells and showed diminished contributions to T-lymphocyte populations. This suggested that the oncogene caused a cell autonomous block in T-lymphocyte commitment in the adult cohort, which was not observed in the fetal cohort. Similar reductions in T-lymphocyte frequencies have been reported in the BM, spleen, and peripheral blood of patients (Oliveira et al. 2016; Krombholz et al. 2016). Furthermore, whereas patient's multipotent progenitors do express JMML-initiating mutations, the majority of peripheral T-lymphocytes do not

(Sakaguchi et al. 2013; Stieglitz, Troup, et al. 2015). This provides clinical validation of the decreased T cell frequencies in our adult cohort and suggests that a more focused clinical evaluation of T-lymphocyte subsets in patients is warranted.

We sought to evaluate the cellular mechanism for this T cell paucity in our adult cohort. The thymus of mutant animals was of normal size and there was a normal distribution of T-cell committed progenitors beyond the DN IIa stage. However, we did observe a striking increase in overall ETPs and dendritic cells in mutant animals. This suggests that the multipotent ETP may preferentially give rise to CD11c+ histiocytes, rather than commit to a T cell lineage (Luc et al. 2012). Indeed, we equally observed a decrease IL2Ra (CD25) expression among thymic progenitors committing to the T cell lineage. This suggests these progenitors may have a dampened response to IL2-mediated proliferative signals. It will be important to determine whether CD25 expression is equally reduced on peripheral T-lymphocyte populations, since such a deficiency is known to contribute to immunodeficiency and could explain the heightened susceptibility of JMML patients to infections (Caudy et al. 2007).

The ability to distinguish PTPN11$^{E76K/+}$ YFP+ cells from PTPN11$^{\Delta/+}$ YFP- cells permitted us to measure cell-autonomous and non-cell autonomous effects of the oncogene. The striking expansion of YFP+ progenitors and YFP+ mature progeny in the BM, spleen, thymus, and blood of mutant animals was indicative of the cell-autonomous effects of PTPN11^{E76K}. However, the frequency of YFP+ cells in each subset was only ~10%. We hypothesized, therefore, that any net differences in population size above a 10% change must be the result of non-cell autonomous effects. Indeed, we observed striking increases in the overall frequency of myeloid and dendritic cells in the spleens of mutant animals along with a concomitant decrease in CD8 T-lymphocytes. This was accompanied by an expansion of splenic HSCs. These net changes were characteristic

of other JMML mouse models where disease-initiating mutations had been knocked-in to the majority of hematopoietic cells (Chan, Kalaitzidis, et al. 2009; Xu et al. 2011)

This mobilization of HSCs may have been the result of an unfavourable niche in the BM, potentially due to the increased cycling and differentiation of downstream progenitors. Indeed, we observed a net decrease of LSK CD135+ CD34+ cells in mutants' bone marrow. Furthermore, when unsorted BM cells were plated in colony forming assays with increasing doses of GM-CSF, we observed a striking GM-CSF hypersensitivity with up to a 10-fold greater number of colonies. This difference could not have been accounted by the mere 10% of BM progenitors that are YFP+. This suggests that mutant YFP+ cells secrete factors that cause $PTPN11^{\Delta/+}$ YFP- cells to show features of JMML. An abnormal microenvironment has already been implicated in JMML. Increased reactive oxygen species, metabolic activity, and inflammatory cytokines have been described (Dong et al. 2016; Liu et al. 2016; Zheng et al. 2013). Our signaling experiments further implicate the microenvironment in JMML. Following GM-CSF stimulation YFP+ and YFP- cells had equal pERK expression; suggesting that they are equally sensitive to this cytokine. On the other hand, myeloid cells from control animals had markedly lower pERK expression than either YFP+ or YFP- cells from mutants. Furthermore, when YFP+ and YFP- cells were sorted from mutants and assayed separately, only the YFP+ fraction demonstrated features of JMML (Figure II-34). This suggests that it is the mutant niche – and not the mutation itself – that is the primary determinant of aberrant GM-CSF signaling. Below we outline future experiments that will more formally evaluate this hypothesis.

JMML patients present with both peripheral manifestations (leukocytosis, monocytosis, anaemia, thrombocytopenia) as well as tissue abnormalities (hepatosplenomegaly, hypercellular BM, cutaneous lesions). One intriguing feature of the three models presented herein is the divergence between the observations in tissues and observations in the peripheral blood. The HSC-independent cohort had YFP+ mutant cells

in the CNS, liver, and heart. Nonetheless, it showed no evidence of peripheral blood manifestations. Similarly, the adult cohort had pronounced hepatosplenomegaly and alterations in progenitor subsets; nonetheless it had a relatively indolent myeloproliferation in the peripheral blood. This suggests that the pathophysiology of the disease may include a latent period. Consider, the disease may initially alter tissue homeostasis, disrupt the BM microenvironment, and initiate extramedullary hematopoiesis. During this time, peripheral blood manifestations may remain undetectable. Given the *in utero* origin of JMML, such a latency period may occur before birth. Only after a sufficient disruption of normal hematopoiesis—potentially from exposure to *ex utero* pathogens—would the MPN become fulminant. Given the decreased T-lymphocyte frequencies, such pathogens may be particularly virulent for JMML patients and for our mutant animals. Indeed, despite the pathogen-free conditions of our animal facility, the few moribund mutant animals we observed had clear evidence of infection, including fulminant monocytosis and peritoneal abscesses. The decreased T-lymphocytes may, in part, explain such a susceptibility. While this notion of a latency period is speculative, it is inherently testable in our model and we outline our proposed future experiments below.

Our findings of non-cell autonomous effects of PTPN11 mutations further suggest why healthy donor HSCT failed to cure VavCre;PTPN11^{D61Y} mice. Any residual host cells that remained following myeloablation would have continued to exert paracrine effects on the healthy donor cells. As such, the environment of the host niche would never have recovered and would have continued to bear features of hyperactive *RAS-ERK* signaling. Nonetheless, the dominance of cell autonomous effects of mutations cannot be overlooked. Both in our animal model and in JMML patients, disease relapse after HSCT occurs from host cells. To our knowledge, there are no reports of JMML patients relapsing with donor-derived disease. Indeed, the importance of representative mouse models of rare hematologic disease such as JMML cannot be overstated.

In this light, consider that a significant proportion of hematopoietic studies rely on transplantations. They generate mutation-expressing progenitors and adoptively transfer them into myeloablated recipients. Post-transplantation hematopoiesis, however, is markedly different from unperturbed hematopoiesis (Busch and Rodewald 2016). Following transplantation, the vast majority of progenitors exhaust within the first few weeks; only a tiny fraction of cells will have durable multi-lineage contribution 4 months after transfer (Yamamoto et al. 2013). In contrast, progenitors in the context of unperturbed hematopoiesis have much greater lifespans (Busch et al. 2015; Sun et al. 2014; Henninger et al. 2017). Our CSF1R-MCM system can induce and monitor mutations in the context of unperturbed hematopoiesis and thereby avoids additional pitfalls of transplantation. For instance, whereas 90% of myeloid cells are labelled by FLT3Cre in unperturbed animals, this drops to nearly 50% following transplantation with a limiting dose of HSCs (Boyer et al. 2011). Additionally, transplantation will permit progenitors to undergo atypical differentiation patterns following exposure to non-physiologic signaling cues (Beaudin et al. 2016; Schlenner and Rodewald 2010). Finally, transplantation disrupts normal embryonic development by removing cells from their *in utero* conditions and transferring them into the foreign host environment. This can equally alter the differentiation potential of donor cells, as we observed in our YS EMP transplants. These readily contributed to splenic macrophage populations but did not contribute to microglia, which is the dominant progeny of YS EMPs in unperturbed hematopoiesis. Therefore, by forgoing transplantation, our studies rely on a more patient-relevant model that is compatible with unperturbed hematopoiesis.

Previous studies modeling myeloid disease with conditional PTPN11 mutant mice have relied on numerous Cre strains: VavCre, Mx1Cre, and LysMCre. Each one has purported benefits: VavCre as being active in all hematopoietic cells *in utero*, Mx1Cre as being inducible by pI:pC administration, and LysMCre as being restricted to the myeloid

lineage. In actuality, none of these claims are accurate. All three demonstrate Cre activity in non-hematopoietic cells, including endothelial cells, osteoblasts, mesenchymal stem cells, alveolar cells, and/or septal cells (Stadtfeld, Ye, and Graf 2007; Desai, Brownfield, and Krasnow 2014; Dong et al. 2016). LysMCre does show activity in up to 10% of B and T-lymphocytes (Ye et al. 2003), and Mx1Cre will become spontaneously active in up to 10% of HSCs by 5weeks of age due to endogenous interferon release (Sabnis et al. 2009). In contrast, we demonstrated that CSF1R-MCM shows no activity in the absence of tamoxifen and negligible activity in non-hematopoietic stromal and endothelial cells. As such, this is the first study to have evaluated the hematopoietic-restricted expression of $PTPN11^{E76K}$ in unperturbed hematopoiesis. Given that expression of other JMML-initiating mutations using VavCre, Mx1Cre, or LysMCre leads to lethality from non-hematopoietic causes (Staffas et al. 2015; Tang et al. 2013; Desai, Brownfield, and Krasnow 2014), it is challenging to directly compare our hematopoietic-restricted model with those published previously. Indeed, the rapid lethality observed in Mx1Cre; $PTPN11^{E76K}$ mice may have been the result of synergistically deleterious effects of the mutation on hematopoietic, endothelial, and stromal cells. This hypothesis is supported by a recent study that showed $PTPN11^{E76K}$ expression restricted to the stromal compartment is sufficient for MPN development (Dong et al. 2016). Therefore, we highlight the pitfalls of using Cre strains that are not cell type specific. We strongly advocate that future studies of neoplasms take advantage of lineage trace methods to monitor oncogene-expressing cells and to track the mutant allele frequency.

In summary, we have characterized the effect of $PTPN11^{E76K}$ expression restricted to three distinct hematopoietic phases. We have shown that the YS HSC-independent phase bears functional features of JMML but that it cannot initiate an MPN either upon transplantation or following unperturbed *in utero* expression. Expression within the fetal HSC-dependent phase causes a mild monocytosis but does not cause an overall

expansion or lineage skewing of YFP+ PTPN11^{E76K} cells. In contrast, expression within the adult HSC-dependent phase showed a drastic increase in YFP+ PTPN11^{E76K} cells and their biased differentiation into myeloid cells. Furthermore, we obtained strong evidence that expression of PTPN11^{E76K} alters the BM niche causing an egress of HSCs to the spleen and causing YFP- PTPN11$^{\Delta/+}$ cells to acquire functional features of JMML progenitors including growth hypersensitivity to GM-CSF due to hyperactive *RAS-ERK* signaling. As such, we have observed non-cell autonomous effects of low frequency hematopoietic restricted expression of PTPN11^{E76K}.

Ongoing Studies and Future Directions

The fetal and adult CSF1R-MCM;PTPN11^{E76K} cohorts described above are part of an ongoing study. We will continue to monitor them until 90 weeks of age. This prolongation of the current 40-60 week study will address key unanswered questions. Will the frequency of YFP+ leukocyte in mutants and controls remain stable? Will the number of T cells continue to decline with a concomitant increase in neutrophils? Will the hepatosplenomegaly continue to progress and will this be accompanied by further exacerbation of extramedullary hematopoiesis? These questions will be addressed by tissue analysis. Progenitors in the fetal cohort will prove particularly interesting given that these animals had an increase in net peripheral neutrophils, but that YFP+ cells did not show a myeloid-bias. This analysis will therefore permit us to further evaluate pathologic features that are distinct between the fetal and adult cohorts.

We will also be better able to correlate MPN features in the peripheral blood with the concomitant progenitor abnormalities in tissues. This will permit us to draw conclusions as to the potential latency period of hematopoietic-restricted PTPN11^{E76K} expression. For instance, it is possible that 90 weeks after tamoxifen administration, in addition to progenitor hypersensitivity to GM-CSF, we may also observe a fulminant MPN in the

peripheral blood. This would support our hypothesis of a latency period between tissue abnormalities and peripheral blood manifestations following clonal JMML-initiating mutations. The prolongation of the study will also make our survival analyses more robust.

It will be imperative to determine the sensitivity and specificity of YFP as a readout for PTPN11^{E76K} expression. Do only YFP+ cells express PTPN11^{E76K}? To answer this question we will use published quantitative PCR protocols that measure the amount of the non-recombined allele (Dong et al. 2016). We will isolate YFP+ and YFP- cells from the blood, spleen, and BM of mutant animals, isolate genomic DNA, and compare the abundance of the non-recombined allele to a reference allele. We anticipate that all sorted YFP+ cells would express the mutation and have little non-recombined allele. In contrast, we anticipate YFP- cells will have complete retention of their non-recombined allele. This would confirm that only YFP+ cells can express the mutation and would validate our conclusions regarding the non-cell autonomous effects of the PTPN11^{E76K} mutation.

Interestingly, we have already obtained some functional data that supports our hypothesis that only YFP+ cells express the mutation (Figure II-34). We sorted YFP+ and YFP- myeloid progenitors from mutant animals and plated them in methylcellulose assays with increasing doses of GM-CSF. YFP+ progenitors demonstrated a marked GM-CSF hypersensitivity compared to the YFP- progenitors that had developed in the same BM niche. Furthermore, when *RAS-ERK* signaling was measured in these sorted progenitors we observed a pronounced hyperactivity in YFP+ cells that was not observed in YFP- cells. This suggests that when cultured in isolation, YFP+ cells behave as JMML-initiating cells whereas YFP- progenitors from the same animal and niche have normal function. This would suggest that the oncogene is indeed only expressed in YFP+ cells. This preliminary experiment will need to be repeated to provide robustness to our conclusions.

These findings also suggest that YFP+ mutant cells do not exert an irreversible effect on the healthy YFP- progenitors. Instead, it suggests that short acting paracrine signals

from mutant cells act directly on healthy progenitors—without first affecting a stromal cell intermediate. Going forward, we will repeat our GM-CSF hypersensitivity and pERK experiments with unfractionated BM cells. Next, we will repeat pERK signaling experiments with three co-cultured cell types: i) YFP+ cells from a mutant animal; ii) YFP- cells from a mutant animal; and iii) CD45.1+ cells from a healthy animal. If CD45.1+ cells have hyperactive signaling, this would confirm the paracrine signal is secreted by the mutant YFP+ cells and would be present in the medium. In contrast, if YFP+ and YFP- cells are hyperactive but CD45.1+ cells are not, this would suggest that the paracrine signal is restricted the BM niche. We will then proceed to measure cytokine levels in the mutant BM and compare it to that of healthy controls. In so doing, we will identify several candidate molecules that may mediate the observed non-cell autonomous effects. Likely candidates are IL1β, CCL3, CXCL12, and TNFα, all of which have been shown to mediate leukemogenic and/or inflammatory effects in tissue niches (Dong et al. 2016; Randhawa et al. 2016; Schiwon et al. 2014). However, novel targets may equally be identified. We would validate them through pharmacological inhibition to see if the MPN features of YFP- cells can be reversed.

Finally, we have demonstrated that the monocytosis in our adult cohort is accompanied by a concomitant decrease in CD8+ T-lymphocytes with additional evidence of abnormal T-lineage commitment in the thymus. We speculate that this may render our animals immune compromised. Whereas we did observe moribund animals with overt evidence of infection, this was not common due to the pathogen-free conditions in which our animals were housed. Therefore, to directly test whether our animals have a compromised immune response, we propose to directly challenge them with an exogenous pathogen (Castro, Dee, and Malek 2012). Mice will be inoculated with *L. monocytogenes* and survival will be monitored. We hypothesize that mutant animals will be more susceptible to infection and death due to a diminished number of CD8 effector T-

lymphocytes. In follow up experiments, we would immunize mutant and littermate animals with the ovalbumin (OVA) peptide and then challenge them 4 weeks later with an *L. monocytogenes* strain that expresses the OVA. This would help determine whether CD4 memory T cells have acquired memory to OVA and are able to help clear infections. Given that JMML patients may have decreased and/or abnormal T-lymphocyte functions and are prone to infections, these studies would help determine the degree to which JMML patients should be protected from pathogen exposure.

In summary, we have described the first mouse model that has hematopoietic restricted expression of $PTPN11^{E76K}$ that is spatiotemporally restricted to distinct developmental phases. We show that whereas YS EMPs do not contribute to disease development, HSC-dependent progenitors from fetal and adult phases provoke a MPN. The adult cohort in particular has pronounced expansion of mutation-expressing cells in all lineages. Using our model we have defined non-cell autonomous effects of hematopoietic-restricted $PTPN11^{E76K}$ expression. We observe extramedullary hematopoiesis, and both YFP+ and YFP- progenitors are hypersensitive to GM-CSF due to hyperactive RAS signaling. These findings provide insight into the hematopoietic niche of JMML patients and suggest that future therapies will need to mitigate the deleterious effects that mutant cells exert on healthy clones.

CHAPTER III

MODELING JMML WITH KRAS^{G12D} MUTATIONS IN MICE

Abstract

Juvenile Myelomonocytic Leukemia is a pediatric myeloproliferative disorder that bears distinct characteristics of a fetal origin. This disease has been extensively modeled with mice bearing conditional JMML-initiating mutations. However, these studies have failed to recapitulate defining features of the disease due to *in utero* lethality, non-hematopoietic expression, and the pervasive emergence of T-ALL. We present a novel model of JMML using FLT3Cre;Kras^{G12D} mice that express Kras^{G12D} *in utero,* are born at normal Mendelian ratio, develop hepatosplenomegaly, anaemia, thrombocytopenia, and succumb to a rapidly progressing and fully penetrant neonatal myeloid disease. FLT3Cre;Kras^{G12D} mice have altered HSC and progenitor populations that are hypersensitive to GM-CSF due to hyperactive *RAS-ERK* signaling. These progenitors have biased differentiation that results in an expansion of neutrophils and dendritic cells with a concomitant decrease in T-lymphocytes. These features can be evoked upon fetal liver transplantation but not upon transplantation of BM progenitors from moribund animals. FLT3Cre;PTPN11^{E76K} mice have an indolent MPN progression and show diminished T-lymphocyte populations. In contrast, CSF1R-MCM; Kras^{G12D} mice develop T-ALL with complete penetrance, irrespective of whether the mutation was expressed in fetal or adult progenitors. In summary, we describe FLT3Cre; Kras^{G12D} as the first mouse model that reproducibly develops a faithful JMML-like disease with this oncogene. This model will prove useful for pre-clinical drug studies and for elucidating the developmental origins of pediatric neoplasms.

Introduction

A. *Ras* Mutations in JMML

Ras proteins are inner plasma membrane-bound GTPases that bind guanosine triphosphate (GTP) and hydrolyze it to guanosine diphosphate (GDP). This hydrolysis reaction is spontaneous, but is catalyzed by mediators including neurofibronin, which is encoded by *NF1.* Ras-GDP is inactive; Ras-GTP is active and can promote signaling via downstream mediators such as the MEK-ERK cascade or Phosphoinositide 3-kinase. These signaling events are vital for numerous biological processes including proliferation, differentiation, apoptosis, and migration (Lodish et al. 2000).

Given the growth-promoting properties of Ras, it may be expected that aberrant Ras signaling would be involved in tumorigenesis. Indeed, *Ras* genes were the first identified oncogenes and they are the most frequently mutated alleles in human cancers (Hunter et al. 2015; Parada et al. 1982). Strikingly, most *Ras* mutations are SNPs, a single amino acid substitution will inhibit the hydrolysis of GTP and lock Ras in an active state. Despite the frequency of *Ras* mutations in cancer, initial studies suggested that in isolation they were not sufficient to initiate tumorigenesis; secondary mutations that target complementary cancer hallmarks—such as immune evasion and DNA repair—were deemed necessary for Ras-induced malignancy (Seeburg et al. 1984; Hanahan and Weinberg 2011).

It was surprising, therefore, to discover that 20-25% of JMML patients harbor mutations in *Nras* or *Kras* (Flotho et al. 1999) and that these polymorphisms are frequently the only genetic abnormality identified in these children (Stieglitz, Taylor-Weiner, et al. 2015; Sakaguchi et al. 2013). This demonstrates that *Ras* mutations are sufficient for the development of pediatric MPN. However, the prognosis of children with somatic *Ras* mutations in hematopoietic cells is unpredictable. Whereas gain of function PTPN11 mutations confer a uniformly poor prognosis without transplantation, there are a subset of

patients with *Ras* mutations who show no signs of disease even into adulthood (Calvo et al. 2015). It has been proposed that these patients have a distinct disorder termed Ras-associated autoimmune leukoproliferative disorder (RALD). However, apart from their clinical course, no features that distinguish RALD and JMML have been identified. Clinicians continue to debate whether these are distinct disorders (Anastas and Calvo 2016).

Interestingly, aberrant Ras function in JMML may occur independently of mutation via DNA methylation. One group has reported that *RASA4* hypermethylation is frequently observed in JMML patients irrespective of the causative genetic mutation and that this modification is associated with an inferior prognosis (Poetsch et al. 2014). This finding further supports the prevailing hypothesis that multiple complementary lesions targeting the RAS-ERK pathway confer worse prognosis to JMML patients (Caye et al. 2015). Importantly, aberrant DNA methylation is widespread in JMML and not restricted to *Ras* genes. Cell cycle mediators that are known to be tumor suppressor genes, such as p15/INK4b encoded by *CDKN2B* and p16 encoded by *CDKN2A,* are hypermethylated in JMML patients (Hasegawa et al. 2005). Indeed, DNA methyltransferase inhibitors have shown some *in vitro* efficacy in reversing the abnormal methylation patterns observed in JMML patients (Wilhelm et al. 2016). Such therapeutic strategies hold promise for *Ras* associated malignancies given that direct pharmacological inhibition of Ras has not been possible (McCormick 2015). Indeed, one clinical trial using DNA methyltransferase inhibitors in JMML is already recruiting patients (NCT02447666). It is therefore important to find animal models that can recapitulate Ras-induced JMML and determine if they have evidence of aberrant DNA methylation. Such a representative model would permit testing of new therapeutic strategies for a disease with a very poor prognosis.

B. FLT3Cre: a Tool in the Study of Fetal Hematopoiesis

We have described in Chapter I the rationale and mechanism of the Cre-loxP system. This is a powerful tool to introduce mutations in animals within specific cell populations and at specific developmental stages. The specificity of the system relies on the cis-regulatory elements that control the expression of the Cre recombinase. We described in detail that the most common Cre strains used to study hematopoiesis and myeloid development–VavCre, Mx1Cre, LysMCre–are all expressed in non-hematopoietic tissues and have poorly characterized temporal expression. Researchers have therefore sought to develop new Cre strains whose expression would be more predictable and restricted to hematopoietic lineages.

The fms-like tyrosine kinase 3 (FLT3; also called Flk2, CD135) is a receptor tyrosine kinase that binds the growth-promoting cytokine FLT3L. *FLT3* is highly expressed in hematopoietic progenitor cells and in other unfractionated tissue samples including brain, placenta, kidney, heart, lung and germ tissues (Matthews et al. 1991). Subsequent studies revealed that within the LSK progenitor population, further depletion of cells expressing FLT3 would enrich for long-term serial repopulating potential (Christensen and Weissman 2001). This suggested that expression of FLT3 was among the first genes upregulated following asymmetric HSC division and differentiation. This hypothesis was confirmed in subsequent studies that identified the LSK FLT3+ cells as the multipotent progenitor (MPP), capable of contributing to all blood lineages but without indefinite self-renewal (Yamamoto et al. 2013). These studies suggested that all hematopoietic cells derived from a *FLT3*-expressing intermediate progenitor.

This hypothesis was formally tested using FLT3Cre;ROSA26$^{mTmG/mTmG}$ mice and a clever lineage trace strategy (Boyer et al. 2011). In this model, cells that express *FLT3* will undergo a fluorescent switch from Tomato to GFP (Figure III-1A). This is achieved through the irreversible excision of a loxP-flanked DNA sequence that encodes both the Tomato

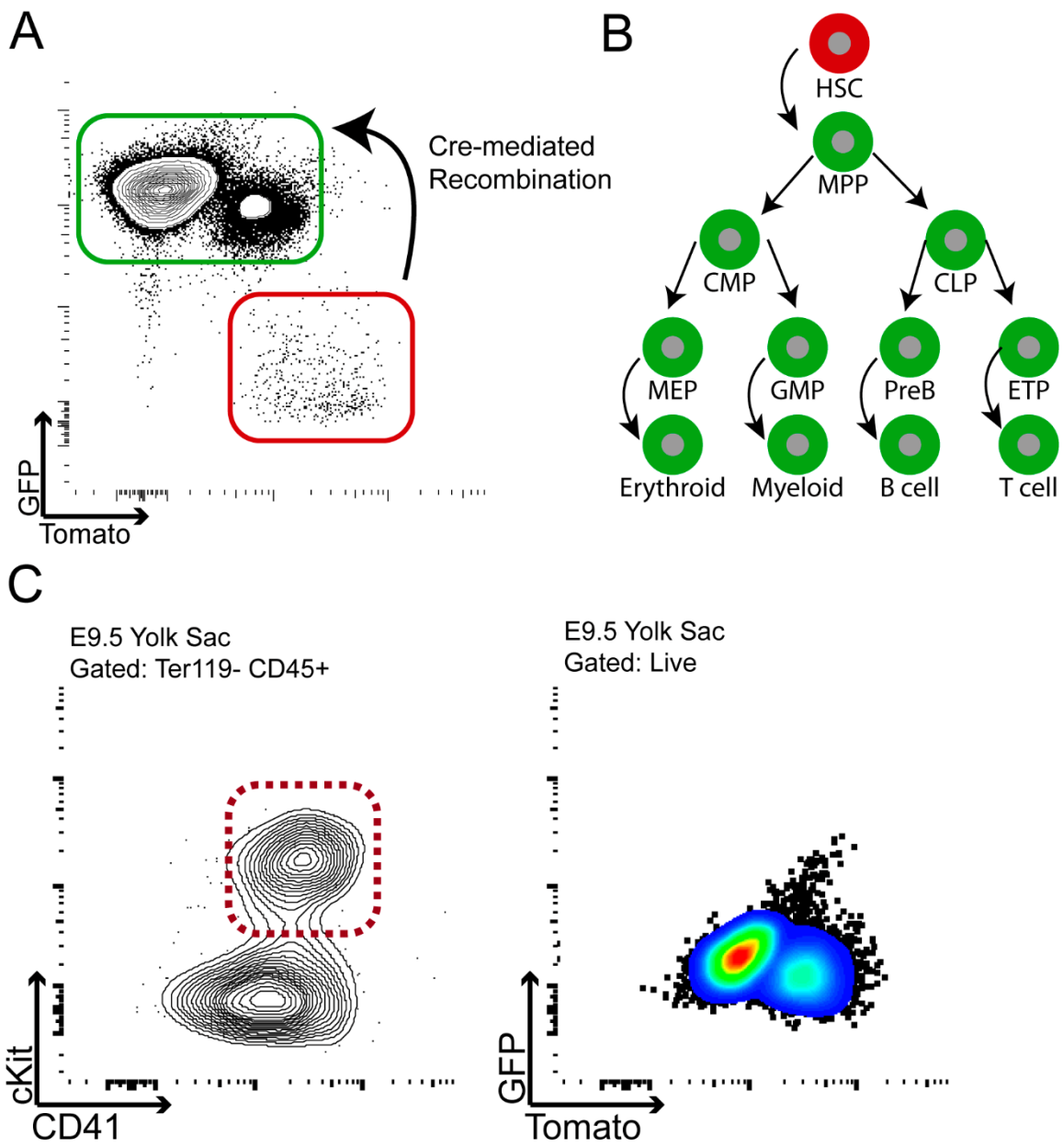

Figure III-1. Analysis of FLT3Cre Activity in HSC-Dependent and HSC-Independent Hematopoiesis. A) Cells that have active Cre recombinase can be monitored by flow cytometry by the irreversible switch from Tomato+ to GFP+ expression. B) FLT3Cre activity was shown to begin in MPPs; it is not active in HSCs in adult BM. C) FLT3Cre activity in E9.5 yolk sacs. No GFP+ cells were observed, including among EMPs, gated in red.

allele and a STOP cassette. The removal of both permits the expression of GFP, which will continue to be expressed in all progeny. This group showed that >90% of myeloid, B cell, T cell, erythroid, and platelet populations were GFP+. Furthermore, they identified that phenotypic HSCs were Tomato+ and that the switch to GFP expression occurred in the MPP compartment. Subsequent functional studies confirmed that only Tomato+ LSK cells from adult BM could be serially transplanted; GFP+ LSK cells had only transient contributions in recipients (Boyer, Beaudin, and Forsberg 2012). These experiments confirmed that FLT3Cre was active downstream of HSCs and that it would label the majority of mature hematopoietic cells in adults (Figure III-1B).

Subsequent studies sought to further characterize the precise embryonic populations labelled by FLT3Cre. Interestingly, it was shown that E8.5 activated CSF1R-MCM and FLT3Cre were active in mutually exclusive populations in the fetal liver (Gomez Perdiguero et al. 2015; Epelman et al. 2014). Additional studies showed that FLT3Cre was not active in HSC-independent hematopoietic cells (Hoeffel et al. 2015), and we independently confirmed that E10.0 Ter119- cKit+ CD45+ yolk sac EMPs were not labelled in all 5 analyzed embryos (Figure III-1C). This feature would prove useful in further discerning the contributions of HSC-independent and HSC-dependent embryonic hematopoiesis to adult tissues. Elegant studies that directly compared (E8.5) CSF1R-MCM and FLT3Cre contributions to myeloid tissues showed that all brain microglia were derived from the yolk sac, all adult intestinal macrophages were HSC-derived, and heart, liver, lung and spleen macrophages had contributions from both phases (Epelman et al. 2014; Bain et al. 2014). Thus, FLT3Cre is a useful tool to distinguish HSC-independent from HSC-dependent hematopoiesis.

Early studies also suggested that FLT3 expression may be able to distinguish fetal vs. adult HSC-dependent hematopoiesis. Whereas FLT3+ LSK cells from adult BM could not self-renew upon transplantation, FLT3+ LSK cells from E14.5 fetal liver cells did

engraft and produce multilineage progeny (Christensen and Weissman 2001). More recent studies using FLT3Cre;ROSA26$^{mTmG/mTmG}$ mice also suggested that a small proportion of fetal HSCs were FLT3+. Given that FLT3 signaling strongly promotes proliferation and that fetal HSCs are actively cycling, the expression of this receptor on fetal HSCs may be an adaptation to promote their rapid growth. Furthermore, these studies suggested a functional difference: that FLT3+ HSCs preferentially gave rise to innate-like lymphoid cells, such as peritoneal B1a and B1b populations.

These studies, however, had numerous shortcomings. First, they transplanted bulk populations of FLT3+ cells. As such, they were unable to evaluate the clonal contribution to progeny—a defining feature of HSCs. Additionally, these studies relied on adoptive transfer experiments; they did not consider if FLT3+ fetal cells functioned as HSCs under unperturbed hematopoiesis. Indeed, evidence suggests that they do not. Since GFP+ cells in adult FLT3Cre;ROSA26$^{mTmG/mTmG}$ mice cannot be transplanted, this indicates that fetal FLT3+ HSCs do not self-renew under homeostatic conditions. Additionally, if FLT3+ fetal progenitors contribute to long-lived innate lymphoid populations, one would expect these populations to have a high frequency of GFP expression. There is no supporting evidence for this in the manuscript. Indeed, our preliminary experiments using unperturbed FLT3Cre;ROSA26$^{mTmG/mTmG}$ mice showed that peritoneal B1a and B1b populations had a lower frequency of GFP expression that BM-derived B2 populations (Figure III-2). As such it is possible that the insights drawn from FLT3+ fetal HSCs are the result of non-physiologic potentials evoked by transplantation. The physiological and developmental relevance of FLT3+ fetal HSCs in unperturbed conditions remains unclear.

Following the differentiation of FLT3+ MPPs, FLT3 is re-expressed on certain hematopoietic cells. Committed lymphoid progenitors (CLPs) and both B-cell restricted and T-cell restricted progenitors express FLT3. This is contrast to common myeloid progenitors (CMPs), which do not express FLT3 (Karsunky et al. 2008). As such, lymphoid

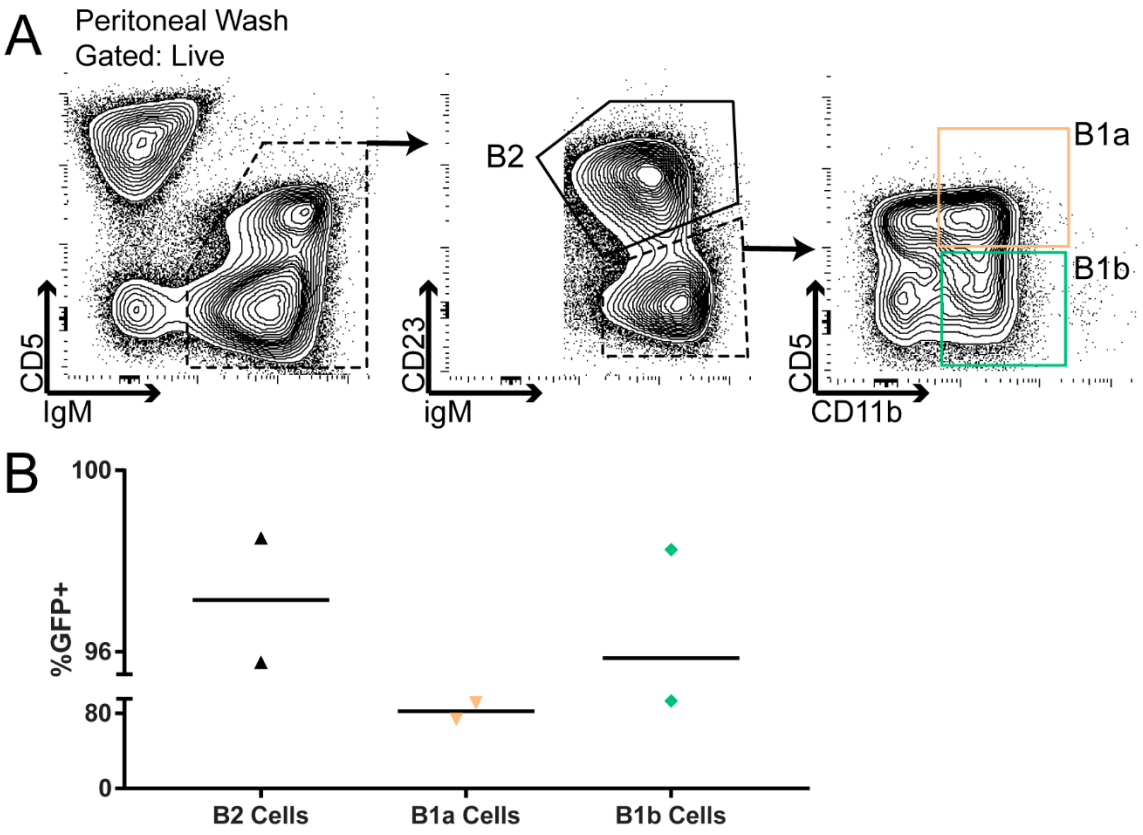

Figure III-2. FLT3Cre Activity in Peritoneal B-Lymphocytes. A) Gating strategy to identify adaptive B2 cells and innate-like B1a and B1b cells. B) Assessment of GFP+ cells in the above gated populations. This study was not adequately powered to detect a difference. This experiment was performed with assistance from Momoko Yoshimoto.

cells in FLT3Cre;ROSA26$^{mTmG/mTmG}$ mice have additional opportunities to transition through a FLT3+ intermediate and thus a greater proportion of them are GFP+ compared with myeloid cells. However, dendritic cells (DCs) are the only mature hematopoietic population to express *FLT3* (Waskow et al. 2008). Since DCs are ubiquitous in all tissues, the original reports showing *FLT3* expression in non-hematopoietic organs need to be re-evaluated. It remains unclear whether *FLT3* expression is restricted to hematopoietic cells. Further complicating this analysis is the finding of multiple transcript lengths encoded by *FLT3.* This suggests context-specific or tissue-specific *FLT3* expression.

Of relevance to our study is the spatiotemporal activity of FLT3Cre, which may be different from the expression pattern of the protein itself. For instance, CSF1R-Cre activity has been shown to only partially overlap with the receptor's expression (Hoeffel et al. 2015). Unfortunately, the original characterization of the FLT3Cre animal did not provide sufficient detail to know the sequence of the cis-regulatory elements that drive Cre expression (Benz et al. 2008). As such, FLT3Cre activity must be measured functionally using a lineage trace strategy such as ROSA^{mTmG}. To date, no reports have suggested non-hematopoietic activity of FLT3Cre mice and we determined it is not expressed in lung and BM endothelial cells. In so doing, we have shown FLT3Cre overcomes the major specificity hurdle of Mx1Cre, VavCre, and LysMCre. As such, we deemed it the best model with which to evaluate hematopoietic-restricted expression of JMML-initiating mutations.

C. Rationale for the FLT3Cre+;Kras^{G12D} Model of JMML

Juvenile Myelomonocytic Leukemia is a pediatric myeloproliferative disorder caused by somatic mutations in RAS-ERK signaling genes, including *KRAS*, *NRAS*, *PTPN11*, *NF1*, and *c-CBL* (Chan, Cooper, et al. 2009). These mutations result in a hypersensitivity of hematopoietic progenitors to GM-CSF and lead to monocytosis, anaemia, thrombocytopenia, hepatosplenomegaly, and infiltration of peripheral tissues

with histiocytes (Loh 2011; Ng et al. 1988). Compared to other pediatric hematologic malignancies, the prognosis of JMML patients is very poor. Allogeneic hematopoietic stem cell (HSC) transplantation is the only curative therapy, which nonetheless has a 5 year overall survival of only 52% (Locatelli et al. 2013).

The majority of JMML cases result from a mutation in a single gene (Stieglitz, Taylor-Weiner, et al. 2015; Sakaguchi et al. 2013; Caye et al. 2015). As such, disease models using the most common JMML-initiating mutations have been readily generated (Xu et al. 2011; Chan, Kalaitzidis, et al. 2009; Le et al. 2004). The Mx1Cre;$Kras^{G12D}$ mouse was the first conditional animal model of JMML and continues to be studied extensively (Braun et al. 2004). However, these mice ultimately die from non-hematopoietic $Kras^{G12D}$ expression or from T cell acute lymphoblastic leukemia/lymphoma (T-ALL) (Kindler et al. 2008; Kong et al. 2013; Staffas et al. 2015; Sabnis et al. 2009). *In utero* $Kras^{G12D}$ expression using LysMCre or VavCre have led to lung adenocarcinoma or to prenatal lethality, respectively, both from non-hematopoietic expression of the oncogene (Desai, Brownfield, and Krasnow 2014; Tang et al. 2013). Thus, existing $Kras^{G12D}$ models have failed to address the fetal origin of JMML and have failed to recapitulate the myeloid nature of the disease.

Converging clinical evidence suggests that the origin of JMML is closely associated with fetal development. Patients present very young with a median age of <2years and retrospective analyses of tissue samples collected at birth suggest that the majority of patients acquire the somatic disease-initiating mutation *in utero* (Kratz et al. 2005; Matsuda et al. 2010; Locatelli and Niemeyer 2015). Furthermore, bone marrow progenitors of most patients exhibit a fetal-like gene expression signature, which correlates with an inferior prognosis (Helsmoortel, Bresolin, et al. 2016). These findings strongly implicate a developmental origin of JMML and imply that a genetic alteration must occur within an appropriate spatial and temporal context to initiate this disease.

Fetal hematopoietic progenitors are functionally distinct from adult progenitors. Murine fetal progenitors have greater engraftment efficiency, biased lineage differentiation, and altered susceptibility to transformation compared with adult counterparts (Bowie et al. 2006; Bowie et al. 2007; Benz et al. 2012; Copley et al. 2013; Yuan et al. 2012; Porter et al. 2016). Analogous studies in humans showed fetal and cord blood CD34+ cells are more proliferative and have a greater propensity to form myeloid colonies in methylcellulose culture than adult BM cells (Lansdorp, Dragowska, and Mayani 1993; Broxmeyer et al. 1992). These characteristics of fetal progenitors suggest a mechanism through which they may evoke clinical features of JMML when challenged with a somatic oncogenic mutation.

We hypothesized that temporal expression of $Kras^{G12D}$ during fetal hematopoiesis and limited functionally to the hematopoietic progenitor population would produce a JMML-like disease. Recently, the expression pattern of FLT3Cre has been extensively studied using lineage-tracing methods (Boyer et al. 2011; Epelman et al. 2014). FLT3Cre activity begins in multipotent progenitors (MPPs) at embryonic day E10.5 and it is subsequently observed in >90% of mature leukocytes. We now demonstrate that $Kras^{G12D}$ is sufficient to produce a perinatal myeloproliferative disease when expressed in fetal hematopoietic progenitors using FLT3Cre. We have thereby defined the crucial cellular and developmental environment needed to produce authentic features of $Kras^{G12D}$-induced JMML.

Results

A. FLT3Cre+;$Kras^{G12D}$ Mice Develop A Transplantable JMML-Like Myeloid Disease

We mated $FLT3Cre^{+}$;$ROSA^{mTmG/mTmG}$ studs with $Kras^{G12D/+}$ dams to generate $FLT3Cre^{+}$;$ROSA^{mTmG/+}$;$Kras^{G12D/+}$ mice (hereafter FLT3Cre;$Kras^{G12D}$) in which oncogene expression can be monitored by a switch from Tomato to Green Fluorescent Protein (GFP)

expression. FLT3Cre;Kras^{G12D} mutants were born at expected Mendelian ratio and had weight gain comparable to littermates until 2 weeks of age (Figure III-3A,B). Mutants and littermates had equivalent activity of FLT3Cre as measured by %GFP+ cells and *Kras^{G12D}* expression in mutant mice was confirmed by PCR (Figure III-1C,D). After 2 weeks, FLT3Cre;Kras^{G12D} mice showed progressive weight loss, leukocytosis, anaemia, thrombocytopenia, hepatosplenomegaly, and died at a median age of 26 days (Figure III-4). Histological organ examination revealed a monocytic infiltrate in the liver and spleen and a marked expansion of CD11b+ Gr1+ cells in the blood, spleen, liver, and bone marrow (BM) was confirmed by flow cytometry (Figure III-5). Notably, the frequency of CD3+ T-lymphocytes and B220+ B-lymphocytes was decreased and FLT3Cre;Kras^{G12D} mice had an atrophied thymus compared to littermates (Figure III-4C). Consistent with a faithful model of hyperactive Ras-induced JMML, BM progenitors from FLT3Cre; Kras^{G12D} animals demonstrated hypersensitivity to GM-CSF in colony forming assays which was corrected by MEK inhibition (Figure III-6). This was strong evidence of hyperactive Ras-ERK signaling. However, as previous studies have shown (Braun et al. 2004), myeloid cells derived from BM progenitors of moribund mutant animals did not demonstrate elevated phosphorylation of ERK (Figure III-7).

To confirm the disease in FLT3Cre;Kras^{G12D} animals was initiated *in utero* and could be propagated autonomously *in vivo*, we transplanted E14.5 fetal liver cells into adult BoyJ animals (Figure III-8). Progenitors from mutant donors showed robust engraftment, and rapidly contributed to monocytosis, anaemia, and thrombocytopenia (Figure III-8B,C). Recipients of mutant cells succumbed to a JMML-like myeloid disease with a median survival of 9 weeks (Figure III-8D). At analysis, mutant recipients had hepatosplenomegaly with expanded donor-derived myeloid populations in the BM and spleen (Figure III-8E-I). In stark contrast to other Kras^{G12D} models, primary recipients of FLT3Cre;Kras^{G12D} progenitors did not develop enlarged thymuses or show signs of T-ALL.

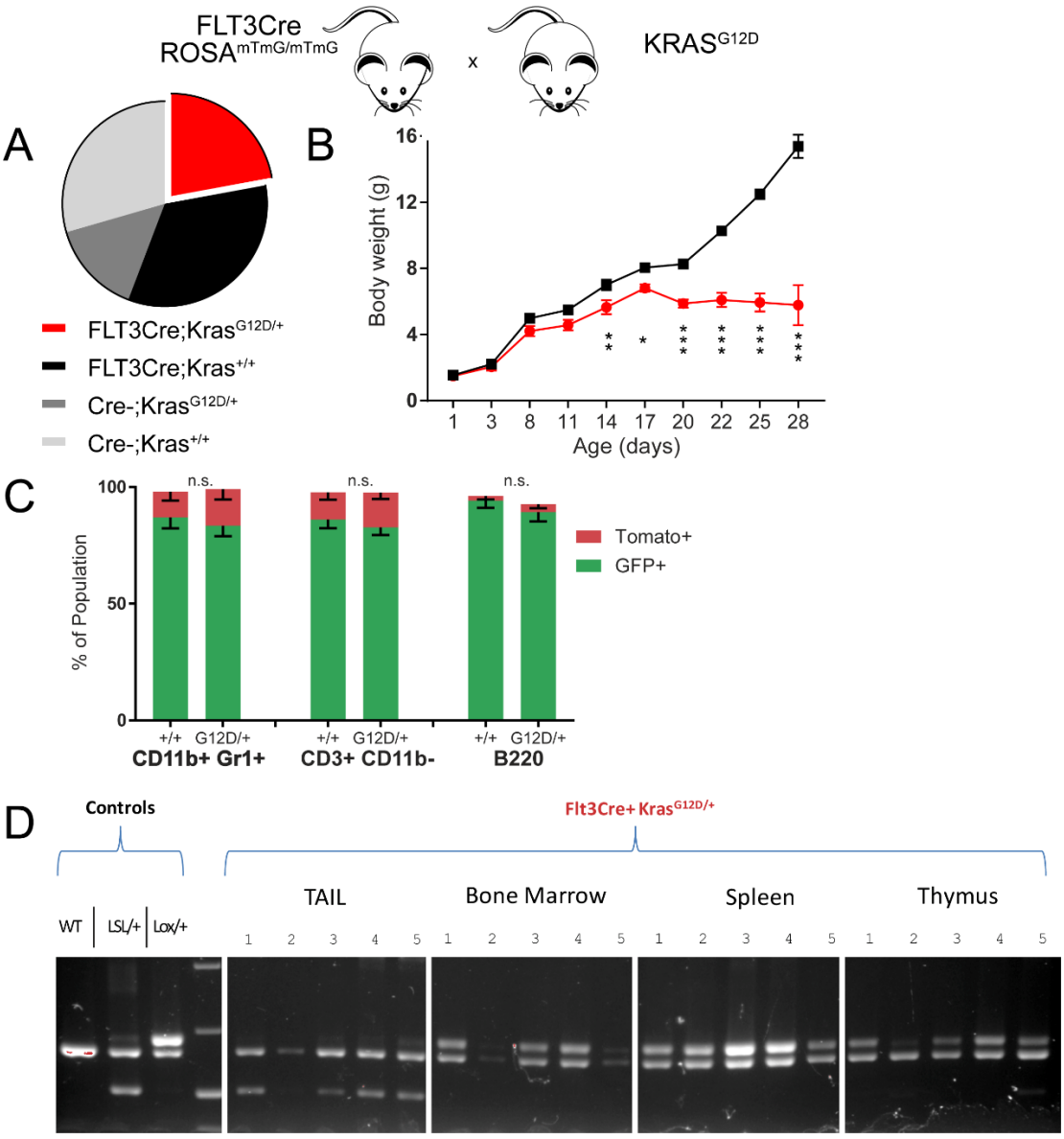

Figure III-3. FLT3Cre;Kras^{G12D}: Birth Ratio, Weight Gain, and Cre Activity. A) Genotypes at birth of Flt3Cre+ ROSA26$^{mTmG/mTmG}$ x Kras$^{G12D/+}$ progeny (N=95, Chi squared p=0.05). B) Weight gain (N=12 mutants, 19 controls). C) Proportion of peripheral blood cell lineages that express Tomato or GFP in mutant animals (N=10) and littermates (N=8). Statistical analysis by two-way ANOVA followed by Tukey's multiple comparisons test. D) PCR gel electrophoresis demonstrating successful recombination of the Lox-STOP-Lox Kras^{G12D} allele in the bone marrow, spleen, and thymus of 5 analyzed Flt3Cre;Kras^{G12D} animals.

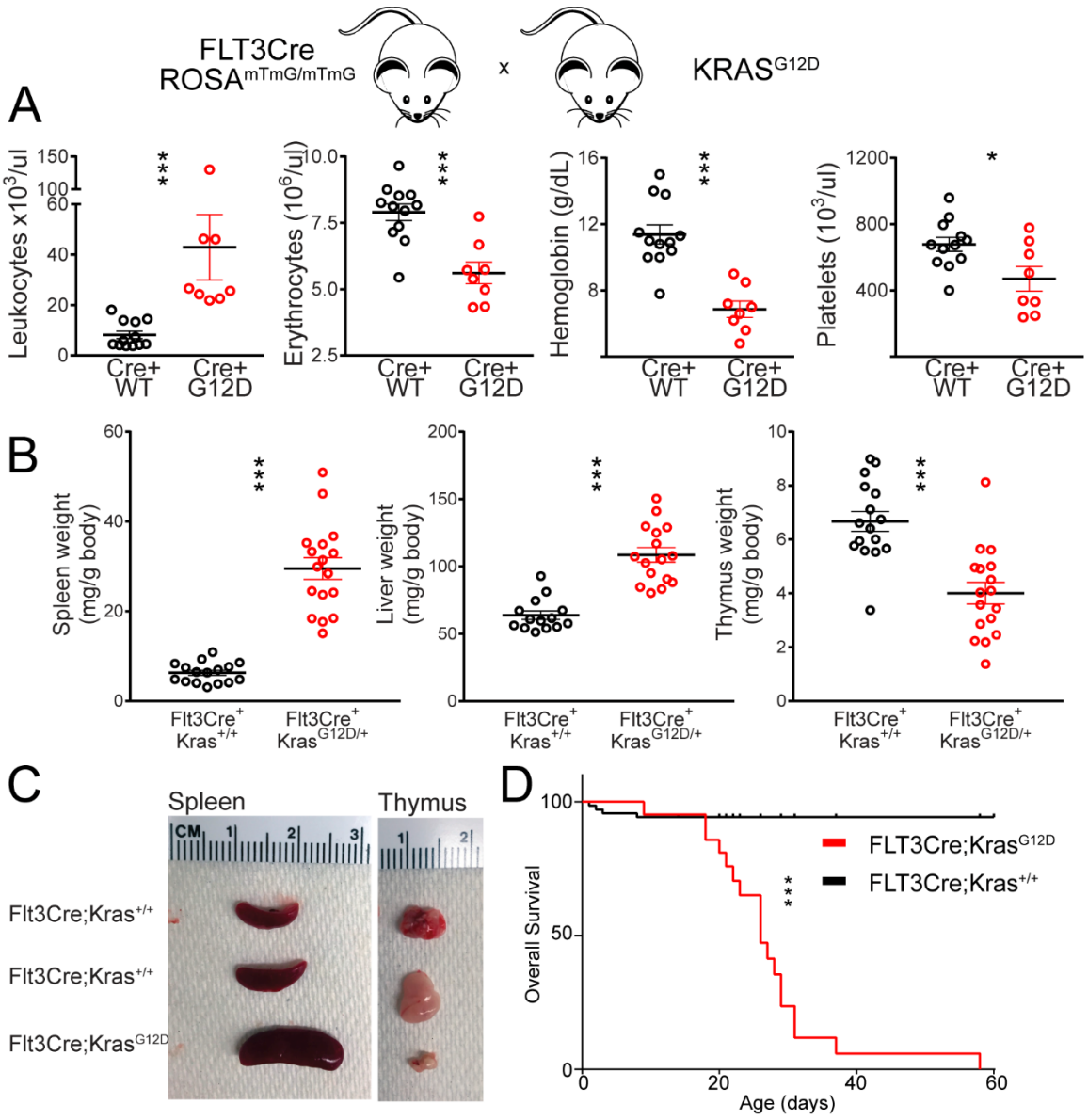

Figure III-4. FLT3Cre;Kras^{G12D}: CBC, Tissue Weights, and Survival. A) Peripheral blood analysis or moribund animals and littermates. B) Spleen, liver, and thymus weights normalized to body weight. C) Representative image of mutant and littermate spleen and thymus. D) Overall survival (analysis by Mantel-Cox test).

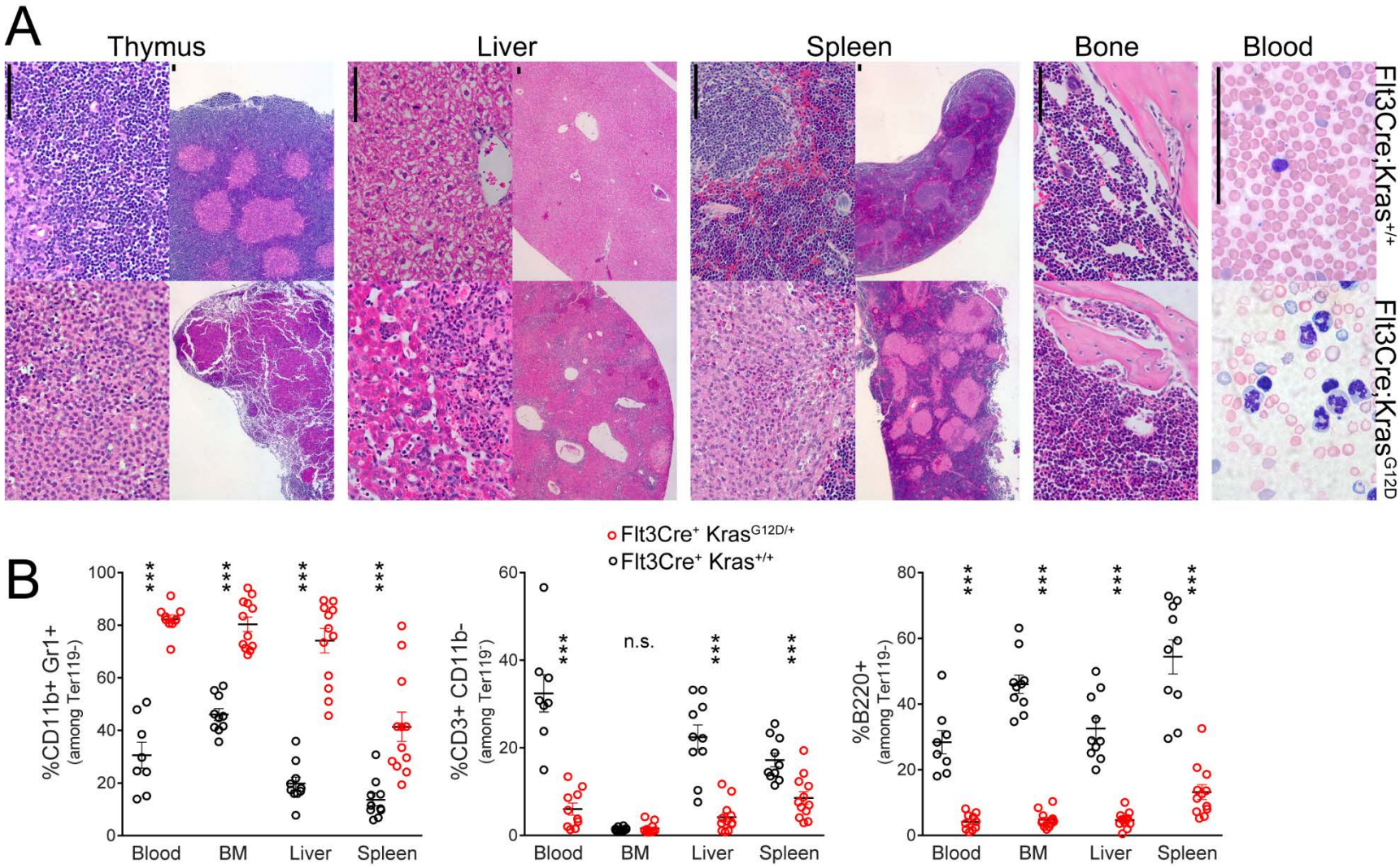
A
Thymus
Liver
Spleen
Bone
Blood
Flt3Cre;Kras+/+
Flt3Cre;KrasG12D
B
Flt3Cre+ KrasG12D/+
Flt3Cre+ Kras+/+
%CD11b+ Gr1+ (among Ter119-)
%CD3+ CD11b- (among Ter119-)
%B220+ (among Ter119-)
Blood
BM
Liver
Spleen
***
n.s.

Figure III-5. FLT3Cre;Kras^{G12D} Mice Develop a Myeloproliferative Disease. A) Pathohistological analysis (scale bars = 100µm, representative of N=2). B) Flow cytometric quantification of tissue leukocytes.

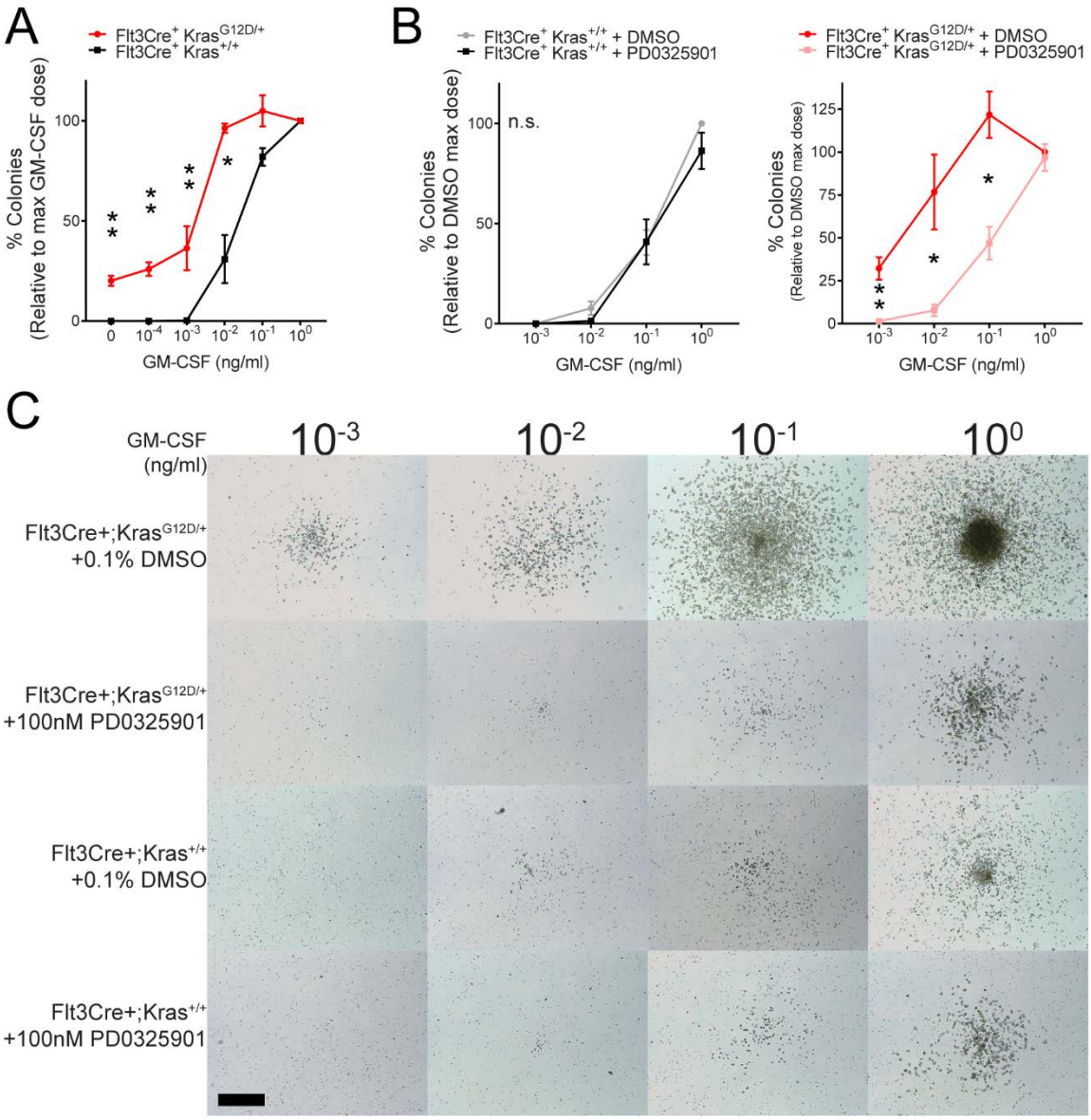

Figure III-6. FLT3Cre;Kras^{G12D}: GM-CSF Growth Hypersensitivity. A) 7 day methylcellulose colony formation of BM cells (N=2 mutant and 3 littermate biological replicates, each plated in triplicate). B) 7 day BM colony formation with 100nM PD0325901 or 0.1% DMSO (N=3 biological replicates/group, each plated in triplicate). C) Representative images of colonies quantified in B; scale bar=0.5mm. All analyses performed on moribund 3-4 week-old Flt3Cre+ Kras$^{G12D/+}$ and age-matched littermates.

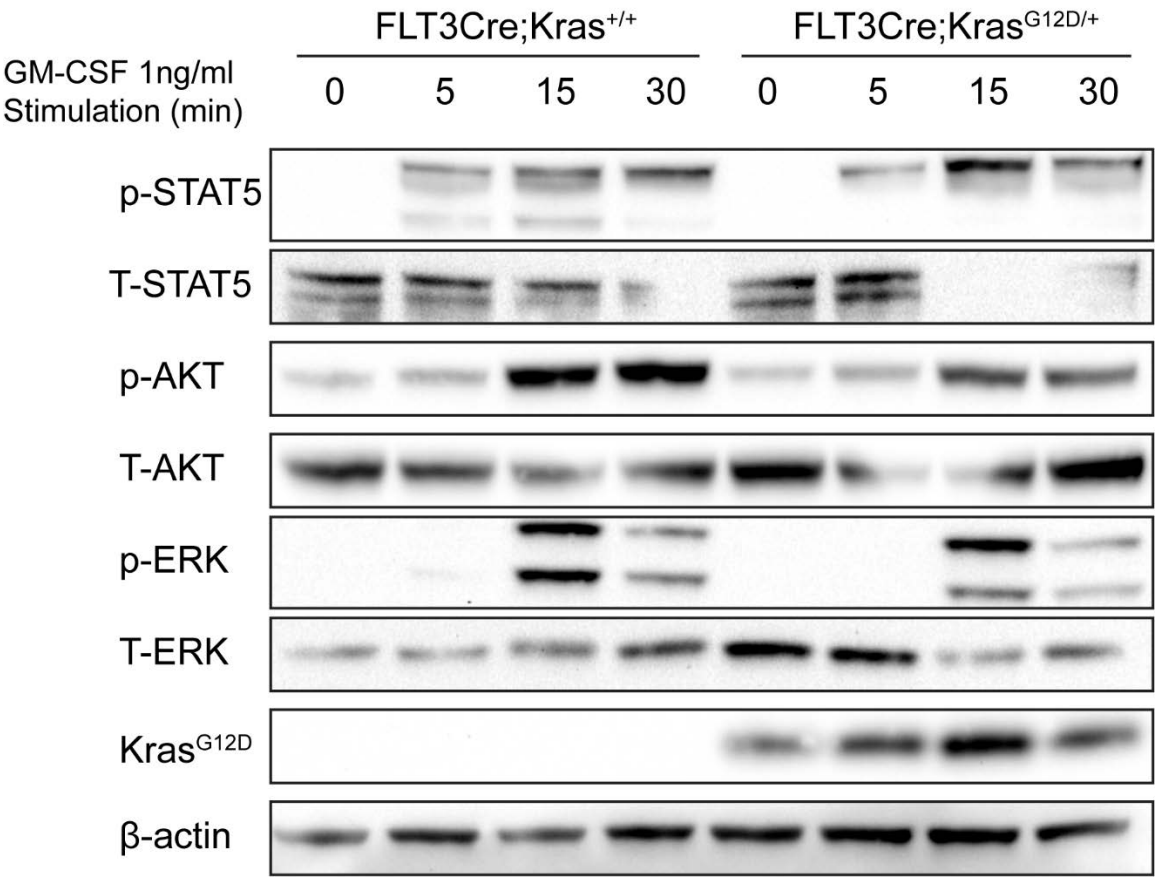

Figure III-7. FLT3Cre;Kras^{G12D}: Signaling Analysis. BM cells from moribund mutants and littermate controls were cultured in M-CSF for 7 days. Cultured cells were starved of serum overnight and then stimulated with 1ng/ml GM-CSF for indicated durations. Cell lysates were probed with the indicated antibodies. Representative image of 3 independent experiments.

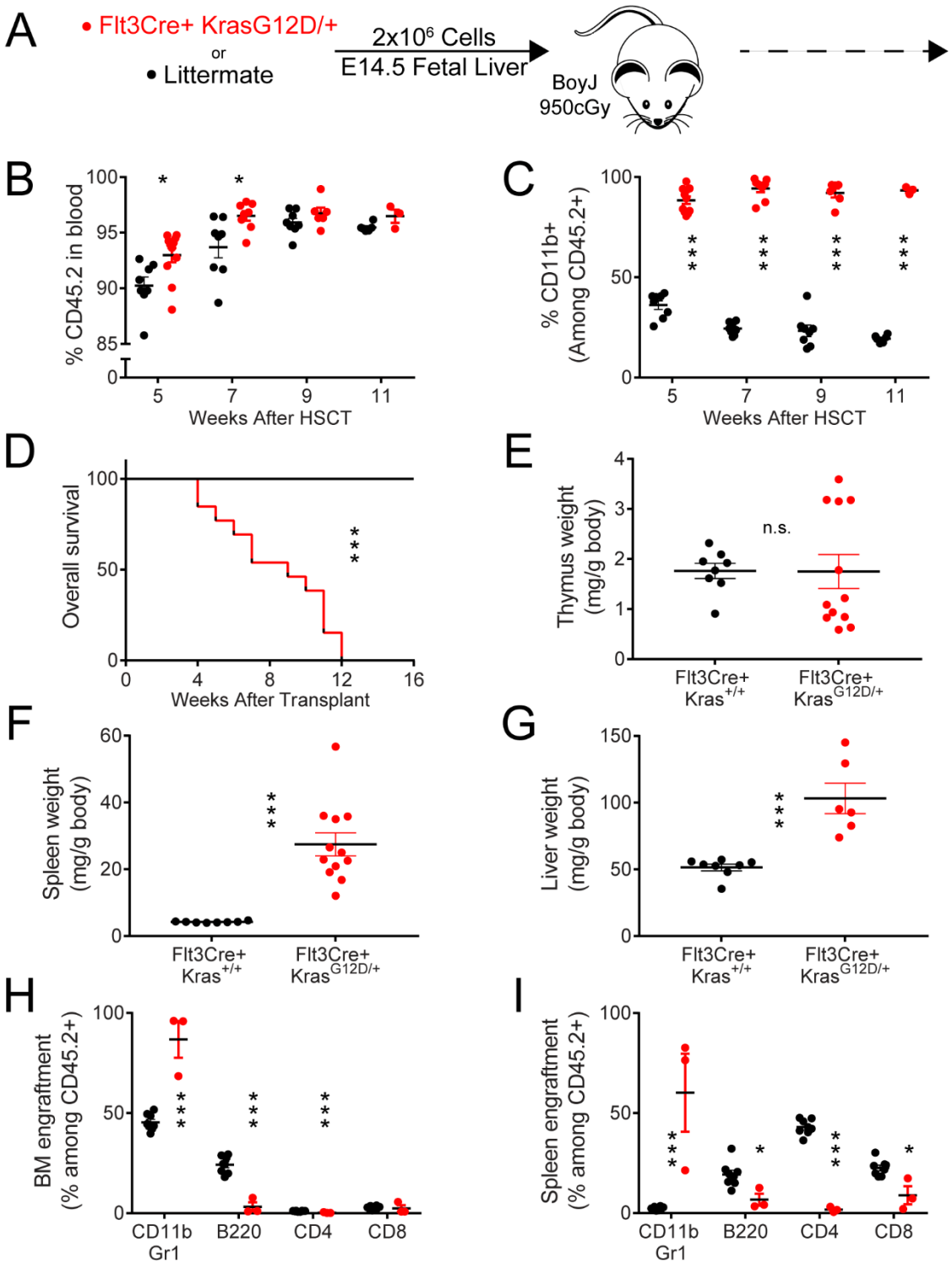

Figure III-8. FLT3Cre;Kras^{G12D}: Fetal Liver Transplantation Propagates a JMML-Like Disease. A) Schematic of fetal liver transplantations (N=12 mutant and 8 control recipients). Analysis of donor cell B) engraftment and C) myeloid contributions in

peripheral blood. D) Overall survival following transplantation (analysis by Mantel-Cox test). E-G) Normalized thymus, spleen, and liver weights of analyzed animals. Flow cytometric quantification of donor leukocytes in H) BM and I) spleen of recipients. Statistical analyses by unpaired t-test unless indicated. $p<0.05$; ** $p<0.01$; ***$p<0.001$.

These findings indicate that temporal expression of $Kras^{G12D}$ *in utero* transforms fetal hematopoietic progenitors into transplantable JMML-initiating cells.

We proceeded to analyze the effect of fetal $Kras^{G12D}$ expression on the frequency and distribution of HSCs and progenitors. In contrast to Mx1Cre;$Kras^{G12D}$ animals (Sabnis et al. 2009) we observed a reduction of HSCs and MPPs in both the BM and spleen of moribund FLT3Cre;$Kras^{G12D}$ mice (Figure III-9A,B). We reasoned this decrease was due to progenitor exhaustion incurred by increased myeloid differentiation in FLT3Cre;$Kras^{G12D}$ animals. In characterizing the progeny of FLT3Cre;$Kras^{G12D}$ progenitors, we found that BM cells cultured in cytokine-free medium gave rise to histiocytes that expressed CD11c+ and CD135+ (Figure III-10A). This finding is reminiscent of reports describing dendritic cell (DC)-like tumor cells in JMML patients (Longoni et al. 2002; Ng et al. 1988; Estrov et al. 1986) and prompted us to analyze DC populations in the tissues of FLT3Cre;$Kras^{G12D}$ animals. We observed a marked increase in the frequency of CD11c+ cells in the BM and spleen (Figure III-10B). Strikingly, the CD11c+ cell expansion was particularly prominent in the atrophied thymus (Figure III-10C), where we saw a concomitant deficit of CD4- CD8- CD25+ committed T-cell progenitors and CD4+ CD8+ double positive cells (Figure III-11). This propensity for preferential DC differentiation was also observed in recipients of FLT3Cre;$Kras^{G12D}$ fetal liver progenitors (Figure III-10D,E), in which we confirmed that splenic CD11c+ MHCII+ DCs were distinct from the equally expanded CD11b+ Gr1+ neutrophil population.

We present the first $Kras^{G12D}$ model to unify JMML disease-defining features: an *in utero* origin, viability at birth followed by a failure to thrive, anaemia, thrombocytopenia, monocytosis, hepatosplenomegaly, and infiltration of tissues with histiocytes. All FLT3Cre;$Kras^{G12D}$ mice succumbed to a myeloid disease that could be recapitulated following fetal liver transplantation. This is in stark contrast to existing $Kras^{G12D}$ models,

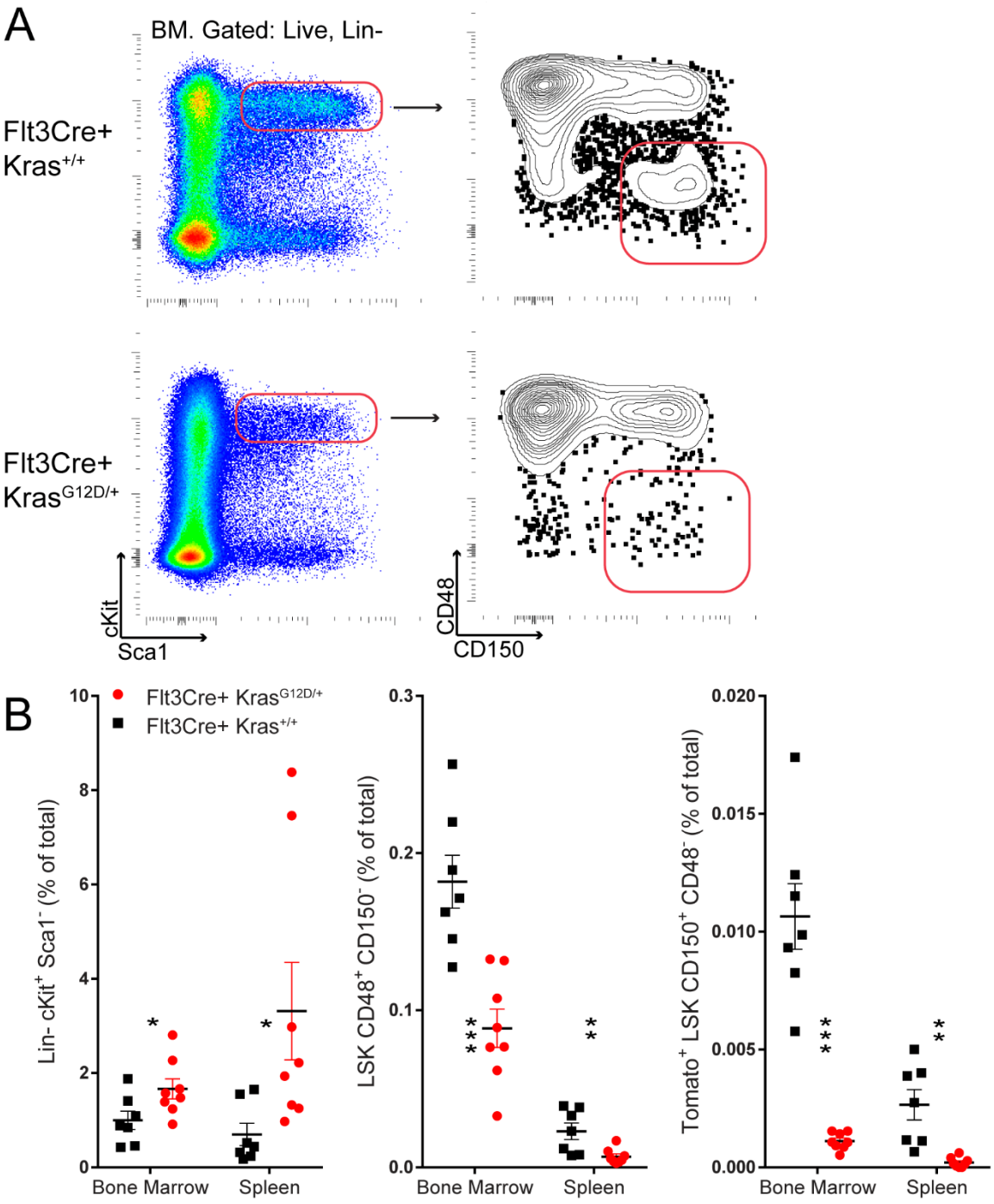

Figure III-9. FLT3Cre;Kras^{G12D}: Depletion of BM and Splenic HSCs. A) Representative gating of LSK CD150+ CD48- HSCs in the BM of mutants and littermates. B) Quantification of HSCs and progenitor subsets in the BM and spleen of moribund mutants and littermates

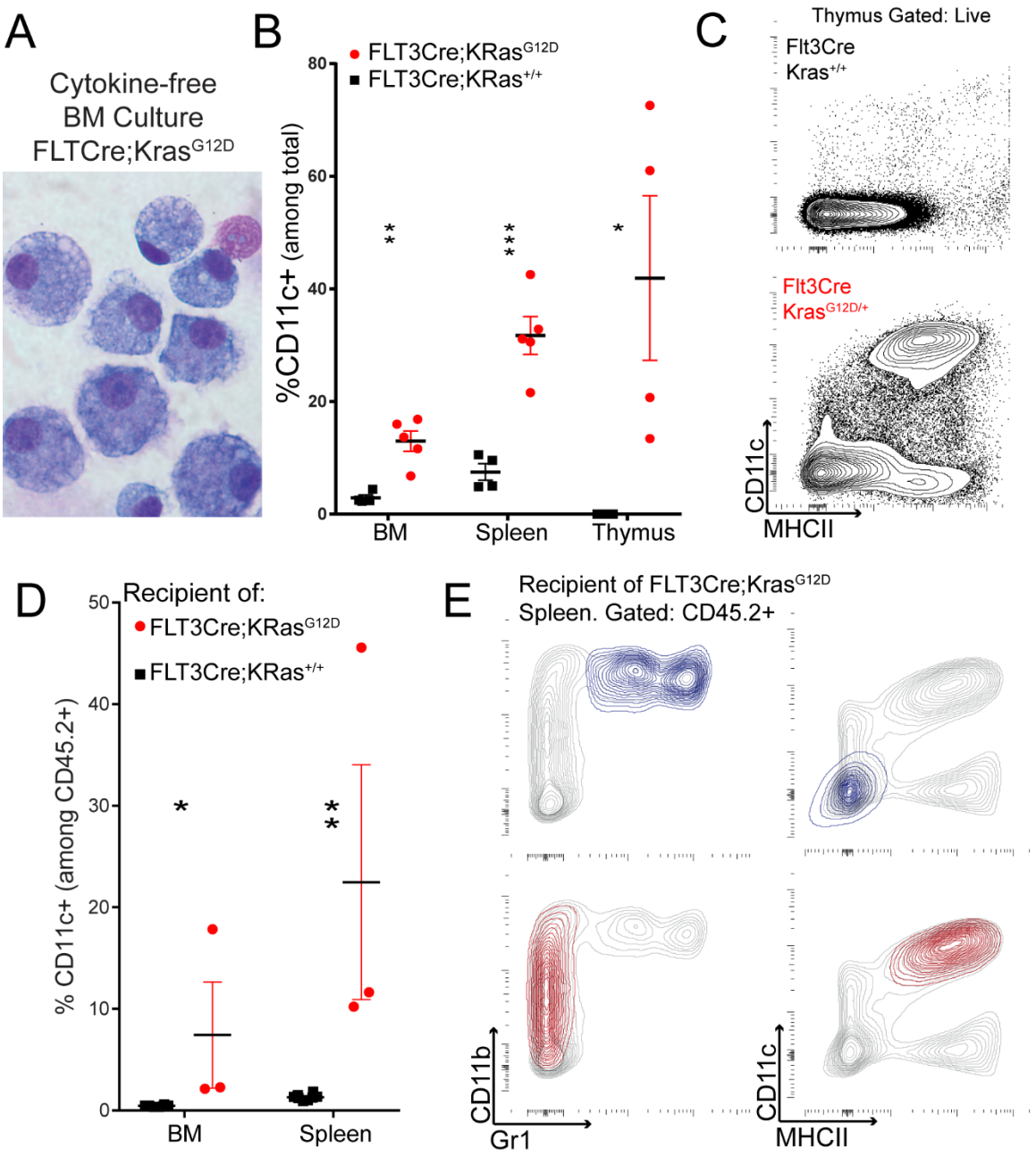

Figure III-10. FLT3Cre;Kras^{G12D}: Enhanced Dendritic Cell Differentiation. A) Histiocytes obtained from cytokine-free culture of BM cells. B) Quantification of CD11c+ dendritic cells in BM, spleen, and thymus. C) Representative gating of thymic dendritic cells D) Quantification of dendritic cell frequency following fetal liver transplants E) Representative gating demonstrating CD11c+ MHCII+ dendritic cells (red) are distinct from CD11b+ Gr1+ neutrophils (blue).

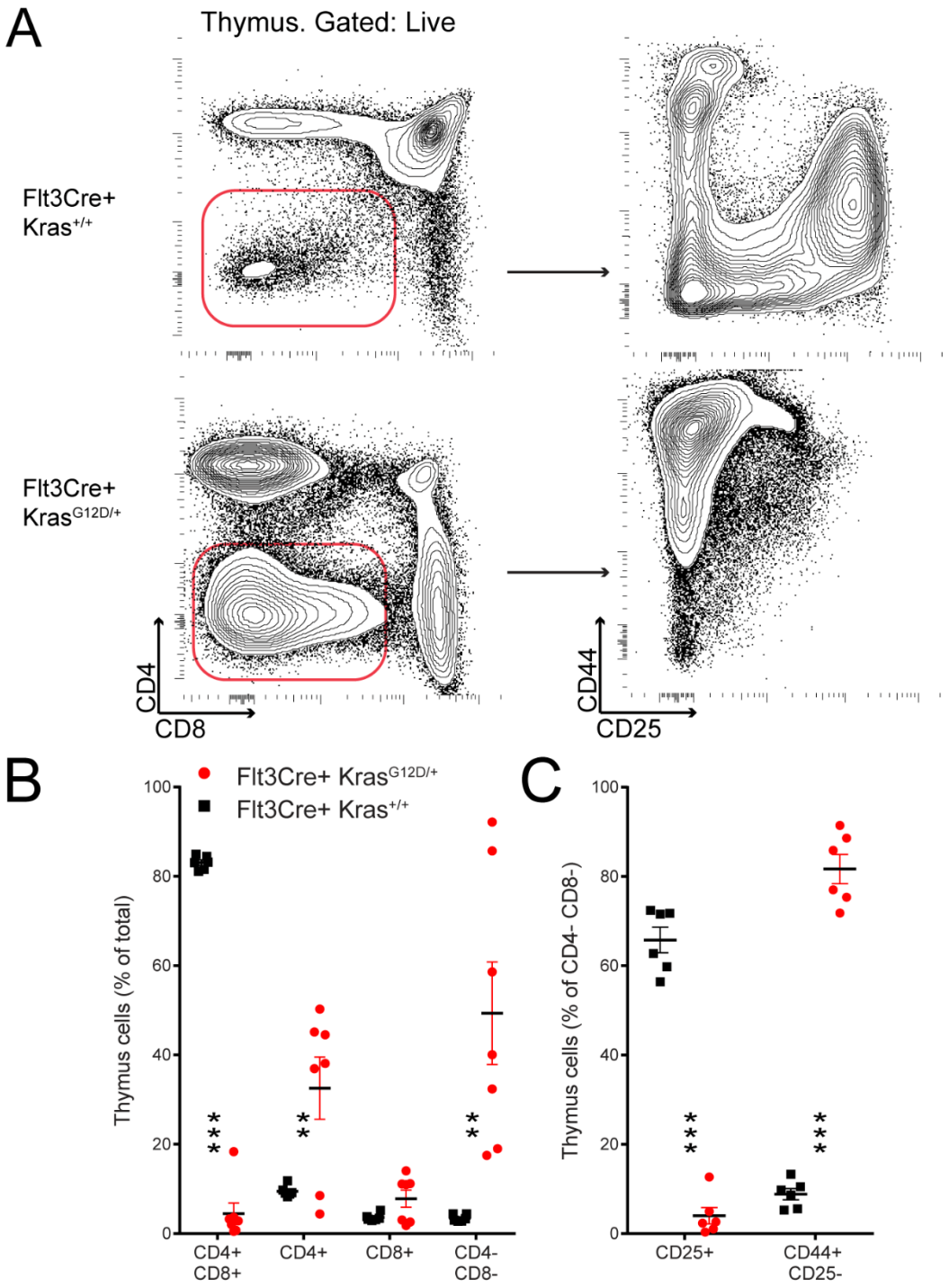

Figure III-11. FLT3Cre;Kras^{G12D}: Defective T-cell Differentiation. A) Representative gating of T-cell generation in thymuses of moribund mutants and littermates. B,C) Flow cytometric quantification of thymic progenitors.)

which die from T-ALL or non-hematopoietic expression (Staffas et al. 2015; Desai, Brownfield, and Krasnow 2014; Tang et al. 2013).

B. In-depth Analysis of FLT3Cre;Kras^{G12D} Transplantations

Hematopoietic transplantations bypass normal developmental processes by removing hematopoietic progenitors from their native niche and requiring them to engraft a foreign host. It is possible, however, to use age-matched donors and recipients to minimize the differences between native and host environments. Experiments that have used such donor-recipient matching have identified novel progenitor types with novel differentiation potentials (Yoder et al. 1997). However, this approach has not been applied to the study of disease-initiating cells. Given that fetal liver progenitors from FLT3Cre;Kras^{G12D} mice could serially propagate a JMML-like disease when transplanted into adult recipients, we sought to determine if the same disease would be observed when neonatal recipients and/or adult BM progenitors from moribund mice were used (see schematic in Figure III-12).

We observed that recipients of FL cells had a diminished survival compared to recipients of 4week old BM cells (Figure III-13A). No difference in survival was observed when neonatal and adult primary recipients were compared. However, adult recipients of secondary transplants succumbed more rapidly than neonatal recipients of adult transplants (Figure III-14). This suggests that the duration a progenitor resides in a particular niche may influence the rate of disease progression. All recipients of mutant progenitors had hepatosplenomegaly compared to control recipients. However, we did not observe differences in spleen or liver weights based on the age of the recipient or the phase of the donor cells (Figure III-13B).

Adult recipients of FL progenitors had leukocytosis 5 weeks after transplant (Figure III-15A). However, this leukocytosis was not evident in subsequent blood draws from these

Recipient / Donor	 2day old	 8 week old
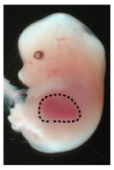 E14.5 Fetal Liver	**Matched Donor : Recipient**	**Mismatched**
 Adult BM	**Mismatched**	**Matched Donor : Recipient**

Figure III-12. Developmentally Coordinate Transplants. Schematic of transplantations used to assess the contribution i) fetal vs. adult progenitors and ii) neonatal vs. adult hematopoietic niche to the development of disease following transplantation of $Kras^{G12D}$-expressing progenitors.

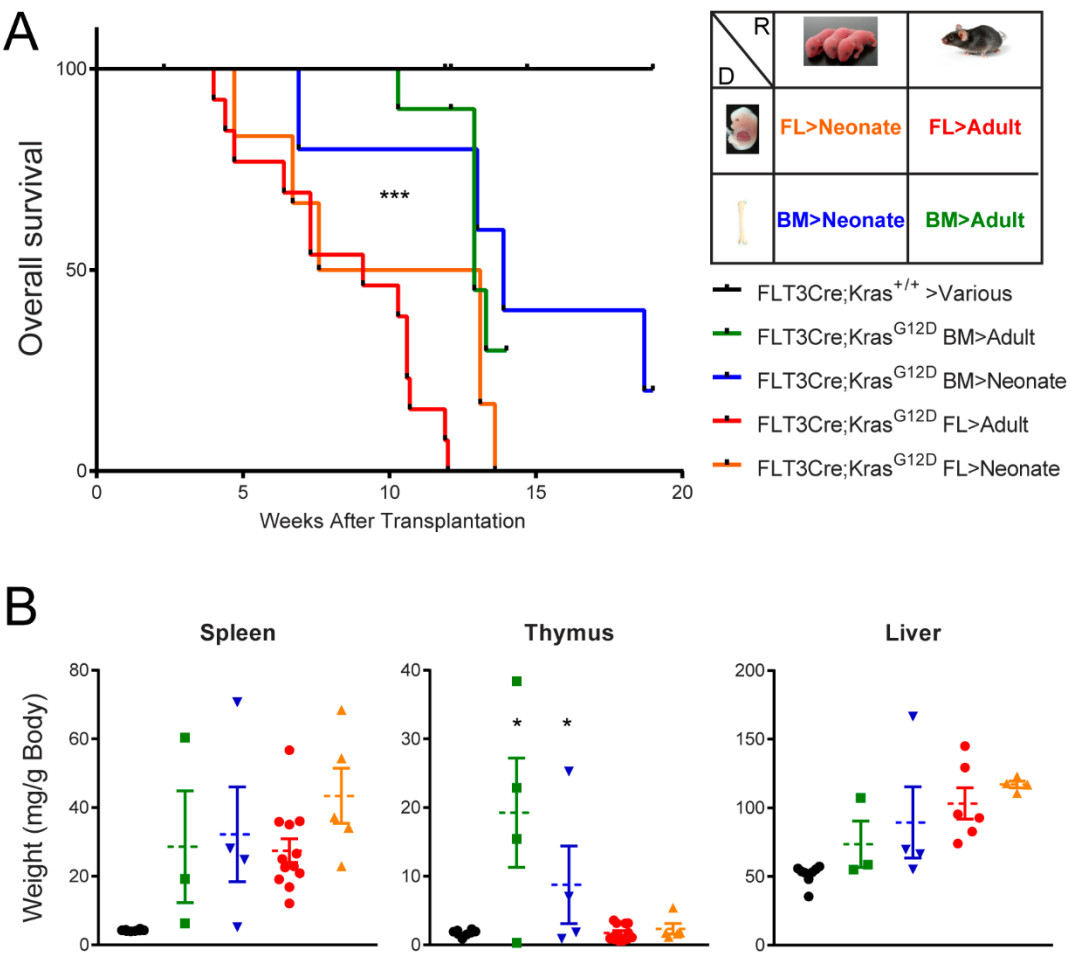

Figure III-13. FLT3Cre;Kras^{G12D}: Primary Transplants. A) Overall survival of recipients. P-value denotes FL vs. adult donor cohorts. Survival differences between adult vs. neonatal recipients are not significant (N= 12 FL>Adult; 6 FL>Neonate; 5 BM>Neonate; 10 BM>Adult). B) Normalized spleen, thymus, and liver weights of moribund recipients. Donor cell numbers: FL>Adult=2x10^6 iv; FL>Neonate=1x10^6 iv; BM>Adult=2x10^6 iv; BM>Neonate=5x10^6 ip.

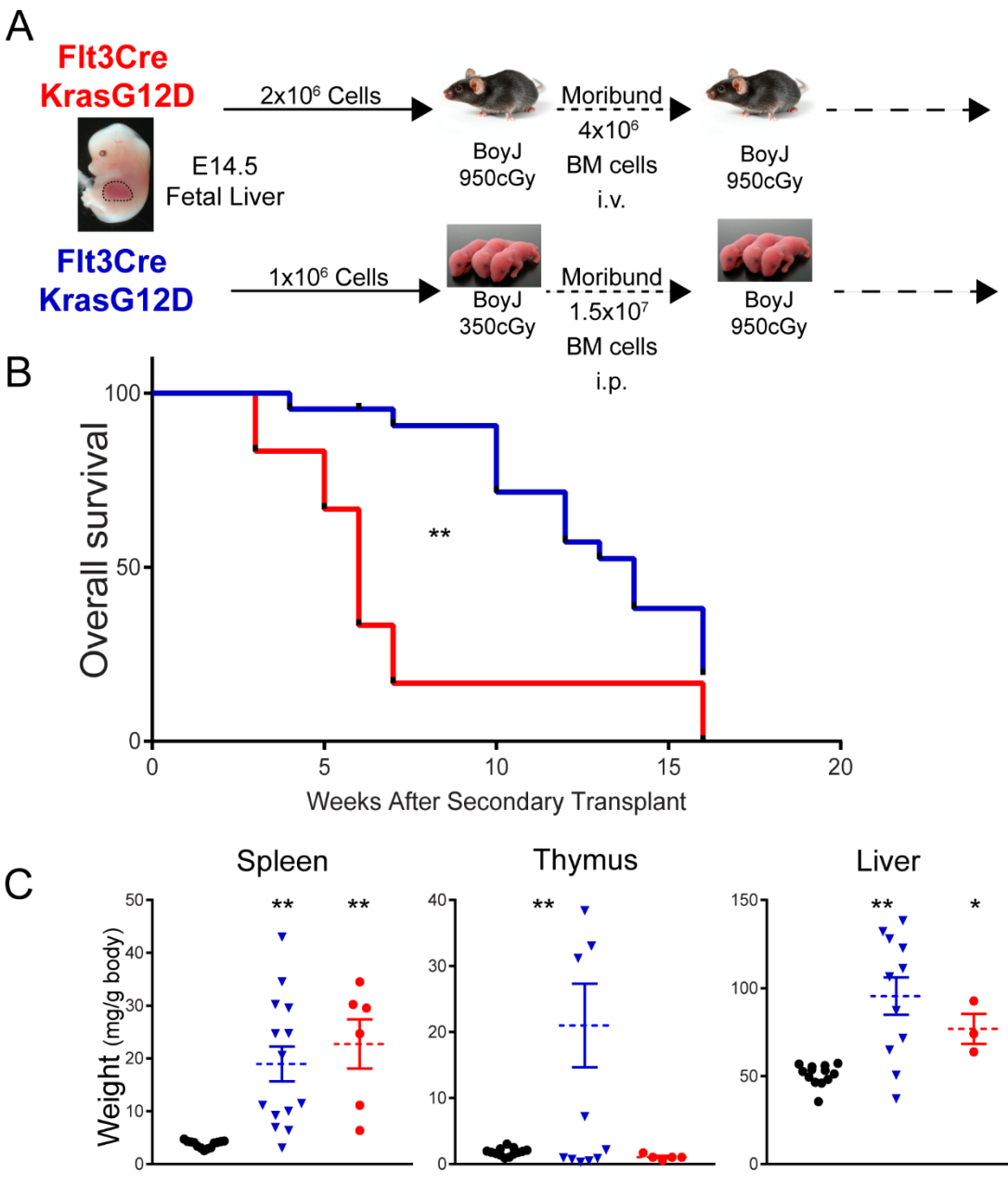

Figure III-14. FLT3Cre;Kras^{G12D}: Secondary Transplants. A) Schematic of transplantations. B) Overall survival of secondary transplant recipients with >0.5% donor engraftment (N=6 Adult; 22 Neonates). C) Normalized spleen, thymus, and liver weights of moribund recipients, p-values are relative to primary recipients of littermates, shown in black and in Figure III-13B. Donor cell numbers: FL>Adult>Adult=4x10^6 iv; FL>Neonate>Neonate=8x10^6 ip.

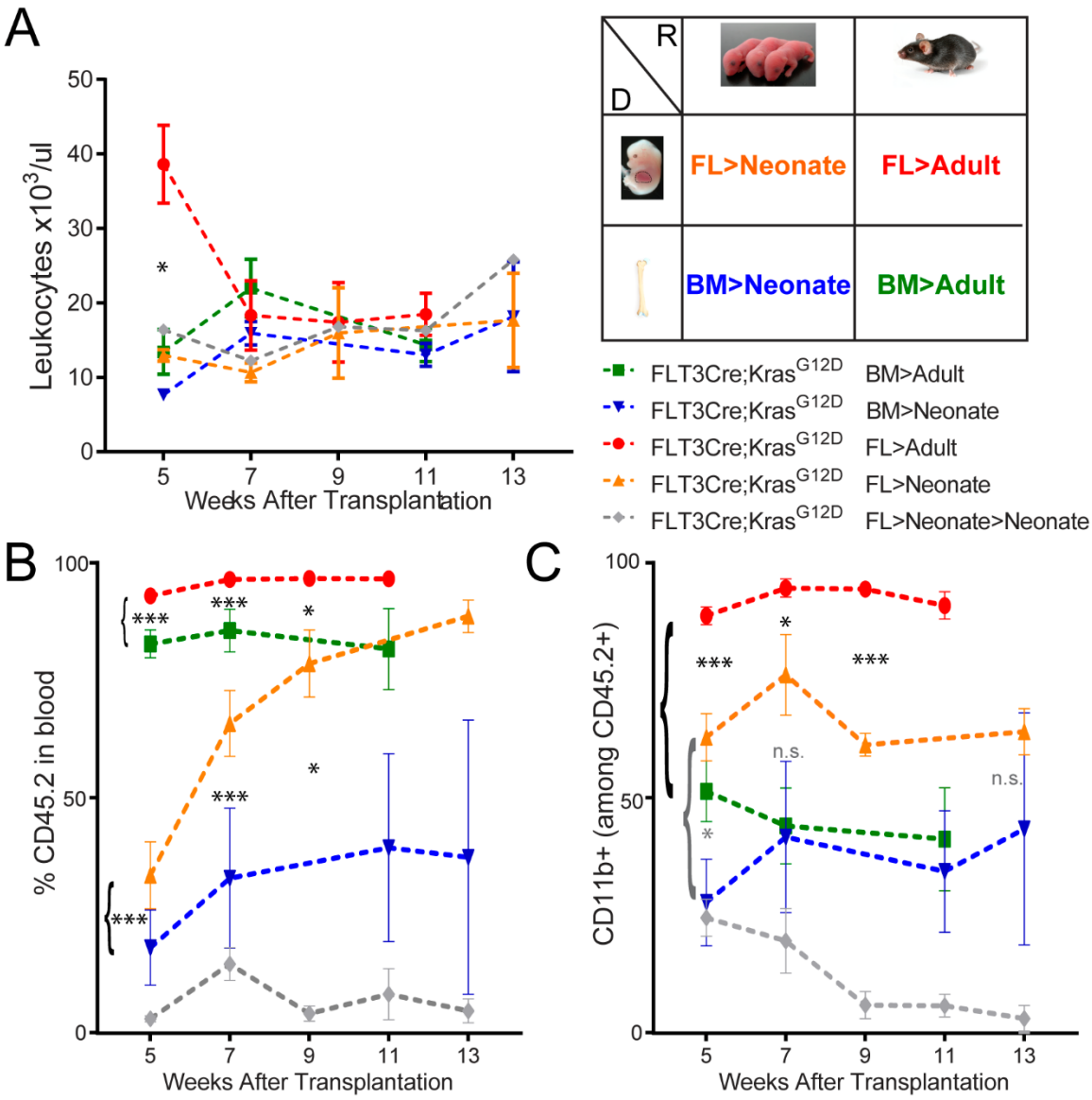

Figure III-15. FLT3Cre;Kras^{G12D} Transplants: Engraftment, Leukocytosis, Monocytosis. A) Leukocyte counts of transplant cohorts. B) Peripheral blood engraftment of transplant cohorts. C) Contribution of donor cells to CD11b+ neutrophils in peripheral blood. Statistical analysis compares BM>Neo with BM>Adult & FL>Neo with FL>Adult; p-values obtained by unpaired t-tests. Neonatal secondary recipients that had <0.5% engraftment were excluded from this analysis.

animals. Furthermore, no other transplant cohort had signs of leukocytosis. However, there were pronounced differences in engraftment efficiency (Figure III-15B). FL>Adult had better donor engraftment than BM>Adult. Neonatal recipients had a significantly inferior engraftment that their adult counterparts. However, FL>Neonate engraftment markedly increased over time whereas BM>Neonate did not. Importantly, fetal progenitors had significantly greater contribution to CD11b+ myeloid cells compared to BM donors when transplanted into either neonates or adults (Figure III-15C).

We set out to determine the relationship between engraftment efficiency and the propensity for myeloid-biased differentiation. In all recipients of mutant donors there was a direct correlation between CD45.2 engraftment and donor differentiation into CD11b+ cells (Figure III-16A-D). This correlation was not seen in recipients of healthy littermate progenitors (Figure III-16E). This suggests that myeloid-biased differentiation of mutant progenitors is not entirely a cell autonomous decision. Rather, the presence of mutant cells in the niche may influence the lineage output of progenitors. This suggests that the development of MPN is determined, in part, by the proportion of total cells that express the mutation. Importantly, residual and competitive CD45.1 host cells did not show this myeloid biased differentiation (Figure II-16F). This suggests that the non-cell autonomous effect of transplanted $Kras^{G12D}$ cells are restricted to the mutant progenitors themselves.

Whereas fetal donors gave rise to a JMML-like disease in both adult and neonatal recipients, FLT3Cre;$Kras^{G12D}$ BM cells from 4 week old moribund animals preferentially gave rise to T-ALL upon transplantation (Table III-1). This propensity for lymphoid disease was observed following BM transplantation into both adult and neonatal recipients. This shows that the microenvironment does not have a decisive role in determining the lineage of $Kras^{G12D}$-induced disease. Rather, it suggests that innate properties of fetal and adult progenitors cause myeloid and lymphoid diseases, respectively. The FLT3Cre;$Kras^{G12D}$ model provides a tool to seek the nature of those innate differences.

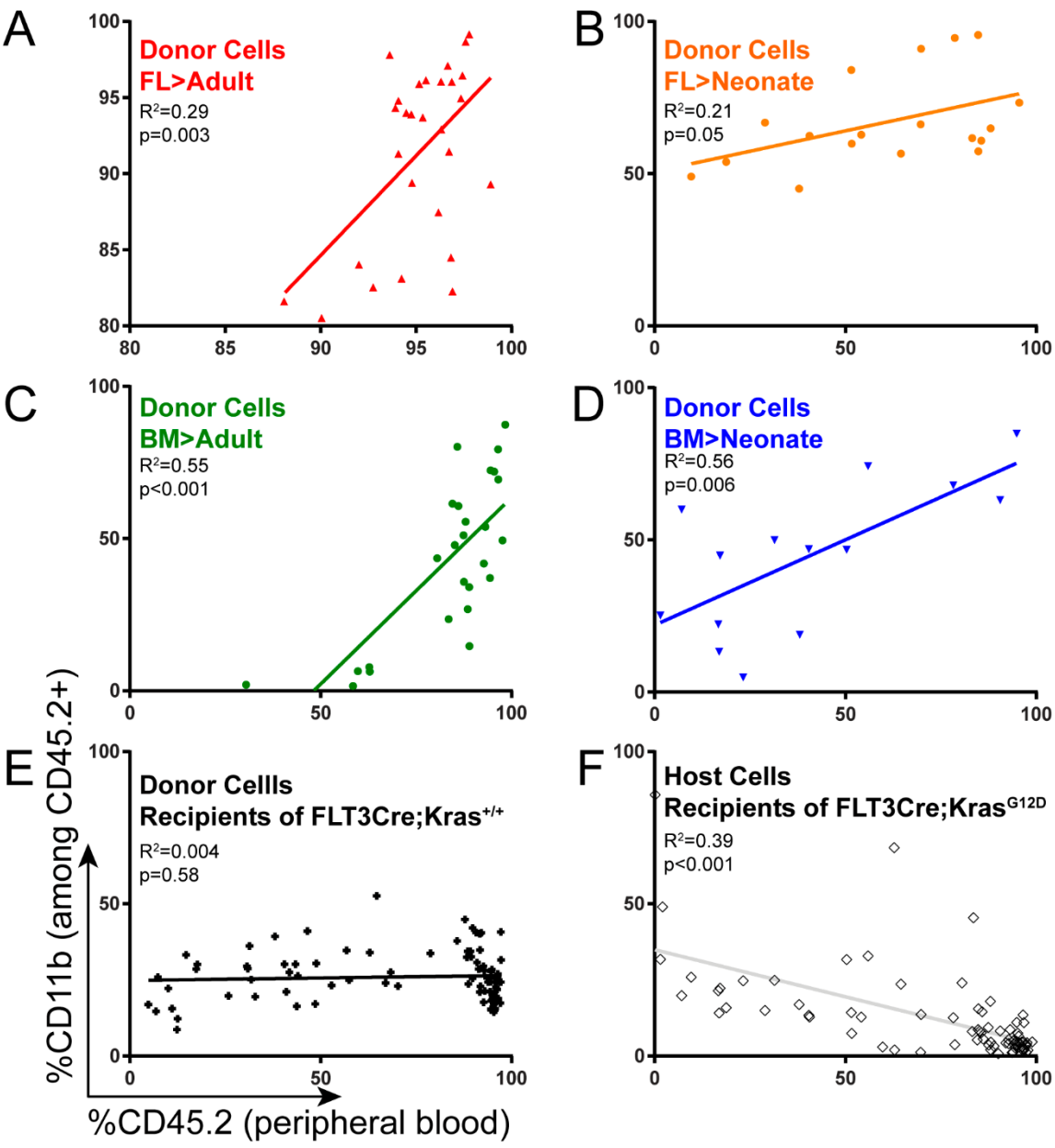

Figure III-16. FLT3Cre;Kras^{G12D} Transplants: Correlation Between Engraftment and Monocytosis. Relationship between %CD45.2 engraftment and donor cell biased differentiation into CD11b+ neutrophils. A-D) FLT3Cre;Kras^{G12D} donor transplants. E) Littermate transplants. F) Competitive and residual CD45.1+ cells in recipients of FLT3Cre;Kras^{G12D}. Each dot represents one peripheral blood draw. Analysis of the same animal at multiple timepoints are included in this analysis. P-values calculated using Pearson's correlation.

Donor	Recipient	Donor Cells	Cohort Size	Median survival (weeks)	JMML-like (# deaths)	T-ALL (# deaths)
N/A	FLT3Cre Kras^{G12D} (No Transplant)	N/A	18 (NA)	3.7	100% (18)	0%
		2x10^6 (iv)	12 (12)	9.1	100% (12)	0%
		1x10^6 (iv)	6 (6)	10.4	100% (6)	0%
		2x10^6 (iv)	10 (10)	12.9	17% (1)	83% (5)
		5x10^6 (ip)	5 (5)	13.9	20% (1)	40% (2)
	 Secondary	4x10^6 (iv)	6 (6)	6.0	83% (5)	17% (1)
	 Secondary	8x10^6 (iv)	22 (12)	14.0	25% (3)	50% (6)

Table III-1. Summary of FLT3Cre;Kras^{G12D} Cohorts and Survival. Death totals may not add up to 100% due to deaths from uncertain causes. Donors were unfractionated cells from E14.5 fetal livers or BM from 4 week-old moribund animals.

C. FLT3Cre;PTPN11^{E76K} Develop An Indolent Myeloproliferative Disease.

Given the successful modeling of JMML using FLT3Cre;Kras^{G12D} mice, we proceeded to evaluate whether the same Cre strain would produce a faithful disease model using the PTPN11^{E76K} oncogene. FLT3Cre+;PTPN11^{E76K};ROSA$^{mTmG/+}$ (hereafter FLT3Cre;PTPN11^{E76K}) mice were born at expected Mendelian ratio (Figure III-17A). However, unlike the Kras^{G12D} cohort, FLT3Cre;PTPN11^{E76K} mice developed an indolent disease with transient leukocytosis, minor anaemia, and thrombocytopenia (Figure III-18). Nonetheless, peripheral blood analysis revealed markedly elevated CD11b+ cells with a concomitant reduction of CD3+ or CD4/CD8 single positive T-lymphocytes in PTPN11^{E76K} mutants compared to controls (Figure III-17B-D). The overall survival of mutants was lower than that of controls, but a mean survival could not be calculated due to an 80% survival rate at 60 weeks of age (Figure III-18E).

An interesting observation in FLT3Cre;PTPN11^{E76K} mice was the progressive decline in the %GFP+ cells (Figure III-19A,B). Since GFP+ cells are the progeny of progenitors with active Cre, these GFP+ cells should also be the only cells that recombined the PTPN11^{E76K} allele and express the oncogene. We considered two hypotheses to explain diminishing GFP+ frequency. First, healthy clones may be preferentially contributing to hematopoiesis in mutant animals. Alternatively, the finding may be an ancillary consequence of monocytosis. Recall, myeloid cells have a lower frequency of GFP expression than either B- or T-lymphocytes because only CLPs and not CMPs express FLT3. Therefore, a relative monocytosis would cause the total frequency of GFP+ leukocytes to diminish. To address these hypotheses we analyzed the %GFP+ cells in each lineage over time (Figure III-19C). Using two-way ANOVA analysis, we confirmed that %GFP+ by lineage was T-cells > B-cells > myeloid cells in mutants (P-value<0.0001; accounting for 17% of the variance). In contrast, the age of the animal had a minor contribution to %GFP+ among CD11b+ cells (5.4% of the variance; P-value 0.03).

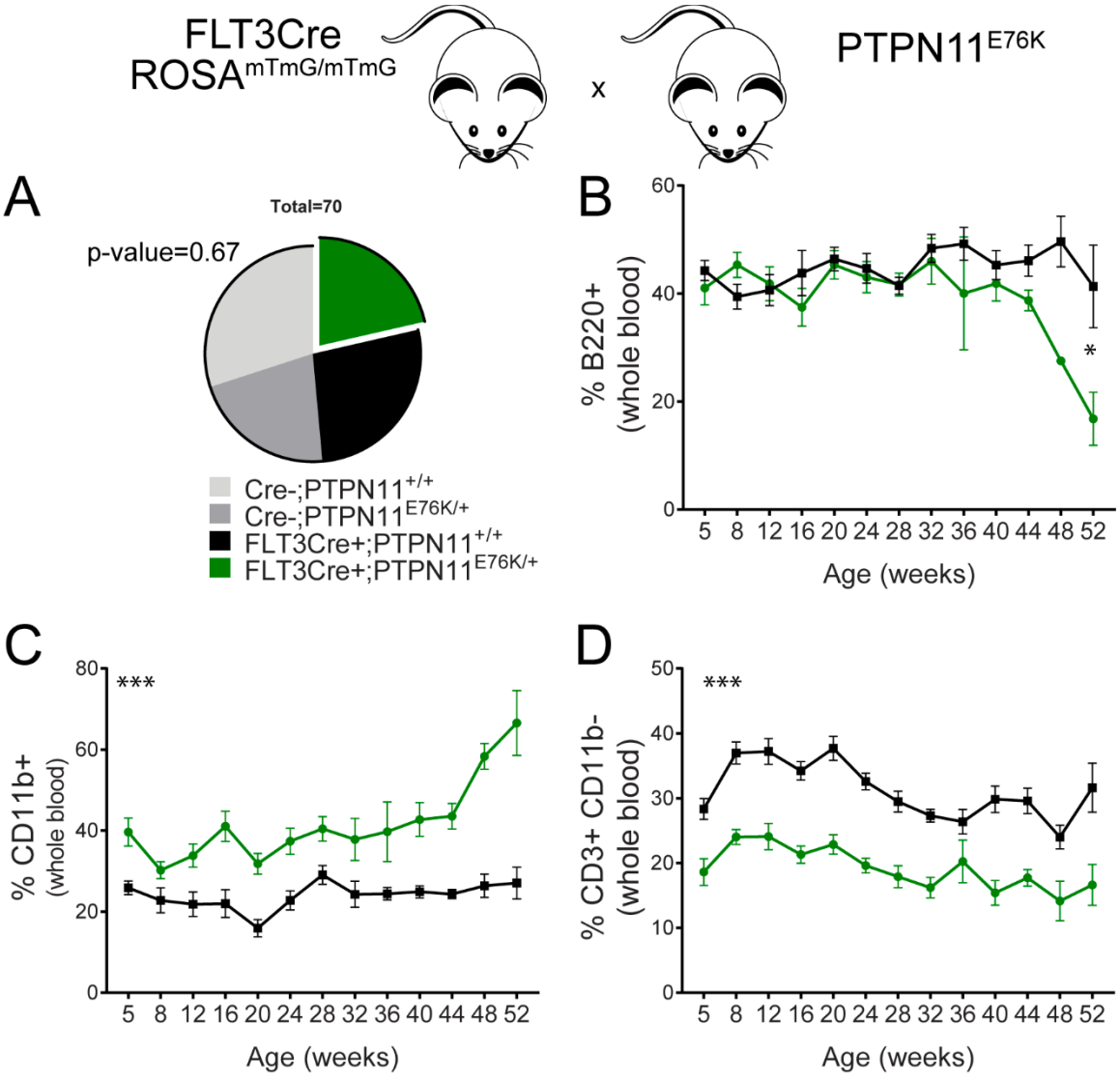

Figure III-17. FLT3Cre;PTPN11^{E76K}: Birth Ratio and Peripheral Leukocyte Analysis. Birth ratios at weaning of FLT3Cre;ROSA$^{mTmG/mTmG}$ x PTPN11$^{E76K/+}$ matings. B-D) Analysis of peripheral blood lineages in mutant (N=13) and control (N=18) animals. P-values in C and D are significant at all time points.

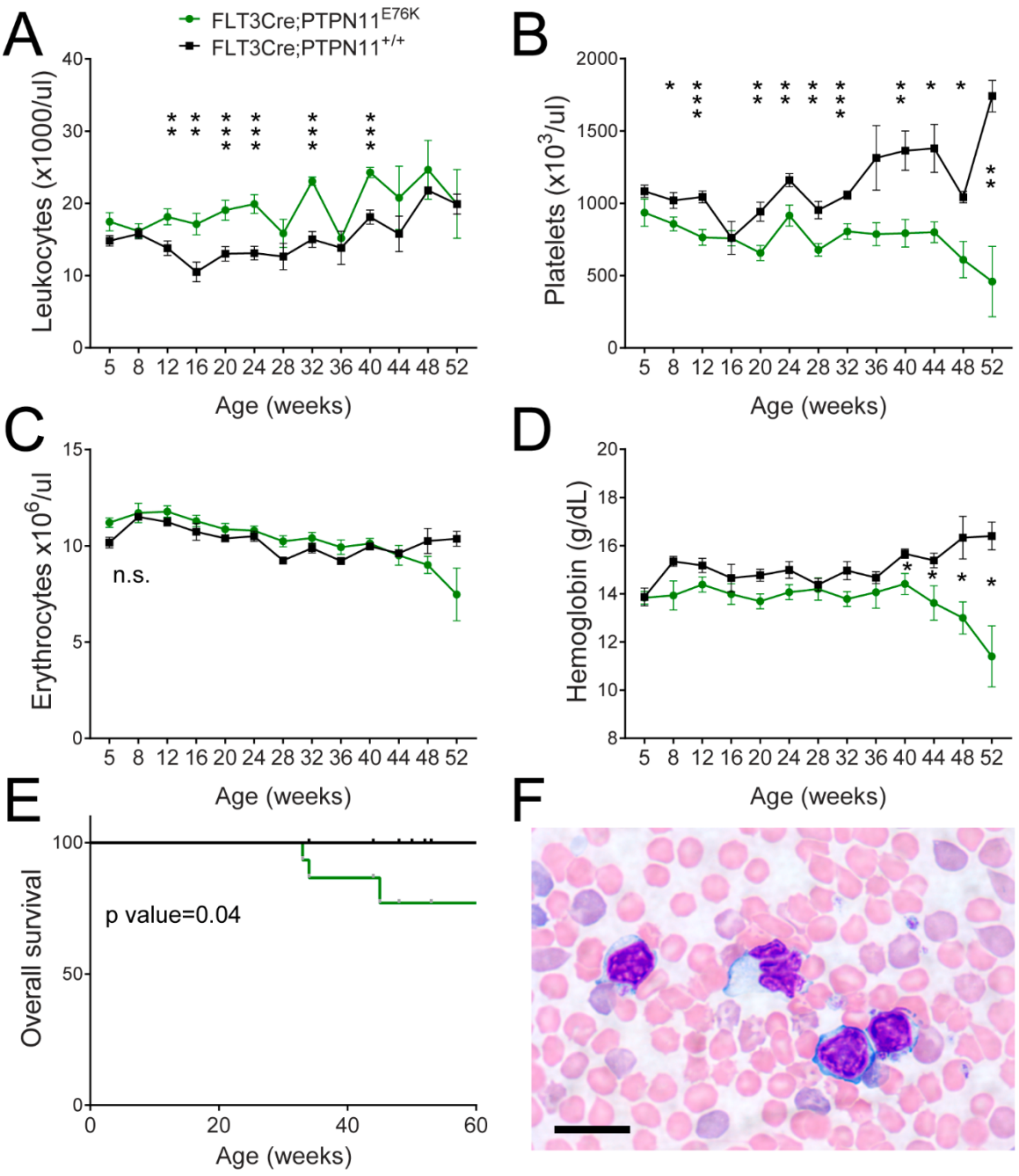

Figure III-18. FLT3Cre;PTPN11^{E76K}: CBC and Survival Analyses. A-D) FLT3Cre; PTPN11^{E76K} develop a leukocytosis, thrombocytopenia, and late-onset anaemia. E) Overall survival; p-values calculated by Mantel-Cox test. F) Representative image of FLT3Cre; PTPN11^{E76K} peripheral blood. Scale bar=20um.

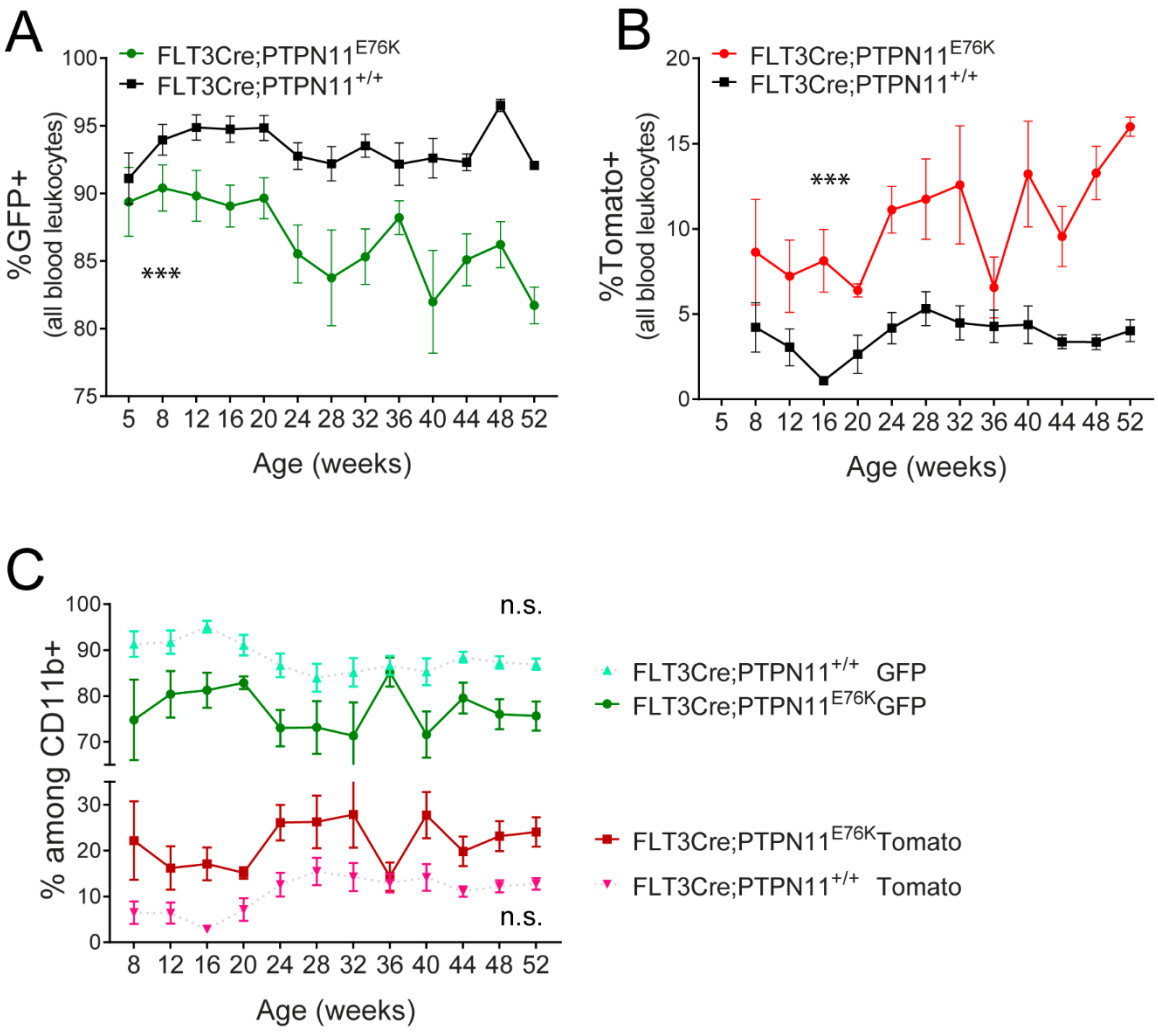

Figure III-19. FLT3Cre;PTPN11^{E76K}: Analysis of GFP+ Leukocytes. A,B) Frequencies of GFP+ and Tomato+ leukocytes in peripheral blood at indicates ages C) Analysis of GFP+ and Tomato+ expression among CD11b+ cells in mutants and littermates. Two-way ANOVA indicates that genotype accounts for 17% of variance in GFP+ myeloid cells (p-value<0.001) whereas age accounts for 5.4% of variance (p-value=0.03).

These results strongly suggest that the dominant contribution to decreasing %GFP+ cells in the peripheral blood is the result of the relative monocytosis and not due to preferential expansion of non-mutated Tomato+ clones.

Three FLT3Cre;PTPN11^{E76K} animals died in the course of our study. Two died at 33 weeks of age, from the same cage, had normal sized spleens and thymuses, and showed no evidence of disease. One mutant died at 45 weeks of age with limb weakness (Figure III-20). On examination, this animal had an atrophied thymus, pronounced hepatosplenomegaly and BM hypercellularity. The spleen was infiltrated with CD11c+ MHCII+ DCs and both BM and spleen had expanded CD11b+ Gr1+ neutrophil populations. Interestingly, the spleen had an increased CD71+ Ter119- erythroblast population, suggesting marked extramedullary erythropoiesis. Consistently, the frequency of LSK CD34- CD135- HSCs was also greater in the spleen than BM (Figure III-20B,C), suggesting that hematopoietic progenitors had shifted out of the BM. Inexplicably, the %GFP+ among both BM and spleen HSCs was increased (74% and 58%, respectively), which is much greater than historic, non-littermate controls (Boyer et al. 2011). This suggests that the HSC compartment has inappropriately begun to express the Cre recombinase and the PTPN11^{E76K} oncogene.

D. Comparing the Contributions of Fetal vs. Adult Hematopoietic Phases to Kras^{G12D}-Induced Disease

In Chapter II we described the CSF1R-MCM model as a tool to monitor the temporal expression of oncogenes in hematopoietic progenitors. In this chapter, we have described that fetal Kras^{G12D} expression in unperturbed animals leads to a JMML-like myeloid disease and that transplantation of fetal liver progenitors can propagate this MPN. In contrast, transplantation of adult progenitors from moribund FLT3Cre;Kras^{G12D} frequently resulted in T-ALL. These results suggest that the fetal hematopoietic phase can

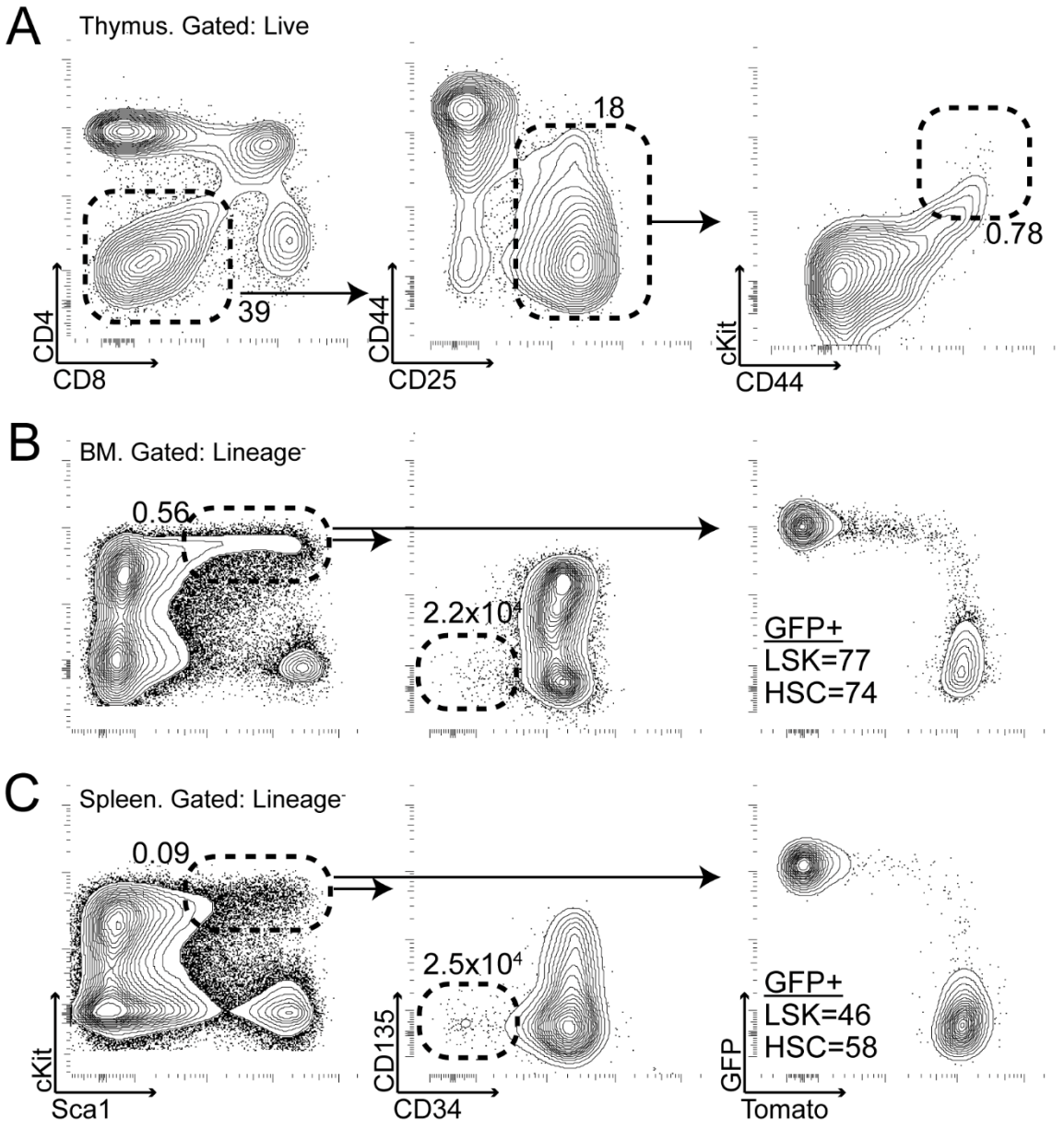

Figure III-20. FLT3Cre;PTPN11^{E76K}: Moribund Animal Analysis. FE-51 succumbed at 45 weeks of age with splenomegaly (982mg), hepatomegaly (1890mg), and thymic atrophy (11mg). Flow cytometric analysis revealed A) an expanded CD4- CD8- population in the thymus with a marked decrease of CD44+ CD25+ DNIIa and DNIIb cells. B-C) There was a marked decrease in BM HSCs and a minor expansion of splenic HSCs. LSK cells in both tissues were actively cycling and differentiating, as measured by the visualization of Tomato to GFP switch.

uniquely provide the appropriate spatial and temporal milieu for $Kras^{G12D}$-induced myeloid disease. We sought to formally test this hypothesis using the CSF1R-MCM+;$ROSA26^{YFP/YFP}$ system, which we showed in Chapter II to permit restricted expression of conditional mutations to specific phases of hematopoiesis.

We mated CSF1R-MCM+;$ROSA26^{YFP/YFP}$ studs with loxP-STOP-loxP-$Kras^{G12D}$ dams to generate CSF1R-MCM+;$ROSA26^{YFP/+}$;loxP-STOP-loxP-$Kras^{G12D}$ (hereafter CSF1R-MCM+;$Kras^{G12D}$), CSF1R-MCM;$Kras^{+/+}$, and Cre- littermate controls. In these animals, Cre-mediated recombination may be detected by the expression of the fluorescent protein YFP. As such, YFP+ cells in CSF1R-MCM+;$Kras^{G12D}$ mice express the oncogene and YFP- do not or have silenced their ROSA26 locus, as has been reported by other groups (Sabnis et al. 2009). We proceeded to inject these animals 3x with 75ug/g tamoxifen at 4 weeks of age to induce Cre activity in hematopoietic stem and progenitors cells of the adult phase (Figure III-21A).

Peripheral blood examination showed no evidence of leukocytosis in CSF1R-MCM;$Kras^{G12D}$ mutants compared to CSF1R-MCM;$Kras^{+/+}$ controls (Figure III-21B). Mutants developed anaemia and thrombocytopenia 12 weeks after tamoxifen injection. Flow cytometric analysis revealed YFP labelling in mutant and controls was equivalent 1 week after tamoxifen. Thereafter, %YFP+ leukocytes expanded in mutants, peaking at 12 weeks (Figure III-22B). Concomitantly, mutant animals had an expansion of CD11b+ myeloid cells and a paucity of CD3+ T-lymphocytes up to 12weeks after tamoxifen (Figure III-22C-E). Importantly, in mutant animals, YFP+ cells showed a much greater contribution to CD11b+ myeloid cells than to CD3+ T-cells, suggesting biased, cell autonomous differentiation (Figure III-22F-G). Nonetheless, mutant animals showed a rapid demise with a median survival of 18 weeks (Figure III-23A). Upon autopsy, these animals uniformly had massively enlarged spleens and thymuses, suggestive of a T cell leukemia/lymphoma (T-ALL) (Figure III-23B).

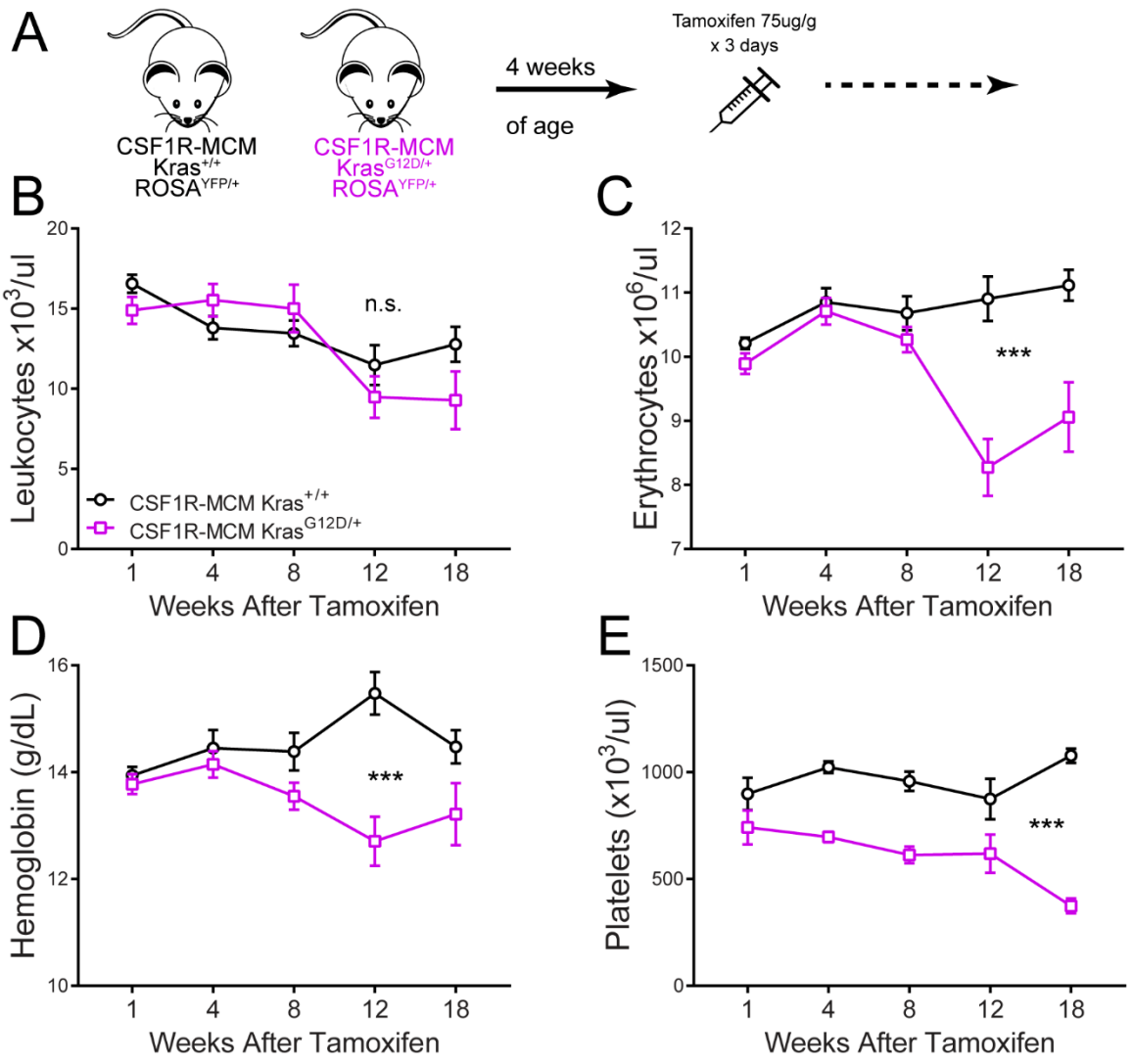

Figure III-21. Adult CSF1R-MCM;Kras^{G12D}: CBC Analysis. A) Schematic of experimental design. 8 mutants and 12 controls were serially analyzed over time. B-E) Mutant animals show anaemia and thrombocytopenia without leukocytosis.

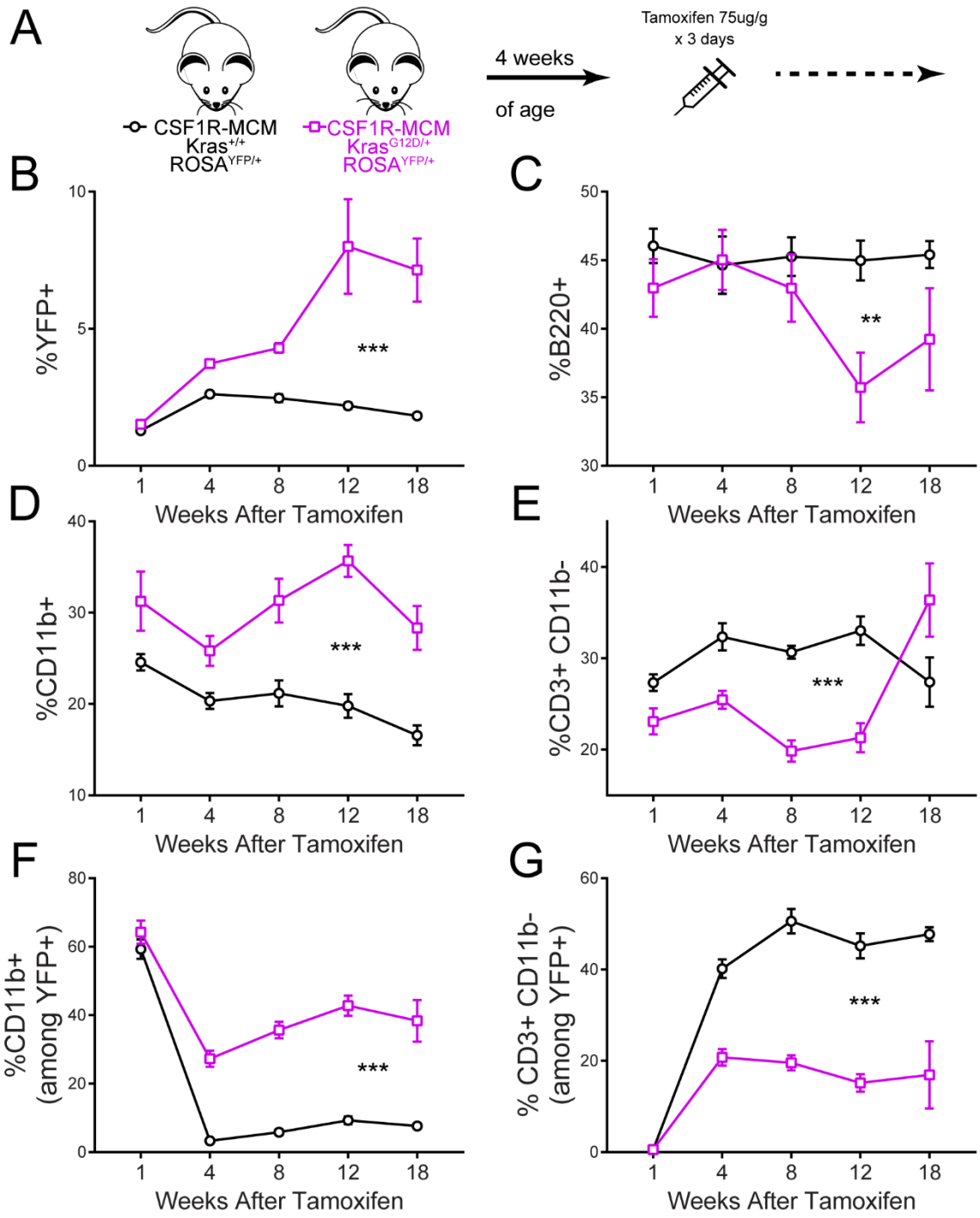

Figure III-22. Adult CSF1R-MCM;Kras^{G12D}: Peripheral Blood Leukocytes Analysis. B-E) Flow cytometric analysis of overall (YFP+ and YFP-) leukocytes in peripheral blood reveals monocytosis and a paucity of T-cells. F-G) YFP+ cells preferentially contribute to CD11b+ neutrophils rather than CD3+ CD11b- T-cells in mutants.

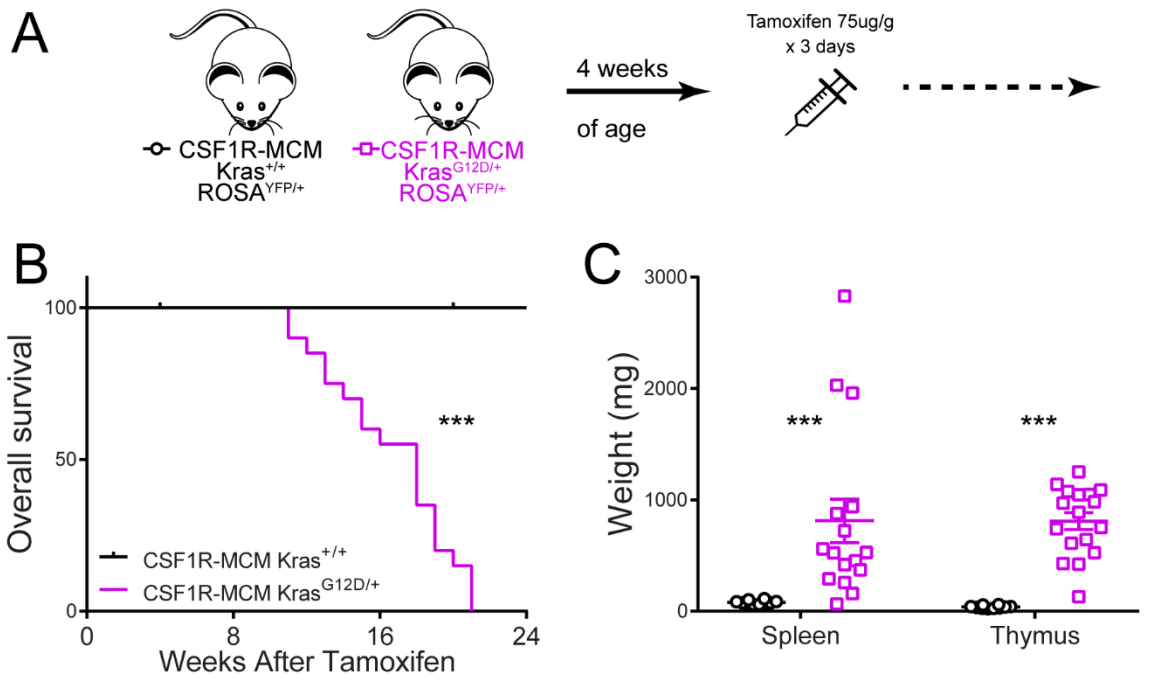

Figure III-23. Adult CSF1R-MCM;Kras^{G12D}: Survival and Tissue Weights. A) Adult cohort mutants succumb with a median survival of 18 weeks (N=22 mutants and 12 controls). B) Moribund mutants die with large spleens and strikingly enlarged thymuses.

We proceeded to analyze the lineages present in the organs of moribund animals. We observed a striking increase in the frequency of CD11b+ neutrophils in the spleens of mutants (Figure III-24B,C). There was a concomitant decrease in the frequency of CD4 and CD8 single positive T-lymphocytes. However, there was an appreciable infiltration of CD4+ CD8+ double positive (DP) T-lymphocytes. This phenotypic population is usually restricted to the thymus; we therefore proceeded to characterize thymus progenitor frequencies. Within the enlarged thymuses of mutant animals, we observed a striking increase of CD8 single positive or CD4 CD8 double positive cells (Figure III-25,26). Interestingly, these cells were YFP-, which suggests that this abnormal population was able to silence its ROSA26 locus. Concomitantly, we saw a decrease in the number of CD4+ or CD4-CD8- (DN) cells and a profound reduction of CD25+ DN II and DN III populations in mutants (Figure II-26C). This strongly suggests the occurrence of a differentiation block in T-lymphocyte commitment.

We hypothesized that CSF1R-MCM;$Kras^{G12D}$ mutants would have abnormal hematopoietic progenitors. Indeed, we observed a striking reduction in the frequency of LSK progenitors in the BM and their concurrent expansion in the spleen (Figure III-27D,E). Interestingly, we also observed an increase in the frequency of LK cells in both the BM and spleen. However, whereas BM progenitors saw an expansion of granulocyte-macrophage progenitors (GMP), the spleen had a pronounced increase in megakaryocytic-erythroid progenitors (MEPs, see Figure III-27F,G). This suggests that whereas the BM has become committed to myeloid cell production, the spleen of mutant animals has become the dominant site of erythropoiesis. The decrease in common myeloid progenitors (CMPs) in both in BM and spleen, together with the very rapid disease onset, suggests a tremendously high rate of myeloid and erythroid differentiation in mutant animals. Importantly, whereas the frequency of YFP+ cells was increased in progenitors compared to CSF1R-MCM;$Kras^{+/+}$ controls, this frequency was only ~7.5% (Figure III-

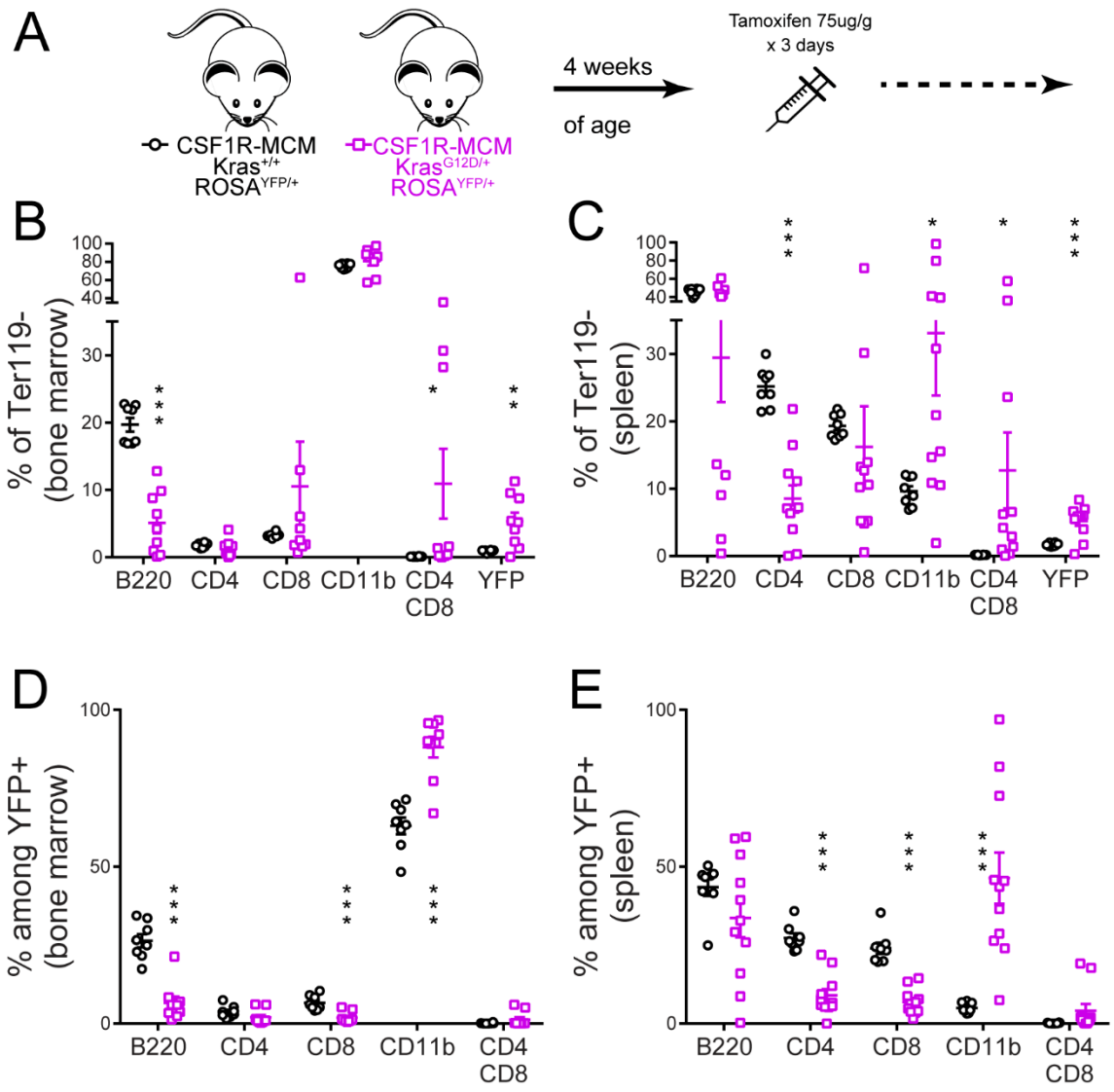

Figure III-24. Adult CSF1R-MCM;Kras^{G12D}: Tissue Leukocyte Analysis. B-C) Analysis of net leukocytes in BM and spleen reveals a paucity of splenic CD4+ cells, a concomitant expansion of CD11b+ splenic neutrophils and the presence of abnormal CD4 CD8 double positive thymocytes in both spleen and BM. D-E) Mutant YFP+ preferentially contribute to CD11b+ neutrophils at the expense of contributions to CD4+ and CD8+ mature T-lymphocytes as well as abnormal CD4 CD8 double positive malignant cells.

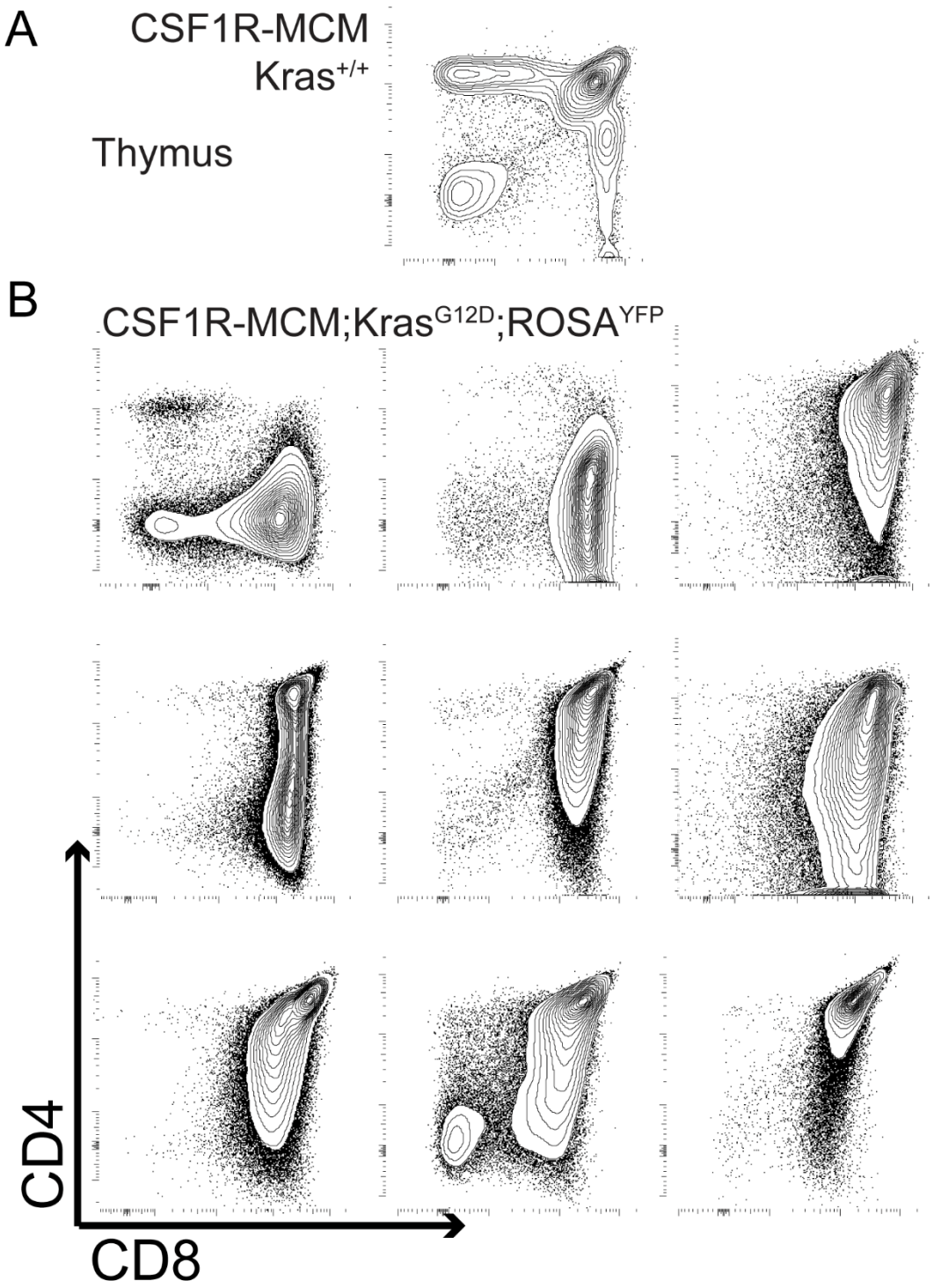

Figure III-25. Adult CSF1R-MCM;Kras^{G12D}: T-ALL Immunophenotype. Representative thymus flow cytometric gating of A) healthy littermate and B) 9 mutant animals.

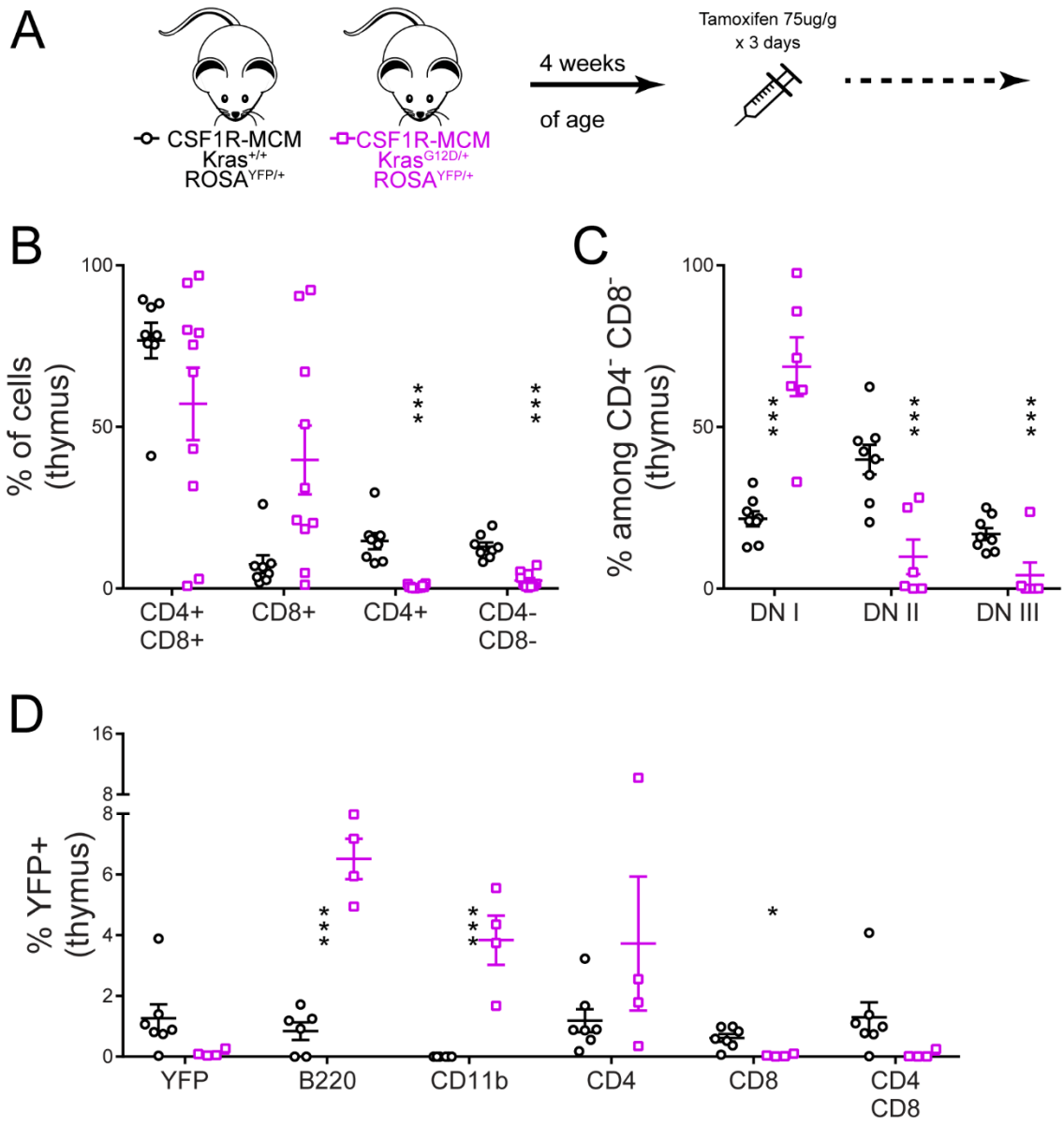

Figure III-26. Adult CSF1R-MCM;Kras^{G12D}: Thymocyte Analysis. B) Mutant thymuses have relative decrease of CD4+ and DN populations due to abnormal CD8+ cells. C) There is a lack of CD25+ DN II and DN III committed T cell progenitors in mutant thymuses. D) YFP+ cells in mutants contribute to myeloid and B cell populations but do not label CD8+ malignant cells; see also Figure III-31.

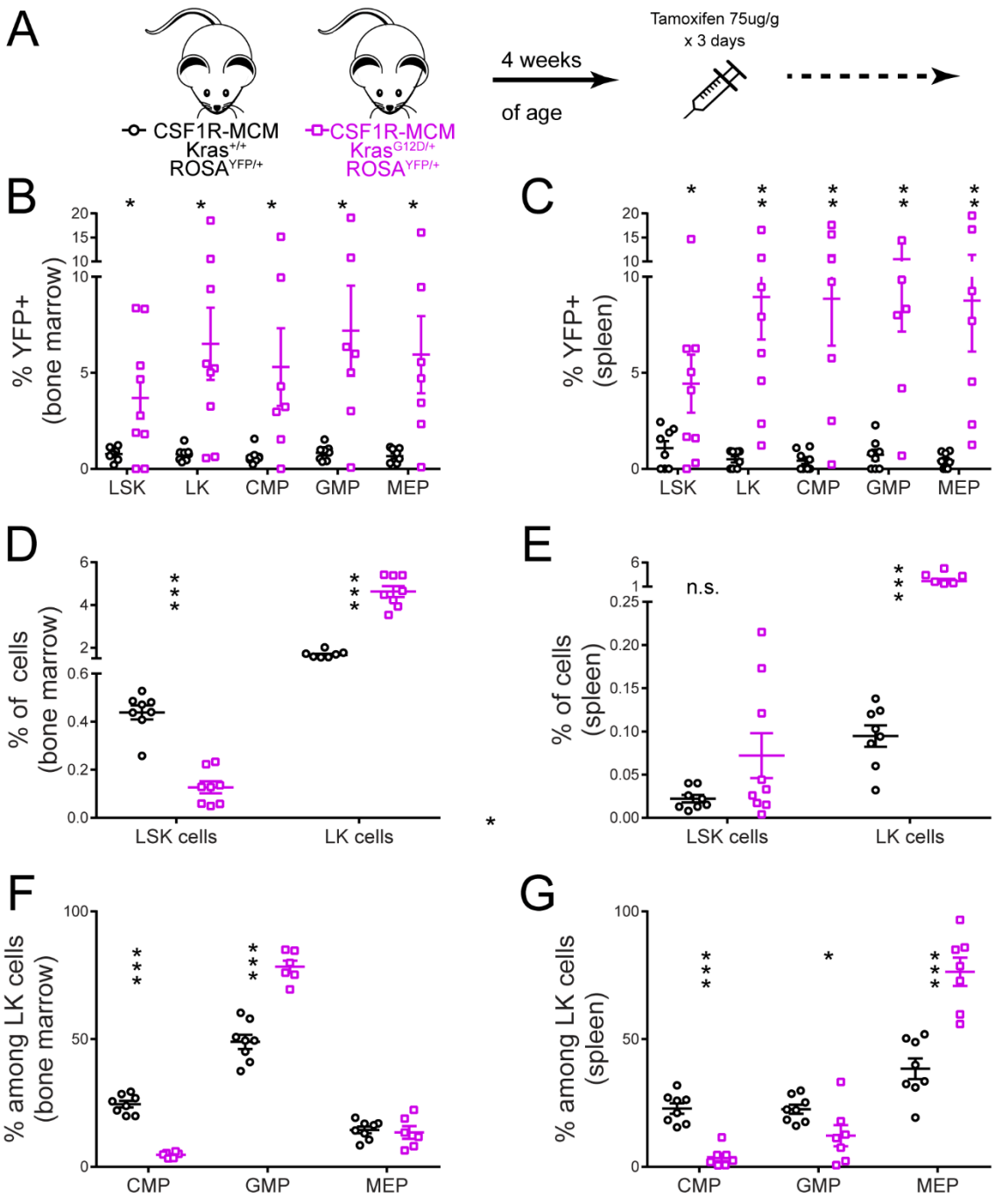

Figure III-27. Adult CSF1R-MCM;Kras^{G12D}: Hematopoietic Progenitor Analysis. B-C) Compared to littermates, mutants have BM and splenic progenitors that are more frequently YFP+. D-E) Net BM LSK cells are depleted whereas net LK cells are expanded in both the BM and spleen of mutants. F) GMPs are enriched in mutant BM whereas MEPs are enriched in spleens.

27B,C). This suggests that either i) a large proportion of oncogene-expressing cells are silencing their ROSA26 locus or ii) moribund mice have a low mutant allele frequency but that mutated progenitors are having non-cell autonomous effects of on healthy clones.

These results in CSF1R-MCM;Kras^{G12D} activated with tamoxifen at 4 weeks of age closely parallel previous studies in Mx1Cre;Kras^{G12D} mice. This is not surprising since both Cre systems were used to target the adult HSC-dependent hematopoietic phase. We proceeded to repeat these studies with a cohort that had their mutation activated in the fetal HSC-dependent phase via E14.5 injection of 4-hydroxy tamoxifen (Figure III-28A). We hypothesized that restricted expression of Kras^{G12D} in fetal hematopoietic progenitors with CSF1R-MCM would produce a faithful JMML-like disease similar to that of the FLT3Cre;Kras^{G12D} animals.

Due to a high frequency of late-term abortions, we obtained 7 mutants and 7 littermate controls. All were delivered by C-section. We saw that a considerably smaller frequency of YFP+ cells in the blood of this fetal cohort compared with previous CSF1R-MCM cohorts (Figure III-28B). Nonetheless, whereas there was no difference in the %CD11b+ cells, there was a striking decrease in CD4+ T-lymphocytes in our fetal cohort mutants compared to littermates (Figure III-28E). We did not observe leukocytosis or anaemia in these mice (Figure III-29B-D). Nonetheless, all fetal-cohort CSF1R-MCM;Kras^{G12D} mice succumbed to a T-ALL disease by 18 weeks of age (Figure III-29F,G)

The decrease in CD4+ T-lymphocytes prompted us to analyze the lymphoid progenitors in these mutants. We observed a striking decrease in the frequency of common lymphoid progenitors (CLPs) in the bone marrow of our mutants compared to controls (Figure III-30B,D). The frequency of MDP and CMoP myeloid progenitors were not changed. Consistently, we observed a decrease in the frequency of CD4- CD8- cells in the thymus with a concomitant lack of CD25+ committed T-lymphocyte progenitors. As was observed in adult-cohort CSF1R-MCM;Kras^{G12D} animals, our fetal-cohort mutants had

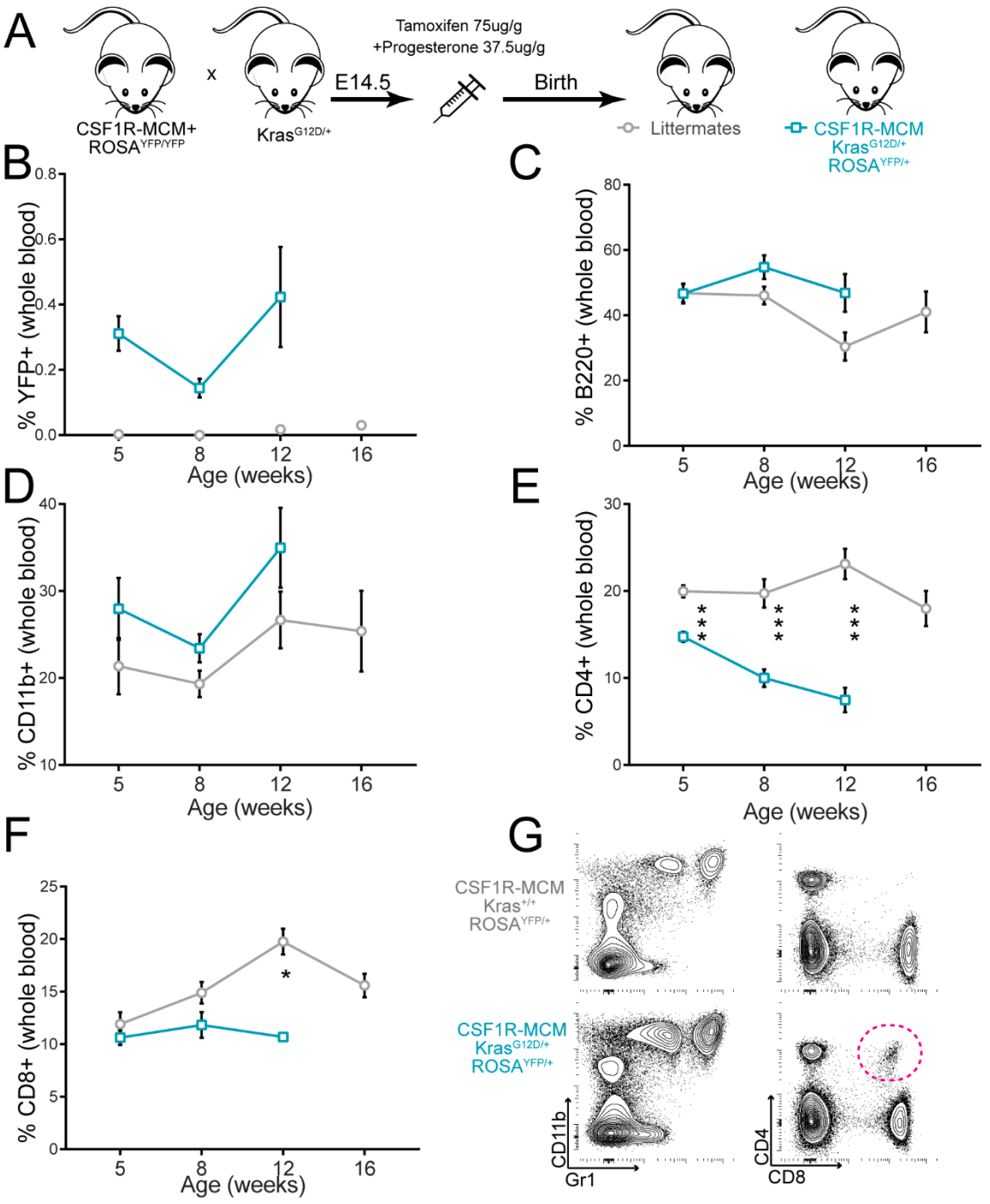

Figure III-28. Fetal CSF1R-MCM;Kras^{G12D}: Peripheral Blood Leukocytes Analysis. B) This cohort has low YFP expression in peripheral blood. C-F) mutants have a paucity of CD4 T-lymphocytes from an early age. G) Representative gating demonstrates expanded neutrophils and abnormal CD4 CD8 double positive cells in peripheral blood.

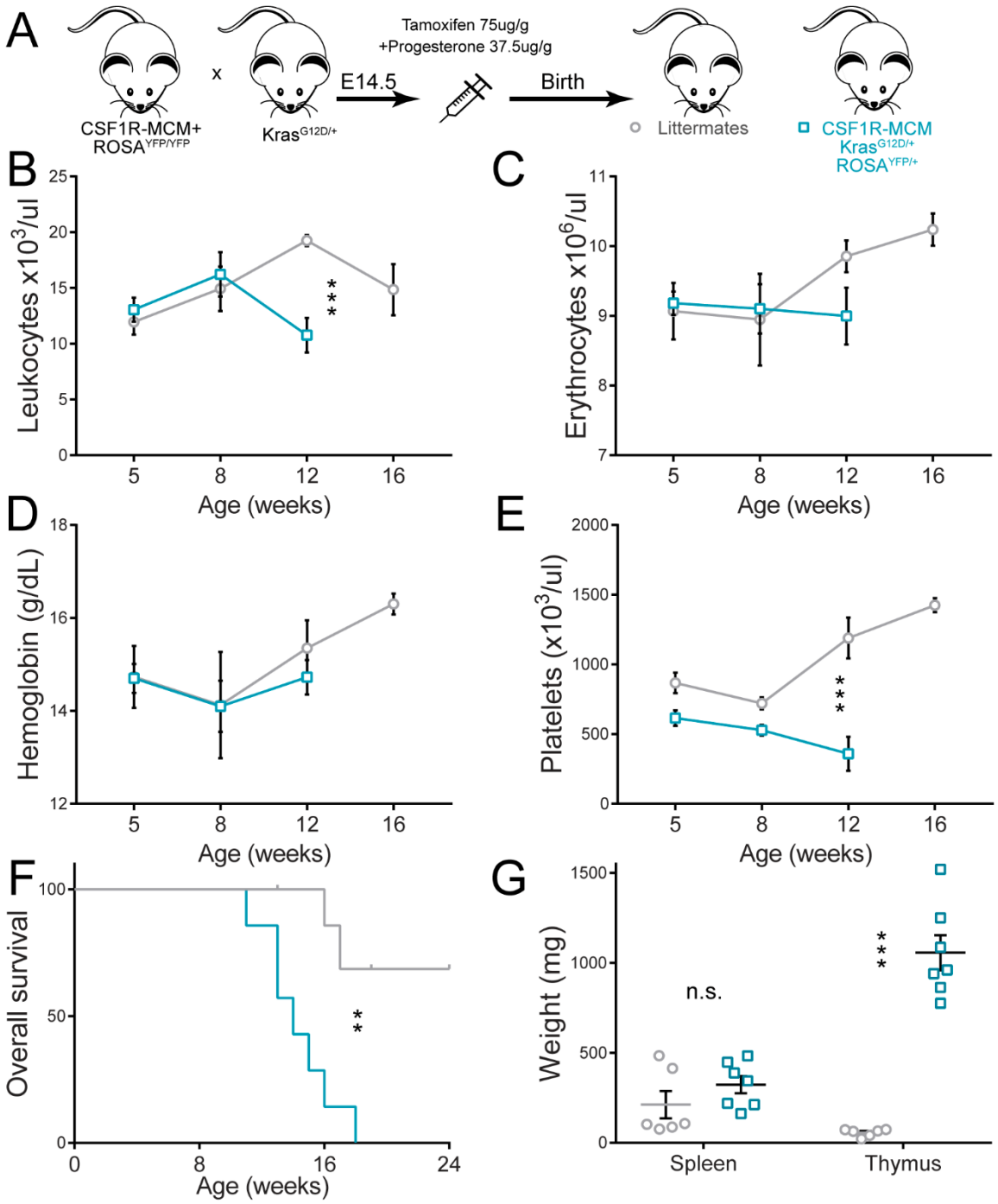

Figure III-29. Fetal CSF1R-MCM;Kras^{G12D}: CBC and Survival Analysis. B-E) Mutants show late-onset leukopenia and thrombocytopenia. F) Overall survival (N=7 mutants and 7 littermates). G) Tissue weights or moribund animals and littermates.

a striking expansion of CD4+ CD8+ or CD8+ single positive T-lymphocytes in the spleen. These mutant cells were uniformly YFP-, again suggesting that abnormal regulatory elements were silencing the ROSA26 locus. In contrast with our FLT3Cre;Kras^{G12D} mice, we did not see an expansion of CD11c+ dendritic cells in the BM, spleen, or thymuses of our CSF1R-MCM;Kras^{G12D} mice.

We have observed a very similar phenotype in both fetal-cohort and adult-cohort CSF1R-MCM;Kras^{G12D} animals. Both succumb 12-20 weeks after tamoxifen treatment from a T-ALL that does not express the YFP+ reporter. Preceding the animals' demise, they show myeloproliferation and a decrease of circulating T-lymphocytes. The overlapping features of myeloproliferation and T cell disease were strongly indicative of a particular T-ALL subset: early thymic progenitor (ETP) T-ALL. The hallmarks of ETP T-ALL is that it bears distinct features of dual lineage expansion (Zhang et al. 2012). BM progenitors from these patients have gene expression profiles that are enriched for myeloid progenitors in addition to T-cell progenitors. Additionally, only 17% of ETP-ALL had mutations in Notch1, compared with over 50% in other T-ALL cases, suggesting an alternate disease mechanism. Hyperactive *RAS* signaling is common in ETP-ALL and *K-ras* mutations have been observed in these patients (Zhang et al. 2012). Finally, abnormal methylation has been recently characterized in ETP-ALL and has been associated with silencing of specific genes including GATA3, a well-characterized regulator of T-cell development in the thymus (Naito et al. 2011; Fransecky et al. 2016). Importantly, with the exception of the ETP-ALL subgroup, GATA3 is typically overexpressed in T-ALL. We therefore proceeded to analyze the expression of GATA3 and other genes whose expression is known to regulate T cell development. We found that that mutants from both the fetal and adult cohorts had lower expression of GATA3 and Bcl11b in their thymuses compared to littermate controls (Figure III-30E). This strongly suggests that the disease emerging in CSF1R-MCM;Kras^{G12D} mice is a model of human ETP-ALL.

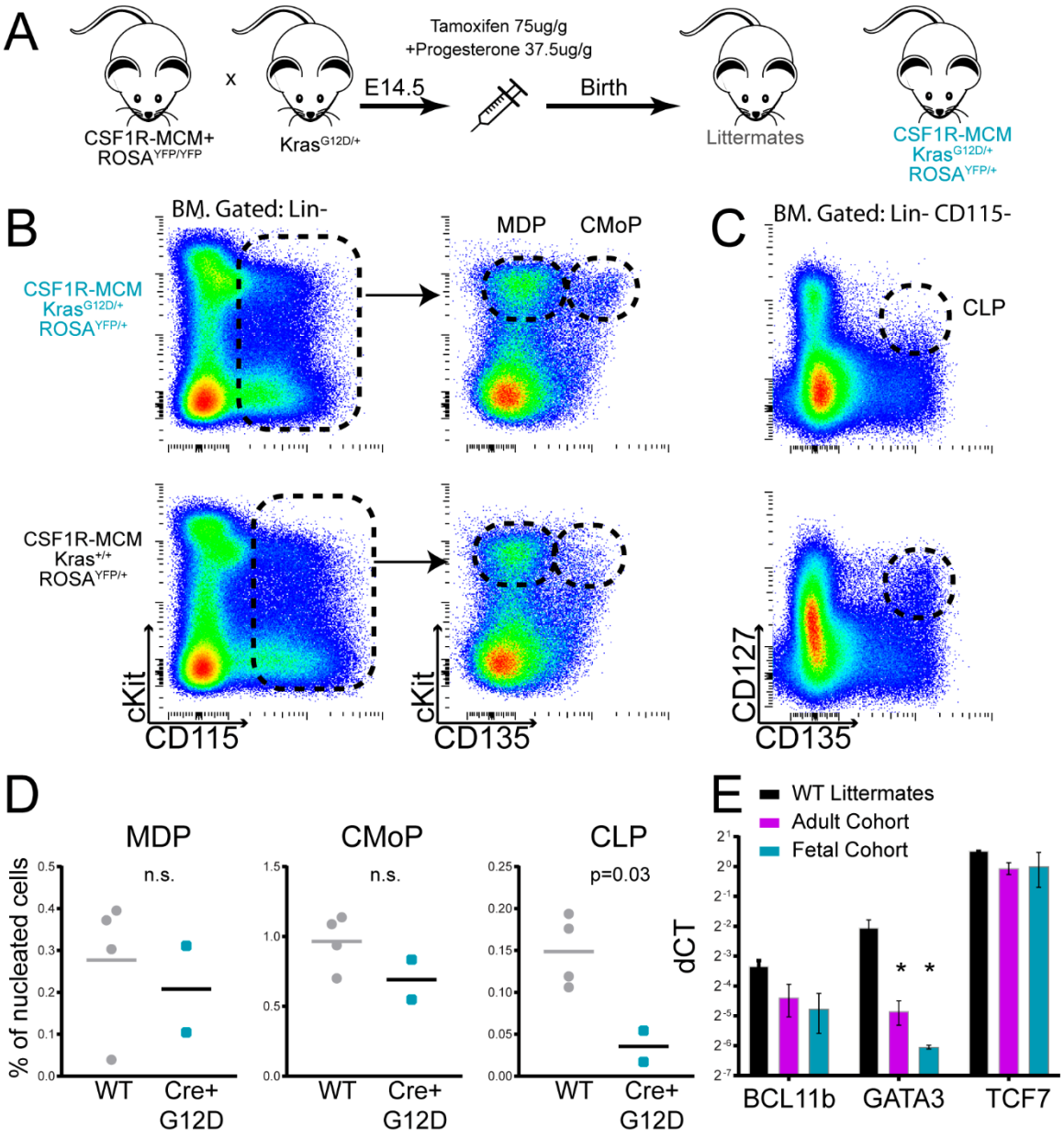

Figure III-30. Fetal CSF1R-MCM;Kras^{G12D}: Progenitor Analysis. B,C) Representative flow cytometry plots of myeloid and lymphoid progenitors in BM of fetal cohort mutants and littermates. D) Quantification of progenitors shown in B,C. E) Gene expression in unfractionated thymocyte samples; CT values normalized to GAPDH expression.

Discussion

A. The FLT3Cre+ Kras^{G12D} Model of JMML

We present the first murine Kras^{G12D} model to unify JMML disease-defining features: an *in utero* origin, viability at birth followed by a failure to thrive, anaemia, thrombocytopenia, monocytosis, hepatosplenomegaly, and infiltration of tissues with histiocytes. All FLT3Cre;Kras^{G12D} mice succumbed to a myeloid disease that could be recapitulated following fetal liver transplantation. This is in stark contrast to existing Kras^{G12D} models, which die from T-ALL or non-hematopoietic expression (Staffas et al. 2015; Desai, Brownfield, and Krasnow 2014; Tang et al. 2013; Braun et al. 2004).

FLT3Cre has a markedly different expression pattern from Mx1Cre, which may explain the observed respective myeloid vs lymphoid disease outcomes. Mx1Cre is used to target adult progenitors whereas FLT3Cre becomes active in fetal MPPs (Beaudin et al. 2016). As such, FLT3Cre initiates Kras^{G12D} expression within an *in utero* progenitor that is more proliferative, has greater repopulating ability, and has enhanced myeloid cell production compared to adult progenitors targeted by Mx1Cre (Benz et al. 2012; Copley et al. 2013; Dykstra et al. 2007). This context emulates JMML patient studies that highlighted the fetal origins of this disease: the causative somatic mutations occur before birth and BM cells have a gene expression signature that is characteristic of fetal – and not adult – progenitors (Matsuda et al. 2010; Helsmoortel, Bresolin, et al. 2016). Therefore, in contrast to Mx1Cre, FLT3Cre targets Kras^{G12D} expression to the appropriate progenitor at the appropriate developmental stage to recapitulate the origin of JMML.

Previous studies have suggested that the HSC is the cell of origin for Kras^{G12D}-evoked T-ALL (Zhang et al. 2009; Sabnis et al. 2009). In contrast, FLT3Cre is not expressed in adult HSCs; its activity is restricted to MPPs and their progeny (Boyer, Beaudin, and Forsberg 2012). As such, HSCs in FLT3Cre;Kras^{G12D} animals do not express the mutation and therefore would not be able to initiate T-ALL. In the setting of

transplantation, however, the circumstances change. We show that the majority of recipients of BM from moribund FLT3Cre;Kras^{G12D} mice do develop T-ALL. This finding further highlights the differences between unperturbed and post-transplant hematopoiesis. Additionally, since FLT3Cre is not active in BM HSCs, our study challenges the hypothesis that T-ALL is initiated from an HSC. Instead it suggests that oncogene expression within MPPs is sufficient for T-ALL development in a transplantation setting.

The lack of recombinase activity in HSCs also permits analysis of HSC-intrinsic vs extrinsic effects of oncogene expression. For instance, we were surprised to observe that FLT3Cre;Kras^{G12D} mice have decreased frequencies of HSCs in both the BM and spleen. This suggests that non-mutated HSCs may exhaust from the increased cycling of oncogene-expressing downstream progenitors. Our results suggest that studies that rely on Mx1Cre-induced genetic alterations to draw conclusions about HSC functions should distinguish: i) intrinsic effects of genetic alterations on HSCs and ii) extrinsic effects in downstream progeny that affect HSC function via feedback mechanisms.

The cellular origin of JMML has been controversial. On the one hand, case reports have shown CD34+ CD38- patient cells express disease-initiating mutations (Busque et al. 1995; Stieglitz, Taylor-Weiner, et al. 2015) and xenotransplantation of patient progenitors will produce mutated myeloid, B, and T cells with a common clonal origin (Nakamura et al. 2005). On the other hand, circulating T-lymphocytes from most patients do not express the disease-initiating mutation (Flotho et al. 1999; Sakaguchi et al. 2013). These findings suggest that JMML is initiated within a multipotent progenitor that subsequently undergoes a differentiation block during T-lymphocyte commitment. Consistent with this hypothesis, case reports have noted decreased T cell frequencies in the blood, bone marrow, and spleen of JMML patients (Weinberg et al. 1990; Krombholz et al. 2016; Oliveira et al. 2016). These findings parallel our FLT3Cre;Kras^{G12D} model, which has an atrophied thymus and decreased peripheral T-lymphocytes. It will be

important to understand the significance of abnormal T-cell development in JMML and its contribution to patient morbidity; we discuss this is more detail below.

Another group found similarly skewed T-lymphocyte development when $Kras^{G12D}$ expression was restricted to dendritic cells in $p53^{-/-}$ mice via Clec9a-Cre (Bottcher et al. 2015). Importantly, this group demonstrated that $Kras^{G12D}$-expressing DCs are capable of antigen presentation to T-lymphocytes and that these DCs permit proliferation and normal T-Cell Receptor gene rearrangements. These mice had diminished overall survival but the cause of their lethality was not explicitly stated. Our results build on these findings and suggest that $Kras^{G12D}$ expression in a fetal multipotent progenitor is sufficient for preferential DC differentiation in the thymus.

Dendritic cell biased differentiation was observed in tissues apart from the thymus. BM progenitors from FLT3Cre;$Kras^{G12D}$ mice could spontaneously differentiate into DC-like cells *in vitro*, as has been observed in patient samples (Longoni et al. 2002; Estrov et al. 1986). DCs were also markedly expanded in the BM and spleen of our model and were distinct from neutrophils, which were also increased in number. Importantly, case reports have equally noted JMML patient tissues are infiltrated by atypical histiocytes (Ozono et al. 2011; Ng et al. 1988). Future clinical studies will need to evaluate whether these cells are functional antigen presenting DCs and whether they contribute to JMML patient morbidity.

In summary, we describe the first $Kras^{G12D}$ mouse model that recapitulates defining features of JMML. FLT3Cre;$Kras^{G12D}$ mice are viable, develop monocytosis, anaemia, thrombocytopenia, hepatosplenomegaly, and they die from a fully penetrant and transplantable myeloid disease. This model further emulates underappreciated features of JMML such as the paucity of mature T-lymphocytes and an expansion of dendritic cells and thereby hints at potential new therapeutic strategies. FLT3Cre;$Kras^{G12D}$ mice will

prove useful for preclinical drug studies targeting the RAS-MEK-ERK signaling pathway and will help elucidate the developmental origins of JMML and pediatric leukemias.

B. FLT3Cre;Kras^{G12D} Age-Matched Transplantations

We performed age-matched transplantations of E14.5 fetal liver (FL) and 4 week-old BM from FLT3Cre;Kras^{G12D} mice into both neonatal and adult congenic recipients. These studies permitted us to gauge the relative importance of the fetal progenitor and of the fetal niche in contributing to our JMML-like disease. We show that—compared to BM donors—FL progenitors lead to more rapid mortality when transplanted into either adult or neonatal recipients. Equally, we determined that whereas all recipients of fetal progenitors developed a JMML-like disease, the majority of BM recipients developed T-ALL. These results suggest, that the primary determinant of myeloid vs. lymphoid disease and the rate of onset is the progenitor itself; not its microenvironment.

We did not find differences in survival when comparing adult and neonatal recipients of FL progenitors. Upon secondary transplantation, however, we saw that adult secondary recipients succumbed more rapidly than neonatal recipients. This is likely due to the competitive nature of neonatal transplantations. Since sublethal conditioning regimens must be used, the donor cells compete with the newborn's native progenitors. Therefore, whereas adult recipients of fetal progenitors had >90% engraftment 5 weeks after transplantation, neonatal recipients showed 35% engraftment. Secondary neonatal recipients showed less than 10% engraftment even 13 weeks after transplantation.

Another striking difference between fetal and BM donors was that the proportion of fetal progenitors that contributed to CD11b+ myeloid cells was much greater than that of adult donors. Whereas 90% of donor cells in FL>Adult and 75% of FL>Neonate were CD11b+, less than 50% were CD11b+ when BM donors were used. These findings agree with previous studies that show fetal progenitors are more proliferative and produce more

and larger myeloid colonies than BM progenitors (Broxmeyer et al. 1992; Lansdorp, Dragowska, and Mayani 1993). Notably, this does not contradict single cell studies that showed fetal HSCs preferentially contribute to lymphoid cells whereas adult HSCs preferentially contribute to myeloid cells (Benz et al. 2012). This is because our study considered the short-term (<13weeks) contribution of MPPs to disease manifestation, whereas the Benz *et al.* study considered the durable (>16week) contribution of single cell HSCs.

We made a remarkable finding when we correlated engraftment with the frequency of donor-derived CD11b+ myeloid cells. The greater the engraftment of CD45.2 cells, the more their differentiation is biased towards CD11b+ myeloid cells (Figure III-16). This trend was observed in all 4 of our transplant cohorts. Importantly, it was not observed among FLT3Cre;$Kras^{+/+}$ control transplant cohorts. This finding suggests that greater engraftment of mutant cells will cause changes in the hematopoietic niche that further exacerbate the MPN phenotype. This change could be a cytokine that causes mutant progenitors to become more proliferative and myeloid biased. If such a cytokine is secreted by mutant cells, then greater engraftment = more secretion = more myeloid proliferation. Such a scenario is consistent with the non-cell autonomous findings in our the CSF1R-MCM;$PTPN11^{E76K}$ model where both YFP+ mutated cells and YFP- WT cells in the same niche are equally hypersensitivity to GM-CSF, presumably due to cytokine secretions.

This parallel prompted us to determine if the residual host CD45.1+ cells that resisted myeloablation were also myeloid-skewed following FLT3Cre;$Kras^{G12D}$ transplantation. Given the results from our CSF1R-MCM;$PTPN11^{E76K}$ cohort, it was surprising that CD45.1+ cells were not myeloid-biased. There are two potential explanations. First, post-transplant hematopoiesis may not recapitulate the unperturbed findings of the CSF1R-MCM cohort. Indeed, residual cells in a lethally-irradiated host are typically long-lived B-cells and T-cells. Alternatively, the effect of the $Kras^{G12D}$ mutation on

the niche may be different from that of the PTPN11^{E76K} mutation. Whereas we did observe non-cell autonomous effects following PTPN11^{E76K} expression, the effects of Kras^{G12D} in the niche may be restricted to cells that express the mutation.

We acknowledge that the findings from these transplants must be considered in context. The donor populations were not sorted and the number of progenitors per recipient varied among the 4 cohorts. For instance, the frequency of MPPs and HSCs in the fetal liver of mutants is 0.4% and 0.03% respectively, whereas the frequencies in the BM are much lower: 0.08% and 0.001%, respectively. Furthermore, engraftment in neonates is much lower than in adult recipients, albeit this difference is less pronounced for fetal progenitors (Arora et al. 2014). As such, the definitive conclusion from these transplants is limited: fetal progenitors propagate a JMML-like disease whereas BM progenitors do not. Additional studies that control for the number of transplanted progenitors and account for engraftment differences would need to be performed to directly compare effects of neonatal vs. adult recipients.

C. Comparison of Kras^{G12D} and PTPN11^{E76K} Models of JMML

Among JMML patients, mutations in *PTPN11* are particularly deleterious and are associated with an inferior prognosis compared to other mutations, including *KRAS*. (Yoshida et al. 2009). Indeed, the presence of *RAS* mutations in JMML patients has been suggested to be correlated with superior overall survival, even the potential of spontaneous remission (Matsuda et al. 2007). However, in murine studies Kras^{G12D} mutants have notably inferior survival to PTPN11^{E76K} mutants. Median survival following pI:pC for Mx1Cre;Kras^{G12D} is 11 weeks, whereas for Mx1Cre;PTPN11^{E76K} it is 28 weeks. This suggests there are differences between murine and human signaling pathways downstream of these nodes.

We also observed differences in signaling between our *PTPN11* and *KRAS* models. Progeny of VavCre;PTPN11^{D61Y} yolk sac EMPs had hyperactive *RAS* as measured by increased phosphorylation of ERK following GM-CSF stimulation. In contrast, we did not observe increased phosphorylation of ERK, STAT5, or AKT in our FLT3Cre;Kras^{G12D} model. These findings are consistent with previous murine studies (Braun et al. 2004) that also failed to see elevated MEK or AKT activation in cells cultured from Mx1Cre;Kras^{G12D} BM. On the other hand, freshly harvested LK cells from these mice do show elevated ERK activation following GM-CSF stimulation (Lyubynska et al. 2011). These findings highlight that signaling downstream of Kras^{G12D} is inadequately understood and that species-specific differences may account for the incongruent survival of human patients and mouse models expressing oncogenic *KRAS*.

As such, our observation that FLT3Cre;PTPN11^{E76K} mice have prolonged survival compared to FLT3Cre;Kras^{G12D} mice is consistent with previous murine models. What may be surprising is the large difference in survival we observed. Whereas FLT3Cre;Kras^{G12D} mice succumb with a median age of 26 days, more than 75% of FLT3Cre;PTPN11^{E76K} mice remained alive 1 year after birth. This finding suggests that previous PTPN11^{E76K} models—which used Mx1Cre, VavCre, or LysMCre—had significant morbidity from non-hematopoietic expression. Unfortunately, these other models did not assess the contribution of endothelial and stromal cell oncogene-expression to disease.

The differential responses of the two oncogenes to expression by CSF1R-MCM vs. FLT3Cre are equally striking. Both FLT3Cre;PTPN11^{E76K} and CSF1R-MCM; PTPN11^{E76K} mice acquire MPN. In contrast, FLT3Cre;Kras^{G12D} uniformly die of MPN whereas all CSF1R-MCM;Kras^{G12D} acquire T-ALL. Notably, the age at which CSF1R-MCM was activated did not alter the dominant disease manifestations in either model. This argues that the fetal vs. adult phase of the progenitor is not *per se* the dominant

determinant of disease manifestation. Rather, it suggests that the mutant allele frequency may determine disease outcome for $Kras^{G12D}$ but not for $PTPN11^{E76K}$.

Cre efficiency is a direct surrogate for measuring the mutant allele frequency. FLT3Cre results in the activation of >80% of hematopoietic progenitors. In contrast, we activated no more than 2% of progenitors using CSF1R-MCM. As such, the initial mutant allele frequency in FLT3Cre cohorts is much greater than that in CSF1R-MCM cohorts. The greater allele frequency in FLT3Cre;$Kras^{G12D}$ may permit myeloid populations to expand sufficiently early and quickly to cause lethality. In contrast, the myeloid expansion in CSF1R-MCM;$Kras^{G12D}$ is pronounced but simply cannot produce monocytosis to the same extent as the FLT3Cre cohort. Instead, the paucity of circulating T-lymphocytes may provoke greater cycling among thymic progenitors and lead to lymphoma.

In contrast, we observed extensive non-cell autonomous effects in the setting of $PTPN11^{E76K}$. Non-mutated YFP- progenitors that cohabit the niche in CSF1R-MCM; $PTPN11^{E76K}$ animals demonstrate the same degree of GM-CSF hypersensitivity as do YFP+ mutant-expressing progenitors. This suggests that even in the setting of a low mutant allele frequency, $PTPN11^{E76K}$ will provoke MPN development due to alterations in the BM niche.

In this light, the comparison between FLT3Cre; $PTPN11^{E76K}$ and CSF1R-MCM; $PTPN11^{E76K}$ mice is remarkable. These cohorts have high and low mutant allele frequencies, respectively. However, the MPN manifestations in these animals are equivalent. Both have nearly 50% net CD11b+ cells and fewer than 20% net T-cells in peripheral blood at 1 year of age. The overall survival is equal ($p=0.45$) and the leukocyte counts are equal. This suggests that the same MPN will emerge in the setting of both high and low hematopoietic-restricted $PTPN11^{E76K}$ allele frequencies.

This finding highlights the importance of murine studies that assess low mutant allele frequency contributions to disease—particularly in the setting of unperturbed

hematopoiesis. Human studies have demonstrated the pervasiveness of clonal hematopoiesis and its direct correlation with all-cause mortality (Jaiswal et al. 2014; Genovese et al. 2014). Therefore, models that permit monitoring of hematopoietic subpopulations within an animal would be very beneficial to this field. However, it will not be possible to use Mx1Cre and VavCre because of their broad and indiscriminate activation patterns. We present CSF1R-MCM has the most readily available tool that is compatible with existing conditional mouse models and can emulate the clonal nature of hematologic malignancies. Given the striking findings of our studies we strongly urge other researchers to adopt similar strategies.

D. T-Lymphocyte Development in JMML

We observed a common feature in all of our models of JMML. Prior to overt disease, all mutant animals demonstrated myeloproliferation with a concomitant decrease in peripheral T-lymphocytes. The frequency of B-lymphocytes was not changed until fulminant disease manifestations. These findings strongly suggest that a convergent pathway is driving this lineage bias. Evidence from both PTPN11 and Kras cohorts suggests that there is a marked defect in the maturation of DN I progenitors to the DN II and DN III stages. Functionally, this transition is normally characterized by expression of CD25, and the downregulation of cKit. As the progenitor loses cKit expression, the DNIIa to DNIIb checkpoint is reached. This transition marks the irreversible commitment to T-lymphocytes. Prior to this point, thymic progenitors are capable of multilineage differentiation including into myeloid cells and dendritic cells (Kueh et al. 2016; Luc et al. 2012). Coordinate cues are required for this commitment including Notch signaling as well as sequential transcription factors: GATA3, TCF7, and BCL11b (Naito et al. 2011).

These findings prompted us to search whether parallel findings have been reported among JMML patients. Indeed, we found several reports that describe reduced T-

lymphocyte numbers in these children (Weinberg et al. 1990; Oliveira et al. 2016; Krombholz et al. 2016). Additionally, reports suggest that T-cells may not express the disease-initiating mutation (Flotho et al. 1999; Sakaguchi et al. 2013). These results are consistent with our finding that oncogene expression causes defective T cell maturation and a concomitant decrease in mature progeny. Interestingly, our findings of decreased CLPs in the BM of CSF1R-MCM;Kras^{G12D} mice suggest that the causes of this block may not be solely restricted to the thymus.

It will be important to understand the significance of this observation in patients. Lack of functional T-lymphocytes would likely exacerbate the morbidity of MPN but may equally suggest alternative treatment strategies. JMML patients' elevated susceptibility to infection further provides evidence that they may lack a normal adaptive immune system. Additionally, several case reports have identified JMML patients who subsequently developed T-ALL with the same mutant clone (Raikar et al. 2016; Cooper et al. 2000). This suggests that under certain conditions, the defect in T cell development may be overcome and cause a leukemia. As such, further evaluate T-cell maturation in JMML patients and probing the mechanisms of a potential differentiation block may identify strategies prevent lineage switching and improve outcomes following infection.

Ongoing Studies and Future Directions

A. Further characterization of FLT3Cre;Kras^{G12D}

We will continue to analyze our JMML model with the intention of understanding the pathophysiology of disease in patients. We have noted a marked expansion of dendritic cells in our model. Whereas case reports present similar patient findings, it is unclear how common DC expansion is in JMML and whether it contributes to morbidity. We will isolate CD11c+ DCs from the spleens of our mice and assess their ability to stimulate T-cells via antigen presentation. DCs from mutants and controls will be

separately co-cultured with naïve CD4+ cells from OT-II mice, which uniquely express a T-cell receptor specific for ovalbumin. Ovalbumin will then be added to the culture medium. If the CD11c+ DCs are *bona fide* antigen presenting cells then they should be able to process the ovalbumin, present it on their MHCII, and thereby stimulate the CD4+ cells to proliferate. This proliferation will be measured through the dilution of a dye, such as CFSE.

We would then proceed to more thoroughly characterize the abundance of DCs in patients. We have been fortunate to acquire tissue blocks of JMML patient spleens. We would section them onto cover slips and stain them with human DC markers, including CD11c, MHCII, CD1c, and CD141. If we saw an expansion, we could then follow up with stains of activated DCs, such as CD80 and CD86, to determine if they were more likely to be presenting antigen than DCs from controls. Finally, if we were able to obtain live cells from human spleens, we could determine whether patient DCs share the same functional antigen presentation characteristics as DCs from our model.

Apart from dendritic cells, we will further characterize the progenitor compartment. We assume that only cells with active Cre recombinase express the mutation and that only GFP+ cells express Cre. Nonetheless, we will directly confirm this using genomic quantitative PCR. We have designed primers that can distinguish recombined vs non-recombined alleles of the LSL-Kras^{G12D} locus. We will therefore sort GFP+ and Tomato+ subsets and quantify the frequency of recombined oncogene to ensure that only GFP+ cells express the oncogene and that Tomato+ cells do not.

If Tomato+ cells truly are WT we will proceed to characterize why we see a depletion of Tomato+ HSCs in our model. Our hypothesis is that increased differentiation of downstream progenitors causes HSCs to enter the cell cycle. We will test this using Ki67 and DAPI staining in Tomato+ Lin- cKit+ Sca1+ CD150+ CD48- HSCs. Alternatively, it is possible that HSCs fail to appropriately seed the BM and spleen. HSCs in mutant animals may remain confined to the liver, potentially due to a lack of chemokine receptors

such as CXCR4, PSGL-1, and CD44 (Magnon and Frenette 2008). If we do not detect a difference in HSC cell cycle, we will proceed to characterize the expression of these markers on peri-natal HSCs.

B. Transplantations with sorted FLT3Cre;Kras^{G12D} subsets

We will further study our progenitors with transplantations using sorted populations. This will enable head-to-head comparison of distinct progenitors from both the fetal and adult (4 week old BM) phases. By enabling transplantations with defined numbers of progenitors, we will build on findings from our CSF1R-MCM;Kras^{G12D} studies, which suggested that the mutant allele frequency was more important than the hematopoietic phase in determining a myeloid vs. lymphoid disease with this oncogene.

There are four variables to consider in these transplant studies: i) fetal vs. adult phases; ii) GFP+ vs. Tomato+, corresponding to the presence and absence of active mutation, respectively; iii) progenitor immunophenotype, be it HSC, MPP, or lineage committed progenitors; and iv) the number of donor cells. In each scenario FLT3Cre; Kras^{G12D} donors will be transplanted alongside CD45.1 supportive cells. Concurrent transplants with FLT3Cre:Kras$^{+/+}$ littermates will be performed as controls. Recipients will be adult BoyJ animals; we will describe novel strategies for neonatal transplants below.

Initially, we will transplant 100 Tomato+ HSCs from fetal and adult phases. Following their engraftment, the progeny of these HSCs will transition through a FLT3+ intermediate whereby they will begin to express GFP and the oncogene. This transplant will determine whether progenitors from the fetal phase cause a JMML-like disease whereas those from the adult phase cause T-ALL. If the fetal transplant results in T-ALL, we will repeat the experiment using 500 fetal Tomato+ donors to gauge if increased mutant allele frequency alters disease outcome. Finally, we will transplant the fetal GFP+ HSCs

(Beaudin et al. 2016), which would assess whether this transient population may contribute to disease manifestations in our model.

Next, we will transplant 500 GFP+ MPPs from fetal and adult phases. These are the populations that actively express the oncogene in our model. As such they are the presumptive candidate for the JMML-initiating cell. We expect that adult MPPs will transiently contribute to peripheral leukocytes but will not durably engraft and will not contribute to disease. This would support similar progenitor transplantations reported using the Mx1Cre;$Kras^{G12D}$ model (Zhang et al. 2009). Fetal MPPs, on the other hand, may be sufficiently proliferative to evoke a fulminant MPN. If fetal MPPs do not cause disease, this would suggest that the MPN in our model was the result of persistent contributions from Tomato+ HSCs to GFP+ MPPs. Each such differentiation would produce a new MPP clone that expresses $Kras^{G12D}$. This would indicate that the MPN observed in our model was not clonal, but rather the result of incessant mutagenesis following each asymmetric HSC division.

Finally, we will transplant lineage-committed cells to determine if they have been transformed and can propagate the disease. We will begin by transplanting dendritic cells from the spleens of moribund mice. Previous work suggested that transfer of $Kras^{G12D}$-expressing DCs is sufficient to kill recipient mice (Bottcher et al. 2015). However, they did not characterize the nature of the resulting disease. Our study could address whether DCs are sufficient to alter the T-cell differentiation observed in the thymus of our animals and whether this contributes to myeloid-biased progenitor differentiation.

C. Neonatal Transplants.

We described the first study that sought to assess disease outcomes following age-matched transplantations. Our goal was to determine if the fetal vs. adult hematopoietic niche contributes to the myeloid vs. lymphoid disease following $Kras^{G12D}$

expression. We noted, however, that it is challenging to interpret these experiments due to differences in the conditioning regimens of neonatal and adult mice. The former can only be sublethally irradiated. As a result, neonatal transplants are inherently competitive. Previous attempts by the Yoder lab to standardize the conditioning regimens and permit head-to-head comparison of neonatal vs. adult recipients have not identified a viable strategy. Below we propose another approach that may prove fruitful.

The transcription factor Myb is required for the emergence and maintenance of HSCs (Mucenski et al. 1991). Previous studies have deleted Myb using Mx1Cre as a conditioning regimen and performed transplants in the absence of irradiation (Schulz et al. 2012). Our proposal is to generate FLT3Cre;$Myb^{fl/fl}$ mice. These animals would have normal development of HSCs (since they do not express FLT3), but the progeny of HSCs would subsequently lose Myb expression and undergo defective differentiation. FLT3Cre is active in >90% of hematopoietic cells, suggesting that the extent of deletion should be pronounced but that an adequate number of leukocytes and erythrocytes should be present to permit viability. We would then compare engraftment into non-irradiated neonatal and adult FLT3Cre;$Myb^{fl/fl}$ mice. In such a setting, both neonatal and adult transplants would be equally competitive, yet the donors would be competing against a highly defective hematopoietic program.

D. Completion of the FLT3Cre;$PTPN11^{E76K}$ Study

Our analysis of FLT3Cre;$PTPN11^{E76K}$ suggests that previous models using this oncogene had extensive morbidity due to non-hematopoietic effects. Our model shows indolent progression of MPN despite a mutant allele frequency that is almost the same as that in Mx1Cre and VavCre models. It will therefore be important to assess the long-term effects of hematopoietic-restricted $PTPN11^{E76K}$ expression. We have already confirmed FLT3Cre is not active in endothelial cells. We will test its activity in stromal populations,

including osteoblasts (Lin- CD140a+ Sca1-) and MSPCs (Lin- CD140a+ Sca1+). Thereafter we will continue our study to address the following questions.

FLT3Cre;PTPN11^{E76K} mice show progressive myeloid bias with development of pronounced anaemia, thrombocytopenia but with rather unremarkable leukocytosis. It will be important to determine whether the total leukocyte counts further increase. Leukocytosis is, after all, a defined feature of JMML. Since FLT3Cre is not active in all hematopoietic progenitors, it is possible that healthy clones will outcompete the mutant clones. As such, we will continue to monitor %GFP+ cells in all lineages as a surrogate for mutant allele frequency. If we continue to see a decline in the frequency of mutant cells, this will suggest that healthy clones are indeed preferentially expanding.

We will be able to confirm this through the analysis of tissue populations. At the end of our study, we will be able to assess the frequency of Tomato+ progenitor subsets. If we see that a greater proportion of MPPs in mutants are Tomato+ than in littermates, we will conclude one of the following: i) healthy clones preferentially expanded in mutants or ii) increased rate of progenitor cycling in mutants resulted in stress hematopoiesis. Others have shown that stress hematopoiesis in the FLT3Cre model results in expansion of Tomato+ cells because each clone spends less time as a FLT3+ intermediate. As a result, the cis-regulatory elements that enable Cre activation are less active and fewer clones have active recombinase. By assessing the number of HSCs in our animals, we would be able to differentiate between scenario i) and ii). In i), we would expect to see an equal number of HSCs in mutants and controls. However, in ii) we would expect mutant HSCs to be depleted due to exhaustion following the increased cycling of downstream progenitors.

As we continue monitoring these animals, we will closely compare their disease manifestations with those of the CSF1R-MCM; PTPN11^{E76K}. Thus far we have seen very similar morbidities in these two cohorts. This is despite FLT3Cre continuously driving

PTPN11^{E76K} expression in ~90% of LSK cells whereas CSF1R-MCM was activated only once at 4 weeks of age and targeted only 1.1% of LSK cells. If we continue to see no differences in survival, leukocytosis, myeloid differentiation, or T-cell differentiation we will seek to further validate non-cell autonomous effects of PTPN11^{E76K}. We will do so by assessing growth hypersensitivity and *RAS-ERK* activation following GM-CSF stimulation among GFP+ and Tomato+ progenitors from FLT3Cre;PTPN11^{E76K} mice. Next, we will assess the clinical relevance of our findings. We hypothesize that the overall survival of patients should be inversely related to their mutant allele frequency at the time of transplant. Furthermore, we will perform pERK signaling studies with patient samples co-cultured with progenitors from healthy children. This will determine if mutant cells secrete a cytokine that evokes GM-CSF hypersensitivity in healthy cells.

E. Methylation in Kras^{G12D} models

We noted in our introduction that methylation is frequently observed in JMML, particularly among those patients that have mutated *RAS*. It has been shown that modulating DNA methylation has therapeutic efficacy in JMML models *ex vivo.* Indeed, an ongoing clinical trial (NCT02447666) is actively recruiting pediatric MDS and JMML patients to test 5-azacytidine—a DNA methyltransferase inhibitor. Therefore, we propose to assess CpG methylation in FLT3Cre;Kras^{G12D} and CSF1R-MCM;KrasG12D mice to determine if they may be suitable pre-clinical models to test future therapeutics.

We have data that suggests aberrant methylation occurs in these animals. ROSA^{mTmG} should be active in all cells that transcribe this locus, which includes all nucleated hematopoietic cells. Since this is a dual fluorescent system, all cells should be either GFP+ or Tomato+. Cells that have silenced their ROSA26 locus would express neither. We observed there was a clear subset of cells that do not express GFP or

Tomato in mutant tissues. We identified that these cells were CD11c+ MHCII+ dendritic cells (Figure III-31). No other lineage demonstrated silencing of the ROSA26 locus in these mice. This finding is consistent with aberrant methylation of the ROSA26 promoter. To formally test this, we will isolate DNA from Tomato- GFP- dendritic cells and bisulfide convert it, such that all non-methylated CpG become UpG. Subsequent sequencing will identify the number of CpG sites that were methylated. We would expect to see increased CpG methylation of the ROSA26 promoter in these mutant DCs.

Fluorescent marking in the ROSA^{YFP} system, on the other hand, is less clear. Whereas YFP+ cells should express the mutation, YFP- cells may either have inactive Cre or they may have silenced their ROSA26 locus. Fortunately, mutant cells in our CSF1R-MCM;Kras^{G12D} have a definitive phenotype: CD4 CD8 double positive cells in non-thymic tissues. It is interesting to see that in nearly all of our mice, these cells were uniformly YFP- (Figure III-31). This also suggests that aberrant DNA methylation is involved in this T-ALL disease. Importantly, aberrant DNA methylation is a hallmark of ETP-ALL, a disease which has similar characteristics as our model, including myeloproliferation, and decreased expression of GATA3. We will therefore perform bisulfide sequencing from mutant cells from our CSF1R-MCM;Kras^{G12D} mice. In particular we will assess the ROSA26 and GATA3 loci, the latter of which is also hypermethylated in ETP-ALL patients. If these preliminary studies are informative we will proceed to seek the cause of the aberrant methylation. We will measure the mRNA expression of DNA methyltransferases and demethylases, including DNMT3A, TET1/2, and IDH1/2 as well as the cell cycle regulators known to be methylated in JMML: *CDKN2A* and *CDKN2B*. Finally, we will proceed to pre-clinical studies to test whether inhibition of methyltransferases would alter morbidity and disease outcomes in our models.

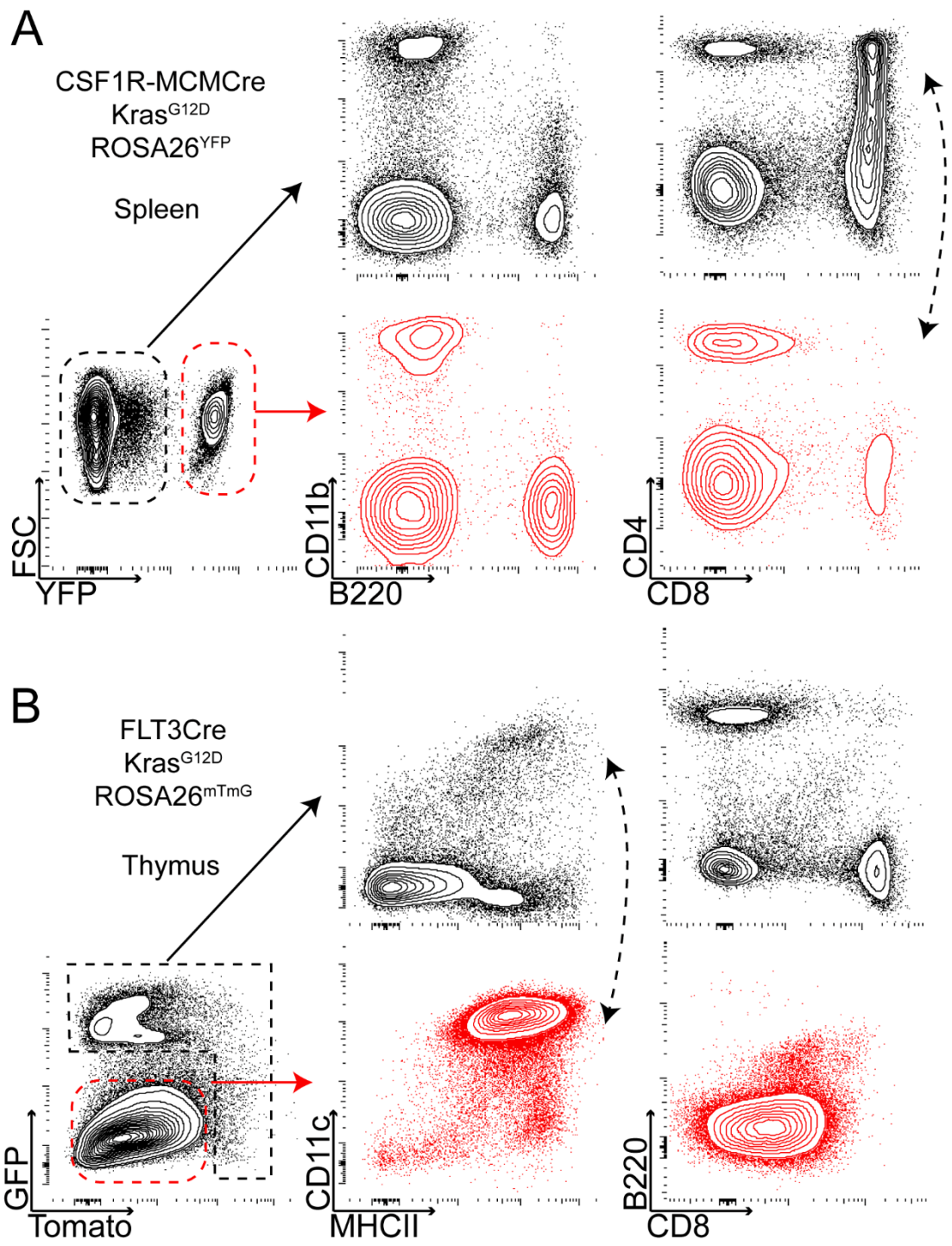

Figure III-31. Neoplastic Kras^{G12D} Cells Silence the ROSA26 Locus. A) CD4+ CD8+ cells in the spleen of moribund CSF1R-MCM;Kras^{G12D};ROSA^{YFP} animal are uniformly YFP-. B) CD11c+ MHCII+ dendritic cells in thymuses of FLT3Cre;Kras^{G12D} animals do not express GFP or Tomato.

APPDENDIX

Reaction	Primers	Interpretation
LSL-KrasG12D	GTCTTTCCCCAGCACAGTGC CTCTTGCCTACGCCACCAGCTC AGCTAGCCACCATGGCTTGAGTAAGTCTGCA	WT Kras Allele=622bp LSL-KrasG12D=500bp loxP-KrasG12D=650bp
Sly / Xlr (gender)	GATGATTTGAGTGGAAATGTGAGGTA CTTATGTTTATAGGCATGCACCATGTA	Male=280bp; Female= 480bp+660bp+685bp
LSL-PTPN11 D61Y	CCTGAATGAACTGCAGGACG GTTTCGCTTGGTGGTCGAAT	NeoR+=248bp
CSF1R-MCM	CTAGGCCACAGAATTGAAAGATCT GTAGGTGGAAATTCTAGCATCATCC AGATGCCAGGACATCAGGAACCTG ATCAGCCACACCAGACACAGAGATC	Cre+ 236bp Control 324bp
E76K genotype	GGGAATTGAACTCAGGACCT CCCACTCACCTTGTCATGTA	E76K=350bp
E76K recombination	TGGGAAGACAATAGCAGGCA CCCACTCACCTTGTCATGTA	WT = 247bp E76K.rec = 336bp
ROSA26-YFP	AAG ACC GCG AAG AGT TTG TC AAA GTC GCT CTG AGT TGT TAT GGA GCG GGA GAA ATG GAT ATG	YFP=320bp WT=600bp
ROSA26-mTmG	CTC TGC CTC CTG GCT TCT CGA GGC GGA TCA CAA GCA ATA TCA ATG GGC GGG GGT CGT T	WT=330bp mTmG=250bp

Primer Sequences Used For Genotyping PCR Analyses.

Primer Pair	Sequence	Efficiency
mGAPDH Fwd	TGGTGAAGCAGGCATCTGAG	92.8% // 96.1%
mGAPDH Rev	TGTTGAAGTCGCAGGAGACAAC	
Lin28b-Fwd	GAGTCCAGGATGATTCCAAGA	87.4%
Lin28b-Rev	TGCTCTGACAGTAATGGCACTT	
HMGA2-Fwd	GGTGCCACAGAAGCGAGGAC	91.7%
HMGA2-Rev	GGGCTCACAGGTTGGCTCTT	
Igf2bp1-Fwd	GGCTCAGTACGGTACAGTGGA	83.7%
Igf2bp1-Rev	ACCACAGCTGTCTCACTTTCAG	
Igf2bp2-Fwd	GGGAAAATCATGGAAGTTGACTA	103.0%
Igf2bp2-Rev	CGGGATGTTCCGAATCTG	
Igf2bp3-Fwd	AAACAGCTTTCTCGCTTTGC	99.1%
Igf2bp3-Rev	TCCGCACTTTAGCATCTGGT	
TCF7-Fwd	CGCAGAGACTTTTCCCGGAC	93.9%
TCF7-Rev	TTGTTATGCAGCGGGGGTTG	
GATA3-Fwd	GCTCCTTGCTACTCAGGTGAT	92.7%
GATA3-Rev	GGAGGGAGAGAGGAATCCGA	
BCL11b-Fwd	GGAGAACATTGCAGGGCCG	97.1%
BCL11b-Rev	TGGGAAGAGGAGGCAGCTAT	
Clec4b2-Fwd	GAAGTGCTCTCTCAGGGGTG	105%
Clec4b2-Rev	GTGCCAGAATGTGGCTCTATC	

Primer Sequences Used For Quantitative RT-PCR.

REFERENCES

Ajami, B., J. L. Bennett, C. Krieger, W. Tetzlaff, and F. M. Rossi. 2007. 'Local self-renewal can sustain CNS microglia maintenance and function throughout adult life', *Nat Neurosci*, 10: 1538-43.

An, W., S. A. Nadeau, B. C. Mohapatra, D. Feng, N. Zutshi, M. D. Storck, P. Arya, J. E. Talmadge, J. L. Meza, V. Band, and H. Band. 2015. 'Loss of Cbl and Cbl-b ubiquitin ligases abrogates hematopoietic stem cell quiescence and sensitizes leukemic disease to chemotherapy', *Oncotarget*, 6: 10498-509.

Anastas, Vollter, and Katherine Calvo. 2016. "Whole Exome Sequencing Suggests Indolent Phenotype of RAS-Associated Autoimmune Leukoproliferative Disorder (RALD) is Characterized by Single Somatic Mutations in RAS Genes with Absence of Cooperating Mutations." In *JMML Symposium*. San Diego, CA.

Arber, D. A., A. Orazi, R. Hasserjian, J. Thiele, M. J. Borowitz, M. M. Le Beau, C. D. Bloomfield, M. Cazzola, and J. W. Vardiman. 2016. 'The 2016 revision to the World Health Organization classification of myeloid neoplasms and acute leukemia', *Blood*, 127: 2391-405.

Arora, N., P. L. Wenzel, S. L. McKinney-Freeman, S. J. Ross, P. G. Kim, S. S. Chou, M. Yoshimoto, M. C. Yoder, and G. Q. Daley. 2014. 'Effect of Developmental Stage of HSC and Recipient on Transplant Outcomes', *Dev Cell*, 29: 621-8.

Bain, C. C., A. Bravo-Blas, C. L. Scott, E. Gomez Perdiguero, F. Geissmann, S. Henri, B. Malissen, L. C. Osborne, D. Artis, and A. M. Mowat. 2014. 'Constant replenishment from circulating monocytes maintains the macrophage pool in the intestine of adult mice', *Nat Immunol*, 15: 929-37.

Beaudin, A. E., S. W. Boyer, J. Perez-Cunningham, G. E. Hernandez, S. C. Derderian, C. Jujjavarapu, E. Aaserude, T. MacKenzie, and E. C. Forsberg. 2016. 'A Transient Developmental Hematopoietic Stem Cell Gives Rise to Innate-like B and T Cells', *Cell Stem Cell*, 19: 768-83.

Benz, C., M. R. Copley, D. G. Kent, S. Wohrer, A. Cortes, N. Aghaeepour, E. Ma, H. Mader, K. Rowe, C. Day, D. Treloar, R. R. Brinkman, and C. J. Eaves. 2012. 'Hematopoietic stem cell subtypes expand differentially during development and display distinct lymphopoietic programs', *Cell Stem Cell*, 10: 273-83.

Benz, C., V. C. Martins, F. Radtke, and C. C. Bleul. 2008. 'The stream of precursors that colonizes the thymus proceeds selectively through the early T lineage precursor stage of T cell development', *J Exp Med*, 205: 1187-99.

Bertrand, J. Y., A. Jalil, M. Klaine, S. Jung, A. Cumano, and I. Godin. 2005. 'Three pathways to mature macrophages in the early mouse yolk sac', *Blood*, 106: 3004-11.

Boisset, J. C., W. van Cappellen, C. Andrieu-Soler, N. Galjart, E. Dzierzak, and C. Robin. 2010. 'In vivo imaging of haematopoietic cells emerging from the mouse aortic endothelium', *Nature*, 464: 116-20.

Bonnet, D., and J. E. Dick. 1997. 'Human acute myeloid leukemia is organized as a hierarchy that originates from a primitive hematopoietic cell', *Nat Med*, 3: 730-7.

Bottcher, J. P., S. Zelenay, N. C. Rogers, J. Helft, B. U. Schraml, and C. Reis e Sousa. 2015. 'Oncogenic Transformation of Dendritic Cells and Their Precursors Leads to Rapid Cancer Development in Mice', *J Immunol*, 195: 5066-76.

Bowie, M. B., D. G. Kent, B. Dykstra, K. D. McKnight, L. McCaffrey, P. A. Hoodless, and C. J. Eaves. 2007. 'Identification of a new intrinsically timed developmental checkpoint that reprograms key hematopoietic stem cell properties', *Proc Natl Acad Sci U S A*, 104: 5878-82.

Bowie, M. B., K. D. McKnight, D. G. Kent, L. McCaffrey, P. A. Hoodless, and C. J. Eaves. 2006. 'Hematopoietic stem cells proliferate until after birth and show a reversible phase-specific engraftment defect', *J Clin Invest*, 116: 2808-16.

Boyer, S. W., A. E. Beaudin, and E. C. Forsberg. 2012. 'Mapping differentiation pathways from hematopoietic stem cells using Flk2/Flt3 lineage tracing', *Cell Cycle*, 11: 3180-8.

Boyer, S. W., A. V. Schroeder, S. Smith-Berdan, and E. C. Forsberg. 2011. 'All hematopoietic cells develop from hematopoietic stem cells through Flk2/Flt3-positive progenitor cells', *Cell Stem Cell*, 9: 64-73.

Braun, B. S., J. A. Archard, J. A. Van Ziffle, D. A. Tuveson, T. E. Jacks, and K. Shannon. 2006. 'Somatic activation of a conditional KrasG12D allele causes ineffective erythropoiesis in vivo', *Blood*, 108: 2041-4.

Braun, B. S., D. A. Tuveson, N. Kong, D. T. Le, S. C. Kogan, J. Rozmus, M. M. Le Beau, T. E. Jacks, and K. M. Shannon. 2004. 'Somatic activation of oncogenic Kras in hematopoietic cells initiates a rapidly fatal myeloproliferative disorder', *Proc Natl Acad Sci U S A*, 101: 597-602.

Broxmeyer, H. E., G. Hangoc, S. Cooper, R. C. Ribeiro, V. Graves, M. Yoder, J. Wagner, S. Vadhan-Raj, L. Benninger, P. Rubinstein, and et al. 1992. 'Growth characteristics and expansion of human umbilical cord blood and estimation of its potential for transplantation in adults', *Proc Natl Acad Sci U S A*, 89: 4109-13.

Buchrieser, J., W. James, and M. D. Moore. 2017. 'Human Induced Pluripotent Stem Cell-Derived Macrophages Share Ontogeny with MYB-Independent Tissue-Resident Macrophages', *Stem Cell Reports*, 8: 334-45.

Busch, K., K. Klapproth, M. Barile, M. Flossdorf, T. Holland-Letz, S. M. Schlenner, M. Reth, T. Hofer, and H. R. Rodewald. 2015. 'Fundamental properties of unperturbed haematopoiesis from stem cells in vivo', *Nature*, 518: 542-6.

Busch, K., and H. R. Rodewald. 2016. 'Unperturbed vs. post-transplantation hematopoiesis: both in vivo but different', *Curr Opin Hematol*, 23: 295-303.

Busque, L., D. G. Gilliland, J. T. Prchal, C. A. Sieff, H. J. Weinstein, J. M. Sokol, M. Belickova, A. S. Wayne, K. S. Zuckerman, L. Sokol, and et al. 1995. 'Clonality in juvenile chronic myelogenous leukemia', *Blood*, 85: 21-30.

Calvo, K. R., S. Price, R. C. Braylan, J. B. Oliveira, M. Lenardo, T. A. Fleisher, and V. K. Rao. 2015. 'JMML and RALD (Ras-associated autoimmune leukoproliferative disorder): common genetic etiology yet clinically distinct entities', *Blood*, 125: 2753-8.

Castro, I., M. J. Dee, and T. R. Malek. 2012. 'Transient enhanced IL-2R signaling early during priming rapidly amplifies development of functional CD8+ T effector-memory cells', *J Immunol*, 189: 4321-30.

Caudy, A. A., S. T. Reddy, T. Chatila, J. P. Atkinson, and J. W. Verbsky. 2007. 'CD25 deficiency causes an immune dysregulation, polyendocrinopathy, enteropathy, X-linked-like syndrome, and defective IL-10 expression from CD4 lymphocytes', *J Allergy Clin Immunol*, 119: 482-7.

Caye, A., M. Strullu, F. Guidez, B. Cassinat, S. Gazal, O. Fenneteau, E. Lainey, K. Nouri, S. Nakhaei-Rad, R. Dvorsky, J. Lachenaud, S. Pereira, J. Vivent, E. Verger, D. Vidaud, C. Galambrun, C. Picard, A. Petit, A. Contet, M. Poiree, N. Sirvent, F. Mechinaud, D. Adjaoud, C. Paillard, B. Nelken, Y. Reguerre, Y. Bertrand, D. Haussinger, J. H. Dalle, M. R. Ahmadian, A. Baruchel, C. Chomienne, and H. Cave. 2015. 'Juvenile myelomonocytic leukemia displays mutations in components of the RAS pathway and the PRC2 network', *Nat Genet*, 47: 1334-40.

Chan, G., D. Kalaitzidis, T. Usenko, J. L. Kutok, W. Yang, M. G. Mohi, and B. G. Neel. 2009. 'Leukemogenic Ptpn11 causes fatal myeloproliferative disorder via cell-autonomous effects on multiple stages of hema', *Blood*, 113: 4414-24.

Chan, R. J., T. Cooper, C. P. Kratz, B. Weiss, and M. L. Loh. 2009. 'Juvenile myelomonocytic leukemia: a report from the 2nd International JMML Symposium', *Leuk Res*, 33: 355-62.

Chan, R. J., M. B. Leedy, V. Munugalavadla, C. S. Voorhorst, Y. Li, Y. Menggang, and R. Kapur. 2005. 'Human somatic PTPN11 mutations induce hematopoietic-cell hypersensitivity to granulocyte-macrophage colony-stimulat', *Blood*, 105: 3737-42.

Chan, R. J., and M. C. Yoder. 2013. 'JMML patient-derived iPSCs induce new hypotheses', *Blood*, 121: 4815-7.

Chanda, B., A. Ditadi, N. N. Iscove, and G. Keller. 2013. 'Retinoic acid signaling is essential for embryonic hematopoietic stem cell development', *Cell*, 155: 215-27.

Chen, M. J., Y. Li, M. E. De Obaldia, Q. Yang, A. D. Yzaguirre, T. Yamada-Inagawa, C. S. Vink, A. Bhandoola, E. Dzierzak, and N. A. Speck. 2011. 'Erythroid/myeloid progenitors and hematopoietic stem cells originate from distinct populations of endothelial cells', *Cell Stem Cell*, 9: 541-52.

Chen, M. J., T. Yokomizo, B. M. Zeigler, E. Dzierzak, and N. A. Speck. 2009. 'Runx1 is required for the endothelial to haematopoietic cell transition but not thereafter', *Nature*, 457: 887-91.

Christensen, J. L., and I. L. Weissman. 2001. 'Flk-2 is a marker in hematopoietic stem cell differentiation: a simple method to isolate long-term stem cells', *Proc Natl Acad Sci U S A*, 98: 14541-6.

Christensen, J. L., D. E. Wright, A. J. Wagers, and I. L. Weissman. 2004. 'Circulation and chemotaxis of fetal hematopoietic stem cells', *PLoS Biol*, 2: E75.

Clausen, B. E., C. Burkhardt, W. Reith, R. Renkawitz, and I. Forster. 1999. 'Conditional gene targeting in macrophages and granulocytes using LysMcre mice', *Transgenic Res*, 8: 265-77.

Cooper, L. J., K. M. Shannon, M. R. Loken, M. Weaver, K. Stephens, and E. L. Sievers. 2000. 'Evidence that juvenile myelomonocytic leukemia can arise from a pluripotential stem cell', *Blood*, 96: 2310-3.

Copley, M. R., S. Babovic, C. Benz, D. J. Knapp, P. A. Beer, D. G. Kent, S. Wohrer, D. Q. Treloar, C. Day, K. Rowe, H. Mader, F. Kuchenbauer, R. K. Humphries, and C. J. Eaves. 2013. 'The Lin28b-let-7-Hmga2 axis determines the higher self-renewal potential of fetal haematopoietic stem cells', *Nat Cell Biol*, 15: 916-25.

Copley, M. R., P. A. Beer, and C. J. Eaves. 2012. 'Hematopoietic stem cell heterogeneity takes center stage', *Cell Stem Cell*, 10: 690-7.

Copley, M. R., and C. J. Eaves. 2013. 'Developmental changes in hematopoietic stem cell properties', *Exp Mol Med*, 45: e55.

Croker, BA, Donald Metcalf, Lorraine Robb, Wei Wei, S Mifsud, L DiRago, LA Cluse, KD Sutherland, L Hartley, E Williams, J-G Zhang, DJ Hilton, NA Nicola, and WS Alexander. 2004. 'SOCS3 is a critical physiological negative regulator of G-CSF signaling and emergency granulopoiesis', *Immunity*, 20: 153-65.

de Boer, Jasper, Adam Williams, George Skavdis, Nicola Harker, Mark Coles, Mauro Tolaini, Trisha Norton, Keith Williams, Kathleen Roderick, Alexandre J Potocnik, and Dimitris Kioussis. 2003. 'Transgenic mice with hematopoietic and lymphoid specific expression of Cre.', *Eur J Immunol*, 33: 314-25.

Desai, T. J., D. G. Brownfield, and M. A. Krasnow. 2014. 'Alveolar progenitor and stem cells in lung development, renewal and cancer', *Nature*, 507: 190-4.

Dong, L., W. M. Yu, H. Zheng, M. L. Loh, S. T. Bunting, M. Pauly, G. Huang, M. Zhou, H. E. Broxmeyer, D. T. Scadden, and C. K. Qu. 2016. 'Leukaemogenic effects of

Ptpn11 activating mutations in the stem cell microenvironment', *Nature*, 539: 304-08.
Doulatov, S., L. T. Vo, S. S. Chou, P. G. Kim, N. Arora, H. Li, B. K. Hadland, I. D. Bernstein, J. J. Collins, L. I. Zon, and G. Q. Daley. 2013. 'Induction of multipotential hematopoietic progenitors from human pluripotent stem cells via respecification of lineage-restricted precursors', *Cell Stem Cell*, 13: 459-70.
Dykstra, B., D. Kent, M. Bowie, L. McCaffrey, M. Hamilton, K. Lyons, S. J. Lee, R. Brinkman, and C. Eaves. 2007. 'Long-term propagation of distinct hematopoietic differentiation programs in vivo', *Cell Stem Cell*, 1: 218-29.
Eaves, C. J. 2015. 'Hematopoietic stem cells: concepts, definitions, and the new reality', *Blood*, 125: 2605-13.
Elmore, M. R., A. R. Najafi, M. A. Koike, N. N. Dagher, E. E. Spangenberg, R. A. Rice, M. Kitazawa, B. Matusow, H. Nguyen, B. L. West, and K. N. Green. 2014. 'Colony-stimulating factor 1 receptor signaling is necessary for microglia viability, unmasking a microglia progenitor cell in the adult brain', *Neuron*, 82: 380-97.
Ema, H., and H. Nakauchi. 2000. 'Expansion of hematopoietic stem cells in the developing liver of a mouse embryo', *Blood*, 95: 2284-8.
Emanuel, P. D., L. J. Bates, R. P. Castleberry, R. J. Gualtieri, and K. S. Zuckerman. 1991. 'Selective hypersensitivity to granulocyte-macrophage colony-stimulating factor by juvenile chronic myeloid leukemia hematopoietic progenitors', *Blood*, 77: 925-9.
Epelman, S., K. J. Lavine, A. E. Beaudin, D. K. Sojka, J. A. Carrero, B. Calderon, T. Brija, E. L. Gautier, S. Ivanov, A. T. Satpathy, J. D. Schilling, R. Schwendener, I. Sergin, B. Razani, E. C. Forsberg, W. M. Yokoyama, E. R. Unanue, M. Colonna, G. J. Randolph, and D. L. Mann. 2014. 'Embryonic and adult-derived resident cardiac macrophages are maintained through distinct mechanisms at steady state and during inflammation', *Immunity*, 40: 91-104.
Espin-Palazon, R., D. L. Stachura, C. A. Campbell, D. Garcia-Moreno, N. Del Cid, A. D. Kim, S. Candel, J. Meseguer, V. Mulero, and D. Traver. 2014. 'Proinflammatory signaling regulates hematopoietic stem cell emergence', *Cell*, 159: 1070-85.
Estrov, Z., B. Zimmerman, T. Grunberger, J. Chao, I. E. Teshima, H. S. Chan, and M. H. Freedman. 1986. 'Characterization of malignant peripheral blood cells of juvenile chronic myelogenous leukemia', *Cancer Res*, 46: 6456-61.
Feil, S., J. Krauss, M. Thunemann, and R. Feil. 2014. 'Genetic inducible fate mapping in adult mice using tamoxifen-dependent cre recombinases', *Methods Mol Biol.*, 1194: 113-39.
Ferkowicz, M. J. 2003. 'CD41 expression defines the onset of primitive and definitive hematopoiesis in the murine embryo', *Development*, 130: 4393-403.
Flotho, C., S. Valcamonica, S. Mach-Pascual, G. Schmahl, L. Corral, J. Ritterbach, H. Hasle, M. Arico, A. Biondi, and C. M. Niemeyer. 1999. 'RAS mutations and clonality analysis in children with juvenile myelomonocytic leukemia (JMML)', *Leukemia.*, 13: 32-7.
Frame, J. M., K. H. Fegan, S. J. Conway, K. E. McGrath, and J. Palis. 2016. 'Definitive Hematopoiesis in the Yolk Sac Emerges from Wnt-Responsive Hemogenic Endothelium Independently of Circulation and Arterial Identity', *Stem Cells*, 34: 431-44.
Frame, J. M., K. E. McGrath, and J. Palis. 2013. 'Erythro-myeloid progenitors: "definitive" hematopoiesis in the conceptus prior to the emergence of hematopoietic stem cells', *Blood Cells Mol Dis*, 51: 220-5.
Fransecky, L., M. Neumann, S. Heesch, C. Schlee, J. Ortiz-Tanchez, S. Heller, M. Mossner, S. Schwartz, L. H. Mochmann, K. Isaakidis, L. Bastian, U. R. Kees, T. Herold, K. Spiekermann, N. Gokbuget, and C. D. Baldus. 2016. 'Silencing of

GATA3 defines a novel stem cell-like subgroup of ETP-ALL', *J Hematol Oncol*, 9: 95.

Gandre-Babbe, S., P. Paluru, C. Aribeana, S. T. Chou, S. Bresolin, L. Lu, S. K. Sullivan, S. K. Tasian, J. Weng, H. Favre, J. K. Choi, D. L. French, M. L. Loh, and M. J. Weiss. 2013. 'Patient-derived induced pluripotent stem cells recapitulate hematopoietic abnormalities of juvenile myelomonocytic leukemia', *Blood*, 121: 4925-9.

Gekas, C., F. Dieterlen-Lievre, S. H. Orkin, and H. K. Mikkola. 2005. 'The placenta is a niche for hematopoietic stem cells', *Dev Cell*, 8: 365-75.

Genovese, G., A. K. Kahler, R. E. Handsaker, J. Lindberg, S. A. Rose, S. F. Bakhoum, K. Chambert, E. Mick, B. M. Neale, M. Fromer, S. M. Purcell, O. Svantesson, M. Landen, M. Hoglund, S. Lehmann, S. B. Gabriel, J. L. Moran, E. S. Lander, P. F. Sullivan, P. Sklar, H. Gronberg, C. M. Hultman, and S. A. McCarroll. 2014. 'Clonal hematopoiesis and blood-cancer risk inferred from blood DNA sequence', *N Engl J Med*, 371: 2477-87.

Georgiades, P., S. Ogilvy, H. Duval, D. R. Licence, D. S. Charnock-Jones, S. K. Smith, and C. G. Print. 2002. 'VavCre transgenic mice: a tool for mutagenesis in hematopoietic and endothelial lineages', *Genesis*, 34: 251-6.

Ghiaur, G., M. J. Ferkowicz, M. D. Milsom, J. L. Bailey, D. Witte, J. A. Cancelas, M. C. Yoder, and D. A. Williams. 2008. 'Rac1 is essential for intraembryonic hematopoiesis and for the initial seeding of fetal liver with definitive hem', *Blood*, 111: 3313-21.

Ginhoux, F., M. Greter, M. Leboeuf, S. Nandi, P. See, S. Gokhan, M. F. Mehler, S. J. Conway, L. G. Ng, E. R. Stanley, I. M. Samokhvalov, and M. Merad. 2010. 'Fate mapping analysis reveals that adult microglia derive from primitive macrophages', *Science*, 330: 841-5.

Gomez Perdiguero, E., K. Klapproth, C. Schulz, K. Busch, E. Azzoni, L. Crozet, H. Garner, C. Trouillet, M. F. de Bruijn, F. Geissmann, and H. R. Rodewald. 2015. 'Tissue-resident macrophages originate from yolk-sac-derived erythro-myeloid progenitors', *Nature*, 518: 547-51.

Goodwin, C. B., Z. Yang, F. Yin, M. Yu, and R. J. Chan. 2012. 'Genetic disruption of the PI3K regulatory subunits, p85alpha, p55alpha, and p50alpha, normalizes mutant PTPN11-induced hypersensitivity to GM-CSF', *Haematologica*, 97: 1042-7.

Gosselin, D., V. M. Link, C. E. Romanoski, G. J. Fonseca, D. Z. Eichenfield, N. J. Spann, J. D. Stender, H. B. Chun, H. Garner, F. Geissmann, and C. K. Glass. 2014. 'Environment drives selection and function of enhancers controlling tissue-specific macrophage identities', *Cell*, 159: 1327-40.

Greaves, M. 2015. 'Evolutionary determinants of cancer', *Cancer Discov*, 5: 806-20.

Hanahan, D., and R. A. Weinberg. 2011. 'Hallmarks of cancer: the next generation', *Cell*, 144: 646-74.

Haniffa, M., F. Ginhoux, X. N. Wang, V. Bigley, M. Abel, I. Dimmick, S. Bullock, M. Grisotto, T. Booth, P. Taub, C. Hilkens, M. Merad, and M. Collin. 2009. 'Differential rates of replacement of human dermal dendritic cells and macrophages during hematopoietic stem cell transplantation', *J Exp Med*, 206: 371-85.

Hasegawa, D., A. Manabe, T. Kubota, H. Kawasaki, I. Hirose, Y. Ohtsuka, T. Tsuruta, Y. Ebihara, Y. Goto, X. Y. Zhao, K. Sakashita, K. Koike, M. Isomura, S. Kojima, A. Hoshika, K. Tsuji, and T. Nakahata. 2005. 'Methylation status of the p15 and p16 genes in paediatric myelodysplastic syndrome and juvenile myelomonocytic leukaemia', *Br J Haematol*, 128: 805-12.

Hashimoto, D., A. Chow, C. Noizat, P. Teo, M. B. Beasley, M. Leboeuf, C. D. Becker, P. See, J. Price, D. Lucas, M. Greter, A. Mortha, S. W. Boyer, E. C. Forsberg, M.

Tanaka, N. van Rooijen, A. Garcia-Sastre, E. R. Stanley, F. Ginhoux, P. S. Frenette, and M. Merad. 2013. 'Tissue-resident macrophages self-maintain locally throughout adult life with minimal contribution from circulating monocytes', *Immunity*, 38: 792-804.

He, S., I. Kim, M. S. Lim, and S. J. Morrison. 2011. 'Sox17 expression confers self-renewal potential and fetal stem cell characteristics upon adult hematopoietic progenitors', *Genes Dev*, 25: 1613-27.

Helsmoortel, H. H., S. Bresolin, T. Lammens, H. Cave, P. Noellke, A. Caye, F. Ghazavi, A. de Vries, H. Hasle, V. Labarque, R. Masetti, J. Stary, M. M. van den Heuvel-Eibrink, J. Philippe, N. Van Roy, Y. Benoit, F. Speleman, C. Niemeyer, C. Flotho, G. Basso, G. Te Kronnie, P. Van Vlierberghe, and B. De Moerloose. 2016. 'LIN28B overexpression defines a novel fetal-like subgroup of juvenile myelomonocytic leukemia', *Blood*, 127: 1163-72.

Helsmoortel, H. H., B. De Moerloose, T. Pieters, F. Ghazavi, S. Bresolin, H. Cave, A. de Vries, V. de Haas, C. Flotho, V. Labarque, C. Niemeyer, P. De Paepe, N. Van Roy, J. Stary, M. M. van den Heuvel-Eibrink, Y. Benoit, J. Schulte, S. Goossens, G. Berx, J. J. Haigh, F. Speleman, P. Van Vlierberghe, and T. Lammens. 2016. 'LIN28B is over-expressed in specific subtypes of pediatric leukemia and regulates lncRNA H19', *Haematologica*, 101: e240-4.

Henninger, J., B. Santoso, S. Hans, E. Durand, J. Moore, C. Mosimann, M. Brand, D. Traver, and L. Zon. 2017. 'Clonal fate mapping quantifies the number of haematopoietic stem cells that arise during development', *Nat Cell Biol*, 19: 17-27.

Hettinger, J., D. M. Richards, J. Hansson, M. M. Barra, A. C. Joschko, J. Krijgsveld, and M. Feuerer. 2013. 'Origin of monocytes and macrophages in a committed progenitor', *Nat Immunol*, 14: 821-30.

Hoeffel, G., J. Chen, Y. Lavin, D. Low, F. F. Almeida, P. See, A. E. Beaudin, J. Lum, I. Low, E. C. Forsberg, M. Poidinger, F. Zolezzi, A. Larbi, L. G. Ng, J. K. Chan, M. Greter, B. Becher, I. M. Samokhvalov, M. Merad, and F. Ginhoux. 2015. 'C-myb(+) erythro-myeloid progenitor-derived fetal monocytes give rise to adult tissue-resident macrophages', *Immunity*, 42: 665-78.

Hofer, T., K. Busch, K. Klapproth, and H. R. Rodewald. 2016. 'Fate Mapping and Quantitation of Hematopoiesis In Vivo', *Annu Rev Immunol*, 34: 449-78.

Hunter, J. C., A. Manandhar, M. A. Carrasco, D. Gurbani, S. Gondi, and K. D. Westover. 2015. 'Biochemical and Structural Analysis of Common Cancer-Associated KRAS Mutations', *Mol Cancer Res*, 13: 1325-35.

Inagaki, J., R. Fukano, T. Nishikawa, K. Nakashima, D. Sawa, N. Ito, and J. Okamura. 2013. 'Outcomes of immunological interventions for mixed chimerism following allogeneic stem cell transplantation in children with juvenile myelomonocytic leukemia', *Pediatr Blood Cancer*, 60: 116-20.

Inlay, M. A., T. Serwold, A. Mosley, J. W. Fathman, I. K. Dimov, J. Seita, and I. L. Weissman. 2014. 'Identification of Multipotent Progenitors that Emerge Prior to Hematopoietic Stem Cells in Embryonic Development', *Stem Cell Reports*, 2: 457-72.

Jaiswal, S., P. Fontanillas, J. Flannick, A. Manning, P. V. Grauman, B. G. Mar, R. C. Lindsley, C. H. Mermel, N. Burtt, A. Chavez, J. M. Higgins, V. Moltchanov, F. C. Kuo, M. J. Kluk, B. Henderson, L. Kinnunen, H. A. Koistinen, C. Ladenvall, G. Getz, A. Correa, B. F. Banahan, S. Gabriel, S. Kathiresan, H. M. Stringham, M. I. McCarthy, M. Boehnke, J. Tuomilehto, C. Haiman, L. Groop, G. Atzmon, J. G. Wilson, D. Neuberg, D. Altshuler, and B. L. Ebert. 2014. 'Age-related clonal hematopoiesis associated with adverse outcomes', *N Engl J Med*, 371: 2488-98.

Johnson, S. A., and M. C. Yoder. 2005. 'Reconstitution of hematopoiesis following transplantation into neonatal mice', *Methods Mol Med.*, 105: 95-106.

Kalwak, K., J. Porwolik, M. Mielcarek, E. Gorczynska, J. Owoc-Lempach, M. Ussowicz, A. Dyla, J. Musial, D. Pazdzior, D. Turkiewicz, and A. Chybicka. 2010. 'Higher CD34(+) and CD3(+) cell doses in the graft promote long-term survival, and have no impact on the incidence of severe acute or chronic graft-versus-host disease after in vivo T cell-depleted unrelated donor hematopoietic stem cell transplantation in children', *Biol Blood Marrow Transplant*, 16: 1388-401.

Karsunky, H., M. A. Inlay, T. Serwold, D. Bhattacharya, and I. L. Weissman. 2008. 'Flk2+ common lymphoid progenitors possess equivalent differentiation potential for the B and T lineages', *Blood*, 111: 5562-70.

Kiel, M. J., T. Iwashita, O. H. Yilmaz, and S. J. Morrison. 2005. 'Spatial differences in hematopoiesis but not in stem cells indicate a lack of regional patterning in definitive hematopoietic stem cells', *Dev Biol*, 283: 29-39.

Kierdorf, K., D. Erny, T. Goldmann, V. Sander, C. Schulz, E. G. Perdiguero, P. Wieghofer, A. Heinrich, P. Riemke, C. Holscher, D. N. Muller, B. Luckow, T. Brocker, K. Debowski, G. Fritz, G. Opdenakker, A. Diefenbach, K. Biber, M. Heikenwalder, F. Geissmann, F. Rosenbauer, and M. Prinz. 2013. 'Microglia emerge from erythromyeloid precursors via Pu.1- and Irf8-dependent pathways', *Nat Neurosci*, 16: 273-80.

Kim, I., T. L. Saunders, and S. J. Morrison. 2007. 'Sox17 dependence distinguishes the transcriptional regulation of fetal from adult hematopoietic stem cells', *Cell*, 130: 470-83.

Kim, I., O. H. Yilmaz, and S. J. Morrison. 2005. 'CD144 (VE-cadherin) is transiently expressed by fetal liver hematopoietic stem cells', *Blood*, 106: 903-5.

Kindler, T., M. G. Cornejo, C. Scholl, J. Liu, D. S. Leeman, J. E. Haydu, S. Frohling, B. H. Lee, and D. G. Gilliland. 2008. 'K-RasG12D-induced T-cell lymphoblastic lymphoma/leukemias harbor Notch1 mutations and are sensitive to gamma-secretase inhibitors', *Blood*, 112: 3373-82.

Kong, G., J. Du, Y. Liu, B. Meline, Y. I. Chang, E. A. Ranheim, J. Wang, and J. Zhang. 2013. 'Notch1 gene mutations target KRAS G12D-expressing CD8+ cells and contribute to their leukemogenic transformation', *J Biol Chem*, 288: 18219-27.

Koulnis, M., R. Pop, E. Porpiglia, J. R. Shearstone, D. Hidalgo, and M. Socolovsky. 2011. 'Identification and analysis of mouse erythroid progenitors using the CD71/TER119 flow-cytometric assay', *J Vis Exp*.

Kratz, C. P., C. M. Niemeyer, R. P. Castleberry, M. Cetin, E. Bergstrasser, P. D. Emanuel, H. Hasle, G. Kardos, C. Klein, S. Kojima, J. Stary, M. Trebo, M. Zecca, B. D. Gelb, M. Tartaglia, and M. L. Loh. 2005. 'The mutational spectrum of PTPN11 in juvenile myelomonocytic leukemia and Noonan syndrome/myeloproliferative disease', *Blood*, 106: 2183-5.

Kreso, A., and J. E. Dick. 2014. 'Evolution of the cancer stem cell model', *Cell Stem Cell*, 14: 275-91.

Krombholz, C. F., K. Aumann, M. Kollek, D. Bertele, S. Fluhr, M. Kunze, C. M. Niemeyer, C. Flotho, and M. Erlacher. 2016. 'Long-term serial xenotransplantation of juvenile myelomonocytic leukemia recapitulates human disease in Rag2-/-gammac-/- mice', *Haematologica*, 101: 597-606.

Kueh, H. Y., M. A. Yui, K. K. Ng, S. S. Pease, J. A. Zhang, S. S. Damle, G. Freedman, S. Siu, I. D. Bernstein, M. B. Elowitz, and E. V. Rothenberg. 2016. 'Asynchronous combinatorial action of four regulatory factors activates Bcl11b for T cell commitment', *Nat Immunol*, 17: 956-65.

Kuhn, R., F. Schwenk, M. Aguet, and K. Rajewsky. 1995. 'Inducible gene targeting in mice', *Science*, 269: 1427-9.
Kuhn, R., and R. M. Torres. 2002. 'Cre/loxP recombination system and gene targeting', *Methods Mol Biol*, 180: 175-204.
Kunisaki, Y., I. Bruns, C. Scheiermann, J. Ahmed, S. Pinho, D. Zhang, T. Mizoguchi, Q. Wei, D. Lucas, K. Ito, J. C. Mar, A. Bergman, and P. S. Frenette. 2013. 'Arteriolar niches maintain haematopoietic stem cell quiescence', *Nature*, 502: 637-43.
Lansdorp, P. M., W. Dragowska, and H. Mayani. 1993. 'Ontogeny-related changes in proliferative potential of human hematopoietic cells', *J Exp Med*, 178: 787-91.
Lapidot, T., T. Grunberger, J. Vormoor, Z. Estrov, O. Kollet, N. Bunin, R. Zaizov, D. E. Williams, and M. H. Freedman. 1996. 'Identification of human juvenile chronic myelogenous leukemia stem cells capable of initiating the disease in primary and secondary SCID mice', *Blood*, 88: 2655-64.
Lavin, Y., D. Winter, R. Blecher-Gonen, E. David, H. Keren-Shaul, M. Merad, S. Jung, and I. Amit. 2014. 'Tissue-resident macrophage enhancer landscapes are shaped by the local microenvironment', *Cell*, 159: 1312-26.
Le, D. T., N. Kong, Y. Zhu, J. O. Lauchle, A. Aiyigari, B. S. Braun, E. Wang, S. C. Kogan, M. M. Le Beau, L. Parada, and K. M. Shannon. 2004. 'Somatic inactivation of Nf1 in hematopoietic cells results in a progressive myeloproliferative disorder', *Blood*, 103: 4243-50.
Li, Y., V. Esain, L. Teng, J. Xu, W. Kwan, I. M. Frost, A. D. Yzaguirre, X. Cai, M. Cortes, M. W. Maijenburg, J. Tober, E. Dzierzak, S. H. Orkin, K. Tan, T. E. North, and N. A. Speck. 2014. 'Inflammatory signaling regulates embryonic hematopoietic stem and progenitor cell production', *Genes Dev*, 28: 2597-612.
Liu, W. J., and P. J. Hansen. 1993. 'Effect of the progesterone-induced serpin-like proteins of the sheep endometrium on natural-killer cell activity in sheep and mice', *Biol Reprod*, 49: 1008-14.
Liu, X., H. Zheng, X. Li, S. Wang, H. J. Meyerson, W. Yang, B. G. Neel, and C. K. Qu. 2016. 'Gain-of-function mutations of Ptpn11 (Shp2) cause aberrant mitosis and increase susceptibility to DNA damage-induced malignancies', *Proc Natl Acad Sci U S A*, 113: 984-9.
Locatelli, F., and C. M. Niemeyer. 2015. 'How I treat juvenile myelomonocytic leukemia', *Blood*, 125: 1083-90.
Locatelli, Franco, Alessandro Crotta, Annalisa Ruggeri, and Mary Eapen. 2013. 'Analysis of risk factors influencing outcomes after cord blood transplantation in children with juvenile myelomonocytic leukemia: a EUROCORD, EBMT, EWOG', *Blood*, 122: 2135-41.
Lodish, Harvey , Arnold Berk, S Lawrence Zipursky, Paul Matsudaira, David Baltimore, and James Darnell. 2000. *Molecular Cell Biology* (W. H. Freeman: New York).
Loh, M. L. 2011. 'Recent advances in the pathogenesis and treatment of juvenile myelomonocytic leukaemia', *Br J Haematol*, 152: 677-87.
Loh, M. L., S. Vattikuti, S. Schubbert, M. G. Reynolds, E. Carlson, K. H. Lieuw, J. W. Cheng, C. M. Lee, D. Stokoe, J. M. Bonifas, N. P. Curtiss, J. Gotlib, S. Meshinchi, M. M. Le Beau, P. D. Emanuel, and K. M. Shannon. 2004. 'Mutations in PTPN11 implicate the SHP-2 phosphatase in leukemogenesis', *Blood*, 103: 2325-31.
Longoni, D., G. D'Amico, G. Gaipa, S. Bernasconi, M. Vulcano, P. Onnis, C. M. Niemeyer, P. Allavena, and A. Biondi. 2002. 'Commitment of juvenile myelo-monocytic (JMML) leukemic cells to spontaneously differentiate into dendritic cells', *Hematol J*, 3: 302-10.
Luc, S., T. C. Luis, H. Boukarabila, I. C. Macaulay, N. Buza-Vidas, T. Bouriez-Jones, M. Lutteropp, P. S. Woll, S. J. Loughran, A. J. Mead, A. Hultquist, J. Brown, T.

Mizukami, S. Matsuoka, H. Ferry, K. Anderson, S. Duarte, D. Atkinson, S. Soneji, A. Domanski, A. Farley, A. Sanjuan-Pla, C. Carella, R. Patient, M. de Bruijn, T. Enver, C. Nerlov, C. Blackburn, I. Godin, and S. E. Jacobsen. 2012. 'The earliest thymic T cell progenitors sustain B cell and myeloid lineage potential', *Nat Immunol*, 13: 412-9.

Lux, C. T., M. Yoshimoto, K. E. McGrath, S. J. Conway, J. Palis, and M. C. Yoder. 2008. 'All primitive and definitive hematopoietic progenitor cells emerging before E10 in the mouse embryo are products of the yolk sac', *Blood*, 111: 3435-38.

Lyubynska, N., M. F. Gorman, J. O. Lauchle, W. X. Hong, J. K. Akutagawa, K. Shannon, and B. S. Braun. 2011. 'A MEK inhibitor abrogates myeloproliferative disease in Kras mutant mice', *Sci Transl Med*, 3: 76ra27.

Magnon, C, and PS Frenette. 2008. 'Hematopoietic stem cell trafficking.' in David Scadden (ed.), *StemBook* (Harvard Stem Cell Institute: Cambridge (MA)).

Man, N., X. J. Sun, Y. Tan, M. Garcia-Cao, F. Liu, G. Cheng, M. Hatlen, H. Xu, R. Shah, N. Chastain, N. Liu, G. Huang, Y. Zhou, M. Sheng, J. Song, F. C. Yang, R. Benezra, S. D. Nimer, and L. Wang. 2016. 'Differential role of Id1 in MLL-AF9-driven leukemia based on cell of origin', *Blood*, 127: 2322-6.

Matsuda, K., K. Sakashita, C. Taira, M. Tanaka-Yanagisawa, R. Yanagisawa, M. Shiohara, H. Kanegane, D. Hasegawa, K. Kawasaki, M. Endo, S. Yajima, S. Sasaki, K. Kato, K. Koike, A. Kikuchi, A. Ogawa, A. Watanabe, M. Sotomatsu, and S. Nonoyama. 2010. 'Quantitative assessment of PTPN11 or RAS mutations at the neonatal period and during the clinical course in patients with juvenile myelomonocytic leukaemia', *Br J Haematol*, 148: 593-9.

Matsuda, K., A. Shimada, N. Yoshida, A. Ogawa, A. Watanabe, S. Yajima, S. Iizuka, K. Koike, F. Yanai, K. Kawasaki, M. Yanagimachi, A. Kikuchi, Y. Ohtsuka, E. Hidaka, K. Yamauchi, M. Tanaka, R. Yanagisawa, Y. Nakazawa, M. Shiohara, A. Manabe, S. Kojima, and K. Koike. 2007. 'Spontaneous improvement of hematologic abnormalities in patients having juvenile myelomonocytic leukemia with specific RAS mutations', *Blood*, 109: 5477-80.

Matthews, W., C. T. Jordan, G. W. Wiegand, D. Pardoll, and I. R. Lemischka. 1991. 'A receptor tyrosine kinase specific to hematopoietic stem and progenitor cell-enriched populations', *Cell*, 65: 1143-52.

Maximow, AA. 1909. 'Untersuchungen uber blut und bindegewebe 1. Die fruhesten entwicklungsstadien der blut- und binde- gewebszellan bein saugetierembryo, bis zum anfang der blutbilding unden leber.', *Arch Mikroskop Anat*, 73: 444–561.

McCormick, F. 2015. 'KRAS as a Therapeutic Target', *Clin Cancer Res*, 21: 1797-801.

McGrath, K. E., J. M. Frame, K. H. Fegan, J. R. Bowen, S. J. Conway, S. C. Catherman, P. D. Kingsley, A. D. Koniski, and J. Palis. 2015. 'Distinct Sources of Hematopoietic Progenitors Emerge before HSCs and Provide Functional Blood Cells in the Mammalian Embryo', *Cell Rep*, 11: 1892-904.

Medvinsky, A., and E. Dzierzak. 1996. 'Definitive hematopoiesis is autonomously initiated by the AGM region', *Cell*, 86: 897-906.

Migliaccio, G., A. R. Migliaccio, S. Petti, F. Mavilio, G. Russo, D. Lazzaro, U. Testa, M. Marinucci, and C. Peschle. 1986. 'Human embryonic hemopoiesis. Kinetics of progenitors and precursors underlying the yolk sac----liver transition', *J Clin Invest*, 78: 51-60.

Mildner, A., H. Schmidt, M. Nitsche, D. Merkler, U. K. Hanisch, M. Mack, M. Heikenwalder, W. Bruck, J. Priller, and M. Prinz. 2007. 'Microglia in the adult brain arise from Ly-6ChiCCR2+ monocytes only under defined host conditions', *Nat Neurosci*, 10: 1544-53.

Mohi, M. G., I. R. Williams, C. R. Dearolf, G. Chan, J. L. Kutok, S. Cohen, K. Morgan, C. Boulton, H. Shigematsu, H. Keilhack, K. Akashi, D. G. Gilliland, and B. G. Neel. 2005. 'Prognostic, therapeutic, and mechanistic implications of a mouse model of leukemia evoked by Shp2 (PTPN11) mutations', *Cancer Cell*, 7: 179-91.

Moore, M.A., and D. Metcalf. 1969. 'Ontogeny of the Haemopoietic System Yolk Sac Origin of In Viuo and In Vitro Colony Forming Cells in the Developing Mouse Embryo', *Br J Haematol*, 18: 279-96.

Mucenski, M. L., K. McLain, A. B. Kier, S. H. Swerdlow, C. M. Schreiner, T. A. Miller, D. W. Pietryga, W. J. Jr. Scott, and S. S. Potter. 1991. 'A functional c-myb gene is required for normal murine fetal hepatic hematopoiesis', *Cell*, 65: 677-89.

Mulero-Navarro, S., A. Sevilla, A. C. Roman, D. F. Lee, S. L. D'Souza, S. Pardo, I. Riess, J. Su, N. Cohen, C. Schaniel, N. A. Rodriguez, A. Baccarini, B. D. Brown, H. Cave, A. Caye, M. Strullu, S. Yalcin, C. Y. Park, P. S. Dhandapany, G. Yongchao, L. Edelmann, S. Bahieg, P. Raynal, E. Flex, M. Tartaglia, K. A. Moore, I. R. Lemischka, and B. D. Gelb. 2015. 'Myeloid Dysregulation in a Human Induced Pluripotent Stem Cell Model of PTPN11-Associated Juvenile Myelomonocytic Leukemia', *Cell Rep*, 13: 504-15.

Muller, A. M., A. Medvinsky, J. Strouboulis, F. Grosveld, and E. Dzierzak. 1994. 'Development of Hematopoietic in the Mouse Embryo Stem Cell Activity', *Immunity*, 1: 291-301.

Naito, T., H. Tanaka, Y. Naoe, and I. Taniuchi. 2011. 'Transcriptional control of T-cell development', *Int Immunol*, 23: 661-8.

Nakamura, Y., M. Ito, T. Yamamoto, X. Y. Yan, H. Yagasaki, Y. Kamachi, K. Kudo, and S. Kojima. 2005. 'Engraftment of NOD/SCID/gammac(null) mice with multilineage neoplastic cells from patients with juvenile myelomonocytic leukaemia', *Br J Haematol*, 130: 51-7.

Naramura, M., N. Nandwani, H. Gu, V. Band, and H. Band. 2010. 'Rapidly fatal myeloproliferative disorders in mice with deletion of Casitas B-cell lymphoma (Cbl) and Cbl-b in hematopoietic stem cells', *Proc Natl Acad Sci U S A*, 107: 16274-9.

Ng, C. S., T. K. Lam, J. K. Chan, P. K. Hui, H. K. Ng, S. C. Szeto, and C. S. Feng. 1988. 'Juvenile chronic myeloid leukemia. A malignancy of S-100 protein-positive histiocytes', *Am J Clin Pathol*, 90: 575-82.

Oliveira, A. F., A. Tansini, D. O. Vidal, L. F. Lopes, K. Metze, and I. Lorand-Metze. 2016. 'Characteristics of the phenotypic abnormalities of bone marrow cells in childhood myelodysplastic syndromes and juvenile myelomonocytic leukemia', *Pediatr Blood Cancer*.

Osumi, T., M. Kato, M. Ouchi-Uchiyama, D. Tomizawa, K. Kataoka, Y. Fujii, M. Seki, J. Takita, S. Ogawa, T. Uchiyama, K. Ohki, and N. Kiyokawa. 2017. 'Blastic transformation of juvenile myelomonocytic leukemia caused by the copy number gain of oncogenic KRAS', *Pediatr Blood Cancer*.

Ozono, S., H. Inada, S. Nakagawa, K. Ueda, H. Matsumura, S. Kojima, H. Koga, T. Hashimoto, K. Oshima, and T. Matsuishi. 2011. 'Juvenile myelomonocytic leukemia characterized by cutaneous lesion containing Langerhans cell histiocytosis-like cells', *Int J Hematol*, 93: 389-93.

Palis, J., R. J. Chan, A. Koniski, R. Patel, M. Starr, and M. C. Yoder. 2001. 'Spatial and temporal emergence of high proliferative potential hematopoietic precursors during murine embryogenesis', *Proc Natl Acad Sci U S A*, 98: 4528-33.

Palis, J., S. Robertson, M. Kennedy, C. Wall, and G. Keller. 1999. 'Development of erythroid and myeloid progenitors in the yolk sac and embryo proper of the mouse.pdf', *Development*, 126: 5073-84.

Parada, L. F., C. J. Tabin, C. Shih, and R. A. Weinberg. 1982. 'Human EJ bladder carcinoma oncogene is homologue of Harvey sarcoma virus ras gene', *Nature*, 297: 474-8.

Park, I. K., D. Qian, M. Kiel, M. W. Becker, M. Pihalja, I. L. Weissman, S. J. Morrison, and M. F. Clarke. 2003. 'Bmi-1 is required for maintenance of adult self-renewing haematopoietic stem cells', *Nature*, 423: 302-5.

Poetsch, A. R., D. B. Lipka, T. Witte, R. Claus, P. Nollke, M. Zucknick, C. Olk-Batz, S. Fluhr, M. Dworzak, B. De Moerloose, J. Stary, M. Zecca, H. Hasle, M. Schmugge, M. M. van den Heuvel-Eibrink, F. Locatelli, C. M. Niemeyer, C. Flotho, and C. Plass. 2014. 'RASA4 undergoes DNA hypermethylation in resistant juvenile myelomonocytic leukemia', *Epigenetics*, 9: 1252-60.

Porter, S. N., A. S. Cluster, W. Yang, K. A. Busken, R. M. Patel, J. Ryoo, and J. A. Magee. 2016. 'Fetal and neonatal hematopoietic progenitors are functionally and transcriptionally resistant to Flt3-ITD mutations', *Elife*, 5.

Qian, B. Z., J. Li, H. Zhang, T. Kitamura, J. Zhang, L. R. Campion, E. A. Kaiser, L. A. Snyder, and J. W. Pollard. 2011. 'CCL2 recruits inflammatory monocytes to facilitate breast-tumour metastasis', *Nature*, 475: 222-5.

Raikar, S. S., J. D. Scarborough, H. Sabnis, J. Bergsagel, D. Wu, T. M. Cooper, F. G. Keller, B. L. Wood, and S. T. Bunting. 2016. 'Early T-Cell Precursor Acute Lymphoblastic Leukemia in an Infant With an NRAS Q61R Mutation and Clinical Features of Juvenile Myelomonocytic Leukemia', *Pediatr Blood Cancer*, 63: 1667-70.

Randhawa, S., B. S. Cho, D. Ghosh, M. Sivina, S. Koehrer, M. Muschen, A. Peled, R. E. Davis, M. Konopleva, and J. A. Burger. 2016. 'Effects of pharmacological and genetic disruption of CXCR4 chemokine receptor function in B-cell acute lymphoblastic leukaemia', *Br J Haematol*, 174: 425-36.

Rufer, N., T. H. Brummendorf, S. Kolvraa, C. Bischoff, K. Christensen, L. Wadsworth, M. Schulzer, and P. M. Lansdorp. 1999. 'Telomere fluorescence measurements in granulocytes and T lymphocyte subsets point to a high turnover of hematopoietic stem cells and memory T cells in early childhood', *J Exp Med*, 190: 157-67.

Sabnis, Amit J., Laurene S. Cheung, Monique Dail, Hio Chung Kang, Marianne Santaguida, Michelle L. Hermiston, Emmanuelle Passegu??, Kevin Shannon, and Benjamin S. Braun. 2009. 'Oncogenic Kras Initiates Leukemia in Hematopoietic Stem Cells', *PLoS Biology*, 7.

Sakaguchi, H., Y. Okuno, H. Muramatsu, K. Yoshida, Y. Shiraishi, M. Takahashi, A. Kon, M. Sanada, K. Chiba, H. Tanaka, H. Makishima, X. Wang, Y. Xu, S. Doisaki, A. Hama, K. Nakanishi, Y. Takahashi, N. Yoshida, J. P. Maciejewski, S. Miyano, S. Ogawa, and S. Kojima. 2013. 'Exome sequencing identifies secondary mutations of SETBP1 and JAK3 in juvenile myelomonocytic leukemia', *Nat Genet*, 45: 937-41.

Samokhvalov, I. M., N. I. Samokhvalova, and S. Nishikawa. 2007. 'Cell tracing shows the contribution of the yolk sac to adult haematopoiesis', *Nature*, 446: 1056-61.

Schiwon, M., C. Weisheit, L. Franken, S. Gutweiler, A. Dixit, C. Meyer-Schwesinger, J. M. Pohl, N. J. Maurice, S. Thiebes, K. Lorenz, T. Quast, M. Fuhrmann, G. Baumgarten, M. J. Lohse, G. Opdenakker, J. Bernhagen, R. Bucala, U. Panzer, W. Kolanus, H. J. Grone, N. Garbi, W. Kastenmuller, P. A. Knolle, C. Kurts, and D. R. Engel. 2014. 'Crosstalk between sentinel and helper macrophages permits neutrophil migration into infected uroepithelium', *Cell*, 156: 456-68.

Schlenner, S. M., and H. R. Rodewald. 2010. 'Early T cell development and the pitfalls of potential', *Trends Immunol*, 31: 303-10.

Schulz, C., E. Gomez Perdiguero, L. Chorro, H. Szabo-Rogers, N. Cagnard, K. Kierdorf, M. Prinz, B. Wu, S. E. Jacobsen, J. W. Pollard, J. Frampton, K. J. Liu, and F. Geissmann. 2012. 'A lineage of myeloid cells independent of Myb and hematopoietic stem cells', *Science*, 336: 86-90.

Seeburg, P. H., W. W. Colby, D. J. Capon, D. V. Goeddel, and A. D. Levinson. 1984. 'Biological properties of human c-Ha-ras1 genes mutated at codon 12', *Nature*, 312: 71-5.

Serrano, M., A. W. Lin, M. E. McCurrach, D. Beach, and S. W. Lowe. 1997. 'Oncogenic ras provokes premature cell senescence associated with accumulation of p53 and p16INK4a', *Cell*, 88: 593-602.

Sheng, J., C. Ruedl, and K. Karjalainen. 2015. 'Fetal HSCs versus EMP2s', *Immunity*, 43: 1025.

Shyh-Chang, N., and G. Q. Daley. 2013. 'Lin28: primal regulator of growth and metabolism in stem cells', *Cell Stem Cell*, 12: 395-406.

Sidorov, I., M. Kimura, A. Yashin, and A. Aviv. 2009. 'Leukocyte telomere dynamics and human hematopoietic stem cell kinetics during somatic growth', *Exp Hematol*, 37: 514-24.

Siegemund, S., J. Shepherd, C. Xiao, and K. Sauer. 2015. 'hCD2-iCre and Vav-iCre mediated gene recombination patterns in murine hematopoietic cells', *PLoS One*, 10: e0124661.

Srinivas, S., T. Watanabe, C-S. Lin, C.M. William, Y. Tanabe, T.M. Jessell, and F. Costantini. 2001. 'Cre reporter strains produced by targeted insertion of EYFP and ECFP into the ROSA26 locus', *BMC Dev Biol*, 1.

Stadtfeld, M., and T. Graf. 2005. 'Assessing the role of hematopoietic plasticity for endothelial and hepatocyte development by non-invasive lineage tracing', *Development*, 132: 203-13.

Stadtfeld, M., M. Ye, and T. Graf. 2007. 'Identification of interventricular septum precursor cells in the mouse embryo', *Dev Biol*, 302: 195-207.

Staffas, A., C. Karlsson, M. Persson, L. Palmqvist, and M. O. Bergo. 2015. 'Wild-type KRAS inhibits oncogenic KRAS-induced T-ALL in mice', *Leukemia*, 29: 1032-40.

Stieglitz, E., A. N. Taylor-Weiner, T. Y. Chang, L. C. Gelston, Y. D. Wang, T. Mazor, E. Esquivel, A. Yu, S. Seepo, S. R. Olsen, M. Rosenberg, S. L. Archambeault, G. Abusin, K. Beckman, P. A. Brown, M. Briones, B. Carcamo, T. Cooper, G. V. Dahl, P. D. Emanuel, M. N. Fluchel, R. K. Goyal, R. J. Hayashi, J. Hitzler, C. Hugge, Y. L. Liu, Y. H. Messinger, D. H. Mahoney, Jr., P. Monteleone, E. R. Nemecek, P. A. Roehrs, R. J. Schore, K. C. Stine, C. M. Takemoto, J. A. Toretsky, J. F. Costello, A. B. Olshen, C. Stewart, Y. Li, J. Ma, R. B. Gerbing, T. A. Alonzo, G. Getz, T. A. Gruber, T. R. Golub, K. Stegmaier, and M. L. Loh. 2015. 'The genomic landscape of juvenile myelomonocytic leukemia', *Nat Genet*, 47: 1326-33.

Stieglitz, E., C. B. Troup, L. C. Gelston, J. Haliburton, E. D. Chow, K. B. Yu, J. Akutagawa, A. N. Taylor-Weiner, Y. L. Liu, Y. D. Wang, K. Beckman, P. D. Emanuel, B. S. Braun, A. Abate, R. B. Gerbing, T. A. Alonzo, and M. L. Loh. 2015. 'Subclonal mutations in SETBP1 confer a poor prognosis in juvenile myelomonocytic leukemia', *Blood*, 125: 516-24.

Sturgeon, C. M., A. Ditadi, G. Awong, M. Kennedy, and G. Keller. 2014. 'Wnt signaling controls the specification of definitive and primitive hematopoiesis from human pluripotent stem cells', *Nat Biotechnol*, 32: 554-61.

Sun, J., A. Ramos, B. Chapman, J. B. Johnnidis, L. Le, Y. J. Ho, A. Klein, O. Hofmann, and F. D. Camargo. 2014. 'Clonal dynamics of native haematopoiesis', *Nature*, 514: 322-7.

Tanaka, Y., M. Hayashi, Y. Kubota, H. Nagai, G. Sheng, S. Nishikawa, and I. M. Samokhvalov. 2012. 'Early ontogenic origin of the hematopoietic stem cell lineage', *Proc Natl Acad Sci U S A*, 109: 4515-20.

Tang, P., C. Gao, A. Li, J. Aster, L. Sun, and L. Chai. 2013. 'Differential roles of Kras and Pten in murine leukemogenesis', *Leukemia*, 27: 1210-4.

Taoudi, S., and A. Medvinsky. 2007. 'Functional identification of the hematopoietic stem cell niche in the ventral domain of the embryonic dorsal aorta', *Proc Natl Acad Sci U S A*, 104: 9399-403.

Till, J. E., and E. A. McCulloch. 1961. 'A direct measurement of the radiation sensitivity of normal mouse bone marrow cells', *Radiat Res*, 14: 213-22.

Tober, J., A. Koniski, K. E. McGrath, R. Vemishetti, R. Emerson, K. K. de Mesy-Bentley, R. Waugh, and J. Palis. 2007. 'The megakaryocyte lineage originates from hemangioblast precursors and is an integral component both of primitive and of definitive hematopoiesis', *Blood*, 109: 1433-41.

Tober, J., A. D. Yzaguirre, E. Piwarzyk, and N. A. Speck. 2013. 'Distinct temporal requirements for Runx1 in hematopoietic progenitors and stem cells', *Development*, 140: 3765-76.

Vanhee, S., K. De Mulder, Y. Van Caeneghem, G. Verstichel, N. Van Roy, B. Menten, I. Velghe, J. Philippe, D. De Bleser, B. N. Lambrecht, T. Taghon, G. Leclercq, T. Kerre, and B. Vandekerckhove. 2014. 'In vitro human embryonic stem cell hematopoiesis mimics MYB-independent yolk sac hematopoiesis', *Haematologica*.

Waskow, C., K. Liu, G. Darrasse-Jeze, P. Guermonprez, F. Ginhoux, M. Merad, T. Shengelia, K. Yao, and M. Nussenzweig. 2008. 'The receptor tyrosine kinase Flt3 is required for dendritic cell development in peripheral lymphoid tissues', *Nat Immunol*, 9: 676-83.

Weinberg, R. S., D. Leibowitz, M. E. Weinblatt, J. Kochen, and B. P. Alter. 1990. 'Juvenile chronic myelogenous leukaemia: the only example of truly fetal (not fetal-like) erythropoiesis', *Br J Haematol*, 76: 307-10.

Wilhelm, T., D. B. Lipka, T. Witte, J. A. Wierzbinska, S. Fluhr, M. Helf, O. Mucke, R. Claus, C. Konermann, P. Nollke, C. M. Niemeyer, C. Flotho, and C. Plass. 2016. 'Epigenetic silencing of AKAP12 in juvenile myelomonocytic leukemia', *Epigenetics*, 11: 110-9.

Wilson, C. H., I. Gamper, A. Perfetto, J. Auw, T. D. Littlewood, and G. I. Evan. 2014. 'The kinetics of ER fusion protein activation in vivo', *Oncogene*, 33: 4877-80.

Wilson, N. K., D. G. Kent, F. Buettner, M. Shehata, I. C. Macaulay, F. J. Calero-Nieto, M. Sanchez Castillo, C. A. Oedekoven, E. Diamanti, R. Schulte, C. P. Ponting, T. Voet, C. Caldas, J. Stingl, A. R. Green, F. J. Theis, and B. Gottgens. 2015. 'Combined Single-Cell Functional and Gene Expression Analysis Resolves Heterogeneity within Stem Cell Populations', *Cell Stem Cell*, 16: 712-24.

Xu, D., X. Liu, W. M. Yu, H. J. Meyerson, C. Guo, S. L. Gerson, and C. K. Qu. 2011. 'Non-lineage/stage-restricted effects of a gain-of-function mutation in tyrosine phosphatase Ptpn11 (Shp2) on malignant transformation of hematopoietic cells', *J Exp Med*, 208: 1977-88.

Yamamoto, R., Y. Morita, J. Ooehara, S. Hamanaka, M. Onodera, K. L. Rudolph, H. Ema, and H. Nakauchi. 2013. 'Clonal analysis unveils self-renewing lineage-restricted progenitors generated directly from hematopoietic stem cells', *Cell*, 154: 1112-26.

Ye, M., H. Zhang, G. Amabile, H. Yang, P. B. Staber, P. Zhang, E. Levantini, M. Alberich-Jorda, J. Zhang, A. Kawasaki, and D. G. Tenen. 2013. 'C/EBPa controls acquisition and maintenance of adult haematopoietic stem cell quiescence', *Nat Cell Biol*, 15: 385-94.

Ye, Min, Hiromi Iwasaki, Catherine V Laiosa, Matthias Stadtfeld, Huafeng Xie, Susanne Heck, Bjorn Clausen, Koichi Akashi, and Thomas Graf. 2003. 'Hematopoietic Stem Cells Expressing the Myeloid Lysozyme Gene Retain Long-Term , Multilineage Repopulation Potential'.

Yoder, M. C., and K. Hiatt. 1997. 'Engraftment of Embryonic Hematopoietic Cells in Conditioned Newborn Recipients', *Blood*, 89: 2176-83.

Yoder, M. C., K. Hiatt, P. Dutt, P. Mukherjee, D. M. Bodine, and D. Orlic. 1997. 'Characterization of definitive lymphohematopoietic stem cells in the day 9 murine yolk sac', *Immunity*, 7: 335-44.

Yoshida, N., H. Yagasaki, Y. Xu, K. Matsuda, A. Yoshimi, Y. Takahashi, A. Hama, N. Nishio, H. Muramatsu, N. Watanabe, K. Matsumoto, K. Kato, J. Ueyama, H. Inada, H. Goto, M. Yabe, K. Kudo, J. Mimaya, A. Kikuchi, A. Manabe, K. Koike, and S. Kojima. 2009. 'Correlation of clinical features with the mutational status of GM-CSF signaling pathway-related genes in juvenile myelomonocytic leukemia', *Pediatr Res*, 65: 334-40.

Yoshimoto, M., E. Montecino-Rodriguez, M. J. Ferkowicz, P. Porayette, W. C. Shelley, S. J. Conway, K. Dorshkind, and M. C. Yoder. 2010. 'Embryonic day 9 yolk sac and intra-embryonic hemogenic endothelium independently generate a B-1 and marginal zone progenitor lacking B-2 potential', *Proc Natl Acad Sci U S A*, 108: 1468-73.

Yoshimoto, M., P. Porayette, N. L. Glosson, S. J. Conway, N. Carlesso, A. A. Cardoso, M. H. Kaplan, and M. C. Yoder. 2012. 'Autonomous murine T-cell progenitor production in the extra-embryonic yolk sac before HSC emergence', *Blood*, 119: 5706-14.

Yuan, Joan, Cuong K Nguyen, Xiuhuai Liu, Chrysi Kanellopoulou, and Stefan A Muljo. 2012. 'Lin28b Reprograms Adult Bone Marrow Hematopoietic Progenitors to Mediate Fetal-Like Lymphopoiesis', *Science*, 335: 1195-200.

Zhang, J., L. Ding, L. Holmfeldt, G. Wu, S. L. Heatley, D. Payne-Turner, J. Easton, X. Chen, J. Wang, M. Rusch, C. Lu, S. C. Chen, L. Wei, J. R. Collins-Underwood, J. Ma, K. G. Roberts, S. B. Pounds, A. Ulyanov, J. Becksfort, P. Gupta, R. Huether, R. W. Kriwacki, M. Parker, D. J. McGoldrick, D. Zhao, D. Alford, S. Espy, K. C. Bobba, G. Song, D. Pei, C. Cheng, S. Roberts, M. I. Barbato, D. Campana, E. Coustan-Smith, S. A. Shurtleff, S. C. Raimondi, M. Kleppe, J. Cools, K. A. Shimano, M. L. Hermiston, S. Doulatov, K. Eppert, E. Laurenti, F. Notta, J. E. Dick, G. Basso, S. P. Hunger, M. L. Loh, M. Devidas, B. Wood, S. Winter, K. P. Dunsmore, R. S. Fulton, L. L. Fulton, X. Hong, C. C. Harris, D. J. Dooling, K. Ochoa, K. J. Johnson, J. C. Obenauer, W. E. Evans, C. H. Pui, C. W. Naeve, T. J. Ley, E. R. Mardis, R. K. Wilson, J. R. Downing, and C. G. Mullighan. 2012. 'The genetic basis of early T-cell precursor acute lymphoblastic leukaemia', *Nature*, 481: 157-63.

Zhang, J., J. Wang, Y. Liu, H. Sidik, K. H. Young, H. F. Lodish, and M. D. Fleming. 2009. 'Oncogenic Kras-induced leukemogeneis: hematopoietic stem cells as the initial target and lineage-specific progenitors as the potential targets for final leukemic transformation', *Blood*, 113: 1304-14.

Zhang, Y., C. Riesterer, A. M. Ayrall, F. Sablitzky, T. D. Littlewood, and M. Reth. 1996. 'Inducible site-directed recombination in mouse embryonic stem cells', *Nucleic Acids Res*, 24: 543-8.

Zheng, H., S. Li, P. Hsu, and C. K. Qu. 2013. 'Induction of a tumor-associated activating mutation in protein tyrosine phosphatase Ptpn11 (Shp2) enhances mitochondrial metabolism, leading to oxidative stress and senescence', *J Biol Chem*, 288: 25727-38.

Zovein, A. C., J. J. Hofmann, M. Lynch, W. J. French, K. A. Turlo, Y. Yang, M. S. Becker, L. Zanetta, E. Dejana, J. C. Gasson, M. D. Tallquist, and M. L. Iruela-Arispe. 2008. 'Fate tracing reveals the endothelial origin of hematopoietic stem cells', *Cell Stem Cell*, 3: 625-36.

CURRICULUM VITAE

Stefan Pasichnyk Tarnawsky

Education

M.D. 2019 Indiana University School of Medicine
Indianapolis, IN.

Ph.D. 2017 Indiana University
Department of Biochemistry and Molecular Biology
Indianapolis, IN.

B.Sc. 2011 University of Toronto
Departments of Biochemistry (Specialty) and English (Minor)
Toronto, ON, Canada.

Publications

Tarnawsky SP, Chan RJ, and Yoder MC. FLT3Cre+ $Kras^{G12D/+}$ mice develop a transplantable JMML-like myeloid disease. J. Clin. Invest. 2017. *Under Review.*

Palazzo AF, Mahadevan K, and Tarnawsky SP. ALREX-elements and introns: two identity elements that promote mRNA nuclear export. Wiley interdisciplinary reviews RNA. 2013;4(5):523-33.

Tarnawsky SP, and Palazzo AF. Positional requirements for the stimulation of mRNA nuclear export by ALREX-promoting elements. Mol Biosyst. 2012;8(10):2527-30.

Cenik C, Chua HN, Zhang H, Tarnawsky SP, Akef A, Derti A, et al. Genome analysis reveals interplay between 5'UTR introns and nuclear mRNA export for secretory and mitochondrial genes. PLoS genetics. 2011;7(4):e1001366.

Gueroussov S, Tarnawsky SP, Cui XA, Mahadevan K, and Palazzo AF. Analysis of mRNA nuclear export kinetics in mammalian cells by microinjection. Journal of visualized experiments: JoVE. 2010(46).

Presentations

2016 American Society of Hematology
San Diego, CA.

JMML International Symposium
San Diego, CA.

2015 European Working Group on Myelodysplastic Syndromes in Childhood
Aarhus, Denmark.

2014 JMML International Symposium
San Diego, CA.

Department of Biochemistry Research Day
Indianapolis, IN.

Awards

2015-2017 NIH-NHLBI 5F30HL128011-02
"HSC-Independent Progenitors Contribute to JMML."

2015 IUSCC Merilyn Hester Scholarship.

2015 IUSCC Research Day poster award: 1st place.

2013-2015 Supported by NIH-NIDDK 5T32DK007519-2 to Dr. H.E. Broxmeyer,
"Regulation of Hematopoietic Cell Production."

2011-2013 Supported by NIH-NIGMS 5T32GM077229-05 to Dr. R.G. Mirmira,
"IUSM Medical Scientist/Engineer Training Program."

Travel American Society of Hematology Abstract Achievement Award 2016.

JMML International Symposium Abstract Award 2016.

IUSM Travel Grant 2016.

NIDDK Abstract Award 2015.

JMML International Symposium Abstract Award 2014.

IUPUI Graduate Student Travel Fellowship 2014.